REFERENCE ONLY

UNIVERSITY OF LONDON THESIS

Degree PhD Year 2006 Name of Author DAWSON, LF

A novel mechanism regulating DNA-damage repair in *Mycobacterium tuberculosis*

Lisa Frances Dawson

A thesis submitted in fulfilment of the requirements of University College London for the degree of Doctor of Philosophy

September 2005

Division of Mycobacterial Research
National Institute for Medical Research
The Ridgeway
Mill Hill
London

ProQuest LLC
789 East Eisenhower Parkway
P.O. Box 1346
Ann Arbor, MI 48106-1346

Abstract

The intracellular pathogen *Mycobacterium tuberculosis* (*M. tuberculosis*) resides in macrophages and is the causative agent of human tuberculosis. Infected macrophages produce reactive oxygen and nitrogen intermediates, known to damage DNA; therefore DNA damage repair is thought to be important in survival of *M. tuberculosis* in the host. The expression of many bacterial DNA repair genes is often regulated by the SOS response, in which RecA is an integral part; however, in *M. tuberculosis* the majority of genes in the DNA-damage regulon are regulated independently of the RecA/LexA system. In this study two potential mechanisms for this alternative mode of gene regulation were investigated.

The first hypothesis addressed was that regulation of expression following DNA-damage is controlled by an alternative sigma factor. Sigma factors are protein subunits of RNA polymerase, which confer specificity of binding to particular promoters. The function/expression of alternative sigma factors is usually regulated by various mechanisms. The sigma factor SigG is the most highly induced of all 13 sigma factors of *M. tuberculosis* in response to DNA-damage in both wild-type and *ΔrecA* strains. A knockout of *sigG* in *M. tuberculosis* was constructed, and found to be more susceptible to mitomycin C stress than wild-type H37Rv and attenuated in mice. *ruvC* was shown to possesses 2 transcriptional start sites, and although neither were regulated by SigG, the P1 promoter appeared to be dual regulated by LexA and the RecA/LexA independent mechanism. Microarray analysis revealed that SigG was not significantly involved in regulation of the RecA/LexA independent DNA-damage regulon, but that SigG directly or indirectly regulated expression of 127 genes in the absence of DNA-damage.

The other possible mode of RecA/LexA independent regulation was via a repressor/activator protein. Gel shifts assays using *M. tuberculosis* cell free extracts were used to attempt to identify a repressor or activator protein that bound to the operator of the *recA* P1 promoter, known to be induced independently of RecA, but failed to detect specific binding. Published microarray data revealed that Rv2017, a predicted regulatory protein, was upregulated in both wild-type and Δ*recA* strains of *M. tuberculosis* in response to DNA-damage. Therefore, a gene inactivation knockout of Rv2017 was constructed and analysed in *M. tuberculosis*. The ΔRv2017 strain was hyposensitive to mitomycin C stress and preliminary mouse *in-vivo* infection data suggested that the ΔRv2017 strain may be hypervirulent. Microarray data revealed that Rv2017 plays a direct/indirect role in regulation of a large regulon, including some genes in the DNA-damage repair regulon.

Acknowledgements

I would like to take this opportunity to thank my supervisor Dr. Elaine Davis for giving me the opportunity to study for my PhD, and would like to thank her, along with my second supervisor Dr. Roger Buxton for their critical analysis and guidance. I would also like to extend my thanks to all the members of the mycobacterial research group, past and present who have helped, guided and discussed both practical and technical problems.

My thanks are extended to Dr. Krishna Gopaul for the pGardee2 construct, from which I constructed the *sigG* mutant strain of *M. tuberculosis*. I would also like to thank Dr. Ricardo Tascon and the animal technicians for performing *in-vivo* mouse infections and Dr. Jason Hinds at the BμGS microarray facility in St. Georges Hospital Medical School for the *M. tuberculosis* microarrays, and for technical assistance.

Finally I would like to thank my family and friends for their unmoving support throughout my PhD. I would particularly like to thank Jonny for all his Mac technical support, without which, I would have been lost, and I would like to also thank Paul for making me smile. I would also like to thank Rox, Jude and Kat for listening relentlessly to my problems.

List of figures

List of tables

Abbreviations

Abbreviations

AIDS	Acquired immunodeficiency syndrome
APC	Antigen presenting cell
APS	Ammonium persulphate
AraLAM	Arabinose capped lipoarabinomannan
ATP	Adenosine triose phosphate
BCG	Bacillus Calmette-Guerin
bp	Base pair
CAP	Catabolite activator protein
cDNA	Complementary deoxyribonucleic acid
CFE	Cell free extract
CFU	Colony forming units
CR	Complement receptor
dATP	deoxyadenosine triphosphate
ddATP	Dideoxyadenosine triphosphate
dCTP	Deoxycytosine triphosphate
ddCTP	Dideoxycytosine triphosphate
ddGTP	Dideoxyguanine triphosphate
ddTTP	Dideoxytyrosine triphosphate
DEPC	diethylpyrocarbonate
dGTP	Deoxyguanine triphosphate
dH_20	Deionized water
DMEM	Dulbecco's modified Eagels media

DMSO	dimethyl sulphoxide
DNA	Deoxyribonucleic acid
DNase	Deoxyribonuclease
DOTS	Directly observed short course therapy
dsDNA	Double stranded deoxyribonucleic acid
DTT	Dithiothreitol
dTTP	Deoxytyrosine triphosphate
EDTA	Diaminoethanetetraacetic acid
FCS	Foetal calf serum
HIV	Human immunodeficiency virus
H-NS	Histone like nucleoid structuring protein
Hyg^R	Hygromycin resistant
LAM	lipoarabinomannan
INF-γ	Gamma interferon
IL	interleukin
LPS	Lipopolysaccharide
IPTG	isopropyl β-D-thiogalactopyranoside
Km^R	Kanamycin resistant
kb	Kilo base (1Kb = 1000bp)
KCl	Potassium chloride
KDa	Kilo dalton
LB-Broth	Luria-Bertani medium
log	Logarithmic
ManLAM	Mannose capped lipoarabinomannan
MBq	MegaBequerels

MHC1	Major histocompatibility complex class 1
MMLV	Moloney murine leukamia virus derrived thermostable reverse transcriptase
MOPS	4-Morpholinepropanesulfonic acid
MR	Mannose receptor
mRNA	Messanger ribonucleic acid
NaOAC	Sodium acetate
OD	Optical density
Paraquat	Methly violgen (1,1-dimethyl 1-4'-dipryriminim dichloride methyl violgen)
PBS	Phosphate buffered saline
PCR	Polymerase chain reaction
PiLAM	Phospho-myo-inositol capped lipoarabinomannan
ppGpp	alarmone guanosine 3', 5'-bisphosphate
RE	Restriction endonuclease
RecA-ND	RecA non-dependent promoter
RNA	Ribonucleic acid
RNAP	RNA polymerase
RNAP-σ	RNA polymerase-sigma factor complex
RNase A	Ribonuclease A
RNase T1	Ribonuclease T1
RNI	Reactive nitrogen intermediates
ROI	Reactive oxygen intermediates
RT-PCR	Reverse transcriptase PCR
σ	Sigma factor
SSC	Standard short course chemotherapy
SDS	Sodium dodecyl sulphate

SDS-PAGE	Sodium dodecyl sulphate-polyacrylamide gel electrophoresis
SSC	Standard saline citrate
SSPE	Standard saline phosphate EDTA
TAE	Tris-acetate EDTA
TBE	Tris-borate EDTA
TE	Tris EDTA
TLR	Toll like receptor
Tris	Tris (hydroxymethyl) aminomethane (2-amino-2-hydroxymethylpropane-1,3-diol
Tris-Cl	Tris chloride
TEMED	N,N,N',N'-tetramethylethylenediamine
Tween 80	Polyoxyethylene sorbitan monooleate
WHO	World Health Organisation
X-Gal	5-Bromo-4-chloro-3-indolyl-β-D-galactoside

1 Introduction

1.1 Tuberculosis

1.1.1 Global incidence of *M. tuberculosis*

Today, tuberculosis is one of the top three killers in developing countries, along with malaria and HIV (Saeyers, 2002), and is responsible for over 2 million deaths a year (WHO, 2002). After the discovery of a treatment for *M. tuberculosis* in the early 1950's, health programs were set up in Europe and the US to combat and irradicate *M. tuberculosis* (O'Brien and Nunn, 2001). The initial success of these programmes led to the steady decline of *M. tuberculosis* in these areas, and the subsequent transfer of resources away from the *M. tuberculosis* programme, to other health programmes. However in the mid 1980's the cases of *M. tuberculosis* were on the increase, then in 1993, the WHO proclaimed *M. tuberculosis* a global emergency (WHO, 1993).

1.1.2 Efficacy of *M. tuberculosis* vaccine bacillus Calmette-Guerin (BCG).

Since the 1920's over 3 billion vaccinations with BCG have been widely administered to combat *M. tuberculosis.* Certain aspects of the BCG vaccine have fuelled an ongoing debate about the suitability and safety of BCG as a vaccine; this live attenuated vaccine was derived by 230 passages over 13 years of a virulent strain of *Mycobacterium bovis* (*M. bovis*) (Agger and Andersen, 2002). The efficacy varies between 0 and 80%, with widespread ineffectiveness in preventing pulmonary tuberculosis (O'Brien and Nunn, 2001). The nature of the vaccine renders the PPD skin test for *M. tuberculosis* ineffective, resulting in vaccinated individuals being indistinguishable from infected individuals (Agger and Andersen, 2002). It has been

hypothesised that the ineffectiveness of the BCG vaccine is linked to exposure of individuals to environmental mycobacteria, which elicits an immune response, whereby antibodies to environmental mycobacteria result in clearance of BCG prior to establishment of protective immunity (Agger and Andersen, 2002). This could explain the wide variation in efficacy, particularly as the lowest level of protection was observed in developing countries. However, BCG exhibits good efficacy at preventing *Mycobacterium leprae* (*M. leprae*) infections along with miliary and meningeal tuberculosis in children (Agger and Andersen, 2002).

1.1.3 Monitoring strategy to limit the spread of *M. tuberculosis*

Tuberculosis is particularly rife among the homeless and refugees world wide, with over 50% of the worldwide refugee population suffering from TB (WHO, 2002), due to poor living conditions and malnutrition. In developing countries, inadequate control practices for tuberculosis alongside the widespread ineffectiveness of the BCG vaccine (O'Brien and Nunn, 2001), has resulted in a global surge in the number of cases, reaching almost pandemic levels. In an effort to tackle the growing problem, the world health organisation (WHO) set up a strategy called directly observed therapy, short course (DOTS); a strategy for detection, monitoring and cure of tuberculosis. It encompasses 5 elements: surveillance/monitoring systems, microscopy services, drug supplies, directly observed effective treatment regimes, and political commitment (WHO, 2002). Without extensive multiple drug treatment, the fatality rate of those with acute tuberculosis is as high as 50% (Saeyers, 2002).

1.1.4 Co-infections with HIV

M. tuberculosis infections are most prevalent in south-east Asia, sub-Saharan Africa and Eastern Europe (WHO, 2002). The rise of *M. tuberculosis* cases has been fuelled by the HIV epidemic sweeping through Africa and Asia; 70% of the total 36.1 million people worldwide suffering from HIV and AIDS, localised to Sub-Saharan Africa (WHO, 2003). Co-infected patients are more likely to develop acute pulmonary tuberculosis (Dye *et al.*, 2002a), due to a depletion of CD4+ T-cells and subsequent decreased levels of interferon-γ (IFN-γ) in HIV patients. CD4+ T-cells are known to secrete IFN-γ, which has been shown in mouse models to be key in combating acute pulmonary tuberculosis (Agger and Andersen, 2002). This absence of CD4+ T cells results in *M. tuberculosis* being the leading cause of death of HIV positive patients (WHO, 2002).

1.1.5 Emergence of multiple-drug resistant *M. tuberculosis* (MDR-TB)

In recent years, there has been a rapid increase in the prevalence of MDR-TB, which is characterised by resistance to at least two of the most important and widely used first line drugs for *M. tuberculosis* treatment, namely rifampicin and isoniazid (Bone, 2001), which are given as part of combination drug therapy (Dye *et al.*, 2002a). Standard short course chemotherapy (SCC) consists of a cocktail of 4 first line drugs, including rifampicin, isoniazid, pyrazinamide and ethambutol given for 2 months, followed by just rifampicin and isoniazid for a further 4 months. These drugs are more effective, cheaper and less toxic than second line drugs, such as capreomycin, kanamycin, ethionamide, cycloserine, and para-aminosalicylate (Lordi, 2000), which are used to treat MDR-TB, for as long as 2 years (Dye *et al.*, 2002b). The treatment of

MDR-TB costs up to 50 times more than the standard short course chemotherapy regime used to treat drug susceptible cases (Dye *et al.*, 2002a). However, the rapid spread of MDR-TB is a cause for concern, as in the latter stages of acute pulmonary infections with MDR-TB there is no real effective treatment, therefore, even with good compliance during the 2 year chemotherapy course, the prognosis is poor. There is a particular problem with the spread of MDR-TB in Eastern Europe (Bone, 2001), namely in prisons in Russia, due to poor living conditions and lack of compliance with drug regimes, compounded by the lack of constant availability of anti-tuberculosis drugs (Bone, 2001).

The decline in the number of new cases of pulmonary tuberculosis in developed countries led to the dismantling of the health programmes in the 1970's, which in turn lead to the withdrawal of major pharmaceutical companies from novel drug discovery for *M. tuberculosis*, as it was no longer deemed a threat in the developed world, and therefore thought to be no longer profitable (Saeyers, 2002). This resulted in a gap in the research, causing a short fall in new drug therapy to treat the rapidly increasing worldwide burden of MDR-TB.

1.2 *M. tuberculosis* classification

M. tuberculosis is a member of the actinomycetes family of Gram-positive, rod shaped bacteria; it is an obligate aerobe, which can be visualised by a Ziehl Nielsen stain, as it is acid-fast (Saeyers, 2002). *M. tuberculosis* is also highly GC-rich and forms the *M. tuberculosis* complex along with; *M. bovis*, *Mycobacterium microti*, *M. bovis* (BCG), *Mycobacterium africanum*, and *Mycobacterium canetti* (Wayne, 1982). Mycobacteria are generally defined as slow growing bacteria in comparison to other species, such as *Bacillus*, or *Escherichia coli* (*E. coli*): the generation time varies from 30 minutes in *E. coli* to 17 hours in *M. tuberculosis*. However,

there are inter-species differences in generation time for mycobacterial species. Fast-growing mycobacteria are defined by the ability to produce colonies on a plate in one week, whereas slow growing mycobacteria take considerably longer (up to 4 weeks) (Goodfellows, 1986). The saprophyte *Mycobacterium smegmatis* is a fast growing mycobacteria, which is often used as a model of *M. tuberculosis.* The slow-growing mycobacteria include the pathogenic mycobacteria; *M. tuberculosis*, *M. leprae* and *M. bovis.* However, *M. leprae* is non-culturable *in-vitro* and can only be cultured outside its natural host (humans) using mouse foot pads, or the nine banded armadillo (Ravisse *et al.*, 1984).

A defining feature of *M. tuberculosis* is the lipid rich envelope, which makes it relatively impenetrable (Jarlier and Nikaido, 1994) and is thought to contribute to the ability of *M. tuberculosis* to survive in phagocytes (Kaufmann, 2001).

1.2.1 Structure of the cell wall

The lipid rich cell wall of *M. tuberculosis* is comprised of at least 4 layers, which overlay the cell membrane (see figure 1.1). The membrane consists of a lipid bi-layer (plasma membrane), encased in peptidoglycan. The peptidoglycan is covalently linked via phosphodiester bonds to arabinogalactan. Mycolic acids are attached to the distal portion of the arabinogalactan (Fenton and Vermeulen, 1996), and glycolipid surface molecules are associated with the mycolic acid. The mannose capped lipoarabinomannan (ManLAM), is tethered via a phosphatidylinositol anchor to the plasma membrane, and extends to the glycolipid surface molecules (Karakousis *et al.*, 2004). There are three classes of mycobacterial lipoarabinomannan (LAM), ManLAM, present in virulent strains, which contains extensive mannose capping, at the arabinan termini, whereas the rapid growing mycobacteria such as *M. smegmatis* possess phospho-myo-inositol

Figure 1.1

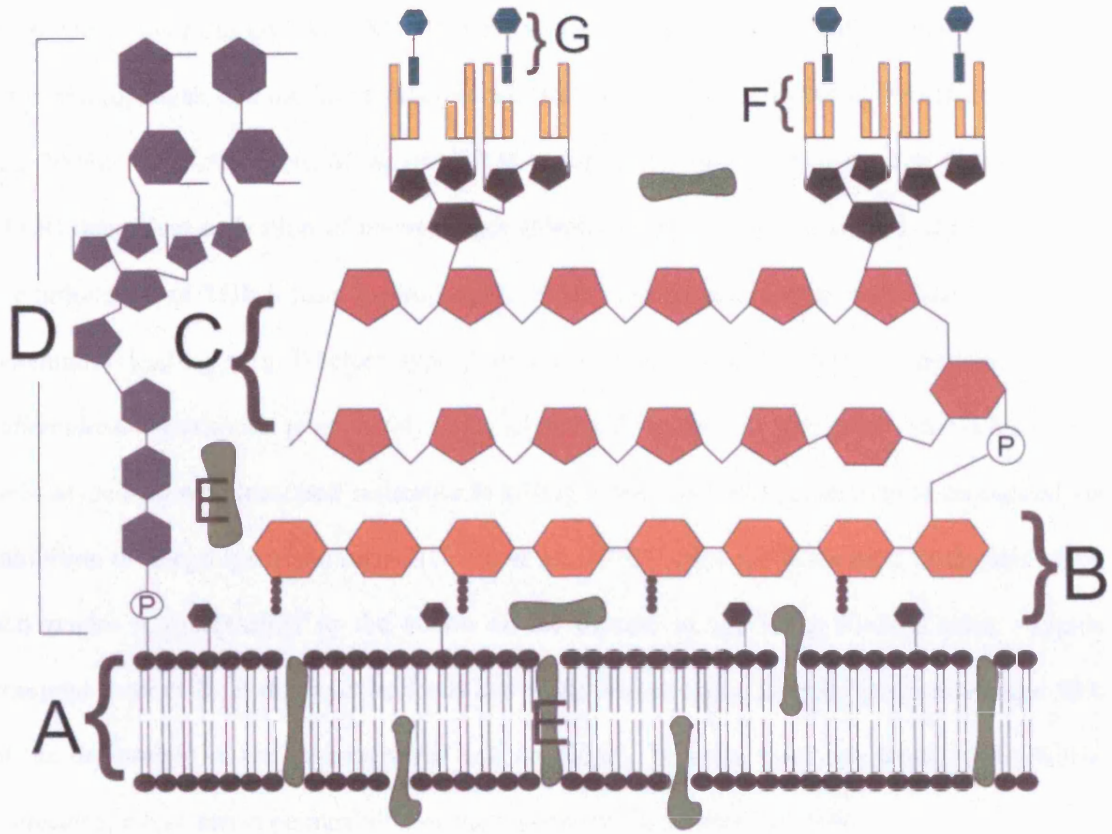

Figure 1.1: A schematic representation of the cell wall of *M. tuberculosis*. Adapted from (Karakousis *et al.*, 2004). The components are plasma membrane (A), peptidoglycan (B), arabinogalactan (C), Mannose-capped lipoarabinan (D), plasma membrane and cell envelope associated proteins (E), mycolic acids (F) and glycolipid surface molecules associated with mycolic acid (G).

capped LAM (PILAM). The third type of LAM, arabinose capped LAM (AraLAM), was described in *M. chelonae*, a rapidly growing mycobacteria, and lacks mannosylation at the arabinan termini. Constituent parts of the mycobacterial cell wall have potential immunogenic properties. Interestingly, AraLAM, is a more potent inducer of pro-inflammatory cytokines from macrophages, and unlike *M. tuberculosis*, induced the production of TNF-α (Karakousis *et al.*, 2004). ManLAM from *M. bovis* and *M. tuberculosis* do not elicit the toll like receptors (TLR) dependent activation of macrophages (Means *et al.*, 1999). ManLAM can also induce the production of TGF-β from macrophages, which inhibits macrophage and T-cell activation, potentially leading to a T-helper type 2 immune response, and decreased immunity to *M. tuberculosis* (Karakousis *et al.*, 2004). The sulpholipids in the cell wall of *M. tuberculosis* have been associated with increased resistance to killing in the macrophage, thought to be elicited via inhibition of phago-lysosome fusion (Goren *et al.*, 1976). Mycolic acids bind to the acid stain, and render it inaccessible to the action of the destain in the Ziehl-Nielson stain. Lipids comprise over 60% of the mycobacterial cell wall; interestingly, mycolic acid constitutes 50% of the dry weight of the mycobacterial cell envelope. Mycolic acids are strong hydrophobic molecules, which affect permeability of the mycobacteria (Chatterjee, 1997).

1.3 Pathogen-host interactions

Tuberculosis or consumption as it was known was initially thought to be caused by a virus, until 1892 when Robert Koch isolated the bacteria from infected lung tissue. The causative agent of tuberculosis, *M. tuberculosis* is a slow growing intracellular human pathogen (Mariani *et al.*, 2000) which is transmitted via aerosol (Saeyers, 2002); tiny water droplets produced by coughing or sneezing enter the lungs via the upper respiratory tract, carrying between 1 and 3 bacilli into the lung alveoli (Graham and Clark-Curtiss, 1999). The bacteria are then

phagocytosed by unactivated macrophages, where they reside in the phagosomal compartment (Goren *et al.*, 1976). After the alveolar macrophages have engulfed the bacteria, specific T cells are stimulated in the draining lymph nodes, which induces containment of the bacteria in granulomas in the lung. These granulomas are comprised of *M. tuberculosis* infected macrophages, which sometimes fuse to create giant cells, along with various T cell populations (Kaufmann, 2001). Interestingly, *M. tuberculosis* prevents phago-lysosome production by inhibiting the fusion of the lysosome with the infected phagosome (Goren *et al.*, 1976). Unactivated macrophages fail to harm *M. tuberculosis*, however activated macrophages (in presence of IFN-γ) can control the growth of the bacteria, but rarely achieve sterile eradication of the pathogen (Kaufmann, 2001). Therefore the bacteria can remain in a dormant state, in the phagosomal compartment of the macrophage, resulting in latent *M. tuberculosis*, or can replicate and form active/acute *M. tuberculosis* (Saeyers, 2002). It has been observed particularly in immuno-compromised patients that most cases of tuberculosis emerge from reactivation of a latent infection (Flynn and Chan, 2001), rather than progression to direct primary tuberculosis (Kaufmann, 2001). It is relevant to note that *M. tuberculosis* is an obligate aerobe but when exposed to gradual oxygen deprivation, like inside a forming granuloma, they are able to survive for extended periods (Sohaskey and Wayne, 2003).

Macrophages are the primary effector cells of the innate immune system, activated following IFN-γ exposure, which subsequently produce reactive oxygen and reactive nitrogen intermediates as part of their anti-microbial repertoire (Kaufmann, 2001). The cytokines TNF-α and lymphotoxin-α3 are important in formation and maintenance of the granuloma, as patients treated with anti-TNF-α for Rheumatoid Arthritis, suffer from reactivation of latent tuberculosis (Kaufmann, 2001). The anti-microbial effects of the macrophage are present via two distinct pathways, both activated by IFN-γ, NADPH phagocyte oxidase (phox) and

inducible nitric oxide synthase (iNOS). Phox catalyses the reduction of molecular oxygen to superoxide (O_2^-), which can be further reduced to hydrogen peroxide (H_2O_2), thus forming the reactive oxygen intermediates. The reactive nitrogen intermediates are formed using iNOS, whereby nitric oxide (NO), formed directly is oxidised to derivatives such as NO_2^- and N_2O_3. The reactive oxygen and nitrogen intermediates can combine to produced compounds such as peroxynitrite ($ONOO^-$), which have potent antimicrobial properties (Lindgren *et al.*, 2005). The intracellular pathogen *Francisella tularensis* is killed in macrophages by $ONOO^-$, however interestingly, other intracellular pathogens such as *M. tuberculosis* and *S. enterica* serovar *typhimurium* have the ability to detoxify ONOO- via peroxyredoxins (Lindgren *et al.*, 2005).

1.3.1 Receptor mediated phagocytosis

Phagocytosis of *M. tuberculosis* is mediated by receptors. There is evidence to suggest that receptor mediated phagocytosis takes place via complement receptor (CR), and mannose receptor (MR) (Fenton and Vermeulen, 1996; Means *et al.*, 1999).

The CR1, CR3 and CR4 receptors have been associated with receptor-mediated phagocytosis of *M. tuberculosis* (Fenton and Vermeulen, 1996). Lipoarabinomannan is a major surface lipoglycan of *M. tuberculosis* (Chatterjee *et al.*, 1992), which is recognised by the MRs (Schlesinger *et al.*, 1994), that are important for phagocytosis of intracellular pathogens and it has been suggested that they contribute to antigen presentation and granuloma formation (Kang and Schlesinger, 1998). The role of Toll like receptor (TLR) mediated activation of macrophages is not completely understood, yet TLR activation induces production of interleukin-12 (IL-12), a pro-inflammatory cytokine, whose activation of T-cells is thought to be important, therefore the loss of IL-12 induction may be a potential mechanism for avoidance of the immune response by *M. tuberculosis* (Karakousis *et al.*, 2004). TLR's are expressed

mainly on dendritic cells and macrophages, and prime the adaptive immune response, by controlling activation of antigen presenting cells (APC) (Barton and Medzhitov, 2002; Medzhitov, 2001). Different TLR's recognise different antigens, TLR2 and 4 generally recognise bacterial lipopolysaccharide (LPS), whereas TLR9 recognise bacterial CpG DNA: however, TLR2 and TLR4 have been shown to recognise the mycobacterial glycoprotein LAM (Means *et al.*, 1999). Interestingly, TLR4 does not require the CD14 ligand when binding LAM from *M. tuberculosis* (Means *et al.*, 1999).

1.3.2 Active versus latent tuberculosis infection

The development of active tuberculosis infection, or the reactivation of a latent infection only happens in a small proportion of individuals (Song *et al.*, 2003), particularly those that are immuno-compromised. It has therefore been suggested that it is important for *M. tuberculosis* to sense the environment of the host, and possess the ability to adapt to the physiological changes of the host, which would result in carefully regulated gene expression in response to the changing host signals during the course of the infection (Shi *et al.*, 2003). It has been suggested that the low ratio of active tuberculosis compared to latent infections is important for the successful survival of the pathogen (Kaufmann, 2001).

1.3.3 Immunogenicity of *M. tuberculosis*

Recent publication of the entire genome sequence (Cole *et al.*, 1998), revealed two distinct gene family clusters, PE-PEGRS. These clusters encode glycine-rich proteins, and comprise about 10% of the genome. They share a conserved amino terminus, and are thought to be immunologically important because either these regions could cause antigenic variation,

resulting in evasion from the host immune response or they could impair antigen processing (Kaufmann, 2001). This is particularly relevant as they have homology to some Pro-Glu family proteins in Epstein-Barr virus which interfere with major histocomptability complex class 1 (MHCI) presentation for T cells (Kaufmann, 2001). Deletion of certain PE-PGRS genes in *M. marinum* impaired growth in granulomas and macrophages (Ramakrishnan *et al.*, 2000).

1.3.4 Immunology of tuberculosis infection

Control of the *M. tuberculosis* infection is brought about by CD4+ and CD8+ T cells, along with natural killer cells, macrophages, which produce INF-γ, and dendritic cells, which activate other cell-types via IL-12 and IL-18 (Kawakami *et al.*, 2004). This activates the antimicrobial pathways in macrophages, producing a hostile environment for the bacteria, particularly as the phagosomal compartments are low in both nutrients and oxygen, and the activated macrophages produce reactive oxygen (ROI) and nitrogen intermediates (RNI), known to damage lipids, proteins, DNA (Cabiscol et al., 2000; Park and Imlay, 2003; Storz and Imlay, 1999) and RNA (Farr and Kogoma, 1991).

1.4 Exposure to DNA-damage

DNA is dynamic, and is continually exposed to a variety of types of DNA-damage, which have lead to the development of mechanisms designed to tolerate and repair the damage to DNA in all living organisms (Friedberg, 2003). An example of the kind of DNA-damage incurred is deamination, which results in miscoding lesions, hence leading to mutations during replication.

1.4.1 Types, effects and repair of DNA-damage

In the case of *M. tuberculosis*, the bacilli are thought to be exposed to a number of DNA damaging agents during infection and persistence in the macrophage, including exposure to ROI and RNI (Nathan and Shiloh, 2000). There are a number of cellular processes, which result in the formation of ROI/RNI, including peroxisomal metabolism, mitochondrial respiration, nitric oxide synthesis, and phagocytic leukocyte metabolism (Friedberg, 1995), suggesting oxidative stress is both an environmental phenomenon and an unavoidable by-product of an aerobic existence (Farr and Kogoma, 1991; Storz and Imlay, 1999). However, it has been suggested that during host-pathogen interactions, it is primarily within phagocytes that the bacteria are exposed to oxidants such as peroxide radicals ($^{\bullet}O_2$), hydrogen peroxide (H_2O_2), hydroxyl radicals ($^{\bullet}OH$) and singlet oxygen (Friedberg, 1995; Miller and Britigan, 1997). ROI and RNI cause damage to DNA, proteins, lipids and RNA, so pathogens have three options: to interfere with host production of ROI/RNI, to catabolize them or to repair damage caused by these agents (Nathan and Shiloh, 2000). Therefore the repair of damaged DNA is thought to be important for survival and replication of the tubercle bacillus (Davis et al., 2002a).

There are three main DNA repair mechanisms that have been extensively studied in *E. coli*, by which damaged bases are repaired, base excision repair (BER), nucleotide excision repair (NER) and homologous recombination (Friedberg, 2003). More recently non-homologous end joining (NHEJ) was also identified in some bacteria with a role in double-stranded break repair.

BER is a two stage process involved in repair of oxidised and alkylated DNA (Sancar, 1994). Initially the damaged bases are recognised by a DNA glycosylase e.g. *fpg* or *mutY*, and excised

then an Apurinic/apyrimidinic (AP) endonuclease *xthA* or *end* catalyses the formation of single stranded breaks, repaired via DNA polymerase I and ligase (Friedberg, 2003).

NER involves *uvrABC* and *D*, which function synergistically to remove pyrimidine dimers, whereby the *uvr*A_2B complex detects lesions in the DNA by sensing disruption of the double helix (Smith *et al.*, 2002), the strands are then separated, and *uvrB* remains bound, while *uvrA* dissociates. *uvrC* then binds and functions in unison with *uvrB* and the *uvrD* to excise a small 13bp region of ssDNA, including the damaged base, which is then repaired by DNA polymerase I and ligase (Friedberg, 2003; Smith *et al.*, 2002).

Homologous recombination is involved in both generation of novel genetic combinations, brought about by processes such as horizontal gene transfer, and the repair of DNA-damage (Colston M. J., 2000; Lorenz and Wackernagel, 1994). Allelic exchange has been utilised to produce gene inactivation knockouts in *M. tuberculosis* among other species. RecA plays a central role in repair, along with RecBCD complex, to form the major pathway of repairing double stranded breaks. RecBCD can act as an ATP-dependent dsDNA exonuclease and a helicase, to produce a single stranded DNA tail, which allows the binding of RecA (Friedberg, 2003). However, RecBCD can also function as a Chi (χ) specific endonuclease, which recognises specific chi sites (Chedin and Kowalczykowski, 2002). The second or minor pathway requires RecA along with the RecFOR complex to repair lesions at replication forks, and single stranded breaks (Friedberg, 2003). There are a number of other recombination repair genes, *recQ*, *recJ*, *recG* and *ruvABC*. RecQ is a helicase and RecJ an endonuclease involved in pre-synaptic stages. RecG and RuvAB are helicases, which function along with the nuclease RuvC, in resolution of cross-overs post synapsis (Friedberg, 2003).

1.4.2 Response to DNA-damage in prokaryotes

The response of exposure to DNA damaging agents has been most extensively studied in *E. coli*. In this organism, there are two pathways, which modulate gene expression in response to oxidative damaging agents; OxyR and SoxRS. In addition there is the SOS response, a further regulatory system, which responds to DNA-damage (Raivio and Silhavy, 2001).

1.4.2.1 OxyR and SoxRS pathways

Redox regulation is the modulation of protein activity by oxidation and reduction, brought about by redox signalling molecules such as ROI and RNI, e.g. superoxide, hydrogen peroxide and nitric oxide (Zheng and Storz, 2000). OxyR and SoxR are redox sensing transcription factors, extensively studied in *E. coli*, which detect elevated levels in ROI and act by regulating expression of bacterial antioxidant genes, to combat the effects of the ROI (Zheng and Storz, 2000). The OxyR regulon in *E. coli* is thought to control at least eight genes (Farr and Kogoma, 1991). The transcriptional activation of these genes is thought to be mediated directly via activated OxyR (activated by oxidation) binding to the α subunit of the RNA polymerase (Pomposiello and Demple, 2001; Zheng and Storz, 2000), which binds to the promoter regions of the OxyR regulon (Pomposiello and Demple, 2001). SoxR responds to superoxide and nitric oxide in a two step activation cascade (Zheng and Storz, 2000), where SoxR regulates transcription of *soxS*, then SoxS in turn activates transcription of genes involved in the antioxidant response (Zheng and Storz, 2000) by binding to the promoter regions and recruiting RNA polymerase (Pomposiello and Demple, 2001). It has been suggested that both OxyR and SoxRS are autoregulated (Georgiou, 2002; Zheng and Storz, 2000). However, interestingly the sigma factor, σ^E, is implicated in the regulation of gene expression of a number of genes involved in the stress responses, and has been shown to regulate expression of several

antioxidant genes, including some of those regulated by OxyR and SoxRS (Storz and Imlay, 1999).

OxyR homologues have been characterised in a number of bacteria (Storz and Imlay, 1999), yet a functional homologue has not been found in *M. tuberculosis* (Deretic et al., 1997). It has been shown that all the members of the *M. tuberculosis* complex contain multiple deletions and termination codons in the *oxyR* pseudogene. There is also no homologue in *M. tuberculosis* of *soxR*, suggesting *M. tuberculosis* may have an alternative mechanism of regulation in response to DNA damaging agents such as ROI/RNI.

M. tuberculosis, like other bacterial pathogens have evolved protective mechanisms against reactive oxygen and nitrogen intermediates (Zahrt and Deretic, 2002), to which they are exposed in their intracellular life style. It has been suggested that the response to ROI is of particular importance, which involves catalase-peroxidase (*KatG*) and catalytic subunit of alkyl hydroperoxide reductase (*ahpC*). KatG is involved in peroxide stress response and in many bacteria, is generally positively regulated by OxyR (Zahrt *et al.*, 2001), however *M. tuberculosis* lacks a functional *oxyR* (Deretic *et al.*, 1995; Deretic *et al.*, 1997). It was discovered that regulation of *katG* in *M. tuberculosis* takes place via FurR, a negative regulator, which forms part of the KatG locus (Zahrt *et al.*, 2001). KatG and AphC are implicated in the sensitivity of *M. tuberculosis* to isoniazid, particularly as *M. leprae* lacks a functional *katG*, but retains functional *aphC* and *oxyR* genes, and is insensitive to isoniazid (Eiglmeier *et al.*, 1997). Oxidative stress response genes often exhibit coupled expression with genes involved in iron metabolism, such as *sodA* and *sodB*; metalloproteins, which encode superoxide dismutase (Niederhoffer *et al.*, 1990). It has been suggested that Fur negatively regulates *sodA* via Fe^{2+}

dependent repression, whereas Fur positively regulates *sodB* in an indirectly manner (Niederhoffer *et al.*, 1990).

1.4.2.2 DNA damage repair in organisms other than *E. coli*

Many basic genetic mechanisms for replication, repair and recombination are conserved between bacterial species. However there appears to be many differences between species in the mechanistic properties, biological functions and molecular components involved in these processes (Kline *et al.*, 2003). One mechanism that appears to be relatively conserved is the SOS response.

1.4.2.3 SOS response

The term SOS response was first coined by Mirolsav Radman in the 1970's (Radman, 1975), and this response has been extensively studied in Gram-negative bacteria, with *E. coli* being the main focus (Courcelle *et al.*, 2001). Current literature indicates that at least 40 genes have been defined as co-ordinately expressed in the *E. coli* LexA regulon (Courcelle *et al.*, 2001; Fernandez De Henestrosa *et al.*, 2000).

The *recA* gene is part of the *E. coli* SOS regulon, which has been shown to be under the control of LexA (Little, 1982), a transcriptional repressor, which binds to a specific region termed the SOS box located in the promoter of SOS response genes (Bertrand-Burggraf *et al.*, 1987; Fernandez De Henestrosa *et al.*, 2000). Some of the genes in the SOS regulon are still expressed to significant levels in the uninduced state, where LexA is bound as a repressor molecule to the SOS box. This is particularly notable with *recA*, which appears to be basally

expressed under uninduced conditions (Friedberg, 1995). This basal level of RecA is possibly required for detection and response to DNA damage, as the SOS response is a dual component system: RecA is an activator (Fernandez De Henestrosa *et al.*, 2000), which recognises single-stranded DNA, often created by blockage of replication forks following DNA-damage (Courcelle et al., 2001). RecA binds to the single-stranded regions and becomes activated, which causes the autocatalytic cleavage of LexA (Sassanfar and Roberts, 1990), in the presence of a nucleoside triphosphate (Friedberg, 1995). The cleaved LexA is no longer able to bind effectively to the SOS box to suppress expression of genes in the SOS regulon (Bertrand-Burggraf et al., 1987), resulting in de-repression of these genes and therefore increased expression. Some proteins have been identified that are DNA-damage inducible, but are independent of the LexA/RecA system (Courcelle et al., 2001).

1.4.2.4 SOS response in *M. tuberculosis*

Although a classical SOS system has been identified in *M. tuberculosis*, where a number of genes have been shown to be DNA-damage inducible independently of LexA and RecA, including *recA* itself. *recA* has two promoters; P2 possesses a defined palindromic LexA binding site, which is regulated by the LexA/RecA system, but the other promoter, P1, does not possess a LexA binding site, and remains DNA-damage inducible in both a *recA* mutant as well as in wild-type H37Rv (Laboratory strain of *M. tuberculosis*) (Davis et al., 2002b).

M. tuberculosis recA contains an intein (Davis et al., 1991), which is removed from the precursor protein while the mature protein is re-ligated concomitantly. The intein is not thought to play a role in regulation of *recA* (Frischkorn *et al.*, 1998; Papavinasasundaram *et al.*, 1998).

Interestingly, a knockout of *recA* in *M. bovis* BCG shows little attenuation in mouse model (Sander *et al.*, 2003).

1.4.2.5 Absence of the SOS response in other pathogenic microorganisms

RecA is thought to be essential for transformation, where integration of foreign DNA is required (Koomey and Falkow, 1987) with RecA and RecX being involved in both recombinational repair pathways, via RecBCD and RecF (Koomey and Falkow, 1987; Stohl and Seifert, 2001). However, the part that *recA* plays in recombinational repair may explain the necessity of the gene in transformation and therefore genetic diversity (Kline et al., 2003). This is thought to be of importance to the human pathogen *Neisseria* (*Neisseria meningitides* and *Neisseria gonorrhoea*) as gene transfer occurs frequently, via transformation of DNA. The transformed DNA was initially thought to be made available by cell lysis, but recent studies show that *Neisseria* is able to secrete DNA via a type IV secretion system, encoded on a genetic island. The ability of *Neisseria* to take up and integrate DNA is especially interesting as it is missing homologues to a substantial number of key SOS response genes; alkylation repair, recombinational repair, replication repair, as well as a few genes involved in; methyl-dependent mismatch repair and base excision repair (Kline et al., 2003).

Neisseria resides solely in the human body; the nasopharynx, blood stream, or the genital tract. Therefore, it has been suggested that *Neisseria* is not subjected to extreme environmental conditions, UV radiation or desiccation (Kline et al., 2003). On that basis, it has been predicted that *Neisseria* has developed a DNA-damage repair system specialised to the type of DNA-damage that would occur in its niche (Kline et al., 2003). Notably, genome comparisons between *N. meningitides*, *N. gonorrhoea* and *E. coli* have shown the absence of both a *lexA*

homologue, and LexA binding sites/SOS boxes, upstream of the promoters of known *E. coli* LexA regulated SOS response genes. It has therefore been suggested that *Neisseria* does not possess the classical SOS response (Black et al., 1998), but may have an alternative damage inducible repair system other than the classical SOS response (Kline et al., 2003).

1.5 Regulation of bacterial gene expression

Bacterial gene regulation takes place at a number of different levels, but it has been suggested that particularly in eubacteria, regulation of transcription initiation is the most significant control point (Hughes and Mathee, 1998), owing to the rapid turnover of transcripts. However regulation also occurs at other levels, including transcriptional termination (Henkin, 1996), as well as post-translational processing (Paget *et al.*, 1999).

1.5.1 Transcription

The transcription process comprises of three stages, initiation, elongation and termination (Borukhov and Nudler, 2003). During transcription the RNAP covers approximately a 35bp region of DNA, 12-15bp of this region are unwound, thus forming the transcription bubble. Inside the melted region the template forms a constant heteroduplex with the 3′ region of the transcript, covering approximately 8-9bp (Toulme *et al.*, 1999). Site-specific repressor proteins and chromosomal proteins can block transcription elongation, and RNA polymerase has the ability to oscillate back or forward at each template position, stabilising the complex before re-initiating the elongation process. Nevertheless, the DNA template sequence can cause lateral oscillation of the ternary complex, which can result in the slowing down of elongation of RNA, or can result in a pause, or even cessation of transcription (Toulme *et al.*, 1999).

1.5.2 Transcriptional activators/repressors

A common mechanism of gene regulation involves proteins, which act as transcriptional activators or repressors to initiate or suppress gene expression respectively. A repressor binds to the operator, which often overlaps the promoter, and in these instances this inhibits the interaction of the promoter with RNA polymerase, preventing it forming an open complex (Gralla, 1996; Lodish H, 1995). Activator proteins come in two distinct forms: those that bind upstream of, but close to promoters and interact with either the carboxy-terminal domain of the α-subunit of RNA polymerase, or with the σ factor (Gomez M, 2000) to activate or enhance transcription (Lodish H, 1995) and those that act as distant enhancers (Gralla, 1996). Although distant enhancers are rare, in *E. coli*, they are associated with a holoenzyme containing an alternative sigma factor known as σ^{54} (Gralla, 1996).

Master regulatory proteins work as part of the cell cycle machinery to organise and co-ordinate multiple proteins, required to function co-ordinately in order to execute a particular function (McAdams and Shapiro, 2003). Examples of master regulatory proteins are the general stress response proteins in *E. coli* (Hengge-Aronis, 1999). The presence of these master regulatory proteins, directing modular or co-ordinate functions, may simplify the control signals in communication pathways, and may also facilitate the short and long term abilities of an organism to adapt to changes in environmental conditions (McAdams and Shapiro, 2003).

SoxR and OxyR are examples of transcriptional activators, which enhance transcription (Volkert and Landini, 2001), whereas LexA is a repressor protein, which binds to the operator to repress transcription (Bertrand-Burggraf *et al.*, 1987). Many genes and operons are subject to dual regulation, by repressors and activators, as seen with *uspA* in *E. coli* (Kvint *et al.*, 2000).

1.5.3 Architectural proteins

H-NS is a histone like nucleoid structuring protein and pleiotropic/global regulator. It works by adapting cellular responses to external signals, such as osmotic stress, oxidative stress, cold shock, motility and acid tolerance (Hansen et al., 2005) and binds DNA with a preference for bent DNA of AT rich sequence (Dole *et al.*, 2004). The binding of H-NS to DNA forms an oligomeric structure, which prevents binding of the RNA polymerase, or traps it at the promoter (Dole *et al.*, 2004). The way in which the activity of the H-NS is regulated is unknown, but *hns* is autoregulated, whereby H-NS acts to repress transcription from its own promoter. However, the DNA binding protein FIS activates transcription of *hns* (Dole *et al.*, 2004). The *bgl* operon in *E. coli* is an example of regulation partially controlled by H-NS and is also responsible for regulating the sigma factor RhoS, which is expressed during early stationary phase. This sigma factor is responsible for regulating gene expression in early stationary phase in response to nutrient starvation/ limitation and decreased pH (Hansen et al., 2005).

1.5.4 Multi-factorial concordant regulation

The expression of certain genes can include more than one regulatory mechanism, as shown in the *bgl* promoter in *E. coli.* Expression from the bgl promoter is controlled by an activator protein, known as CAP (catabolite gene activator), whose binding site is located upstream of the promoter. However, under normal physiological conditions, the gene is repressed by the presence of silencing elements flanking the promoter (Schnetz and Wang, 1996). DNA topology, in conjunction with cellular factors such as H-NS is important for the expression from the *bgl* promoter. Reporter assays were performed with a wild-type *bgl* promoter, a *bgl* promoter with enhanced CAP binding, and a *bgl* promoter containing a deletion in the upstream

silencing element. These assays showed that crude cell extract in the absence of CAP represses transcription, where as negative supercoiling overcomes this repression and enables transcription in the presence of the CAP-cAMP complex (Schnetz and Wang, 1996). It has been suggested that H-NS, DNA topology and other cellular factors are involved in the formation of a nucleoprotein structure in the region of the gene silencer, which renders the promoter inactive, until it is activated by the presence of CAP (Schnetz and Wang, 1996), therefore the regulation of the *bgl* protein is multi-factorial.

Temporal control of gene expression can also be achieved by alarmone guanosine 3', 5'-bisphosphate (ppGpp), which can negatively affect transcription of *rrn* operon in *E. coli*, but can positively affect transcription of a large number of σ^{70} regulated genes. ppGpp affects the induction of these genes in response to environmental stress (Nystrom, 2004b). When bacteria enter into nutrient limitation, the levels of ppGpp increase, and this enhances transcription of genes regulated in response to stress by alternative sigma factors. The hypothesis is that there is a transcriptional trade off between stress defence and growth and proliferation.

1.5.5 Negative feedback regulation

Different types of physiological and environmental stresses cause different types of damage to a cell, and therefore require different mechanisms to repair the damage. Molecular chaperones (DnaK, GroE, DnaJ and GrpE) and ATP dependent proteases (ClpAP, ClpXP and Lon) are responsible for disposing of potentially toxic protein aggregates, which are formed by damaged or misfolded proteins. These malformed proteins can be formed under normal conditions, but aggregate in response to stress, such as heat shock or pathophysiological stresses (Bucca *et al.*, 2003). The tight regulation of the response to this type of stress is vital, and unravelling the

genetic response to these physiological stresses, may potentially lead to the uncovering of a similar mechanism for the regulation of response to environmental stresses, such as DNA-damage.

The regulation of heat shock gene expression in *Streptomyces* is of particular interest, as like *M. tuberculosis*, *Streptomyces coelicolor* (*S. coelicolor*) is a highly GC rich member of the actinomyces family of gram positive bacteria, and unlike in *E. coli*, the expression of heat shock genes in *Streptomyces* is controlled by negative regulation (Bucca *et al.*, 2003).

The *dnaK* operon in *S. coelicolor* is negatively autoregulated by the binding of a repressor molecule to a specific inverted repeat sequence in the operator (Bucca *et al.*, 2003). It has been suggested that DnaK binds HspR (co-expressed with DnaK), to form a complex, which interacts with the specific inverted repeat sequences, to repress transcription of the *dnaK* regulon (which includes the *dnaK* operon, *clpB* and *lon*). Under normal growth conditions, DnaK depletion experiments showed high level transcription of the *dnaK* operon (Bucca *et al.*, 2003). This method of autoregulation, termed the HspR repressor/operator system is found in other actinomyces species, including *M. tuberculosis* (Stewart *et al.*, 2001).

1.5.6 Bacterial promoters

The promoter of a particular gene is generally defined by two regions, the –10 and –35 sites, which are 5' non-coding regions upstream of the transcriptional start site and which have sequence-specific affinity to RNA polymerase holoenzyme (Hughes and Mathee, 1998). Some promoters also include an element UP, which lies upstream of the –35 site (Gralla, 1996); these

are generally AT-rich elements and interact with the RNA polymerase (Hughes and Mathee, 1998), to enhance transcription.

1.5.6.1 Control of bacterial promoters

There are a number of different mechanisms that have been described for modulating bacterial promoters; DNA topology, activator or repressor molecules (outlined in 1.5.1 and 1.5.1.1), enhancers, UP elements. These regulators control both the temporal and spatial expression of a given promoter.

Temporal control of bacterial promoters is vital for regulation of expression of a given gene at a particular time. Temporal control is important for the maintenance and viability of an organism, particularly with regard to cell cycle, as improper timing of cell-cycle genes has proved to have fatal consequences (McAdams and Shapiro, 2003).

In *Caulobacter*, *ctrA*, encodes a protein CtrA, which is responsible for binding and silencing the chromosomal origin of replication in *Caulobacter*. Like *M. tuberculosis recA*, the gene has two promoters, P1 and P2; however, unlike *recA*, the mechanisms of regulation of expression from both promoters have been elucidated. The P1 promoter can only be activated when it is hemimethylated (the intrinsic state of newly replicated DNA). The P2 promoter is autoactivated, as a result of elevated CtrA levels produced from the P1 promoter. This autoactivation takes place when a threshold level of phosphorylated CtrA is reached (McAdams and Shapiro, 2003).

1.5.7 RNA polymerase and formation of an active holoenzyme

The core RNA polymerase is comprised of 5 subunits, $\beta\beta'\alpha_2\omega$ (for a review see (Borukhov and Severinov, 2002). Core RNA polymerase is unable to initiate transcription from promoters (Borukhov and Severinov, 2002), but when it combines with a sigma (σ) factor, an active holoenzyme is formed, able to initiate transcription of the sigma factor's regulon. The sigma factor forms the promoter recognition site, with region 2 of the sigma factor interacting with the –10 region of the promoter, and region 4 of the sigma factor interacting with the –35 site of the promoter (Gralla, 1996), thus giving the RNA polymerase its specificity (for a review see (Severinov, 2000). Shortly after the initiation of transcription, within about the first 10 nucleotides, the σ subunit is discharged from the RNA polymerase (RNAP), and transcription continues with the core RNA polymerase (Haldenwang, 1995; Travers and Burgess R.R, 1969).

1.5.7.1 Core RNA polymerase subunits

The core RNA polymerase has a molecular mass of approximately 400kDa (Darst, 2001). The α, β and β' subunits are the larger subunits, whereas ω is the smallest subunit (Darst, 2001). The α subunits are comprised of two functional domains, a C-terminal domain, and an N-terminal domain (Finn *et al.*, 2000). The C-terminal region of the α subunits, present as a dimer, forms the site of interaction between UP elements and RNAP and with upstream transcriptional activators and the RNAP (Busby and Ebright, 1994). The α subunits form a platform, which binds to the β and β' subunits, which are involved in transcriptional activation (Zhang and Darst, 1998). The β and β' subunits form the catalytic centre of the RNAP (Finn *et al.*, 2000) they form a trough for 12bp of duplex DNA, downstream of the ternary elongation complex

(Darst, 2001). The role of the ω subunit is unclear, although it is thought to have an effect on core formation, and interacts solely with the β′ subunit (Naryshkin *et al.*, 2000).

There are differences in *E. coli* and *B. subtilis* between the structure and function of the different subunits, which comprise to form the RNAP. In *B. subtilis*, there is a delta (δ) subunit, which reduces non-specific initiation of the RNAP when complexed with the housekeeping sigma factor σ^A. However in *E. coli* this reduction of non-specific initiation is thought to be carried out by σ^{70}, along with the usual role of a sigma factor as promoter recognition site (Haldenwang, 1995). There are also differences in antibiotic targeting for the different RNAP's but there do not seem to be any major differences between the core enzymes (Haldenwang, 1995).

1.5.7.2 Sigma factor domains

Sigma factors are comprised of 4 regions. Region 1 of σ^{70} prevents the sigma factor binding directly to the promoter in the absence of the RNAP-σ complex (Lonetto *et al.*, 1994). Region 1 can be subdivided into two sections region 1.1, which solely affects DNA binding by σ^{70} and is found only in primary sigma factors (Baldwin and Dombroski, 2001), and region 1.2, which affects promoter binding, open complex formation, along with initiation and the transition to elongation (Baldwin and Dombroski, 2001) and unlike region 1.1, is also present in alternative sigma factors. Region 2 and 4 are the most highly conserved regions (Lonetto *et al.*, 1994); region 2 is further subdivided into 2.1, 2.2, 2.3 and 2.4, although recent publications also annotate region 2.5 (renamed from region 3) (Checroun *et al.*, 2004). Region 2.4 and 4.2 recognise the –10 and –35 promoter elements respectively (Daniels *et al.*, 1990; Siegele *et al.*, 1989), whereas region 2.5 (3) recognises the extended –10 motif (Checroun *et al.*, 2004).

Regions 2.1, 2.2 and 3.2 are thought to be involved in core binding (Sharp *et al.*, 1999). ECF sigma factors appear to have lost most of region 3 (3.1 and 3.2), in comparison to primary sigma factors (Lonetto *et al.*, 1994). As mentioned, region 4 is required for recognition and binding to the –35 sites, particularly 4.2 region.

1.5.8 The role of sigma factors

There are two main types of sigma factor: primary sigma factors, also known as housekeeping sigma factors, and alternative sigma factors.

When complexed with core RNA polymerase, primary sigma factors such as σ^{70} in *E. coli*, or σ^{A} in *M. tuberculosis* are responsible for transcription of house keeping genes (Hu and Coates, 1999; Missiakas and Raina, 1998), such as essential biosynthetic pathways including amino acid biosynthesis (Hughes and Mathee, 1998).

Alternative sigma factors, recognise different –10 and –35 promoter sequences compared to primary sigma factors (Hughes and Mathee, 1998). Extra cytoplasmic family (ECF) sigma factors belong to a sub-family of the sigma 70 (σ^{70}) class of sigma factors, which are highly conserved through many Gram-positive and Gram-negative species (Helmann, 2002), including *Mycobacteria*, *B. subtilis*, *Sulpholobus acidocaldarius*, *S. coelicolor* and *Pseudomonas aeruginoas* (Helmann, 2001; Missiakas and Raina, 1998).

Sequencing of the *M. tuberculosis* genome (Cole *et al.*, 1998), revealed that *M. tuberculosis* has 13 putative sigma factors, each belonging to the σ^{70} class of sigma factors. The principle sigma factor is σ^{A} (Fernandes *et al.*, 1999), whereas σ^{B} and σ^{F} belong to the sporulation/stress response

family of sigma factors and the remaining 10 sigma factors are ECF family (Manganelli *et al.*, 2001).

Sigma factors compete to bind with core RNAP and initiate transcription of their regulon suggesting the levels of competing sigma factors provide an additional layer to the regulation of transcription at different stages during growth (Nystrom, 2004a).

1.5.9 Regulation of alternative Sigma factors

Extra cytoplasmic family (ECF) σ factors are thought to be key regulatory molecules in the bacterial adaptive response to the host (Graham and Clark-Curtiss, 1999). They provide a response mechanism to various environmental stresses (Song *et al.*, 2003), by co-ordinating transcription of their specific regulons (Missiakas and Raina, 1998), which are otherwise physically unlinked genes (Song *et al.*, 2003). Sigma factors are themselves regulated in order to control temporal gene expression of the sigma factors regulon in response to particular stimuli. There are a number of different modes of regulation for specific sigma factors, usually involving different types of both transcriptional and post-translational regulation:

1.5.9.1 Transcriptional and post-translational regulation of sigma factors by proteolysis

Some sigma factors are both transcriptionally and post-translationally regulated, i.e. they are transcribed as a pro-protein, which contains an amino acid extension at the amino terminus. This extension enables the pro-protein to bind to the cytoplasmic membrane where it remains inactive. The pro-protein is then converted into an active sigma factor by developmentally

triggered proteolysis, which removes the membrane bound pro sequence from the sigma factor pro-protein (Ju and Haldenwang, 2003). This type of regulation has been observed in *B. subtilis*, where the sigma factor SigE is transcribed as a pro-protein. SigE is a sporulation specific sigma factor, which responds to nutrient deprivation known to initiate spore formation (Haldenwang, 1995), as part of a signal transduction cascade. SigE is co-transcribed with a protease SpoIIGA, which is also membrane bound, and remains inactive until septum formation, when SpoIIR is synthesised in the forespore, which in turn activates the protease SpoIIGA. SpoIIGA then causes proteolytic cleavage of the pro-protein, to release the active sigma factor SigE (Ju and Haldenwang, 2003). The transcription of the SigE operon is controlled by an activator protein, Spo0A, which binds to the promoter of *spoIIG* to initiate transcription (Haldenwang, 1995). It has been shown in *M. tuberculosis*, that SigH is required for transcription of the SigE operon, however, RNAP-σ^A complex not RNAP-σ^H complex was responsible for transcription from spoIIG promoter, suggesting SigH has an indirect effect on the expression of SigE (Raman et al., 2001).

The post-translational modification of SigE into its active form, requires products from *ftsZ*, *divIC*, *spoIIGA*, *spoIIAA*, *spoIIAC*, *spoIIE* and *spoIIA* (SigF). However the roles of many of the proteins have not been defined, with the data indicating SigF and SpoIIE affect the processing of pro-SigE indirectly (Haldenwang, 1995). This example highlights the complexity and multi-level regulation involved in control of bacterial gene expression.

This process is not limited to *B. subtilis*, as interestingly, an ECF sigma factor BldN in *S. coelicolor* is regulated at both the transcriptional and post-transcriptional level. On the one hand, its transcription is repressed by BldD, whereas BldN is synthesised as a pro-protein, with an 86 residue N-terminal extension, which is cleaved by proteolysis (Bibb and Buttner, 2003).

1.5.9.2 Two component regulators of sigma factors

The sigma factor σ^{54} is involved in a two-component signal transduction cascade to initiate flagella production, in *Campylobacter jejuni* (Hendrixson and DiRita, 2003). The flagella transcription cascade in *Helicobacter pylori*, *Vibero cholerae* and *Pseudomonas aeruginosa* requires two sigma factors, σ^{54} and σ^{28}. FlgR is part of a two component regulatory system, which acts as a transcriptional activator for the σ^{54} regulon, after phosphorylation by FlgS. FlgS is a sensor kinase, which may be able to detect the correct conditions to initiate transcription of the σ^{54} regulon (Hendrixson and DiRita, 2003). It has been suggested that FlgS detects proper formation of the flagella secretory apparatus in the cytoplasm, before initiating σ^{54} dependent expression of the flagella genes. The other sigma factor σ^{28} is regulated via the anti-sigma factor FlgM, which binds to σ^{28}, preventing transcription of σ^{28} regulon (Hendrixson and DiRita, 2003).

In *S. coelicolor*, σ^{E} is regulated by a two-component system and σ^{E} forms an operon with CseA, CseB and CseC, where CseB is a response regulator and CseC is a sensor kinase (Hong *et al.*, 2002) and CseA is a negative regulator of *sigE* expression (Hutchings *et al.*, 2004).

1.5.9.3 Post-translational regulation by anti-sigma factors and anti-anti sigma factors

Sigma factors can be post-translationally regulated by environmental stimuli interacting directly with an anti-sigma factor or via an anti-anti-sigma factor, to regulate a particular sigma factors activity (Hughes and Mathee, 1998). The ECF family of sigma factors are usually negatively regulated by their cognate anti-sigma factors (Raivio and Silhavy, 2001), some of which are membrane bound, which often exhibit transcriptionally coupled expression, with their

sigma factors. Studies in *B. subtilis* have shown that anti-sigma factors are negatively regulated by a co-expressed protein termed an anti-anti-sigma factor (Hughes and Mathee, 1998). Also, many ECF sigma factors are positively auto-regulated; they drive transcription from their own promoters (Helmann, 1999). This is observed in *M. tuberculosis*, where transcription of the ECF sigma factor, SigH is initiated from an auto-regulated promoter, as a result of oxidative and heat stress (Song *et al.*, 2003).

Anti-sigma factors are regulated by a number of different stimuli, depending on the type of sigma factor they regulate. Non-ECF anti-sigma factors such as AsiA in *E. coli*, FlgM in *S. typhimurium*, SpoIIAB in *B. subtilis*, are cytoplasmic proteins. Some ECF family of anti-sigma factors are inner membrane proteins, with at least one transmembrane domain (Hughes and Mathee, 1998), which bind sigma factors as part of a signalling cascade (Hughes and Mathee, 1998). Therefore anti-sigma factors function to negatively regulate their cognate sigma factors, by binding reversibly to the sigma factor (Duncan and Losick, 1993; Song *et al.*, 2003). Studies using the *M. tuberculosis* sigma factor SigH and its cognate anti-sigma factor RshA, have elucidated the importance of conserved cysteine residues in the binding of anti-sigma factors to their cognate sigma factors (Song *et al.*, 2003).

SigF in *B. subtilis* is regulated by the anti-sigma factor SpoIIAB (Haldenwang, 1995; Ju and Haldenwang, 2003) and the anti anti-sigma factor SpoIIAA. These have homology to the SigB anti-sigma factor RsbW and the anti anti-sigma factor RsbV respectively (Haldenwang, 1995).

One of the best characterised ECF σ factor mediated stress responses is that of SigE in *E. coli* (Hughes and Mathee, 1998; Raivio and Silhavy, 2001) and forms an example of the interaction between a sigma factor (SigE) and its cognate anti-sigma factor RseA. RseA is situated in the

cytoplasmic membrane, with predicted periplasmic and cytoplasmic domains. Under uninduced conditions, the cytoplasmic domain of RseA binds to SigE, preventing it from binding to core RNA polymerase. Under environmental stimulation, a protease cascade is initiated which results in the proteolysis RseA. DegS and RseP respond to stress signals generated in the envelope, and alongside ClpX, degrade RseA by proteolysis (Alba *et al.*, 2002, Grigorova *et al.*, 2004), which results in the release of SigE and initiation if sigE dependent transcription. RseB is a sensor, which binds to the periplasmic domain of RseA, and DseG, which detects cellular changes in the form of overexpressed outer membrane porins induced by environmental stresses.

1.5.9.4 The role of anti anti-sigma factors

The mode of action of anti anti-sigma factors varies, and has been shown to range from enzymatic modification of the anti-sigma factor, such as phosphorylation (Helmann, 1999), to export of the anti-sigma factor out of the cell (Hughes and Mathee, 1998), to interactions with extracytoplasmic or small proteins (Helmann, 1999). The anti anti-sigma factor regulating SigF in *M. tuberculosis*, is regulated by redox (Beaucher *et al.*, 2002).

The importance of phosphorylation as a method of regulating sigma factors is outlined in the case of the *B. subtilis* sigma factor, SigB. SigB is co-transcribed with and controlled by its cognate anti-sigma factor (RsbW) and anti anti-sigma factor (RsbV). The interaction between RsbW and RsbV is regulated by phosphorylation. In this case, RsbW is only able to bind unmodified RsbV, which suggests that either RsbW is phosphorylating RsbV to prevent the formation of a RsbV-RsbW complex, or the phosphorylation of RsbV is a consequence of the ability of RsbW to change its specificity for either SigB or RsbV (Haldenwang, 1995).

However under certain stresses, an additional co-factor is required, RsbU. It is not clear however which regulatory protein receives the signal to initiate binding of RsbW to RsbV (Haldenwang 1995).

In *E. coli*, the heat shock response elicits expression of over 40 genes, including *dnaK*, *dnaJ*, *grpE*, *clpB*, *lon* and *clp* operon, under the control of σ^{32}, an alternative sigma factor (Bucca *et al.*, 2003), so called due to its molecular weight.

1.5.10 The importance and mode of detecting environmental signals

SigH, an alternative sigma factor in *M. tuberculosis* is involved in heat and oxidative stress responses (Fernandes *et al.*, 1999; Raman *et al.*, 2001). Its cognate anti-sigma factor, RshA, is part of the SigH operon and inhibits SigH-dependent transcription. The action of the anti-sigma factor RshA is redox dependent, such that it only negatively regulates SigH under reducing conditions. The interaction of SigH and RshA is also disrupted by elevated temperature suggesting the involvement of SigH in response to heat shock, suggesting RshA reacts to both oxidative stress and heat shock (Song *et al.*, 2003). SigH is a particularly interesting sigma factor, as it induces expression of two mycobacterial stress response ECF sigma factors, *sigE* and *sigB* (Hu and Coates, 1999; Manganelli *et al.*, 2001; Raman *et al.*, 2001; Wu *et al.*, 2004). The *rshA* gene is located downstream of *sigH*, and a motif is situated between the coding regions of *sigH* and *rshA*, which is also present downstream of the *M. tuberculosis* sigma factors, *sigE* and *sigL* (Song *et al.*, 2003).

Redox sensing is important for bacteria other than *M. tuberculosis*, which are subject to oxidative or disulphide stresses. This is observed in *S. coelicolor*, whereby SigR-RsrA is

equivalent to the SigH-RshA system in M. tuberculosis. SigR, a redox dependent sigma factor, which is regulated via its redox dependent cognate anti-sigma factor RsrA encoded by *rsrA* (Kang *et al.*, 1999). It has been observed that certain cysteine residues are required for the function of the anti-sigma factor RsrA (Kang *et al.*, 1999; Paget *et al.*, 2001). Interestingly the *S. coelicolor rsrA* shares homology to *rshA*, an anti-sigma factor from *M. tuberculosis*, also thought to be involved in redox sensing (Kang *et al.*, 1999; Paget *et al.*, 1998; Paget *et al.*, 2001). Interestingly RT-PCR has shown that *sigH* is co-transcribed with *rshA* (Song *et al.*, 2003) and both SigR from *S. coelicolor* and SigH from *M. tuberculosis* are subject to autoregulation from one transcriptional start site (Paget *et al.*, 1998; Raman *et al.*, 2001).

1.6 The use of microarrays for global gene expression profiling

It appears that regulation of gene expression is a multi-factorial process; therefore it is conceivable that microarray technology and other high through-put experimental methods may provide a starting point to unravel regulation of gene expression, or a particular regulon. However, it is important to realise that gene expression analysis does not provide information regarding the effects of post-transcriptional mechanisms, which may affect the half life of mRNA, translation initiation, progression, or other modifications, at the structural or chemical level, which may result in differential protein expression (McAdams and Shapiro, 2003).

Microarray technology provides the means to assess genes expression of an entire genome in response to a particular type of stress, or under certain growth conditions. The use of DNA versus RNA arrays also provides the potential to perform inter- and intra- strain comparisons of global gene expression under the desired conditions.

Potentially, it would be a metabolic disadvantage to express DNA-damage repair genes when they are not required. However, there needs to be a tight controlling mechanism, which enables the rapid response of the required DNA-damage repair genes. Therefore it is possible that one or more master regulatory proteins govern the transcriptional regulation of DNA-damage repair genes in *M. tuberculosis*.

1.7 Aims

The overall aim of this project is to investigate the alternative mechanisms of regulation of DNA-damage repair genes in *M. tuberculosis*. Two different hypotheses are investigated:

a) That regulation is controlled by an alternative sigma factor. The expression of the sigma factor SigG has been demonstrated to be induced following DNA-damage. Therefore, any role of SigG in expression of DNA-damage inducible genes is assessed by construction and analysis of a *sigG* mutant strain of *M. tuberculosis*, including a detailed analysis of expression of *ruvC* in comparison to *recA*.

b) That induction is determined by an activator or repressor protein. The P1 promoter of *recA* is known to be DNA-damage inducible independently of RecA/LexA, so any proteins interacting with this region are sought using bandshift assays. In addition, the role of the damage induced regulatory protein Rv2017 is investigated following construction of a gene inactivation mutant of *M. tuberculosis*.

2 Materials and Methods:

2.1 *E. coli* bacterial strains:

E. coli bacterial strains used in cloning and expression are listed below:

DH5α subcloning/library efficiency (Invitrogen): F'ϕ80d*lacZ*ΔM15 Δ(*lacZYA-argF*) U169 *deo*R *recA*1 *end*A1 *hsd*R17(rK-, mk+) *pho*A *sup*E44 *λ-thi-1 gyr*A9 *6rel*A1

XL1 Blue Supercompetent cells (Stratagene): *recA*1 *end*A1 *gyr*A96 *thi-Z hsd*R1 *7sup*E44 *rel*A1 *lac*[F'*proABlac*aZΔM15 *Tn10(Tet^R)*]

XL10 Gold Ultra competent cells (Stratagene): Tet^R Δ (mcrA)183 Δ(mcrCB-hsdSMR-mrr)173 endA1 supE44 thi-1 recA1 gyrA96 relA1 lac Hte [F' proAB lacIqZΔM15 Tn10 (Tet^R) Amy Cam^R]^a

One-shot chemically competent cells (Invitrogen): F- mcrA Δ(mrr-hsdRMS-mcrBC) ϕ80lacZM15 ΔlacX74 recA1 ara139 Δ(ara-leu)7697 galU galK rpsL (Str^R) endA1 nupG

2.2 *M. tuberculosis* bacterial strains:

H37Rv:	Laboratory strain
Δ*recA*	*recA* knockout strain of *M. tuberculosis*
Δ*sigG*:	*sigG* knockout strain of *M. tuberculosis*
Δ*sigG* full operon comp 8T:	Complement of ΔSigG containing entire operon
Δ*sigG* partial comp Δ1:	Complement of ΔSigG containing *sigG* only
ΔRv2017:	Rv2017 knockout strain of *M. tuberculosis*

2.3 Bacterial Media:

M. tuberculosis was grown in Modified Dubos medium (Difco, see appendix I) containing 10% albumin (v/v) for liquid culture, and *E. coli* was grown in L-Broth supplemented with the

appropriate antibiotics (see table 2.1). For solid culture, *M. tuberculosis* and *E. coli* were grown on 7H11 or L-Agar respectively containing the appropriate supplements (see table 2.1):

Table 2.1: Media supplements

Media supplements	Concentration in *E. coli* µg/ml	Concentration in *M. tuberculosis* µg/ml
Kanamycin	50	25
Hygromycin	250	50
Ampicillin	100	n/a
X-gal	100	100

2.4 Plasmids

Table 2.2: Plasmid descriptions

Vector	Description	Source of reference
Vectors for *M. tuberculosis* knockout and complementation		
pUC-Hyg	Hyg^R cassette	(Mahenthiralingam *et al.*, 1998)
pGoal17	*aph* (Km^R), *sacB/lacZ* cassette	(Parish and Stoker, 2000)
pBackbone	Skeleton plasmid + Km^R	(Gopaul, 2002)
pGarthdee2	pBackbone (Km^R) + 5' and 3' *sigG*	(Gopaul, 2002)
pLD1	pGarthdee 2 (Km^R) + Hyg^R + *sacB/lacZ*	This study
pKP186	pMV306 (Km^R) (Stover *et al.*, 1991), no integrase	Papavinasasundaram
pBSINT	contains integrase, Km^R	(Springer *et al.*, 2001)
pLD1comp8T	pKp186 (Km^R) including full *sigG* operon	This study
pLD1 compD1	pKp186 (Km^R) including only *sigG*	This study
pLD2	Pbackbone (Km^R) + 5' and 3' Rv2017	This study
pLD3	pLD2 (Km^R) + Hyg^R + *sacB/lacZ*	This study
Vectors for Primer extension and RNase protection		
pBluescript SK-	Amp^R	Stratagene
pLDseq1	pBluescript Amp^R + 639bp *sigG* inc 512bp upstream	This study
pLDseq2	pBluescript Amp^R + 322bp *ruvC*, inc 242bp upstream	This study
pCR4-Blunt	Amp^R , Km^R	Invitrogen
pLDRNAse1	pCR4-Blunt Amp^R , Km^R + 339bp *sigG*, inc 151bp upstream	This study
pLDRNAse2	pCR4-Blunt Amp^R , Km^R + 322bp *ruvC*, inc 242bp upstream	This study
pLDRNAse3	pCR4-Blunt Amp^R , Km^R + 358bp *recA*, inc 271bp upstream	This study

2.5 DNA preparation

2.5.1 Purification of Plasmid DNA: S.N.A.P. Miniprep Kit (Invitrogen)

This Miniprep kit is designed to purify up to 20μg of high copy number plasmid DNA from cultures of *E. coli.* Silica-gel membranes are used to adsorb plasmid DNA from bacterial lysates. The protocol incorporates a modified alkaline lysis method of the bacteria, the lysate is then neutralized and adjusted to high salt concentrations, which enables the selective adsorption of plasmid DNA to the Silica-gel membrane in the Miniprep columns. RNA, bacterial DNA, proteins and metabolites flow through the silica gel membrane and are therefore discarded. A wash step ensures that endonucleases are removed from the preparation. DNA extraction was performed in accordance with the manufacturer's guidelines.

2.5.2 Purification of plasmid DNA: QIAprep Spin Miniprep Kit Protocol (Qiagen)

This high speed Miniprep kit is designed to purify up to 20μg of high copy number plasmid DNA from cultures of *E. coli.* The manufacturer's QIAprep Spin Miniprep Kit Protocol was followed for the preparation of Plasmid DNA.

2.5.3 Large scale plasmid extraction: HiSpeed Plasmid purification Kit (QIAgen)

This Midiprep kit is designed to purify up to 200μg of high/low copy number plasmid DNA from cultures of *E. coli.* DNA extraction was performed in accordance with the manufacturer's guidelines.

2.6 Nucleic acid preparations from *M. tuberculosis*

2.6.1 DNA extractions

A single *M. tuberculosis* colony was streaked onto either quarter, half or whole plate (7H11) and incubated at 37°C for 3 to 4 weeks. The quarter or half plate (7H11 plates) of *M. tuberculosis* colonies were harvested using a sterile loop, and incubated at 80-90°C for 1 hour in TE. Then a final concentration of 2mg/ml of lysozyme and lipase, and 5µl RNase (DNase free RNase, Boehringer) was added and incubated at 37°C for 2 hrs. Samples were then frozen using dry ice and ethanol, then incubated at 75°C for 10 mins. Samples were cooled to room temperature, then 500µg/ml proteinase K was added, along with 0.5% SDS and 2µl RNase, and were incubated at 50°C for 1hr. DNA was purified with two extractions using an equal volume of phenol:chloroform:isoamyl alcohol, followed by one extraction with an equal volume of chloroform. DNA was then precipitated by the addition of 1/50th volume of 5M NaCl, and 2 volumes of 100% ethanol.

2.6.2 RNA extraction: FastRNA Pro Blue Kit (BIO 101 systems)

RNA was extracted from 100-200ml cultures of an appropriate strain of *M. tuberculosis* in accordance with the manufacturer's guidelines. Cultures were harvested at room temperature for 15 minutes and 10,000rpm. Pellets were resuspended in 1ml RNApro solution (provided in the kit) per 25mls of culture, and transferred to Lysing Matrix B (1ml per tube of Martix B). Samples were then ribolysed at speed 6 for 40 seconds and then centrifuged at 13,000rpm for 10 minutes, after which the supernatent was transferred to 300µl chloroform and vortexed. Samples were centrifuges at 13,000rpm, 4°C for 15 minutes, then the top phase was transferred to 500µl 100% EtOH and ethanol precipitated overnight at -20°C, and after washing in 70%

EtOH, samples were resuspended in 50µl DEPC dH_2O. DNA was then removed from the sample by addition of 20 units RNase-free DNase (Roche), 20 units RNase inhibitor (Invitrogen), 5.7mM $MgSO_4$ and 0.1M NaOAc (final concentration), and the samples were incubated at 37°C for 1 hour. After 1hr, additional DNase and RNase inhibitor were added as outlined above and incubated for an additional hour at 37°C. Samples were purified using RNeasy Minikit (QIAgen), and RNA was analysed by agarose gel electrophoresis and quantitated using a spectrophotometer.

2.7 Preparation of DNA for Cloning

2.7.1 Polymerase Chain Reaction (PCR):

Reactions were carried out in a final volume of 50μl, containing 2 units of *Pfu* turbo DNA Polymerase, 10-250ng template DNA/a single bacterial or yeast colony (Colony PCR), 0.2mM each dATP, dCTP, dGTP and dTTP, 20 pmol each primer, 1X Pfu reaction buffer (Stratagene). Samples were run in a Hybaid Omn-E or Omnigene Thermal Cycler, with an initial step of 95°C for 5 min, followed by 30-35 cycles at 94°C for 30 sec, annealing temp (Tm –5) for 30 sec, 68°C for 1 min per kb. The annealing temperatures were differed depending on the predicted Tm for the specific primers. All programmes were run with the Hybaid Thermal Cycler lid heated to 110°C to prevent evaporation of the samples. PCR products were purified and either restriction digested for cloning 2.7.6. Alternatively they were cloned directly into pCR4-Blunt in accordance with the manufacturers protocol (Invitrogen).

2.7.2 Touch-down PCR:

PCR reactions were set up as outlined in 2.7.1. Samples were run in a Hybaid Omn-E or Omnigene Thermal Cycler with an initial step of 95°C for 5 min, followed by 10 cycles of 94°C for 30 sec, annealing temperature (Tm + 10°C) for 30 sec, 68°C for 1 min per kb with step wise decrease of the annealing temperature (1°C per cycle). The final 25 cycles were carried out at the specific Tm.

2.7.3 Ligation and cloning of PCR products

PCR products were either gel extracted as outlined in section 2.7.5, or were purified using QIAquick PCR purification Kit (Qiagen), to remove unincorporated nucleotides and enzymes from the reaction. Purified PCR products were incubated at 37°C for 1 hour with 1X T4 polynucleotide kinase buffer (70mM Tris-HCl pH 7.6, 10mM $MgCl_2$, 5mM dithiothreitol with 1mM ATP) final concentration and 10 units T4 polynucleotide kinase (New England Biolabs), the polynucleotide kinase was then heat inactivated at 65°C for 10 min. Kinase reaction enables the transfer and exchange of a phosphate group form the ATP to the 5′ hydroxyl terminus of the PCR product, which enables downstream ligation of the insert into the vector of choice, outlined in section.

2.7.4 Agarose Gel Electrophoresis

A solution of agarose powder, 0.8-4% (w/v) was prepared by heating to boiling point with electrophoresis buffer, 1x TBE (40mM Tris-borate pH8.3, 1M EDTA) or 1X TAE (40mM Tris-acetate pH8.3, 20mM sodium acetate, 1mM EDTA), and 0.3μg/ml ethidium bromide was

added. Samples were prepared by adding 1/5th loading buffer (30% (v/v) Glycerol, 0.25% (w/v) Bromophenol blue, 0.25% (w/v) Xylene cyanol FF) and were loaded along with either 1kb-DNA-ladder, λEcoHind, λHind or 100bp ladder marker (Life-Technologies) used to size DNA fragments. A Consort E833 electrophoresis power supply was used to run the agarose gel immersed in 1X TBE or 1X TAE, at 45 to 90 Volts. The DNA in the gel was visualized on 2UV transilluminator at 302nm and photographed with a UPV BioDoc It System.

2.7.5 Extraction of DNA from Agarose gel

Extraction of DNA fragments was achieved using one of two methods: Microcon columns (Micon), were used with the specific NCO (nucleotide cut off) depending on the size of the required fragment. These columns were also used for concentrating samples and removal of unincorporated nucleotides/primers following PCR. Alternatively QIAquick Gel extraction kit (Qiagen) was used to extract 70bp to 10kb fragments of DNA from certified molecular biology agarose (Bio-Rad) in either TAE or TBE buffer. Each method was performed in accordance with the relevant manufacturers' protocol.

2.7.6 Digestion of DNA with Restriction Endonucleases

One unit of restriction endonuclease (RE) is required to cleave 1μg λDNA in 1hour at 37°C. A final concentration of 10 units of RE (Boehringer Mannheim, or New England Biolabs) per μg DNA was incubated with the manufacturer's recommended buffer at the appropriate temperature (usually 37 °C) for 2 hours-overnight.

2.7.7 Dephosphorylation of linearised plasmids

Plasmids were linearised using restriction digestion (as outlined in section 2.6.5), then dephosphorylated by the addition of 6 units of calf alkaline phosphatase (Roche) per 500ng linearized plasmid DNA, samples were incubated at either 37°C for 1 hour, or 50°C for 45 mins. This prevents re-ligation of the plasmid, by removal of the terminal phosphate group. Samples were then extracted with phenol chloroform and ethanol precipitated (as outlined in sections 2.7.8 and 2.7.9).

2.7.8 Ethanol Precipitation of Nucleic Acids

DNA was precipitated and purified from solution by incubation at -20°C for 15 min-o/n, following the addition of 2.5 volumes absolute ethanol (EtOH) with 0.1 volumes 3M NaOAc pH 6.0. RNA was precipitated and purified at -80°C over night following the addition of 2 volumes absolute EtOH with 0.1 volumes 3M NaOAc pH 4.8. Samples were then centrifuged at 13000 rpm for 15 min at 4°C. The pellet was washed with 70% EtOH (made with DEPC treated water (Sigma) for the RNA), and centrifuged at 13,000 rpm for 5 min, at 4°C. The pellet was air dried and resuspended in TE (10mM Tris, 1mM EDTA), dH_2O (for DNA) or DEPC treated water (for RNA).

2.7.9 Phenol-Chloroform extraction of DNA

Phenol chloroform extraction was used to remove protein contaminants from nucleic acid preparations. A solution of 50% phenol, 48% chloroform and 2% isoamylalcohol was used to purify nucleic acids prior to ethanol precipitation. 1 volume of phenol-chloroform was added to the DNA preparation, and centrifuged at 13,000 rpm for 5 min. The top layer containing

aqueous DNA was removed and added to an equal volume of chloroform (24:1, Chloroform:Isoamylalcohol), and centrifuged at 13,000 rpm for 5 min. The top layer was then removed and the DNA was precipitated with ethanol (see section 2.7.8). Alternatively, Phase lock tubes (Eppendorf) were used to separate the phenol-chloroform purification of the sample in accordance with the manufacturer's protocol, after which, a chloroform extraction and EtOH precipitations were performed as previously described.

2.7.10 Ligation of DNA

Ligations were carried out with either blunt-ended or sticky-ended linear DNA produced as a result of restriction digest with the required restriction enzyme(s) (Outlined in section 2.7.5). The inserts were cloned into dephosphorylated linearized vectors in a ratio of either 1:1, 1:2 or 1:4, (vector: insert respectively) depending on the construct. Ligation reactions were carried out using Rapid DNA ligation Kit (Boehringer) in accordance with the manufacturers protocol and were transformed immediately into chemically competent cells as outlined in section 2.7.11.

2.7.11 Transformation of chemically competent *E. coli*

2.7.11.1 DH5α Subcloning efficiency/Library efficiency (Invitrogen)

Transformations were carried out with 10-100ng of plasmid DNA (derived for section 2.5.1) in accordance with the manufacturers' protocol.

2.7.11.2 One-shot chemically competent cells

Transformations were carried out with 10-100ng of plasmid DNA, containing a PCR product cloned directly into pCR4-Blunt. The transformations were carried out in accordance with the manufacturer's protocol

2.7.12 Automated DNA Sequencing: ABI Prism BigDye Terminator Cycle Sequencing Ready Reaction protocol:

After cloning, constructs were checked for accuracy by restriction digest and sequencing. Automated sequencing reactions were carried out in accordance with the manufacturer's protocol. The unincorporated fluorescently labelled ddNTP's were removed using EtOH precipitation, or Dye X kits (QIAgen) in accordance with the manufacturers protocol. The resultant samples were then analysed using an ABI Prism 377 DNA sequencer, in a denaturing polyacrylamide sequencing gel, and analyzed with the recommended software, Sequence Analysis 3.4.

2.7.13 Site directed Mutagenesis (SDM): QuickChange Site directed mutagenesis Kit (Stratagene)

SDM is a rapid in vitro method of producing site-specific mutations in a gene of interest, using *Pfu* DNA polymerase. Primers were designed for the mutagenesis reaction and the experiment was performed using the *sigG* operon in pKP186 as a template, in accordance with the manufacturer's protocol. The plasmid was then *DpnI* digested and transformed into either XL1 Blue supercompetent cells or XLI0 Gold Cells in accordance with the manufacturers protocol.

2.8 Protein analysis

2.8.1 Synthesis of antibodies

Protein sequences were downloaded form the TubercuList website for SigG (RV0182c), Rv0181c and Rv0180c, and potential antigenic peptides were designed and synthesised by

trained technicians at Sigma-Genosys. The three best candidates were then used to raise antibodies in two rabbits per peptide (Sigma-Genosys).

2.8.2 SDS page gel electrophoresis

15% non-denaturing polyacrylamide SDS-PAGE gels were used for protein visualization as outlined in (Sambrook *et al.*, 1989), or Nu-Page Bis-tris gels (Invitrogen) were used in accordance with the manufacturers protocol, using the XCell sure lock Mini-cell gel system (Invitrogen). In brief, samples were heated to 90°C for 2 mins in NuPAGE buffer (Invitrogen) and reducing agent was added (50mM dithiothreitol), then samples were electrophoresed using Nu-Page Bis-tris gels (Invitrogen), with NuPAGE running buffer (Invitrogen). Gels were run at 200volts for 45 mins-1hour and visuaised using Coomassie (Sambrook *et al.*, 1989).

2.8.3 Dot blot

Dot blots were performed using 0.1, 0.3 and 0.6μg of peptide, alongside 10μg *M. tuberculosis* CFE, *E. coli* CFE and SigG inclusion body preparation. Sample volumes were made up to 2μl using phosphate buffered saline (PSB), then 2μl 2X SDS sample buffer (0.15M Tris (pH 6.8), 1.2% SDS, 30% v/v glycerol, 15% β-mercaptoethanol, 1.8μg/ml bromophenol blue) was added. The samples were spotted onto nitrocellulose membrane, and allowed to dry for 30 mins before a western blocking antibody binding and wash steps were performed at outlined in (Sambrook *et al.*, 1989). Dot blots were visualised using Supersignal West Pico chemiluminescence in accordance with the manufacturers protocol (Pierce).

2.8.4 Western Blot

Western blots were performed using the XCell sure lock Mini-cell gel system (Invitrogen), with the XCell II module for transfer of the Western blot (Invitrogen). Briefly, samples were prepared in SDS-loading buffer, heated to 90°C for 5 mins and electrophoresed at 200 volts for 40 mins to 1hour, as outlined in section 2.8.2. The PVDF membrane (Invitrogen) was soaked in methanol, followed by reducing NuPAGE Transfer Buffer (with 10% methanol). The transfer was performed in the XCell II module at 30V for 1 hour. The PVDF membrane was then washed in dH_2O, before being blocked overnight in 5% milk, 0.1% Tween-20 in PBS, with gentle agitation. The primary antibody was added at either 1/500 (anti-Rv0181c and Rv0180c) or 1/250 (anti-SigG), and incubated for 1hour with gentle agitation. Four wash steps were performed with 0.1% tween in PBS, followed by the addition of the secondary antibody into blocking solution (described above) all with gentle agitation. Horse Radish Peroxidae (HRP) goat-anti-rabbit antibodies (BD Biosciences) were used as the secondary antibody, at a 1/5000 dilution. The PVDF membrane was then washed a total of 5 times in 0.1% tween-20 in PBS and visualised using Supersignal West Pico chemiluminescence in accordance with the manufacturers protocol (Pierce).

2.9 Transcriptional analysis

2.9.1 cDNA synthesis

For cDNA synthesis random primers (7.5μg) were annealed to 1μg RNA in a reaction volume of 10μl. Samples were incubated at 65°C for 10 min, and then cooled to room temperature. To the reaction, 1X reaction buffer (Roche), 1μg Acetylated BSA, 0.2mM dNTP's (with DEPC treated dH_2O), 125mM DTT and 1μl RNase inhibitor was added. To the RT+ reaction (with

RNA), 1.5µl Superscript was added. To the negative control RT- reaction (with RNA), 1.5µl of DEPC dH_2O was added. Samples were then incubated at 37°C for 1 hour and the Superscript was heat inactivated at 70°C for 15 mins.

2.9.2 RT-PCR

RT-PCR was used to determine if genes were co-transcribed or to check for expression. RT-PCR reactions were performed using the cDNA (see section 2.8.1). 2µl of RT + or - reactions, were added to 0.2mM dNTPs, 300nM forward primer, 300nM reverse primer, 1X *Pfu* turbo buffer (Stratagene), 2.5µl DMSO, 2.5units *pfu* turbo. Samples were run in a Hybaid Omn-E or Omnigene Thermal Cycler, with an initial step of 94°C for 3 min, followed by 35 cycles at 94°C for 45 sec, 58°C for 45 sec, 72°C for 2 min, and finally 72°C for 7 mins. The programme was run with the Hybaid Thermal Cycler lid heated to 110°C to prevent evaporation of the samples.

2.9.3 Taqman real-time PCR

Taqman is a real-time quantitative PCR method, which enables quantitation of both DNA and cDNA to determine a quantitative analysis of gene expression. The method involves a DNA probe labelled with a fluorophore (FAM) and a quencher (TAMRA), as previously outlined in (Brooks *et al.*, 2001). The labelled probe binds to the amplification product. During each PCR cycle, extension from the primer, causes the 5'end of the probe to be displaced and degraded, which separates the fluorophore and the quencher, resulting in fluorescence of the fluorophore, which is in turn detected by the TaqMan machine (ABI7700). Primers and probe were designed using Primer Express as outlined in the manufacturer's protocol, and experiments were performed using the Taqman Universal PCR Master Mix (PE Applied Biosystems). 1µg RNA

was reverse transcribed into cDNA as outlined in section 2.9.1. This was then diluted 1/10 or 1/20 and used in the Taqman reactions with the probe and relevant primer pairs. Both the *sigA* and test probes were used on the same samples of RNA in order to quantify the test PCR product. For each of the test probes an optimization was carried out using a standard 5μM probe along with differing concentrations of each primer (see table 2.3). All reactions were carried out in 96 well plates alongside DNA standards of known concentration ranging from 1ng to 8pg, for each of the probes (*sigA* and test probe).

Table 2.3: Optimization primer concentrations

Reaction:	Concentration of forward and reverse primer (nM)	Reaction:	Concentration of forward and reverse primer (nM)
A	50F/50R	F	300F/900R
B	50F/300R	G	900F/50R
C	50F/900R	H	900F/300R
D	300F/50R	I	900F/900R
E	300F/300R	-	-

2.9.4 End-labelling of oligonucleotides

End-labelling of oligonucleotides was carried out in a final volume of 10μl, using 10pmol specific primer/oligonucleotide, in a 1X T4 polynucleotide kinase (PNK) buffer (Promega), with 10 units of T4 PNK (Promega), and 30μCi [γ-32P]ATP. Reactions were incubated at 37°C for 10 mins, and heated at 90°C for 2 mins to heat inactivate the T4 PNK. 9μl were removed, and added to 41μl nuclease free water, then applied to a G25 Sephadex spin column (Life Tech), to remove any unincorporated [γ-^{32}P]ATP. The volume was adjusted to give a final concentration of the end-labelled primer of 180fmol/μl.

2.9.5 Primer extension reactions

Primers used in primer extension (PE) reactions were end-labelled (as outlined in section 2.9.4). 40-100μg total RNA was EtOH precipitated o/n at -80°C, and resuspended in 5μl DEPC treated dH_2O. In brief, RNA was precipitated overnight as outlined in section 2.7.8, and was resuspended in 5μl DEPC dH_2O. Annealing reactions were performed in a final volume of 11μl, with 5μl RNA, 1X avian myeloblastosis virus (AMV) reverse transcriptase buffer and 180fmol of end-labelled primer and were incubated at 58°C for 30 mins (or Tm-5°C). Samples were left for 1hour to cool to room temperature, and the extension reactions was performed with 1X AMV buffer (Promega), 2.8mM Sodium Pyrophosphate and 1 unit of AMV reverse transcriptase to make a total volume of 20μl, then incubated at 42°C for 30-40mins. Samples were EtOH precipitated over night, and resuspended in Formamide loading dye (Promega). Primer extension reactions were carried out in accordance with the manufacturer's protocol (Promega). PE reactions were run on an 8% denaturing polyacrylamide gel, alongside manual sequencing reactions (outlined in section 2.9.6), and visualized using autoradiography.

2.9.6 Manual Sequencing: T7 Sequenase V2.0 (Amersham LS)

5μg of template DNA was denatured with 0.1 volumes (2M NaOH, 2mM EDTA) at 37°C for 30 min. The reaction was neutralized by adding 0.1 volumes 3M NaOAc (pH 4.8), and EtOH precipitated. Samples were resuspended in 7μl dH_2O. Sequencing reactions were carried out in accordance with the manufacturer's protocol, and run on an 8% denaturing polyacrylamide gel, alongside primer extension reactions (see section 2.9.5).

2.9.7 RNase protection

2.9.7.1 *In-vitro* transcription of the radio-labelled probe

In-vitro transcription reactions were performed using the MAXIscript in-vitro transcription kit (Ambion), with either T3 or T7 polymerase in accordance with the manufacturers protocol. The templates were linearized using either *NotI* (for *ruvC* and *recA*), or *SpeI* (for *sigG*) restriction digests. These were then purified using a PCR clean up column (Qiagen) in accordance with the manufacturers protocol. 2.5μg of template was used in a 20μl in-vitro transcriptional reaction, with 1X transcription buffer, 0.5mM ATP, CTP and GTP, and either 0.25, 0.5, 1 or 5mM UTP, 10mCi/ml [α-32P] UTP, and either 30 units T7 polymerase or 60 units T3 polymerase. Reactions were incubated for 1 hour at 37°C (or 15°C), 2μl yeast RNA was added as a carrier, then DNase treated with 2 units DNase I, incubated at 37°C for 15-30mins, to stop the reaction, 1μl 0.5M EDTA was added. Reactions were purified using NucAway columns (Ambion) in accordance with the manufacturers protocol. In the initial test probe synthesis reactions, 0.25mM, 0.5mM, 1mM and 5mM un-labelled UTP was added to the *in-vitro* transcription reaction. For subsequent probe synthesis reactions 1mM non-labelled UTP was used. The test templates were synthesised using the same protocol except the radio-labelled [α-^{32}P] UTP was omitted. 1μl probe was visualised using autoradiography (denaturing polyacrylamide gel), and then quantified using a scintillation counter and used directly in the RNase protection assays at $5x10^4$ CPM. The century marker (Ambion) was *in-vitro* transcribed in accordance with the manufacturer's guidelines.

2.9.7.2 RNase protection assay

RNase protection assays were performed to identify transcriptional start site, and to approximate the level of transcription from each promoter. 20-50μg RNA were used in the

RNase protection assays with $5X10^4$ CPM of purified probe, negative control (no RNA) and positive control (test templates) were performed alongside. The RNA/controls were co-precipitated with the probe, as outlined in the manufacturers guide lines, then resuspended in 10μl hybridization buffer (Ambion), and incubated at 95°C for 4 mins, followed by an overnight incubation at 42°C in a hybaid oven to ensure even distribution of heat. Yeast RNA was added to all samples as a carrier and digestions were initially tested with a range of RNase A/T1 mix, 1:50, 1:100 and 1:500, alongside RNase T1 alone at 1:50, 1:100 and 1:500. For subsequent reactions, 1:100 ratio of the RNase A/T1 mix was used in all reactions except the negative control (probe only). Digestions were performed at 37°C for 30 mins, then reactions were stopped using the RNase inactivation/precipitation buffer (Ambion). A further 2μl Yeast carrier RNA was added prior to precipitation at -20°C for 15 mins. After precipitation, samples were eluted in 4μl gel loading buffer II (Ambion), the heated for 3 mins at 95°C and loaded onto the 5% denaturing polyacrylamide gel, alongside marker (produced by *in-vitro* transcription), then visualised by autoradiography or using a phosphorimager.

2.9.8 Denaturing polyacrylamide gel electrophoresis

Denaturing polyacrylamide gels 8% (w/v) were used to visualize manual sequencing and primer extension reaction, and 5% for RNase protection assays. The 8% polyacrylamide gel was made using Long Ranger in accordance with the manufacturer's protocol (FMC – Long Ranger Gel Solution). The gel was cast between 2 glass plates, one of which was silicon coated, which were separated by plastic spacers, with both edges and the bottom sealed with gel sealing tape (Life Technologies). A comb was inserted into the top of the gel to enable loading of the samples. The gel was then run in 1X TBE in a vertical tank (Life Technologies, Gibco BR1, SA model) at 5 Volts per cm^2, with a Consort Flowgen E734 power supply. The gel was then

transferred to a 3MM Whatman filter paper and dried using a Savent Slab Gel Dryer SDG4050. Gels were then visualised by autoradiography.

2.10 Detection of DNA-Protein binding

2.10.1 Extraction of Cell Free Extract (CFE) from *M. tuberculosis*

CFE is extracted from *M. tuberculosis* to be used in gel retardation assays to look for proteins binding to specific regions of DNA. CFE were obtained as outlined in figure 2.1, in brief, cultures were grown the modified Dubos (Difco) containing 10% albumin, to an OD_{600} of 0.4. these were then pooled and split. One was induced by the addition of 0.2μg/ml mitomycin C, and both were incubated for a further 24hours at 37°C. Samples were then harvest at 10,000rpm for 30mins and 4°C. Pellets were resuspended in Z-buffer (appendix I) containing pefabloc protease inhibitor (Roche) and pelleted as described. The wash step was repeated three times. Samples were added to 2ml tubes containing 0.5-1mg glass beads and ribolysed at speed 6.5 for 30 sec, these were then placed on ice for 2 mins, then the ribolysing step was repeated. The samples were then applied to Ultrafree-MC 0.22μM spin columns (Millipore) in accordance with the manufacturer's protocol to remove cell debris. Quantitation was achieved using BCA protein assay kit (Pierce) in accordance with the manufacturer's guidelines.

Figure 2.1

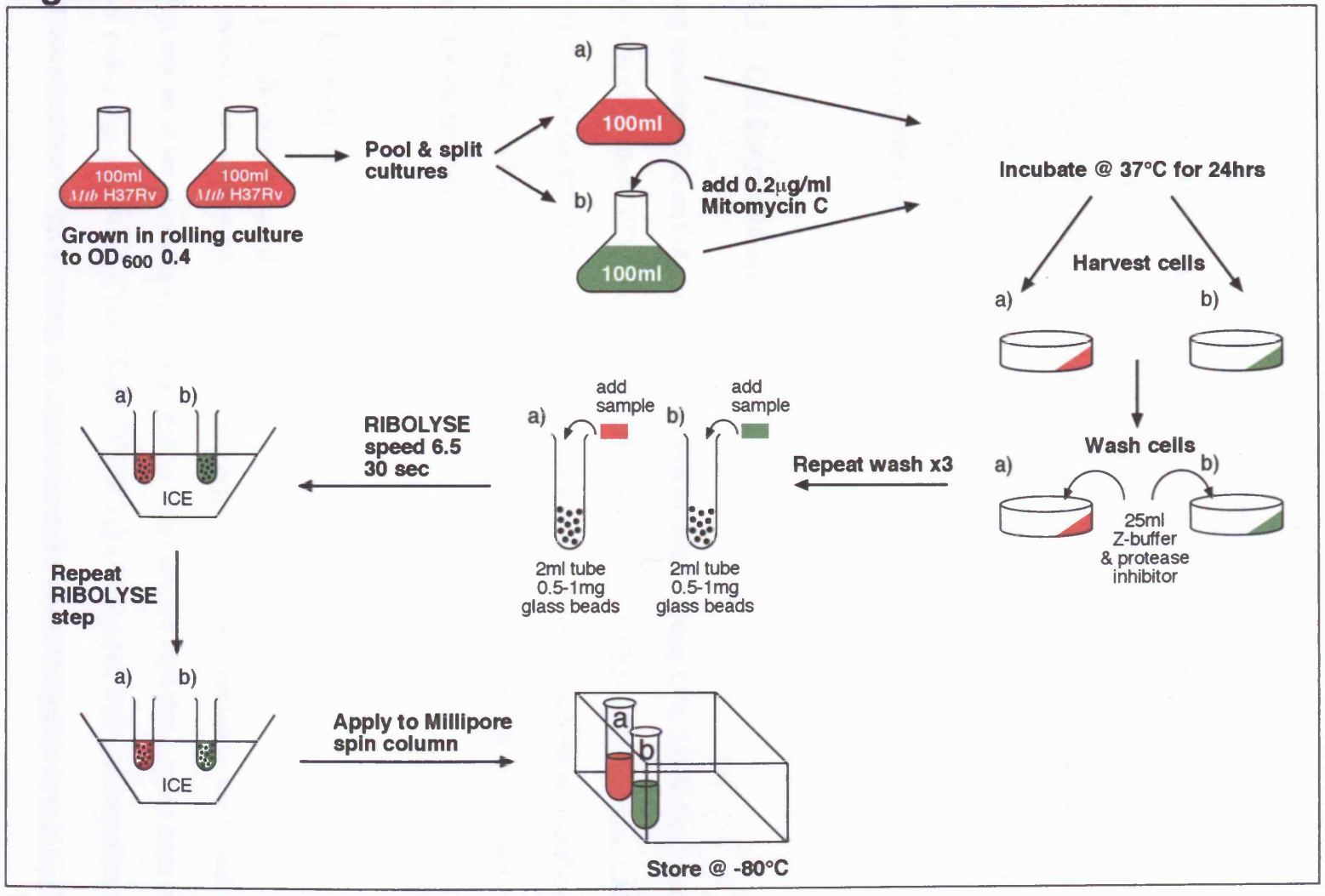

Figure 2.1: Cell free extract protocol in *M.tuberculosis*

2.10.2 Preparation of probes for gel retardation assay

100pmol of single-stranded oligonucleotides were mixed in a 1:1 ratio, with TEN buffer (10mM Tris-HCl, 1mM EDTA, 0.1M NaCl pH8.0), and incubated in a beaker of water at 95°C for 10 mins, then allowed to cool to room temperature in the water. 25μM annealed oligonucleotides were incubated with 1X DNA polymerase buffer (Promega), 5mM [dTTP, dATP, dGTP], 1.1Mbq [α-32P] dCTP, 2 units of Klenow (Promega) for 15 mins at 37°C. The reaction was stopped by the addition of 250mM EDTA, and the reaction was diluted 1:2 with dH_2O. Unincorporated label was removed using G25 spin columns (Pharmacia) in accordance with the manufacturer's guidelines.

2.10.3 Gel Retardation

Binding reactions were carried out at room temperature with 20-30μg CFE, 5X binding buffer (20mM HEPES, 120mM KCl, 0.8mM DTT, 20% glycerol, 0.4μg/μl BSA), 1μg l-lysine, 1.5μg poly d(I-C), 4μM [α-32P]dCTP labelled annealed oligos. The binding reactions were analysed using a Hoefer Se400 Vertical slab electrophoresis unit, with an 8% non-denaturing polyacrylamide gel, containing 1% glycerol.

2.11 Constructing a knockout in *M. tuberculosis*

2.11.1 Cloning into pBackbone

PCR primers were designed to amplify approximately 2kb regions containing the 5′ and 3′ flanking regions of the gene of interest. The primers were designed such that a region from the internal coding region of the gene was deleted. These regions of interest were then sequentially cloned into pBackbone (Gopaul, 2002). A 1.6kb hygromycin resistance cassette from pUC-Hy

(Mahenthiralingam *et al.*, 1998) was then inserted between the 5′ and 3′ regions of the gene. Then a 6.3kb *sacBlacZ* cassette from pGoal17 (Parish and Stoker, 2000) was ligated into the *PacI* site in pBackbone, to enable screening and counter-selection in *M. tuberculosis*. *sacB* encodes levansucrase, which confers sucrose sensitivity and *lacZ* encodes β-galactosidase, which enables blue-white screening with 7H11 plates containing 1.6mg X-Gal (a lactose analogous substrate 5-bromo-4-chloro-3-indoyl-β-D-galactopyranoside which, when cleaved by β-galactosidase produces a blue product). The construct was then electroporated into competent *M. tuberculosis* to select and screen for a mutant strain (see sections 2.11.2 and 2.11.3).

2.11.2 Competent cells and electroporation of *M. tuberculosis*

Cultures were grown to an OD of 1.0 (as outlined in section 2.12.1) and then 0.1 volumes 2M glycine were added and cultures were incubated in the rolling incubator for 24 hours at 37°C. Cells were harvested by centrifugation at 10,000rpm for 30 mins, at room temperature. The pellet was washed 3 times in 1 volume 10% glycerol (filter sterile), then resuspended in 10ml 10% glycerol. 400μl competent cells were electroporated, with 2-5μg plasmid DNA at 25μF, 1000Ω (Bio-Rad gene pulser). Cells were then incubated overnight in static culture at 37°C, then harvested by centrifugation, resuspended in 100μl supernatant, then plated onto 7H11 plus relevant antibiotic. These were incubated at 37°C for 3-4wks. Knockout constructs were selected on 7H11 with 50μg/ml hygromycin and X-Gal.

2.11.3 Selection of a knockout

Initial electroporations were plated onto 7H11 + Hyg +X-Gal for 3/4 weeks. Blue colonies were potential single crossovers, and white colonies were potential double crossovers. The

white colonies were replica plated onto 7H11 + Kan and 7H11 + Hyg. A double crossover would be Hyg^R, but Km^S, indicating the loss of the plasmid. Blue colonies were plated onto 7H11 + Hyg for 3/4weeks, to allow the second cross-over to take place. Colonies were then serially diluted and plated onto 7H11 +Hyg + X-Gal + 2% sucrose, to select for loss of the plasmid. Only colonies that have lost the plasmid should be able to grow on sucrose, and remain white. White colonies were then replica plated on 7H11 + Km and 7H11 + Hyg +X-Gal. Km^S, Hyg^R colonies which remained white were then grown on 7H11 + Hyg for DNA extraction and analysis by PCR and/or Southern blot.

2.11.3.1 Probe Labelling for Southern analysis

50ng of probe DNA was labelled with [α-32P] dCTP using the Ready-to-go DNA labelling beads (Amersham-Pharmacia) following the manufacturer's protocol. Unincorporated [α-32P] dCTP was then removed using Sephadex G-50 Nick Columns (Pharmacia) in accordance with the manufacturer's protocol.

2.11.3.2 Southern Blot

A Southern blot, developed by (Southern, 1975), is a method of transferring restriction digested DNA onto a membrane, then visualizing it by hybridization with a radio-labelled probe. Restriction digested genomic DNA was subjected to electrophoresis in a 1% w/v TBE agarose gel, with EthBr, as outlined in section 2.6.3 at 20 volts overnight. The gel was visualized using an ultraviolet transilluminator at 302nm and photographed with a ruler marker. The gel was then treated with 0.25M HCl for 15 min, then placed in denaturation solution (1.5M NaCl, 0.5M NaOH) for 30 min, then transferred to neutralisation solution (0.5M Tris-HCl pH7.2, 1.5M

NaCl, 1mM EDTA) for 30 min. The blot was then constructed with a wick (Whatman 3MM filter paper) placed in a glass dish containing 20X SSC (3M NaCl, 0.6M trisodium citrate pH7), the gel was placed on top of a filter paper the same size as the gel, on top of the wick. The membrane Hybond N+ (Amersham) was placed on top of the gel, then another three filter papers of the correct size were placed on top of the Hybond N + membrane. All the air bubbles were removed, then Saran Wrap was placed around the sides of the membrane filter sandwich to prevent drying out and 10mm of paper towels were placed on the filter papers. These were then covered with a glass plate and weighted down with two 500ml bottles. The transfer was then left to take place overnight. The wells were marked, and the membrane was then washed in 2XSSC, and crosslinked using optimal crosslink programme, on a SpectrolinkerXL-1500UV crosslinker (Spectronics Corporation). The membrane was then wrapped in gauze and placed in a hybridization bottle with pre-hybridization solution B (5X SSC, 5X Denhardt's solution, 2% (w/v) SDS) and 0.2mg denatured Salmon Sperm DNA and incubated at 65°C overnight. The α-^{32}P labelled denatured probe was then added, and incubated at 65°C overnight. The membrane was then washed twice in wash buffer 1b (2X SSC, 1.0% SDS) at room temperature for 30min, then in wash buffer 2b(1X SSC, 0.1% SDS) at 65°C for 30 min, then in wash buffer 3b (0.1X SSC, 0.1% SDS) at 65°C for 30 min. The membrane was then autoradiographed.

2.11.4 *M. tuberculosis* liquid cultures and Ziehl-Nielson stain

Cultures of *M. tuberculosis* were grown in modified Dubos medium (Difco) containing glycerol and 10% Albumin, at 37°C in rolling bottles at 2rpm. A sample of the culture was applied to a glass slide, which was dried for 10-15 mins, before being fixed for a few seconds in a Bunsen burner flame. Slides were then placed in a formalin jar for at least 15mins for fumigation, then

a Ziehl-Nielson stain was performed (as outlined in Sambrook *et al.*, 1987). Slides were then visualised using light microscopy to look for contaminants.

2.12 Phenotypic analysis of *M. tuberculosis* knockouts

2.12.1 Determination of *in vitro* growth

Static 5ml cultures of modified Dubos medium (Difco), were inoculated using a loop from a 7H11 plate. Theses were incubated for two weeks at 37°C. 1ml of the static culture was used to inoculate a 100ml rolling culture, to an OD of 0.005. These were then incubated at 37°C, in a rolling incubator at 2rpm. 1ml aliquots were removed every 24 hours and the optical density was measured. When the optical density reached 0.4, the aliquot was diluted, either 1/5, 1/10 or 1/15 in modified Dubos medium (Difco), before the optical density was taken.

2.12.2 Viability assays *in vitro*

Two 200ml cultures of H37Rv were grown in modified Dubos medium (Difco), in rolling bottles (1000ml bottles, irradiated to 30KGy - Nalgene, Techmate) at 37°C, in a rolling incubator at 2rpm, to an OD of 0.3-0.4, then combined. 100ml aliquot was removed for the sodium nitrite stress, and centrifuged at 10,000g for 30 mins. The pellet was resuspended in an equal volume of modified Dubos medium pH 5.4. From this aliquots of 40mls were transferred into fresh rolling bottles, one was left untreated and a final concentration of 3mM $NaNO_2$ was added to the other. The remaining 300ml culture was split into 40ml aliquots in rolling bottles, one was left untreated, 0.2μg/ml ofloxacin (final concentration) was added to one aliquot, 0.02μg/ml mitomycin C (final concentration) to another aliquot, 10μM Cumene hydroperoxide

(final concentration) to another, and 25mM paraquat (final concentration) to the final aliquot. These were incubated for 24 hrs at 37°C in a rolling incubator at 2rpm. After 24 hours, serial dilutions were set up using 50µl of each culture, added to 450µl of pre-autoclaved DMEM (Dulbecco's modified Eagles media) containing 50% FCS (heat inactivated foetal calf serum) and 2.5-3.5 mm glass beads. 10µl of the 10^{-2} and 10^{-3} dilutions were plated in duplicate onto 1/4 plates of 7H11. Plates were incubated at 37°C for 13-15 days, and colonies were counted.

For some of the stress agents, further experiments were performed using a range of paraquat and mitomycin C (see table 2.4).

Table 2.4: Mitomycin C and paraquat concentrations

Mitomycin C stress	Paraquat stress
untreated	Untreated
0.02 µg/ml	10mM
0.05 µg/ml	20mM
0.1 µg/ml	30mM
0.2 µg/ml	40mM
	50mM

2.12.3 Viability assays *in vivo*

Single colonies of H37Rv, Δ*sigG* and Δ*sigG* full operon complement (8T) were grown in duplicate in 15ml of supplemented 7H9 media (7H9 + glycerol + tween + ADC), standing culture for 14 days, then were sub-cultured into another 10ml of supplemented 7H9 media, and grown to an optical density (OD) of 0.02. These were then passed onto the animal handling

unit, where a trained animal technician injected 200µl of culture intravenously into 8 week old BALB/C female mice. The lungs and spleen were then harvested at day 1, 30, 60, 90 and 120 to determine the colony forming units(CFU), by serial dilution. A total of four mice were harvested per-strain, per time point.

Alternatively, single colonies of H37Rv, Δ*sigG* and cΔ*sigG*, cΔ*sigG*Δ1 and ΔRv2017 were grown in duplicate in 10ml of modified Dubos medium (Difco), and were incubated in static culture for 14 days at 37°C. 1ml of static culture was then used to inoculate 100mls of modified Dubos medium (Difco), which were incubated at 37°C in a rolling incubator at 2rpm, until an OD of 0.3 was reached. These were then pelleted in a centrifuge, and re-suspended in (phosphate buffered saline) PBS, the OD was re-measures, and were diluted to an OD of 0.02 in PBS. These were then passed onto the animal handling unit, where 200µl of culture was injected intravenously into 3 month old BALB/C female mice. The initial inoculum was plated to determine the dose, then lungs and spleen were then harvested at day 1, 30, 60, 90 and 120 to determine the CFU, by serial dilution. A total of four mice were harvested per-strain, per time point.

2.13 Expression analysis by microarray

2.13.1 Poly-L-lysine coating of microarray slides

Prior to printing of microarray slides, they are coated in poly-L-lysine. The slides (Sigma) were placed in a rack, and were cleaned by being stirred for 2 hours in a specialised container, with an alkaline solution (70g NaOH dissolved in 300ml filtered dH_2O, with 400ml absolute EtOH). Slides were vigorously rinsed 6 times in filtered dH_2O, for 1 minute per rinse. The slides were

then transferred to poly-L-lysine solution (70ml poly-L-lysine, 70ml filtered 10X PBS, 560ml filtered dH_2O) and stirred for 1 hour. Slides were rinsed as outlined above, then dried overnight at 37°C. This protocol has been previously described at:

http://cmgm.stanford.edu/pbrown/protocols/1_slides.html. For early experiments I performed the slide coating and processing, for later experiments, pre-coated Corning GAP slides were ordered by the BμG@S bacterial microarray group, before printing.

2.13.2 Post processing

After poly-L-lysine coating, the slides were printed at St. Georges Hospital by the BμG@S bacterial microarray group. The arrays were post-processed by being rehydrated over stream (boiling dH_2O) for 5 sec, followed by snap drying on a hot plate at 100°C for a few seconds. Slides were then cross-linked to fix the DNA at 1mJ. The array slides were then blocked in succinate anhydride/sodium borate solution (5g succinate anhydride (Sigma) was dissolved in 315ml of N-methyl-pyrrilidinone (Sigma), then 35ml of 0.2M Sodium borate pH 8.0 was added) for 15 minutes. The slides were then washed vigorously in a 95°C water bath (filtered dH_2O) for 2 mins, followed by 1 min in 95% EtOH. Slides were then air dried and stored in an air-tight container.

2.13.3 RNA labelling, hybridization and washing

4-5μg RNA was used as template for 1st strand cDNA synthesis using Superscript II (Invitrogen), with fluorescently labelled cy3-dCTP and cy5-dCTP (Amersham Pharmacia Biotech). Random priming was carried with 6μg random primers (Invitrogen), and was incubated at 95°C for 5 mins, then snap cooled on ice. This was then added to a labelling

reaction, carried out with 1X first strand buffer (Invitrogen), 250mM DTT, 11.5mM [dATP, dGTP, dTTP], 4.6mM dCTP, 1.7µl cy3 or cy5 dCTP and 2.5µl Superscript II (Invitrogen). Samples were incubated for 10 mins at 25°C, then at 42°C for 90 mins. Prehybridized slides (in buffer 3.5X SSC, 0.1% SDS, 10mg/ml BSA, for 20 mins at 60°C) were washed in dH_2O for 1 min, then propan-2-ol for 1 min, and were dried. cy3 and cy5 labelling reactions were pooled, and purified using MinElute spin columns (QIAgen), and eluted in 13.5µl DEPC dH_2O. Samples were added to a final concentration of 4X SSC and 0.3% SDS, denatured at 95°C for 2mins, then cooled briefly (1min), before being applied to the microarray slide. A cover slip was place over the sample, and slides were placed in a waterproof hybridization chamber at 65°C over night. Slides were then washed in 1X SSC with 0.05% SDS for 2 mins, at 65°C, then twice in 0.06X SSC for 2 mins. Slides were then scanned using a GenePix Axon 4000A scanner (Axon Instruments), with dual wavelengths set to 600V. Image data was quantified using GenePix Pro 3.0 software, where any bad/unusable spots were removed. The data was then analysed using GeneSpring 4.1.2 (Silicon Genetics).

2.13.4 DNA versus RNA microarray

The protocol is similar to the RNA versus RNA arrays except the RNA samples are competitively hybridised with DNA to the microarray slides. 1µg DNA is labelled with cy3 after annealing of the random primer (as outlined in section 2.13.3), using 8 units Klenow (1X reaction buffer 50mM Tris-HCl (pH7.2 at 25°C), 10mM MgSO4, 0.1mM DTT) and incubated at 37°C for 90 mins in the dark, whereas the RNA is labelled as outline in section 2.13.3 except with only cy5, and the use of superscript III alters the incubation to 5 mins at 25°C, followed by 60 mins at 50°C. Samples are then pooled and purified as outlined in section 2.13.3.

2.13.5 Microarray data analysis

The microarray slides were scanned using a GenePix Axon 4000A scanner (Axon Instruments) and the collated image data was then processed using GenePix Pro 3.0 software, where the control spots, along with any absent or occluded spots were flagged as absent. The results obtained from GenePix were then transferred to the GeneSpring 4.1.2 (Silicon Genetics) analysis software. The data obtained from all the microarray slides was included in a single experiment in Gene Spring, and the input was annotated as follows:

The experimental normalisations used were:

- Data transformations: set measurements less than 0.01 to 0.01
- Per spot: Divide by control channel
    - Change the cut-off value from 10 to 0.01, to include data where genes are expressed at a low level.
- Per chip: Normalise to the 50th percentile
- Use only measured flags: Anything but absent.

The experimental interpretations used were:

- Log of ratio
- Present
    - This is useful if the data is only present in 5 out of the 6 replicates, it only uses the 5 present data values, thus decreasing the background noise.
- The cross gene error model was not active

The experimental parameters used were:

- Array (slide identification number)
- Strain (H37Rv, Δ*sigG* or ΔRv2017)
- Induction (mitomycin C + or -)
- Biological replicate (1, 2 or 3)
- Technical replicate (A or B)

Altering the interpretation using change display parameters enabled the data to be displayed differently. Initially the data was grouped by strain, in which the array was displayed as continuous, the strain and induction were displayed as non-continuous and the biological and technical replicates were not displayed, this was saved as the group by strain. Then the data was displayed with the strain as non-continuous, induction (mitomycin C +/-) as continuous, and the biological (1,2 and 3) and technical replicates (A and B) were not displayed, this was saved as the log sample replicates. This enabled one to observe the difference between the strains, and the induction. Statistical analysis was in Gene Spring, which enables a range of parametric and non-parametric tests to be performed. A parametric test student T-test, assuming equal variance for the H37Rv and Δ*sigG* strains was performed, however for the analysis comparing the ΔRv2017 and H37Rv strains the Welsh approximation to a Student T-test was performed, which does not assume equal variance, due to the difference in spread of the data observed. The significance value used was either $P<0.05$ or $P<0.01$. The data were further scrutinised using the Benjamini and Hockberg False Discovery Rate correction (FDR), $p<0.01$.

3 Analysis of a sigma factor mutant in *M. tuberculosis*

3.1 Introduction

Regulation of bacterial gene expression takes place at a number of different levels. Sigma factors regulate gene expression at the transcriptional level: they are protein subunits that combine with core RNA polymerase to initiate transcription of their particular regulon, by forming specific interactions with specific promoters (Borukhov and Severinov, 2002). Sigma factors can be divided into 2 major groups, the primary sigma factors (house keeping) or the alternative sigma factors (Lonetto *et al.*, 1994). *M. tuberculosis* has 13 σ^{70} class sigma factors (Cole *et al.*, 1998), of which 10 are ECF family (Manganelli *et al.*, 2001). ECF sigma factors are thought to be important in regulation of adaptive responses to environmental stresses by co-ordinating transcription of a stress response regulon (Missiakas and Raina, 1998; Song *et al.*, 2003). An example is *sigH* in *M. tuberculosis*, which is positively autoregulated in response to oxidative and heat stress (Song *et al.*, 2003) and induces the expression of a set of genes, including known heat shock proteins. Of the 13 sigma factors in *M. tuberculosis*, *sigG* was the most highly upregulated sigma factor in response to DNA-damage (Rand *et al.*, 2003), suggesting that it may have a role in regulation of the response to DNA-damage. Therefore, in this study, a strain of *M. tuberculosis* was constructed, in which *sigG* was inactivated. The phenotype of the knockout was then analysed with respect to *in-vitro* growth and susceptibility to DNA damaging agents, along with *in-vivo* analysis of virulence assessed using a mouse model of infection.

3.2 Construction of a *sigG* knockout

A gene inactivation knockout of *sigG* was constructed in the laboratory strain of *M. tuberculosis*, H37Rv. In brief, the knockout was constructed using a non-integrating plasmid containing a deletion in the *sigG* coding region, replaced by an antibiotic resistance cassette: this was electroporated into H37Rv, where homologous recombination resulted in the replacement of the functional chromosomal copy of *sigG* with the inactivated copy present on the plasmid, as outlined in Parish *et al.*, (1999).

A 4368bp fragment containing the coding region of *sigG* was ligated into the Km^R vector pBackbone, which was derived from pBluescript by K. Gopaul (Gopaul, 2003). Inverse PCR was then used to remove a 691bp region from within the 1110bp predicted coding region of *sigG,* whilst also incorporating *Avr*II sites. A previous member of the laboratory produced this construct (Gopaul, 2003). The *Avr*II site was utilised to enabled cloning of a hygromycin resistance cassette into the deleted region of *sigG.* The construct consisted of a 5′ 1706bp fragment containing part of the 5′ region of *sigG* separated from the 1970bp fragment containing part of the 3′ region of *sigG*, by a hygromycin resistance cassette. A *sacB/lacZ* cassette was cloned into the *Pac*I site within the vector part of this construct, to enable blue-white screening from the *lacZ* gene (which encodes β-galactosidase) and sucrose counter-selection from the sucrose sensitivity gene *sacB* (encodes levansucrase (Jager *et al.*, 1992) in *M. tuberculosis.* This construct (pLD1) was then electroporated into *M. tuberculosis*, H37Rv Mill Hill strain.

The selection and counter selection process was carried out as outlined in section 2.11, to detect potential knockouts, exhibiting Km^S and Hyg^R phenotypes. DNA extractions were then carried out on these potential knockouts, and screened by PCR and Southern blotting.

3.2.1 PCR used to detect potential knockouts

PCR reactions were designed to amplify separately the 5′ flanking region of the mutation and the 3′ flanking region. One primer for each pair was located outside the cloned region of DNA, and the other was located inside the hygromycin resistance cassette. The design of the PCR reaction enabled screening of potential double crossovers, whilst enabling one to distinguish between single crossovers, double cross-overs and random integrations (figure 3.1). Genomic DNA was extracted from potential knockouts and used in both PCR reactions. The PCR reactions gave inconclusive results (data not included). The drawback to this approach of detecting potential knockouts is the lack of a positive control, from which to optimise the PCR reactions, as the PCR reactions potentially produce large products, which may be difficult to amplify.

3.2.2 Southern blot used to detect potential knockouts

A Southern blot was designed such that double cross-over events could be distinguished from wild-type (control), single 3′ or 5′ cross-over events and random integrations. The design required the identification of a restriction enzyme that cuts twice, once in the genomic region, upstream of the knockout cassette and again in the 3′ region of the *sigG* knockout construct (see figure 3.2a). A DNA probe (probe a) was designed to overlap the 5′ coding region of *sigG* and the 5′ upstream flanking region contained within the construct (see figure 3.2a). This design

Figure 3.1

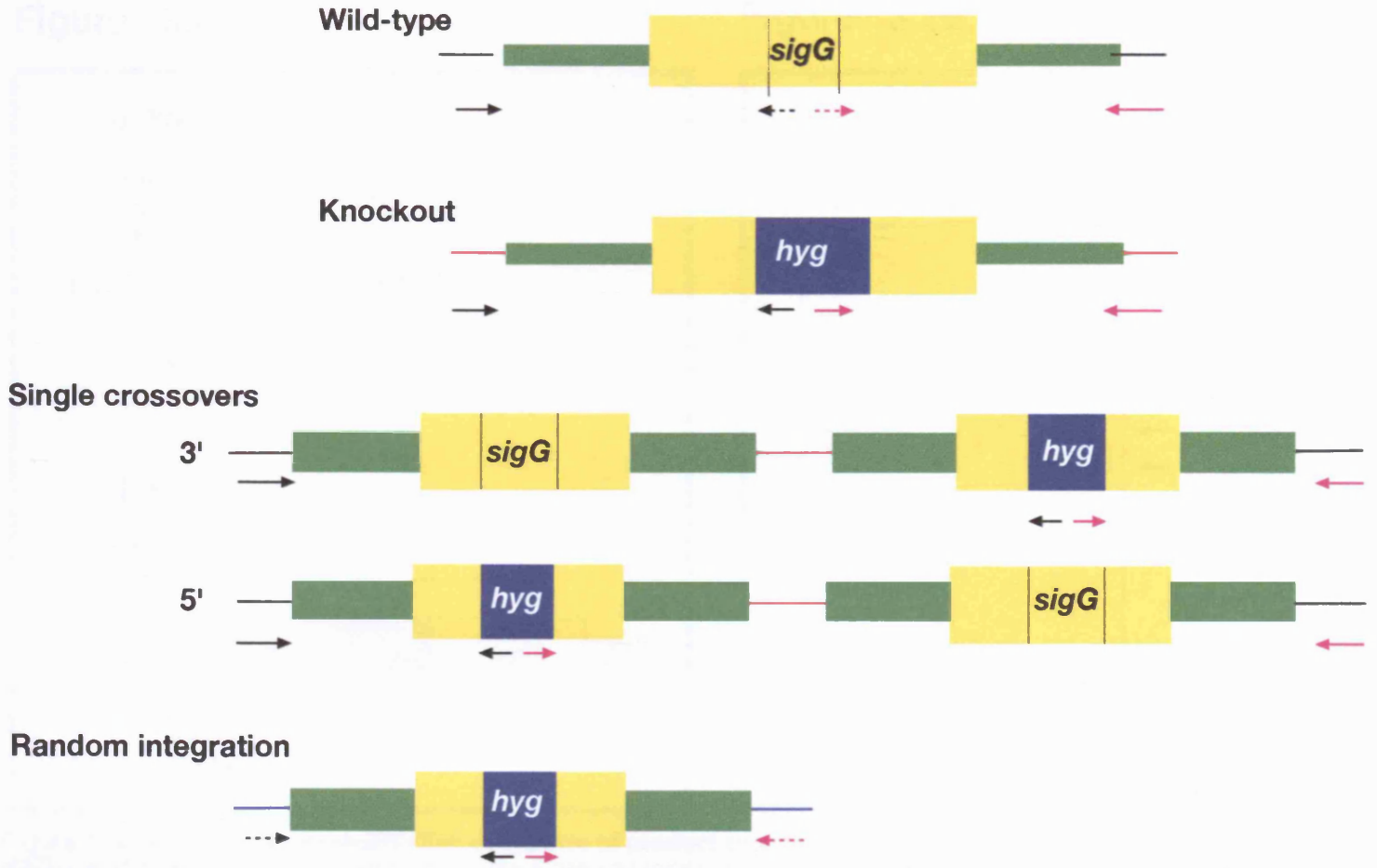

Figure 3.1: A schematic representation of the design of the PCR reaction to screen for potential knockout colonies. The black arrows indicate the PCR primers for the 5' region of the construct and the red arrows indicate the PCR primers for the 3' region of the construct. The dotted arrows indicate the regions that lack homology to the primers and therefore indicate where binding will not take place. The primer locations for the wild-type, knockout, single crossover and random integrations are shown.

Figure 3.2a

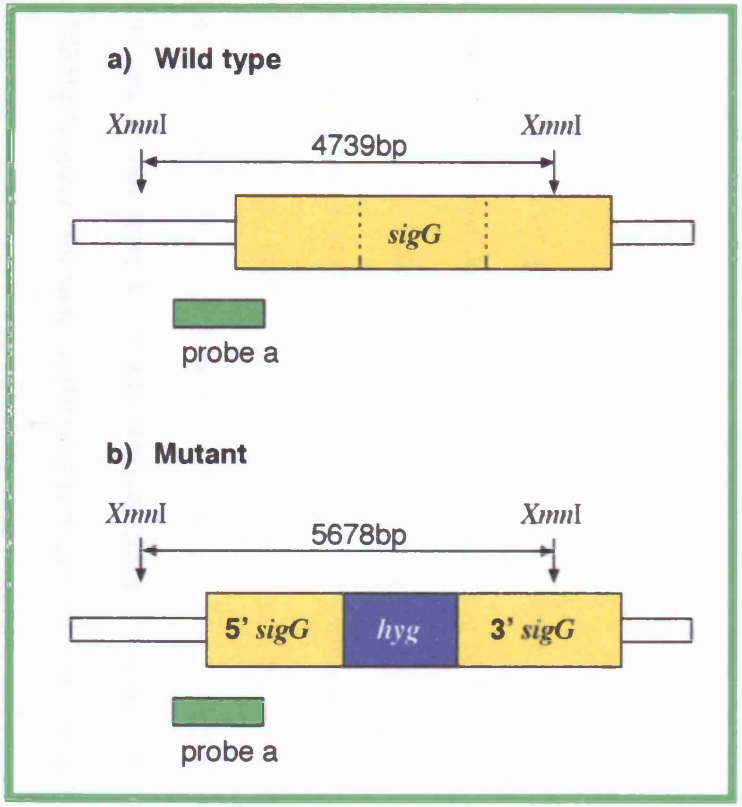

Figure 3.2b

Figure 3.2a: A schematic representation of the size of product produced in a Southern blot for both a Δ*sigG* strain and the H37Rv wild-type. The probe is positioned in the 5' flanking region of *sigG*, and the restriction sites *(XmnI)* are marked with arrows.The size of the expected wild-type and mutant bands are indicated in base pairs (bp).

Figure 3.2b: A southern blot to detect a knockout of *sigG*. DNA was extracted from potential *sigG* knockout colonies and were digested with *XmnI*. A radio-labelled probe was then used to detect potential double cross-overs. Δ*sigG*W1 (track 1) Δ*sigG*W2 (track 2), Δ*sigG*W3 (track 3) and Δ*sigG*W4 (track 4). *M. tuberculosis* genomic DNA (track C) was used as a positive control.

enables the differentiation of 3′ and 5′ cross-over events, double cross-overs, random integration and wild-type. Mutant and wild-type are differentiated by size of a single band whereas single crossovers and random integrations are differentiated by the production of 2 bands. A random integration would produce 2 bands of different size from the 3′ and 5′ single crossovers, due to the positioning of the restriction sites.

*Xmn*I restriction digests were performed on DNA isolated from potential knockout colonies, alongside an *M. tuberculosis* H37Rv genomic DNA control. These digests were then run on an agarose gel and a Southern blot was performed. Probe a, when hybridized to the restriction fragment is expected to visualise a 5678bp fragment with a knockout, and a 4739bp fragment with the wild type (see figure 3.2a and 3.2b). DNA isolated from colonies 1, 2 and 4 showed a band of 5678bp, therefore indicating a knockout (see figure 3.2b), whereas, colony 3 exhibited the same size band as the genomic control, of 4739bp, indicating a wild-type genotype (see figure 3.2b).

A second Southern blot was designed to confirm the identification of *sigG* knockout isolates, by determining if the 691bp deletion of the internal coding region of *sigG* had taken place. *Sca*I sites were identified that cut once in the genomic region upstream of 5′ *sigG*, and once in the genomic region downstream of 3′ *sigG* (see figure 3.3a). Probe b was designed within the 691bp deletion from the *sigG* coding region and therefore only binds to wild-type DNA in a Southern blot (see figure 3.3b). The DNA isolated from colonies 1 and 2 showed no binding of the probe, confirming they were knockouts, whereas colony 3 showed binding to the probe, producing a 3235bp fragment the same as the wild-type genomic control, indicating that colony 3 was wild-type (see figure 3.3b). The knockout *sigG1* (Δ*sigG*) was used in all downstream experiments.

Figure 3.3a

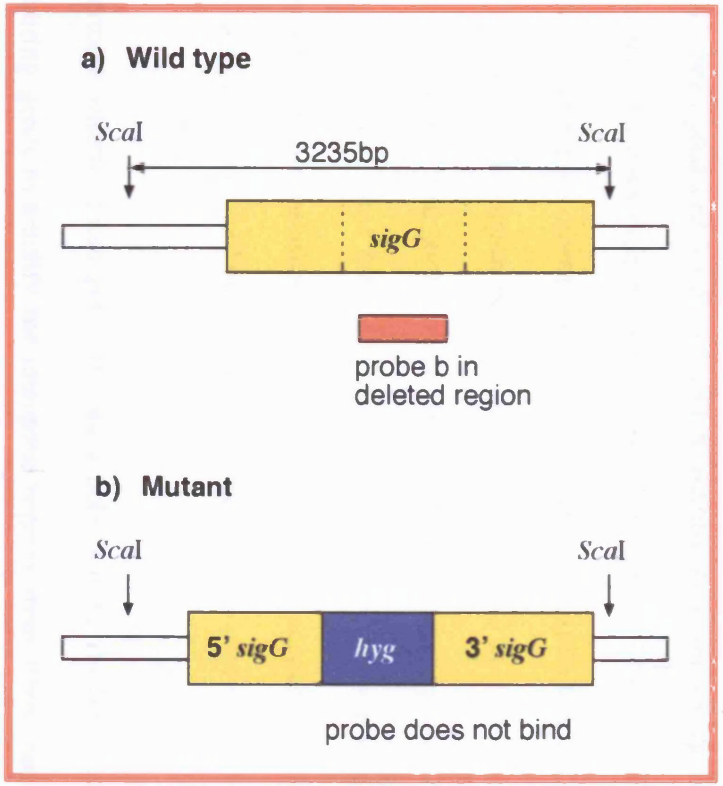

Figure 3.3b

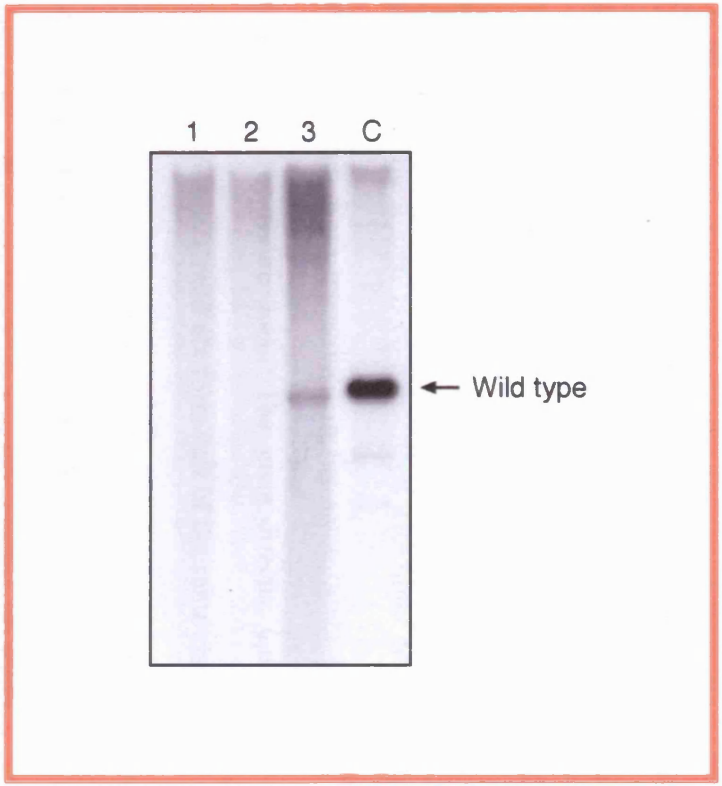

Figure 3.3a: A schematic representation of the size of product produced in a Southern blot using a probe designed in the deleted region of *sigG*. The probe will only bind to the wild-type, and not the *sigG* mutant. The restriction sites (*ScaI*) are indicated along with the size of the wild-type band.

Figure 3.3b: A southern blot to detect a knockout of *sigG*, using a probe designed in the deleted region of *sigG*. DNA was extracted from potential *sigG* knockout colonies DNA was digested with *ScaI* and run on an agarose gel. This was transferred to a nylon memebrane, probed with radio-labelled probe b. Δ*sigG*W1 (track 1) Δ*sigG*W2 (track 2), Δ*sigG*W3 (track 3) and *M. tuberculosis* genomic DNA (track C), was used as a positive control.

3.2.3 Chromosomal location of *sigG*

Current literature suggests some sigma factors are co-transcribed as polycistronic RNA with their cognate anti-sigma factors and even anti-anti sigma factors (Raivio and Silhavy, 2001). If there are genes co-transcribed with *sigG*, the deletion and insertion of a hygromycin resistance cassette may have polar effects on any co-transcribed downstream genes. Therefore, it was important to determine if *sigG* is co-transcribed with other genes. Visual analysis of the locus revealed that 4 genes were transcribed in the same orientation, with *sigG* being positioned furthest upstream (see figure 3.4). The gene directly upstream of *sigG* was divergently transcribed, and therefore, would not form part of the same cistron (see figure 3.4). The size of the intergenic regions, between genes in the same genomic orientation, can be used to predict if genes are co-transcribed as a polycistronic mRNA (Strong *et al.*, 2003). Therefore, genes that are separated by a few base pairs tend to be co-transcribed (Price *et al.*, 2005). A distance model has been produced for *E. coli* and *B. subtilis*, however, intergenic difference may vary across species for conserved operons (Price *et al.*, 2005). The size of the intergenic regions between *sigG* and the 3 downstream genes, Rv0181c, Rv0180c and *lprO* are indicated in figure 3.5a. The intergenic region between Rv0181c and *sigG* is 17bp and the predicted coding regions of Rv0180c and Rv0181c overlap by 27bp, suggesting they may be co-transcribed. However, *lprO* is situated 80bp downstream of Rv0180c, making it more difficult to predict whether they are co-transcribed. One must also take into account that the open reading frames (ORF's) are predictions, and the actual coding regions may vary slightly from these predictions.

To determine whether these genes formed a polycistronic mRNA, primers were designed in neighbouring genes to amplify the intergenic regions from RNA (see figure 3.5a). Internal control primers (see figure 3.5a, primer set D) were designed in the internal coding region of

Figure 3.4

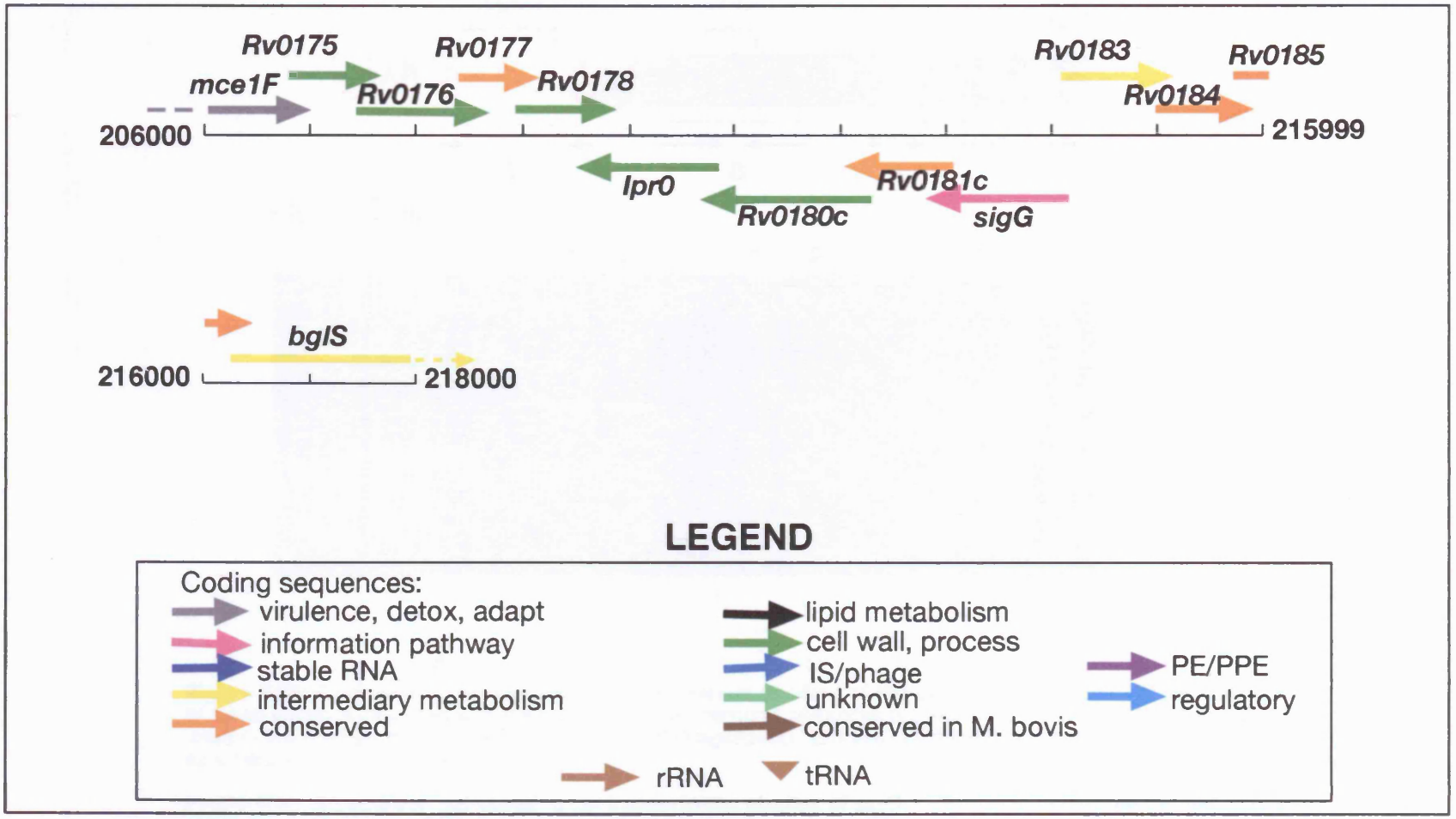

Figure 3.4: A schematic representation of the location of *sigG*. The figure was adapted from the data available on the TubercuList website

Figure 3.5a

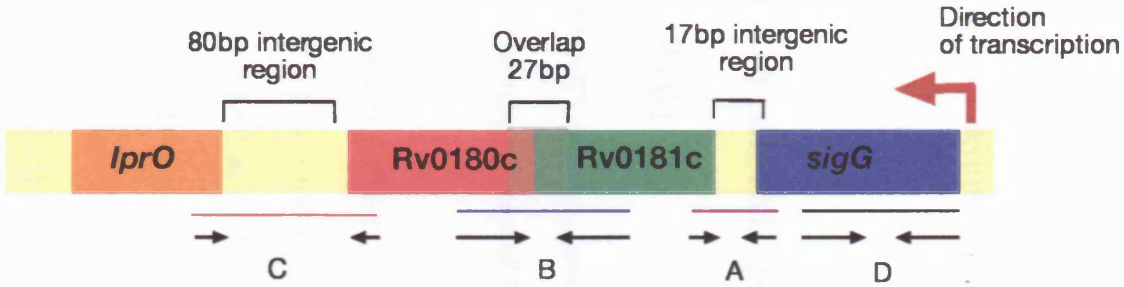

Figure 3.5b

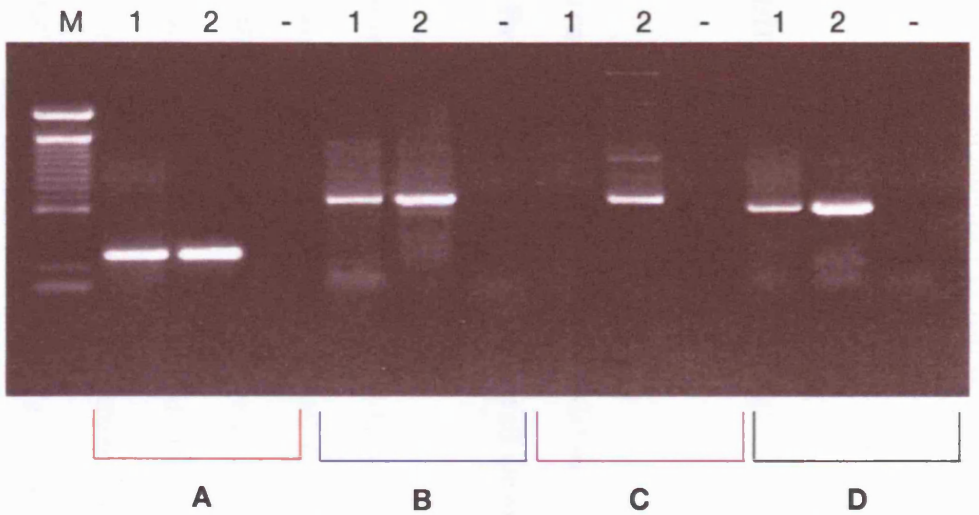

Figure 3.5a: A schematic representation of the relative position of the *sigG*. The direction of transcription of these genes is indicated with the red arrow. The intergenic distances are indicated, along with the primers used in the RT-PCR reaction, A (LD *sigG*Af/r), B (LD *sigG*Bf/r),C (LD *sigG* Cf/r)and D (LD *sigG*f/r). D was used as a positive control for the RT-PCR.

Figure 3.5b: An agarose gel showing co-transcription studies of *sigG*. PCR reactions were performed using cDNA (track 1), positive DNA control (track 2) and a negative control, RT-reaction (tracks -). The primers used in each reaction are marked under the relevant tracks. The sizes were as expected A = 263bp, B =653bp, C = 649bp and D = 571bp

sigG to check the integrity of the cDNA template. The PCR reactions were performed on cDNA, with genomic DNA as a positive control and RT- (omitting superscript) reactions as a negative control. RT- reactions, were performed on RNA, omitting the Superscript (see figure 3.5b). Oligo set A was designed to determine if *sigG* (Rv0182c) and Rv0181c were co-transcribed, oligo set B to determine if Rv0180c and Rv0181c were co-transcribed, and oligo set C to determine if Rv0180c and *lprO* were co-transcribed. Figure 3.5b shows that *sigG*, Rv0181c and Rv0180c are most likely co-transcribed as part of an operon, but *lprO* forms a separate cistron.

3.3 Predicted protein domains of SigG, Rv0181c and Rv0180c

The SMART database, (available on-line at www.samert.embl-heidelberg.de/smart) was used to predict protein domains of SigG, Rv0181c and Rv0180c that might allude to their functions.

SigG contains a PFAM sigma 70 region 2 domain, located at 61-129aa, which corresponds to the most highly conserved of the sigma 70 regions, as region 2 forms the site of interaction with the core-RNAP as well as the –10 recognition helix (Lonetto *et al.*, 1994). SigG from *M. tuberculosis* processes an ECF subfamily signature (TubercuList) and shows high levels of homology to SigG (MB0188C) from *M. bovis* (8e-96), and *M. paratuberculosis* (MAP3621c) e-value (8e-73) and to 2SCK8.21C, a putative ECF family sigma factor in *Streptomyces coelicolor* (3e-65). Alignment of the sequences using the programme Needle of the EMBOSS-Align suite, showed that SigG from *M. tuberculosis* and *M. bovis* shared 100% identity, whereas SigG from *M. paratuberculosis* showed 73.9% identity (Blosum62 matrix, with 10.0 open gap penalty, 0.5 gap extension penalty).

Rv0181c contains the PFAM Pirin domain from position 6-122aa, and shows sequence homology to MB0187C in *M. bovis* (hypothetical protein), (6e-76), which is located in the corresponding location downstream of *sigG*. Rv0181c also shows homology to two putative cytoplasmic proteins, one from *Salmonella typhimurium*, STM3544 (YHHW) (5e-72) and the other from *E. coli*, B3439 (YhhW) (6e-72).

Rv0180c is predicted to contain an N-terminal signal peptide (1-43aa) and five C-terminal transmembrane domains, interspersed with undefined regions, spanning the region 218-414aa. A homology search revealed that Rv0180c shows homology to MB0186C (e-152), a predicted membrane protein from *M. bovis* and ML2600 of *M. leprae*, also a probable conserved membrane protein (e-145). Rv0180c also shows some homology with phage infection protein, BC3083 from *Bacillus cereus* (2e-38), and also to the ABC transporter, FTT0729 of *Francisella tularensis* (subsp. tularensis) (9e-25), a pathogenic aerobic gram negative bacterium, which causes Tularemia.

The domain predictions of Rv0181c and Rv0180c along with the fact that they are co-transcribed with *sigG* in *M. tuberculosis* suggests the possibility that the two downstream genes are involved in regulation of the sigma factor. A number of sigma factors have been found to be co-transcribed with their cognate anti-sigma factors (Raivio and Silhavy, 2001), which negatively regulate them, preventing binding of the sigma factor to the core-RNAP and therefore preventing transcription of the sigma factor's regulon. Anti-sigma factors are in turn regulated by an environmental signal, or by binding of their cognate anti-anti-sigma factors, both of which result in a conformational change of the anti-sigma factor (Humphreys *et al.*, 1999), thus inhibiting binding of the sigma factor and the anti-sigma factor, which enables the sigma factor to bind to core-RNAP and initiate transcription. The predictions regarding the

structure of Rv0180c indicate the presence of a transmembrane domain suggesting that Rv0180c is a transmembrane protein, which may act to detect environmental signals, which could, in turn, result in a conformational change in the structure of the anti-sigma factor (Rv0181c), thus releasing the sigma factor (SigG) to enable transcription of the sigma factor's regulon.

3.4 Complementation of the *sigG* knockout

As previously stated inactivation of *sigG* via deletion and insertion may have polar effects on downstream genes in the operon. Any effects observed in the Δ*sigG* strain may be attributed to a culmination of the global effect of *sigG* knockout and the polar effects this may have on the co-transcribed genes.

To determine whether the genotypic and phenotypic effects exhibited by the knockout are solely due to the effects of constructing an inactivation mutant of *sigG* rather than any polar effects, a full operon complement was produced along side a complement that contained only the coding region of *sigG* (see table 3.1).

	(*sigG*) Rv0182c	Rv0181c	Rv0180c	Deletion size	Construct size
Full operon (8T)	√	√	√	0	6870
Partial δ1	√	X	X	2125	4754

Table 3.1: Comparison between the full operon and *sigG* only complements.

Full operon complementing plasmid was constructed in pKP186. Site directed mutagenesis was performed on the full operon complementing plasmid to produce a deletion containing only *sigG*.

The constructs for complementation were produced in a modified version of the integrating plasmid pMV306 (Stover *et al.*, 1991), called pKP186, in which the integrase gene (*int*) had been deleted in (Papavinasasundaram, personal communication). pMV306 contains genes for both attachment site (*att*) and integrase (*int*), derived from mycobacteriophage L5. These enable integration of the plasmid into the *attB* site of the mycobacterial chromosome. The absence of the excisionase (*xis*) gene means the plasmid should be maintained without the need for selection (Stover et al., 1991). However, problems with maintenance of this plasmid have been observed by others (Springer et al., 2001), which lead to the construction of vectors, in which, the integrase gene has been removed and incorporated into a separate plasmid pBSint (Springer *et al.*, 2001), resulting in increased stability of the vector. pKP186 is one such plasmid in which the integrase has been deleted to increase stability and maintenance.

The full operon complement was constructed, using PCR primers designed to amplify the entire *sigG* operon including enough upstream region to contain the putative *sigG* promoter and downstream of the *sigG* operon, including part of *lprO* gene. This was then cloned into pKP186. The *sigG* only complement was constructed by deletion: primers were designed as outlined in section (2.7.13) to enable site directed mutagenesis to remove a region including the coding regions of Rv0181c and Rv0180c, using the full operon complement as a template (see table 3.1). These constructs were then individually co-electroporated into the Δ*sigG* strain of *M. tuberculosis*, along with pBSint, which contains the integrase gene, thus enabling the complementing plasmid to integrate at *attB* site in the bacterial chromosome. The electroporations were plated onto 7H11 plus kanamycin to select for the presence of the pKP186 construct (see table 3.1 and 2.11.3). The selection was not maintained after integration, thus resulting in loss of non-integrated plasmids, after which, colonies were grown on 7H11 + Km to select for the complementing plasmid.

3.4.1 Checking expression of the SigG, Rv0181c and Rv0180c

To determine if the effects of the deletion and insertion had partial, full or no polar effects on downstream gene expression, data from the DNA vs. RNA microarrays (described in chapter 5) were analysed. These suggest that the levels of *sigG*, Rv0181c and Rv0180c are decreased under both uninduced and induced (0.02μg/ml mitomycin C) conditions, in the Δ*sigG* strain compared to H37Rv wild-type, but not eliminated (see figure 3.6). One would have expected the level of *sigG* expression to have been eliminated in the Δ*sigG* strain, however, *sigG* still appears to be expressed under both uninduced and induced conditions, albeit to a much lower level (significantly different $p<0.01$ Students t-test), and *sigG* does not appears to be induced. Suggesting that expression of *sigG* is not totally SigG dependent. Examination of the location of the microarray probe indicates that the probe overlaps with the retained coding region of *sigG* by 48bp, sufficient to facilitate binding of the probe.

The level of expression of Rv0181c is decreased significantly under uninduced and induced conditions ($p<0.01$ - two-tailed Student t-test), and Rv0180c is significantly decreased under induced conditions ($p<0.01$), (see figure 3.6). It appears that only Rv0181c is still induced, but to a much lower level in Δ*sigG* strain compared to H37Rv.

3.4.2 Design and production of antibodies specific to *sigG*, Rv0181c and Rv0180c

An alternative method of detecting expression of SigG and the downstream co-transcribed genes Rv0181c and Rv0180c was identified, whereby peptides were used to raise antibodies against SigG, Rv0181c and Rv0180c.

Figure 3.6

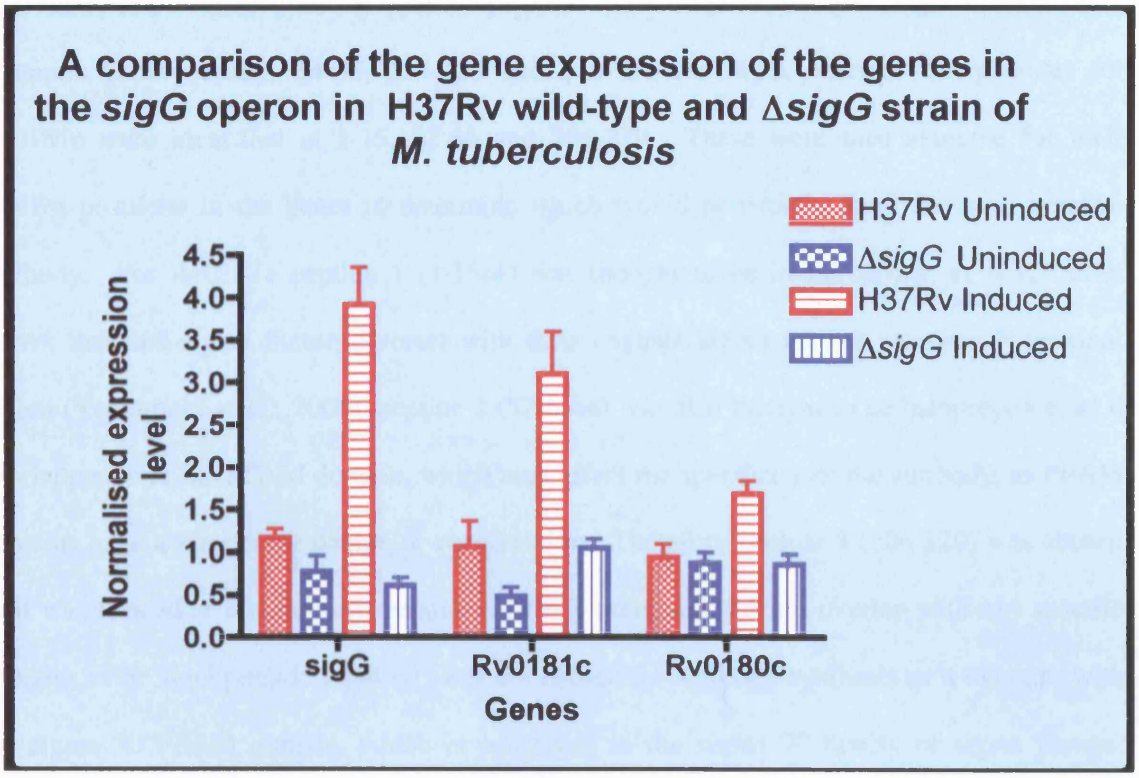

Figure 3.6: Microarray expression data for *sigG* operon in Δ*sigG* strain compared to H37Rv wild-type. DNA versus RNA microarrays were performed with triplicate biological cultures, repeated in duplicate. The uninduced and induced (0.02μg/ml mitomycin C) conditions were compared for both the Δ*sigG* strain and H37Rv. The uninduced conditions were significantly decreased in Δ*sigG* strain compared to H37Rv, at $p<0.01$ (Student t-test) for *sigG* and Rv0181c, and $p<0.05$ for Rv0180c. The induced values were significantly decreased for *sigG*, Rv0181c and Rv0180c at $p<0.01$ (Students t-test).

Protein sequences for SigG, Rv0181c and Rv0180c were sent to Sigma Genosys for the design of potentially immunogenic peptides. There was only one possible peptide detected for Rv0180c at position 88-102, within the region between the signal peptide and the transmembrane domain. Three alternative peptides were identified for both SigG and Rv0181c, at amino acid positions 54-68, 139-153 and 240-254 for SigG, whereas the peptides for Rv0181c were identified at 1-15, 52-66 and 206-220. These were then assessed for their relative positions in the genes to determine which would potentially form the most reactive antibody. For Rv0181c peptide 1 (1-15aa) was thought to be inappropriate, as it has been shown that anti-sigma factors interact with their cognate sigma factors via their N-terminal region (Yoshimura *et al.*, 2004), peptide 2 (52-66aa) was also thought to be inappropriate, as it overlapped with the PFAM domain, which may affect the specificity of the antibody, as PFAM domains have a reasonable degree of conservation. Therefore peptide 3 (206-220) was chosen as it was located at the carboxy terminus of the protein and did not overlap with any specific domains. For SigG peptide 1 (54-68) was not chosen for antibody synthesis as it overlaps with the sigma 70 PFAM domain, which is conserved in the sigma 70 family of sigma factors. Peptide 3 (240-254) was chosen arbitrarily over peptide 2 (139-153) for antibody production. A carboxy terminal cysteine residue was added to all of the peptides to enable conjugation to the carrier protein KLH (keyhole limpet hemocyanin, derived from marine mollusk). Freunds complete adjuvant was omitted from the antibody production protocol as it contains mycobacterial components, which may have compromised antigen specificity, as a result, Freunds incomplete adjuvant was utilised. The synthesised peptides were used to raise antibodies in rabbits. Two rabbits were used per peptide, and the final bleed was used in affinity purification of the antibodies.

3.4.3 Analysis of SigG, Rv0181c and Rv0180c, using antibodies.

Initially, the reactivity and an indication of the specificity of the antibodies raised was assessed using dot blots that included the synthesised peptide specific for each antibody, alongside *M. tuberculosis* cell free extract (CFE) and *E. coli* CFE. The terminal bleeds and purified fractions were compared with the pre-bleeds (null serum) to select fractions and specific dilutions to use in subsequent analysis (data not shown). Western blots were performed to simultaneously examine the expression in the Δ*sigG* strain compared with that of the H37Rv wild-type, to determine if the reactivity of the antibodies raised against SigG, Rv0181c and Rv0180c were specific, using CFE from both uninduced and induced conditions for both Δ*sigG* strain and H37Rv. The western blots were performed with 30μg of H37Rv, Δ*sigG* strain and *E. coli* CFE. For Rv0181c and Rv0180c the purified fractions (F1) were used at a 1/500 dilution for the primary antibody, while for SigG the purified fraction was used at 1/250 dilution (assessed using dot blot, data not shown). The secondary antibody was used at a 1/5000 dilution (goat-anti-rabbit).

The antibody raised against the SigG peptide was not able to detect SigG in any of the cell free extracts, even from H37Rv CFE. The anti-SigG antibody did not cross react with *E. coli* CFE.

In the case of Rv0181c, a single band was obtained, for both the uninduced and induced CFE from H37Rv and Δ*sigG* strains. Although the size of Rv0181c is 26.3kDa, the band appears to run at approximately 48kDa (see figure 3.7, arrow 1), which suggests that Rv0181c maybe running as a dimer, however, even though the anti-Rv0181c antibody did not cross react with *E. coli* CFE, the binding may be non-specific, as a denaturing loading buffer was used.

Figure 3.7

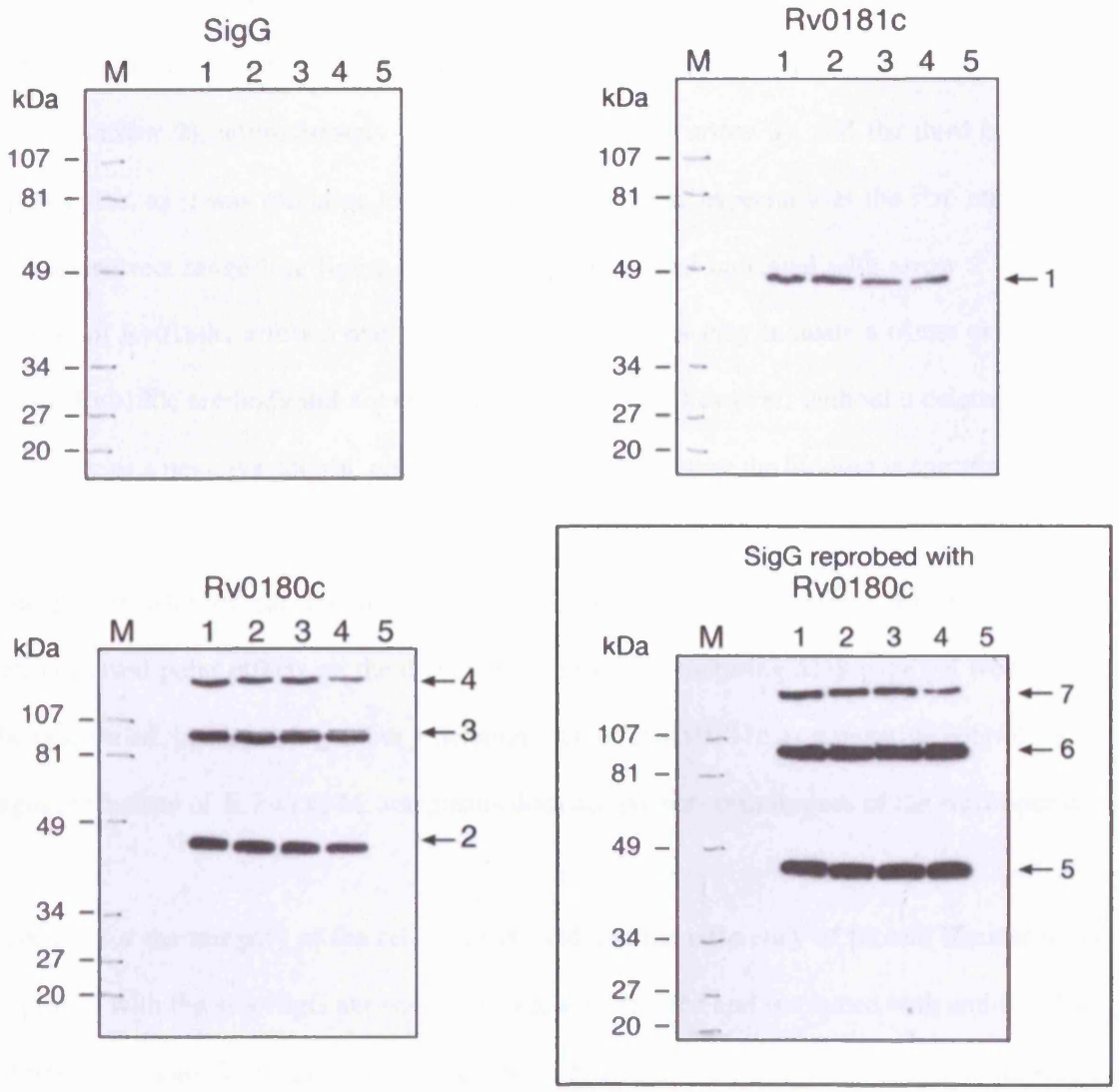

Figure 3.7: Western blot to test specificity of SigG, Rv0181c and Rv0180c antibodies. The Western blots were performed with 30µg H37Rv uninduced CFE (1), 30µg H37Rv induced CFE (2), 30µg Δ*sigG* uninduced CFE (3), 30µg Δ*sigG* induced CFE (4), 30µg *E. coli* uninduced CFE (5). The samples were run on four 10% NuPage Bis-Tris gel (Invitrogen), alongside a low molecular weight marker (M) (BioRad). The transfers were performed with PVDF membrane (Invitrogen). The primary antibodies were used at a dilution of 1/250 SigG, 1/500 Rv0181c and 1/500 Rv0180c. The secondary antibodies were used at a dilution of 1/5000 HRP goat anti-rabbit (SigG, Rv0181c, Rv0180c), Western blots were visualised using chemiluminescence (Pierce). The SigG Western blot was stripped and re-probed with Rv0180c antibody using the protocol as outlined above.

For Rv0180c, three bands were present, for both the uninduced and induced CFE from H37Rv and Δ*sigG* strains. The size of Rv0180c is 47.6kDa, however, bands appear to run at 47kDa (see figure 3.7 arrow 2), approximately 92kDa (see figure 3.7, arrow 3), and the third band is of unknown size, as it was too large to size on this gel system, especially as the size markers are not in the correct range (see figure 3.7, arrow 4). The band indicated with arrow 2 may be a monomer of Rv0180c, arrow 3 may be a dimer, and arrow 4 may indicate a trimer or tetramer. The anti-Rv0180c antibody did not cross react with *E. coli*, however, without a deletion mutant of Rv0180c as a negative control, one can not determine whether the binding is specific.

To determine whether the binding were specific and therefore to assess whether the sigG deletion caused polar effects on the downstream genes, a denaturing SDS-page gel would have to be performed, ideally using either a deletion mutant of Rv0181c as a negative control, or *M. smegmatis* instead of *E. coli* as M. smegmatis does not possess orthologues of the *sigG* operon.

To control for the integrity of the cell extracts used and the efficiency of protein transfer in the blot probed with the anti-SigG antibody, this blot was stripped and re-probed with anti-Rv0180c antibody (see figure 3.7). The Rv0180c antibody bound to the H37Rv and Δ*sigG* strain CFEs, yielding the same three-band pattern as observed previously. This indicates that the CFEs used for this blot were good quality, and that protein transfer from the gel to the membrane had occurred; thus the lack of binding seen with the anti-SigG antibody must be due to the nature of the antibody rather than a problem with the CFE on the blot.

3.5 *In-vitro* analysis of Δ*sigG* strain and complements

3.5.1 Growth curves *in-vitro*

Growth curves for the Δ*sigG* strain, wild-type H37Rv and the two *sigG* complements were produced under normal growth conditions, in a rolling incubator, as outlined in section (Methods – growth curve). The Δ*sigG* strain and two complement strains (8T and Δ1), grew at the same rate as the wild-type H37Rv (see figure 3.8), suggesting that the knockout and complements have the same ability to grow and divide as the wild-type under normal *in-vitro* growth conditions.

3.5.1.1 Viability of Δ*sigG*, complements and wild-type to DNA damaging agents

Alternative sigma factors have been implicated to respond to a number of different environmental signals, as outlined in section 1.5.9.1. Knockouts of some alternative sigma factors have been shown to be more susceptible to certain types of environmental stimuli than wild-type.

To determine if SigG could be involved in the response to DNA-damage in *M. tuberculosis*, the survival of the Δ*sigG* strain following exposure to a number of different DNA damaging agents was compared with that of the wild-type H37Rv. Ofloxacin and mitomycin C are chemical DNA damaging agents; ofloxacin is a quinolone antibiotic, which inhibits DNA gyrase and is toxic to mycobacteria (Movahedzadeh *et al.*, 1997), whereas mitomycin C alkylates guanines to form inter-strand cross-links in DNA (Iyer and Szybalski, 1964). Paraquat and cumene

Figure 3.8

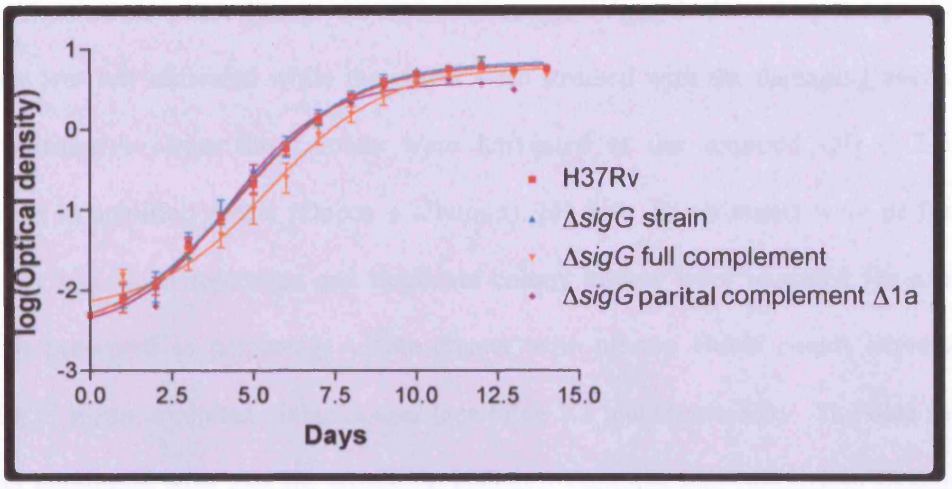

Figure 3.8: The *in-vitro* growth curves of the *sigG* knockout, *sigG* full operon complement, partial complement and H37Rv wild type. For each strain, single colonies were inoculated into 5ml of Dubos plus albumin in triplicate and incubated in static culture for 10 days at 37°C. Static cultures were then then used to inoculate a 100ml rolling culture in Dubos plus albumin, to an OD of 0.005 (approx 1ml). Triplicate cultures were returned to the rolling incubator for a total of 14 days. Optical density readings were taken at the same time daily, and dilutions were made in Dubos + albumin after an OD of 0.4 to enable accurate reading by the spectrophotometer.

hydroperoxide are oxidative agents, which resemble environmental stresses produced in the macrophage (see section 1.4.1). Paraquat generates superoxide, by catalytically diverting electrons from NAD(P)H to oxygen, whereas cumene hydroperoxide generates peroxide stress by oxidising bases and deoxyribose (Demple and Harrison, 1994). Acidified sodium nitrite mimics the exposure of the bacteria to nitric oxide in an activated macrophage (Nathan and Shiloh, 2000), viability assays were performed as outlined in section 2.12.2. Cultures were grown to exponential phase (0.3 to 0.4 optical density (OD_{600})) and were split into aliquots of 40mls, one was left untreated while the others were stressed with the damaging agent. In the case of nitrosative stress the cultures were harvested at the required OD (0.3-0.4) and resuspended in acidified media (Dubos + albumin), pH 5.4. Experiments were performed on two distinct biological replicates and duplicate colony counts were recorded for each. The viability is presented as percentage viable counts, with treated viable counts expressed as a proportion of mean untreated viable counts (see table 3.2 and figure 3.9). The data for *ΔsigG* strain was compared with that for wild-type H37Rv. Paraquat and mitomycin C showed the most dramatic decrease in viability in the knockout compared to the wild-type, with ofloxacin also causing a decrease in viability of the knockout compared to the wild-type (see figure 3.9). However, there was a significant decrease in viability in the *ΔsigG* strain for paraquat ($p<0.01$) and mitomycin C ($p<0.06$) using a Student t-test, but there was no significant difference in viability in *ΔsigG* strain compared to H37Rv, when exposed to ofloxacin ($p=0.20$). There was also no significant difference at the 1% level ($p<0.01$) (Student t-test) between wild-type and knockout in response to cumene ($p=0.26$) and sodium nitrite stress ($p=0.74$).

To analyse the enhanced susceptibility of the *ΔsigG* strain to paraquat and mitomycin C in more detail, further experiments were performed using a titration to determine the effects of different concentrations of the DNA damaging agents on Δ*sigG* strain, wild-type H37Rv and full operon

Figure 3.9

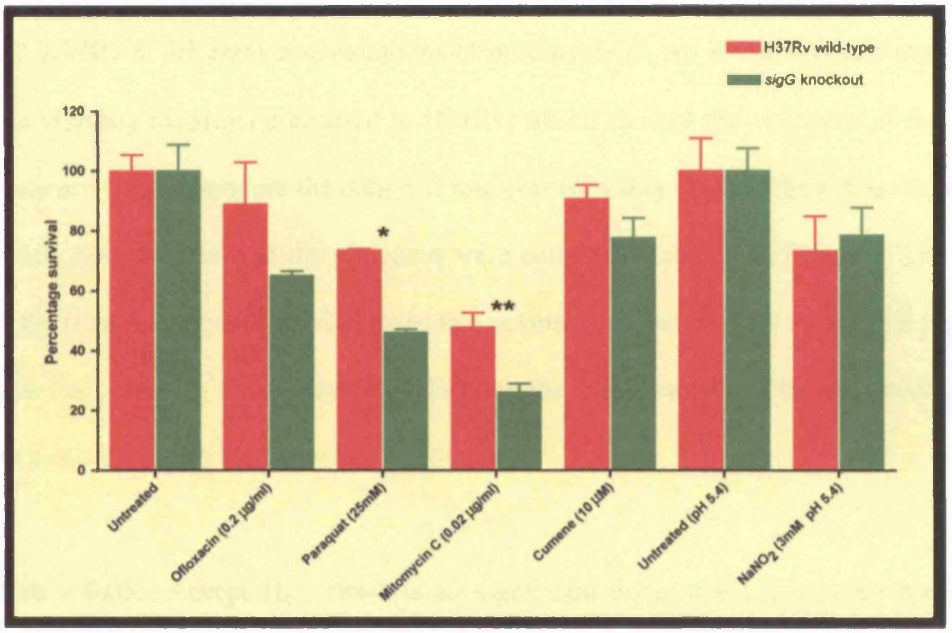

Figure 3.9: Histogram depicting the viability of *sigG* knockout treated with different DNA damaging agents as a percentage of the untreated control.

Cultures of ΔsigG and H37Rv were grown to an OD 0.3-0.4. 40ml aliquots were removed. One was untreated, and the others, were treated with 0.2µg/ml ofloxacin, 0.02µg/ml mitomycin C, 10mM cumene hydroperoxide, 25mM paraquat, or 3mM $NaNO_2$ (for $NaNO_2$ stress, both untreated and test samples were resuspended in Dubos media pH5.4). Cultures were incubated @ 37°C for 24 hours. 50µl of treated culture was serial diluted in DMEM/FCS (50%). Serial dilutions were plated on 7H11 plates and incubated at 37°C for 13-15 days to obtain colony counts. Colony counts are expressed as a percentage of untreated, with mean and standard error for the replicates.

complement (mitomycin C only). Both strains showed a decrease in viability with increasing concentration of paraquat (see table 3.3 and figure 3.10), however, no significant difference was observed between the *ΔsigG* strain and wild-type H37Rv (see table 3.4). The titration with mitomycin C confirmed that the Δ*sigG* strain is considerably more susceptible than wild-type H37Rv (see table 3.5 and figure 3.11). The *ΔsigG* strain exhibits an average viability of only 14% at 0.02μg/ml mitomycin C, whereas the wild-type H37Rv exhibits a 41% viability, this susceptibility increases with increasing concentrations of mitomycin C. Statistical analysis was used to determine whether there was a significant difference between the mean viable count of *ΔsigG* and H37Rv at different concentrations of mitomycin C. An F-test was performed on the percentage viability of *ΔsigG* compared to H37Rv, which showed the variances of the two sets of data were not equal, therefore the data was transformed using log10. The F-test was repeated using the log data, and showed the variances were equal (see table 3.6a, 3.6b and 3.6c), which indicated the transformed data approximates to a normal distribution, and therefore a parametric test such as the t-test was a valid test to perform on the data (see table 3.6a, 3.6b and 3.6c). T-tests were performed with the following hypotheses:

H_0: P value > 0.05. Accept H_0: There is no significant difference between the mean viable counts of *ΔsigG* and H37Rv in response to mitomycin C stress at a given concentration.

H_1: P value < 0.05. Accept H_1: There is a significant difference between the mean viable counts of *ΔsigG* and H37Rv in response to mitomycin C stress at a given concentration.

Two-tailed unpaired t-tests were performed between *ΔsigG* strain and H37Rv untreated transformed data. There was no significant difference between the means at the 95%

Table 3.2

Paraquat (mM)	H37Rv		*sigG* knockout	
	Mean	Standard error	Mean	Standard error
Untreated	100	± 14.754	100	± 0.671
10	72.600	± 11.241	90.604	± 4.698
20	52.693	± 8.197	61.745	± 9.396
30	29.040	± 5.152	48.255	± 5.166
40	30.913	± 2.810	21.846	± 2.798
50	13.665	± 2.758	18.255	± 3.443

Figure 3.10

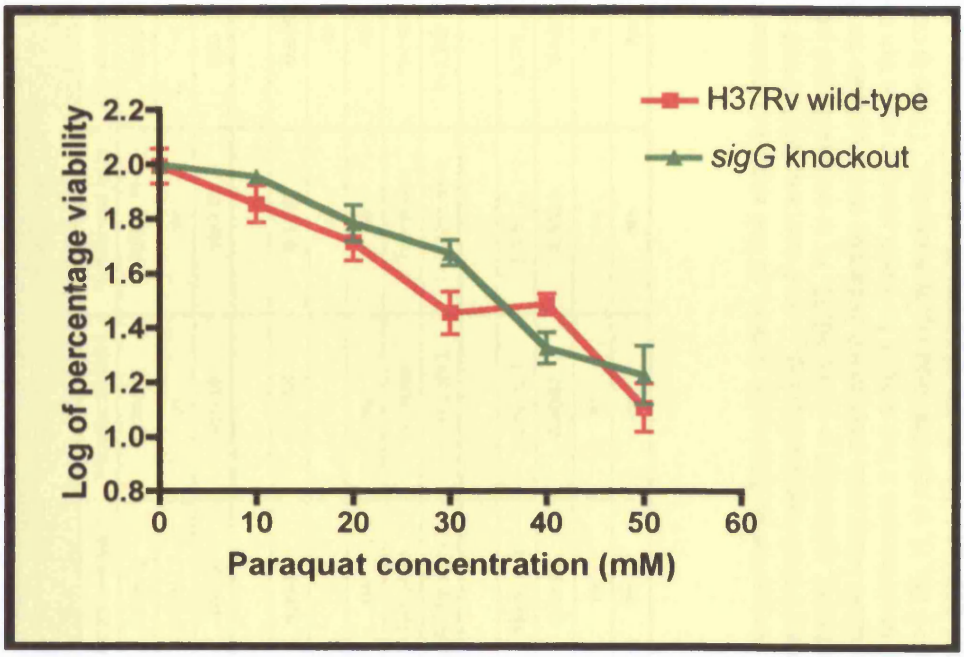

Table 3.2: Percentage viability of H37Rv in comparison to *sigG* knockout in response to paraquat stress. Dulpicate cultures were grown to exponential phase (0.3 to 0.4 OD), 40ml aliquots were incubated for 24hours untreated or with the relavent concentration of Paraquat. After 24hours the cultures were serial diluted and plated on 7H11 plates in duplicate and incubated at 37°C for 16-18 days. Colony counts were taken of at least 2 dilutions. The viable CFU was then expressed as a percentage of the untreated for each sample, and the mean and standard error was calculated.

Figure 3.10: A graph comparing the of viability of the *sigG* knockout to H37Rv wild-type in response to paraquat stress. In Prims 4, the percentage viability data as outlined above was transformed using $\log_{10}$, and plotted on a linear scale. A linear regression sigmoidal dose response curve was fitted to the data.

	Untreated	10mM Paraquat	20mM Paraquat	30mM Paraquat	40mM Paraquat	50mM Paraquat
Table Analyzed	Transformed log10	Transformed log10	Transformed log10	Transformed log10	Transformed log10	Transformed log10
H37Rv wild-type	H37Rv U	H37Rv 10	H37Rv 20	H37Rv 30	H37Rv 40	H37Rv 50
vs	vs	vs	vs	vs	vs	vs
sigG knockout	sigG U	sigG 10	sigG 20	sigG 30	sigG 40	sigG 50
Unpaired t test						
P value	**0.9479**	**0.2934**	**0.5437**	**0.0609**	**0.1463**	**0.4268**
P value summary	ns	ns	ns	ns	ns	ns
Significant difference at 95% (P < 0.05)	**No**	**No**	**No**	**No**	**No**	**No**
One- or two-tailed P value?	Two-tailed	Two-tailed	Two-tailed	Two-tailed	Two-tailed	Two-tailed
t, df	t=0.07381 df=2	t=1.412 df=2	t=0.7251 df=2	t=2.587 df=4	t=1.800 df=4	t=0.8523 df=6
F test to compare variances						
F,DFn, Dfd	490.4, 1, 1	9.046, 1, 1	1.046, 1, 1	1.378, 1, 3	4.151, 3, 1	1.487, 3, 3
P value	**0.0575**	**0.4087**	**0.9858**	**0.6504**	**0.6856**	**0.7521**
P value summary	ns	ns	ns	ns	ns	ns
Are variances significantly different?	**No**	**No**	**No**	**No**	**No**	**No**

Table 3.3: Statistical analysis of the response to Paraquat stress of the sigG knockout compared to H37Rv wild-type. The percentage viability for Δ*sigG* and H37Rv was transformed using $\log_{10}$. An F-test was performed to determine if both samples had equal variance (H_0) (a requirement for parametric tests), when the p-value >0.05, H_0 is accepted, the populations have equal variance and a t-test is appropriate. Then an unpaired, two-tailed t-test was performed between each sample for both *sigG* knockout and H37Rv wild-type, under each stress condition individually, to determine if the means for each sample were the same (H_0) or the means of *sigG* and H37Rv were different (H_1). Where the p-values >0.05, H_1 is rejected and H_{10} is accepted. There is no significant difference between the means, therefore there is no significant difference between the effects of paraquat on *sigG* knockout or H37Rv.

Table 3.4

Mitcomycin C (μg/ml)	H37Rv		*sigG* knockout		*sigG* complement 8T	
	Mean	Standard error	Mean	Standard error	Mean	Standard error
Untreated	100.00	± 12.74	100.00	± 7.78	100.00	± 7.18
0.02	41.16	± 6.89	14.87	± 1.03	29.48	± 2.87
0.05	7.70	± 0.98	2.34	± 0.28	4.40	± 0.6
0.1	1.74	±0.46	0.13	± 0.02	0.75	± 0.17
0.2	0.23	± 0.03	0.02	± 0.006	0.03	± 0.004

Figure 3.11

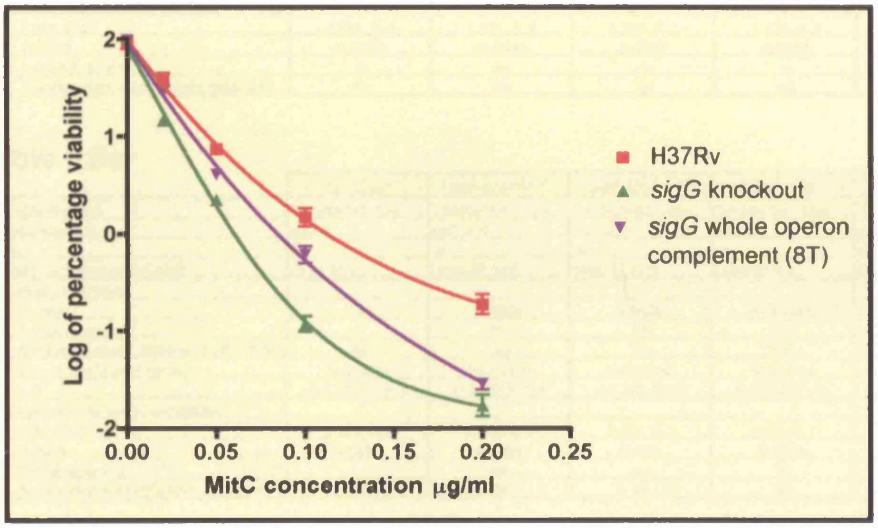

Table 3.4: Percentage viability of H37Rv in comparison to *sigG* knockout and *sigG* full operon complement in response to Mitomycin C stress. Duplicate cultures were grown to exponential phase (0.3 to 0.4 OD), 40ml aliquots were incubated for 24 hours untreated or with the relavent concentration of Mitomycin C. After 24hours the cultures were serial diluted and plated on 7H11 plates in duplicate and incubated at 37°C for 16-18 days. Colony counts were taken of at least 2 dilutions. The viable CFU was then expressed as a percentage of the untreated for each sample, and the mean and standard error was calculated.

Figure 3.11: A graph comparing the of viability of the *sigG* knockout, the *sigG* whole operon complement and H37Rv wild-type to Mitomycin C stress. In Prism 4, the percentage viability data as outlined above was transformed using $\log_{10}$, and plotted on a linear scale. A non-linear regression sigmoidal dose response curve was fitted to the data.

Table 3.5a

	Untreated	0.02µg/ml Mit C	0.05µg/ml Mit C	0.1µg/ml Mit C	0.2µg/ml Mit C
Table Analyzed	Transformed -Log_{10}	Transformed -Log_{10}	Transformed -Log_{10}	Transformed -Log_{10}	Transformed -Log_{10}
H37Rv wild-type	H37rv U	H37Rv 0.02	H37Rv 0.05	H37Rv 0.1	H37Rv 0.2
vs	vs	vs	vs	vs	vs
sigG knockout	sigG U	sigG 0.02	sigG 0.05	sigG 0.1	sigG 0.2
Unpaired t test					
P value	**0.8427**	**0.0001**	**P<0.0001**	**P<0.0001**	**P<0.0001**
P value summary	ns	***	***	***	***
Are means signif. different? (P < 0.05)	**No**	**Yes**	**Yes**	**Yes**	**Yes**
One- or two-tailed P value?	Two-tailed	Two-tailed	Two-tailed	Two-tailed	Two-tailed
t, df	t=0.2060 df=7	t=5.991 df=10	t=7.733 df=14	t=8.982 df=14	t=6.919 df=14
F test to compare variances					
F,DFn, Dfd	8.894, 5, 2	4.519, 5, 5	1.289, 7, 7	1.253, 7, 7	1.089, 7, 7
P value	**0.2083**	**0.1234**	**0.746**	**0.7737**	**0.913**
P value summary	ns	ns	ns	ns	ns
Are variances significantly different?	**No**	**No**	**No**	**No**	**No**

Table 3.5b

	Untreated	0.02µg/ml Mit C	0.05µg/ml Mit C	0.1µg/ml Mit C	0.2µg/ml Mit C
Table Analyzed	Transformed -Log_{10}	Transformed -Log_{10}	Transformed -Log_{10}	Transformed -Log_{10}	Transformed -Log_{10}
H37Rv wild-type	H37rv U	H37Rv 0.02	H367Rv 0.05	H37Rv 0.1	H37Rv 0.2
vs	vs	vs	vs	vs	vs
sigG full operon complement	Comp 8T U	Comp 8T 0.02	comp 8T 0.05	Comp 8T 0.1	Comp 8T 0.2
Unpaired t test					
P value	**0.8142**	**0.0687**	**0.003**	**0.0089**	**P<0.0001**
P value summary	ns	ns	**	**	***
Are means signif. different? (P < 0.05)	**No**	**No**	**Yes**	**Yes**	**Yes**
One- or two-tailed P value?	Two-tailed	Two-tailed	Two-tailed	Two-tailed	Two-tailed
t, df	t=0.2407 df=11	t=1.972 df=14	t=3.533 df=15	t=2.976 df=16	t=6.854 df=14
F test to compare variances					
F,DFn, Dfd	4.371, 5, 6	1.757, 5, 9	1.747, 8, 7	1.203, 9, 7	3.164, 7, 7
P value	**0.1008**	**0.4358**	**0.4767**	**0.8256**	**0.1516**
P value summary	ns	ns	ns	ns	ns
Are variances significantly different?	**No**	**No**	**No**	**No**	**No**

Table 3.5c

	Untreated	0.02µg/ml Mit C	0.05µg/ml Mit C	0.1µg/ml Mit C	0.2µg/ml Mit C
Table Analyzed	Transformed -Log_{10}	Transformed -Log_{10}	Transformed -Log_{10}	Transformed -Log_{10}	Transformed -Log_{10}
sigG knockout	sigG U	sigG 0.02	sigG 0.05	sigG 0.1	sigG 0.2
vs	vs	vs	vs	vs	vs
sigG full operon complement	Comp 8T U	Comp 8T 0.02	comp 8T 0.05	Comp 8T 0.1	Comp 8T 0.2
Unpaired t test					
P value	**0.94**	**0.0001**	**0.0032**	**P<0.0001**	**0.0928**
P value summary	ns	***	**	***	ns
Are means signif. different? (P < 0.05)	**No**	**Yes**	**Yes**	**Yes**	**No**
One- or two-tailed P value?	Two-tailed	Two-tailed	Two-tailed	Two-tailed	Two-tailed
t, df	t=0.07760 df=8	t=5.332 df=14	t=3.501 df=15	t=5.762 df=16	t=1.804 df=14
F test to compare variances					
F,DFn, Dfd	2.035, 6, 2	2.572, 9, 5	1.355, 8, 7	1.508, 9, 7	3.447, 7, 7
P value	**0.7312**	**0.3106**	**0.702**	**0.6019**	**0.1248**
P value summary	ns	ns	ns	ns	ns
Are variances significantly different?	**No**	**No**	**No**	**No**	**No**

Table 3.5a: Statistical analysis of the response to mitomycin C stress of the Δ*sigG* strain compared to H37Rv wild-type. The percentage viability for Δ*sigG* and H37Rv was transformed using log_{10}. An F-test was performed to determine if both samples had equal variance (H_0) (a requirement for parametric tests), when the p-value >0.05, H_0 is accepted, the populations have equal variance and a t-test is appropriate. Then unpaired, two-tailed t-tests were performed between each sample for both Δ*sigG* knockout and H37Rv wild-type, under each stress condition individually, to determine if the means for each sample were the same (H_0) or the means of Δ*sigG* and H37Rv were different (H_1). Where the p-values <0.05, H_0 is rejected and H_1 is accepted. There is a significant difference between the means.

Table 3.5b: Statistical analysis of the response to mitomycin C stress of the Δ*sigG* whole operon complement compared to H37Rv wild-type. Data was treated as outlined in table 3.2a, except the comparison was made between the Δ*sigG* whole operon complement and H37Rv.

Table 3.5c: A statistical analysis of the response to mitomycin C of the ΔsigG strain compared to Δ*sigG* whole operon complement. Data was treated as outlined in table 3.2a, except the comparison was made between the Δ*sigG and the* Δ*sigG* whole operon complement.

confidence level (see Table 3.6a). This shows that the data were comparable, as the untreated samples are not significantly different, as you would expect, as the untreated is set to 100%, and the viability is calculated as a proportion of the untreated. However, there is a significant difference between viability of *ΔsigG* and H37Rv for all concentrations of mitomycin C at the 99% confidence interval ($p<0.01$) (see table 3.6a).

Statistical analysis was also performed to determine whether the *sigG* whole operon complement (8T) was significantly different from H37Rv (see table 3.6b) and Δ*sigG* (see table 3.6c). The data was transformed (log_{10}) to give an approximation to a normal distribution, confirmed by an F-test (see tables 3.6b and 3.6c), and t-tests showed there was no significant difference between the means of H37Rv and the whole operon complement for the untreated and 0.02μg/ml mitomycin C stress, however, there were significant differences at 0.05, 0.1 and 0.2 μg/ml mitomycin C (see table 3.6b). When the t-test was performed between the Δ*sigG* strain and Δ*sigG* full operon complement, H_0 was accepted for untreated and 0.2μg/ml mitomycin C (no significant difference), but H_1 was accepted at 0.02, 0.05 and 0.1μg/ml mitomycin C (significant difference) (see table 3.6c). This suggests the complement does not completely restore sensitivity of the Δ*sigG* strain back to wild-type H37Rv.

3.6 *In-vivo* phenotype of Δ*sigG* strain compared to wild-type

A mouse model of infection was used to determine the *in-vivo* phenotype of the Δ*sigG* strain, in comparison to wild-type H37Rv. Six to eight week old BALB/C female mice were injected intravenously in the tail vain with 200μl of each strain of bacteria, by a trained animal technician (see section 2.12.3). Initial infection colony counts (CFU) were determine from the

inoculum, whereas bacterial load was determined from harvested lungs and spleen at regular intervals throughout the time course, beginning at day 1.

The method of injection accounts for the difference in CFU observed initially between the lungs and the spleen, with the higher CFU being present in the spleen. In a human infection, the route of infection determines that the CFU is highest in the lungs. The only way to mimic this would be to use an aerosol route of infection, which is currently not available at our animal facility.

Figure 3.12a and 3.12b show a difference between CFU in both the lung and the spleen for Δ*sigG* strain compared to the H37Rv wild-type. The Δ*sigG* strain shows greater than a log decrease in CFU at both day 95 and 150.

Statistic analysis using a two-tailed Student T-test shows a significant difference between Δ*sigG* strain and H37Rv: In the spleen, there is a significant difference in CFU in Δ*sigG* strain compared to H37Rv at day 60, 95, 125 and 150 at $p<0.1$, however there is no significant difference at day 2, day 30. In the lung there is a significant difference after inoculation at day 2, $p<0.05$ and also at days 60, 95 and 125 ($p<0.05$), however, there is no significant difference at $p<0.05$ for day 30 or day 150. This analysis suggests that the Δ*sigG* strain is attenuated in the mouse model of infection in comparison to H37Rv.

Figure 3.12a

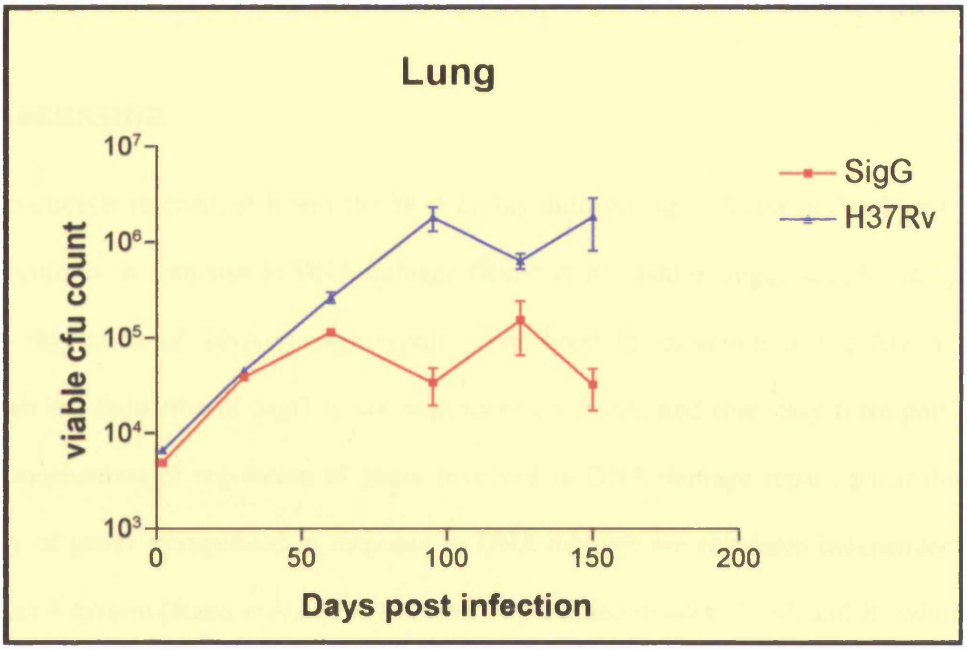

Figure 3.12b

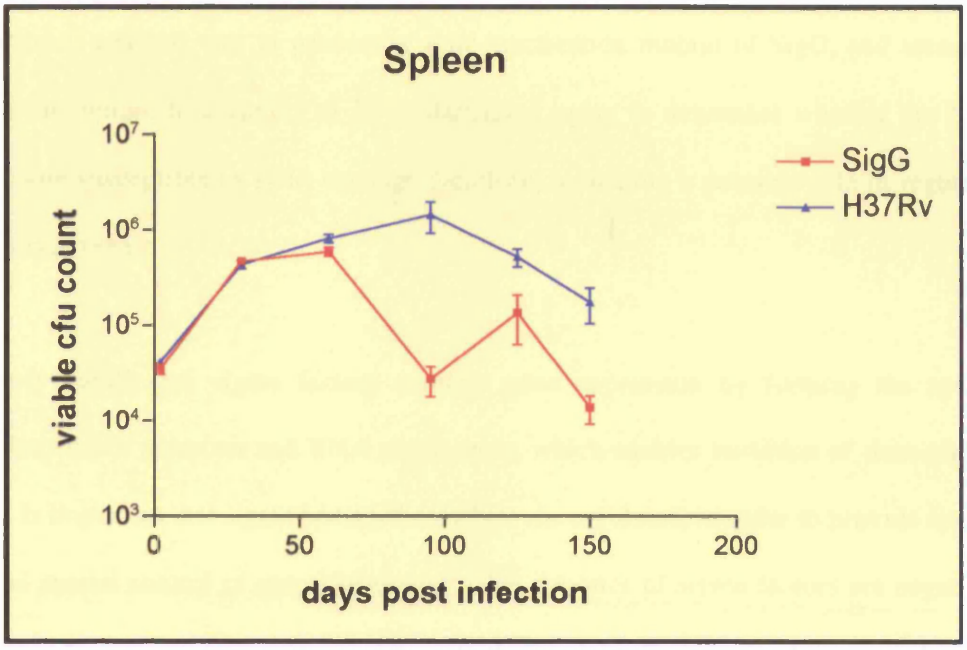

Figure 3.11: Colony counts in lung of BALB/C mice infected with Δ*sigG* strain and H37Rv wild-type. Six to eight week old female BALB/C mice were infected intravenously via the tail vain with Δ*sigG* or wild-type strains of *M. tuberculosis*. Initial colony counts were taken from the inoculum to determine the dose administered. Colony counts were then obtained from the lung (a) and spleen (b) at day 2, 30,60,95,125 and finally day 150.

3.7 Discussion

SigG is of particular interest, as it was the most highly induced sigma factor in the Δ*recA* strain of *M. tuberculosis* in response to DNA-damage (Rand *et al.*, 2003), suggesting it may play a role in the regulation of DNA-damage repair. The level of induction in the Δ*recA* strain indicates that the induction of SigG is not dependent on RecA, and thus may form part of an alternative mechanism of regulation of genes involved in DNA-damage repair, particularly as the majority of genes upregulated in response to DNA-damage are regulated independently of the RecA/LexA system (Rand *et al.*, 2003), extensively studied in both *E. coli* and *B. subtilis*.

In order to determine whether SigG played a role in regulation of DNA-damage repair, the obvious mode of analysis was to produce a gene inactivation mutant of SigG, and assess the response of the mutant to a variety of DNA damaging agent to determine whether the Δ*sigG* strain was more susceptible to DNA-damage therefore, indicating a possible role in regulation of DNA-damage repair.

As previously mentioned, sigma factors regulate gene expression by forming the specific interaction between a promoter and RNA polymerase, which enables initiation of transcription. However, it is important that sigma factors themselves are regulated, in order to provide specific temporal and spatial control of gene expression. The majority of sigma factors are negatively regulated by their cognate anti-sigma factors, which, via a number of alternative mechanisms inhibit binding of the sigma factor to the RNAP, and therefore inhibit transcription of the sigma factor's regulon. The number of different methods the various anti-sigma factors employ to inhibit sigma factor-RNAP binding is wide ranging, as sigma factors can be regulated at transcriptional, translational and post-translational levels (Helmann, 1999). The pathways

controlling anti-sigma factors can be broadly grouped into three categories, export from the cell, as seen with the flagella biosynthesis anti-sigma factor FlgM of *Salmonella typhimurium*, partner switching modules as outlined with SigF of *B. subtilis* (i.e. regulation by an anti-anti sigma factor) and interactions with small molecules or protein ligands (Helmann, 1999). A limited number of sigma factor regulators have been identified, whereby the anti-sigma factor is a transmembrane protein with an intracellular inhibitory domain, which binds and inhibits the cognate sigma factor (Yoshimura *et al.*, 2004), see table 3.7 for a few examples.

Bacterial strain	Sigma factor	Transmembrane anti-sigma factor
E. coli	SigE	RseA
	FecI	FecR
B. subtilis	SigX	RsiX
P. aeruginosa	AlgU	MucA
R. myxococcus	CarQ	CarR

Table 3.6: Sigma factors regulated by transmembrane anti-sigma factors

Interestingly 5 of the 7 ECF family sigma factors in *B. subtilis* are co-transcribed with downstream genes (Yoshimura *et al.*, 2004). SigM in *B. subtilis* is co-transcribed with two downstream genes, known to negatively regulate SigM, *yhdL* and *yhdK*. It appears that YhdL possesses 1 possible transmembrane region, whereas, YhdK the last gene in the operon possesses multiple transmembrane regions. Yeast-2-hybrid studies revealed that SigM interacts with the N-terminal region of YhdL, but not with YhdK. It has also been shown that YhdL and YhdK interact with a highly specific interaction despite the transmembrane regions. Interestingly in deletion experiments removal of regions of the trans-membrane domains nullified the interaction, which suggests the interactions of these proteins YhdL and YhdK, may take place in the cytoplasmic membrane (Yoshimura *et al.*, 2004).

Interestingly, two component regulatory systems are also able to regulate sigma factor activity, as is the case for SigE of *Streptomyces coelicolor*, which is not regulated by a membrane bound anti-sigma factor, but by a two component regulatory system (Paget *et al.*, 1999). CseB and CseC are the response regulator and histidine kinase respectively that regulate SigE (Hong *et al.*, 2002). It is also worth noting that *sigE* is co-transcribed with *cseA*, *cseB* and *cseC* (Hutchings *et al.*, 2004). SigE has been shown to not autoregulate, but is regulated by the sensor kinase CseC and the response regulator CseB, whereby CscC responds to cell wall damage, resulting in autophosphorylation, which, in turn, leads to phosphorylation of the response regulator CseB, which activates transcription from the SigE promoter (Hutchings *et al.*, 2004). It has been suggested, that CseA is a negative regulator of SigE, hypothesised to interact with the sensor kinase CseC, either directly or indirectly negatively regulating SigE (Hutchings *et al.*, 2004).

ECF sigma factors do not solely respond to environmental signals, in the case of SigR from *S. coelicolor*, the regulon is stimulated by the response of the cytoplasmic anti-sigma factor to redox (Paget *et al.*, 1998). RsrA is a member of the ZAS family of zinc binding anti-sigma factors(Li *et al.*, 2003). Under reducing conditions, RsrA binds to the N-terminal region of SigR, encompassing the region 2, thus preventing association with RNAP (Li *et al.*, 2002), then under oxidising conditions (oxidation by molecular oxygen, hydrogen peroxide or diamide), disulfide bonds are formed between the cysteine residues that form the Zn binding motif, this results in release of the Zn, causing a conformational change in RsrA, which results in release of SigR, thus enabling transcription of the SigR regulon (Bae *et al.*, 2004; Li *et al.*, 2003).

The examples of sigma factor regulation have shown that the regulation of activity is diverse. However, *sigG* is co-transcribed with two downstream genes, so, it is possible that these genes

are involved in regulation of the sigma factor, a hypothesis supported by analysis of the domain predictions for the proteins which form the SigG operon.

3.7.1 Inspection of the SigG operon

The close proximity of the two downstream genes (Rv0181c and Rv0180c) to *sigG*, initially indicated that they may be transcribed as a part of a polycistron, especially due to the small intergenic distance between *sigG* and Rv0181c, and the overlap of Rv0181c and Rv0180c. RT-PCR results confirmed that these genes were part of a polycistron. This is of particular interest, as it has been suggested that sigma factors are co-transcribed as polycistronic RNA with their cognate anti-sigma factors and anti-anti sigma factors (Raivio et al., 2001). It is therefore possible that Rv0181c and Rv0180c are required for regulation of the sigma factor SigG.

The domain analysis showed that SigG possesses homology to a sigma 70 region 2 domain, which forms the specific contact between the sigma factor-RNAP complex and the promoter –10 region (Lonetto *et al.*, 1994). Interestingly there are homologues to all three proteins of the *M. tuberculosis* SigG operon in *M. bovis*, yet only to SigG in *M. paratuberculosis*. Rv0181c shows homology to cytoplasmic proteins. Rv0180c contains multiple transmembrane domains, which suggest the protein winds in and out of the membrane, possibly to detect environmental signals. It has been shown that some anti-sigma factors are held at the cytoplasmic membrane by accessory proteins, therefore one could speculate that Rv0181c is an anti-sigma factor which may remain tethered to the cytoplasmic membrane via interactions with the anti-anti sigma factor Rv0180c, then by the mechanism of partner switching, the environmental signal could induce a conformational change in the anti-anti sigma factor, which would then have a downstream effect on the conformation of the anti-sigma factor, thus resulting in the release of

the sigma factor, to initiate transcription of the sigma factor's regulon. This is however, pure speculation, but experiments were designed with the view to analysing the interactions between SigG and the two downstream co-transcribed proteins.

The design of the peptide to produce the antibodies took into account the potential binding sites reported for sigma factors and their putative anti-sigma factors, with anti-sigma factors interacting with sigma factors via their N-terminal region (Yoshimura *et al.*, 2004). The Western did not provide conclusive evidence to determine whether the Rv0181c and Rv0180c antibodies were specific for the respective proteins; however, the SigG antibody did not react with its corresponding peptide. The problems with the SigG antibody may have been due to the poor immunogenic properties of the peptide used in the antibody synthesis. However, there are a number of considerations for the poor reactivity of the antibody. The problems with the sigma factor antibody specificity may lie partially with the location of the antigen. The sigma factors have been reported to bind the anti-sigma factors with the C-terminal region, therefore when the sigma factor is bound to the anti sigma factor, the antibody recognition site may be occluded. Alternatively there may be insufficient SigG present to be detected by a Western blot, or the antibody does not bind under the conditions used. One possibility would be to repeat the Western using more CFE, and use the terminal bleed which appeared to react more strongly by dot blot, rather than the purified fraction.

The antibodies raised to Rv0181c and Rv0180c could also be used along with an improved antibody to SigG in co-immunoprecipitation experiments to determine whether either of the two downstream genes interacts with SigG. This would be a potentially exciting method to determine the interaction of the genes in the SigG operon.

The Westerns did not show any difference between the bands present under uninduced and induced conditions for CFE from either the H37Rv or Δ*sigG* strain of *M. tuberculosis*. This suggests that the two downstream genes Rv0181c and Rv0180c may undergo both transcription and translation in the Δ*sigG* strain, however to determine this properly, the anti-bodies would need to be tested for specificity using deletion mutants of the relevant proteins. It appeared by Western, that the levels of protein are approximately equivalent in both the H37Rv and Δ*sigG* strains for both Rv0180c and Rv0181c, suggesting any potential polar effects do not play a role in the expression of these proteins, despite RT-PCR indicating that the genes are co-transcribed. Thus, to be able to analyse any role of the downstream genes in controlling SigG activity, it would be necessary to construct a new strain of *M. tuberculosis*, in which all three genes are deleted. This would then allow the assessment of expression of a SigG-dependent promoter following the re-introduction of the individual and pairs of genes. The antibodies were also intended for use in co-immunoprecipitations to determine if under certain environmental stimuli such as DNA-damage, the proteins formed an interaction, with the initial hypothesis that sigG may interact with Rv0181c (under uninduced conditions), and that Rv0181c and Rv0180c may interact (under induced conditions). The co-immunoprecipitations were not performed due to the inability of the synthesised SigG antibody to recognise its target.

The construction of the Δ*sigG* strain was such that a non-functional protein would be produced, due to the deletion of part of the coding region and the insertion of the antibiotic resistance cassette. The protein analysis revealed that contrary to microarray analysis, the levels of Rv0181c and Rv0180c were similar in the Δ*sigG* strain to H37Rv, therefore suggesting there were no polar effects of the knockout on the downstream protein expression. There may however, be differences at the transcriptional level as observed by the microarray analysis, which, may not be observed in the translation. The lack of induction detectable by Western

analysis may reflect the limited discrimination of the method in quantitation. The Western may have been saturated, therefore to determine whether the apparent lack of induction was a valid observation, a titration of both the antigen (CFE) and the antibody would need to be performed.

3.7.2 Viability of the Δ*sigG* strain

There does not appear to be any difference between the *in-vitro* growth rates of the Δ*sigG* strain or Δ*sigG* strain complements in comparison to the wild-type H37Rv. However, the Δ*sigG* strain is more susceptible than H37Rv to the DNA damaging agent, mitomycin C (significantly different $p<0.01$). Interestingly, mitomycin C causes inter-strand cross-links of complementary DNA by alkylation of guanine residues, which makes GC rich organisms more susceptible (Iyer and Szybalski, 1964).

Titration experiments revealed that Δ*sigG* strain was not significantly more susceptible to paraquat than H37Rv, contradicting the preliminary results. For the preliminary experiments, using the range of DNA damaging agents, the viability for the wild-type and Δ*sigG* strains were performed separately using different freshly made stocks of the spectrum of chemical damaging agents, whereas the wild-type and Δ*sigG* strain for the titration experiments were performed in parallel using the same freshly made stocks and dilutions of the reagents. This could therefore account for the differences observed in viability across the two experiments. The titration experiments are presumably more reliable due to the use of the same stocks and dilutions for both H37Rv and Δ*sigG* strain, leading to the conclusion that the Δ*sigG* strain is no more susceptible to paraquat stress than H37Rv.

The mitomycin C titration showed that the Δ*sigG* strain is significantly more susceptible to mitomycin C stress than wild-type. However, the full operon complement of Δ*sigG* did not completely restore susceptibility back to wild-type levels, although the complemented strain was significantly less susceptible to mitomycin C than the Δ*sigG* strain. The variation cannot be accounted for simply by the variability in the separate stocks of mitomycin C used for the biological replicates, as the initial experiment for H37Rv and Δ*sigG* strain used one freshly made stock of mitomycin C, which was repeated including the full operon complement, with a different freshly made stock, yet the biological replicates for the H37Rv and the Δ*sigG* strain were almost identical in their viability (data not shown). Strangely there was more variability in the biological replicates of the full operon complement, with one of the replicates mirroring the H37Rv wild-type at all concentrations except 0.2μg/ml. This incomplete restoration to wild-type viability may be due to the location of the integrated plasmid, whereby the topology of the DNA has a negative effect on the gene expression. This type of altered expression is known as position effect variegation in gene expression is readily observed in the more complicated system of eukaryotes, whereby transgenes integrated into or close to heterochromatin (condensed/closed chromatin) show decreased levels of transcription (Festenstein *et al.*, 1996). It may be possible that the complementing construct has integrated (at the *att* site), close to supercoiled DNA, which would hinder the access of transcription factors, and may influence gene expression such that it does not fully return to wild-type. The other possibility is that the complementing construct does not function to fully complement gene expression, or viability.

Decreased viability of the Δ*sigG* strain was also observed in the mouse *in-vivo* model of infection, where the CFU in both the lung and the spleen were significantly decreased in the Δ*sigG* strain compared to H37Rv, suggesting that Δ*sigG* strain was less virulent. This

experiment was repeated using the full and partial operon complements alongside the Δ*sigG* strain and H37Rv. However, due to technical problems with obtaining the CFU in both the lung and spleen after early time points (day 34), no H37Rv colony counts were available, after this time point and high variation was observed in very limited counts that were available for the Δ*sigG* strain and the various complements. The samples were re-streaked from frozen stocks, but technical problems in the animal facilities have prevented CFU reading.

In brief, a gene inactivation knockout of *sigG* was successfully constructed in *M. tuberculosis*; *in-vitro* analysis showed that there was no difference in *in-vitro* growth, although Δ*sigG* strain was more susceptible to mitomycin C than the wild-type, and preliminary mouse *in-vivo* growth indicates that the Δ*sigG* strain is attenuated in the mouse model. Transcriptional analysis revealed that *sigG* is co-transcribed with two downstream genes, which potentially may be involved in regulation of SigG, particularly as other sigma factors are co-transcribed with their regulatory partners. Rv0180c appears to be a transmembrane protein, whereas Rv0181c appears to be a cytoplasmic protein. One could hypothesise that Rv0180c may be involved in detection of environmental signals, which could be transmitted via Rv0181c, to activate SigG; this may be in the form of anti-anti-sigma factor (Rv0180c) and anti-sigma factor (Rv0181c). The antibodies raised to Rv0181c and Rv0180c gave inconclusive data regarding their specificity, due to the *E. coli* CFE not being an ideal negative control. However, the antibodies potentially showed that the levels of Rv0181c and Rv0180c in the Δ*sigG* strain appear to be similar to that in H37Rv, with only slightly decreased levels, therefore suggesting the Δ*sigG* mutation may have limited polar effects on the downstream genes.

4 Regulation of *sigG* and identification of its regulon

The expression level of the sigma factor, SigG (encoded by *sigG*) has been shown to be induced in response to DNA-damage, in both the H37Rv and Δ*recA* strains of *M. tuberculosis* (Rand *et al.*, 2003), suggesting that it may be involved in the response to DNA-damage. The induction of the gene in the Δ*recA* strain of *M. tuberculosis* indicates that any role in DNA-damage repair is thought to be independent of the RecA/LexA system.

It is possible that *sigG* plays a role in the response to DNA-damage, in which case, DNA-damage repair genes may form part of this sigma factor's regulon. To determine whether this was the case, microarray experiments were performed to compare the Δ*sigG* strain of *M. tuberculosis* with the H37Rv wild-type under both uninduced and induced conditions.

As *sigG* is DNA-damage inducible at the transcriptional level, it was important to determine if *sigG* possesses one or more damage inducible transcriptional start sites. The expression from these transcriptional start site(s) could then be assayed in the H37Rv wild-type, Δ*recA*, and Δ*sigG* strains of *M. tuberculosis*, to determine if RecA plays any role in transcription, and to see if *sigG* is autoregulated, which is of particular interest, as several sigma factors drive transcription from their own promoters, including *sigD* from *M. tuberculosis* (Raman et al., 2004).

4.1 Identification of the *sigG* regulon by microarray analysis

Microarray experiments were designed such that inter- and intra-strain comparisons could be made between the levels of expression under uninduced and induced (0.02μg/ml mitomycin C) conditions. This meant that RNA versus DNA arrays were performed, whereby each RNA

sample was labelled with cy5, and competitively hybridized with cy3-labelled DNA, obtained from Colorado State University. The design of the experiment took into account the difficulties observed with differential labelling with one of the dyes, as DNA was used as a normaliser across all samples, thereby enabling direct comparisons between transcriptional levels in Δ*sigG* strain compared to wild-type H37Rv, under both uninduced and induced conditions individually. Traditional microarray data gives an induction ratio, which may be skewed when the expression level of a gene is particularly low. Therefore, the ability to dissect both the uninduced and induced conditions, procures the ability to calculate the induction ratio from the uninduced and induced data. Thus enabling a more thorough picture of the expression levels in response to different environmental conditions to be constructed.

The microarray slides used were PCR spotted whole genome *M. tuberculosis* arrays, produced by the BμGS microarray unit at St. George's Hospital Medical School. Triplicate cultures for RNA samples were harvested from exponentially grown (OD_{600} 0.15) H37Rv and Δ*sigG* strains of *M tuberculosis*, and were either uninduced or induced with 0.02μg/ml mitomycin C. Both the uninduced and induced cultures were incubated for a further 24 hours after the addition of the chemical DNA damaging agent mitomycin C. Any DNA contamination was removed by DNase treatment. The RNA samples were then analysed using a Bioanalyser (Agilent Technologies) to determine the quantity and quality of the RNA preparation.

4.1.1 Analysis and input of the microarray slides

Each triplicate biological sample was used in duplicate for both the uninduced and induced (mitomycin C 0.02μg/ml) cultures of H37Rv wild-type and the Δ*sigG* strain, resulting in a

minimum of 6 slides per strain, per treatment. (Slides were repeated where there was a problem with either scratching of the slide or background fluorescence).

The slides were scanned and analysed as outlined in the methods (see section 2.13.5). The spread of the data was similar in both the H37Rv strain and the Δ*sigG* strain, therefore the statistical analysis performed on the data, was a parametric test; the Student's T-test, which assumes equal variance for the H37Rv and Δ*sigG* strains.

4.1.2 Statistical analysis of microarray data

The microarray data was analysed in two ways, to answer two different questions. The first was to identify whether SigG played a role in the regulation of genes induced by DNA-damage and the second was to look at the difference in expression between genes in the Δ*sigG* and H37Rv strains under each condition separately, producing a comparison between the expression levels of genes in the Δ*sigG* strain compared to H37Rv under uninduced and induced conditions.

4.1.2.1 SigG and the genes involved in the DNA-damage response

To address the possibility that SigG was involved in gene regulation following DNA-damage, a list of genes induced two fold or more in the H37Rv wild-type in response to DNA-damage, was collated using the 'filtering on fold change' option in Genespring, with the minimum cut off value of 2-fold induction. A parametric Student's T-test (equal variance) was then performed on the 2-fold gene list, using the log-of-ratio values, to determine if the expression of these genes was significantly different between uninduced and induced samples of H37Rv ($p<0.01$). A parametric test with equal variance (t-test) was chosen for H37Rv uninduced versus

induced comparisons, as transformation of data (log of ratios) by either $\log_{10}$ or $\log_e$ transforms the data to approximate a normal distribution (see 2.12.2), and is widely recognised as an acceptable approximation of a normal distribution. The resultant gene list contained 115 genes, whose induction ratio was greater than or equal to 2 and the uninduced values were significantly different from the induced values ($p<0.01$) for H37Rv.

Combining the H37Rv and Δ*sigG* data into one experiment in Genespring was very useful when it came to producing gene lists. The gene list of 115 genes was exported into Excel, and contained both the H37Rv and the Δ*sigG* values, which enabled a direct comparison to be made in Excel to determine whether there were any significant differences in the induction ratios of H37Rv and the Δ*sigG* strain. The data downloaded was in the format of the normalised data for each biological (1, 2 and 3) and technical replicate (A and B), for each condition (+/- mitomycin C) in both strains (H37Rv and Δ*sigG*). Calculations were performed to determine the mean, standard deviation and standard error for both the uninduced and induced values for each strain individually. Any standard errors greater than 3 standard deviations from the mean were highlighted, and the individual values were assessed. In some cases, spurious data spots had not been effectively removed in Gene Pix, which could be seen as huge numbers (>1000), usually in one out of the 6 replicates. When the data for 5 out of the 6 biological and technical replicates were within one standard deviation of the mean, and the last replicate was greater than 3 standard deviations away from the mean, these data points were removed as errors. However, outliers that were less than 3 standard deviations from the mean were included in the data.

After the removal of outliers, the induction ratios were calculated for each of the biological and technical replicates individually. The mean, standard deviation and standard error of the

induction ratios were calculated for each of the 115 genes in the list. A two-tailed Student T-test was performed in Excel to determine if there were any significant differences in induction ratio between the H37Rv wild-type and Δ*sigG* strains, using a $P<0.05$ as a cut off. Of the 115 genes tested, 17 showed a significantly different induction ratio in the Δ*sigG* strain compared to H37Rv ($P<0.05$). Of those 17, 4 had a significantly lower induction ratio in the Δ*sigG* strain compared to H37Rv (see figure 4.1a), whereas 13 had a significantly higher induction ratio in the Δ*sigG* strain compared to H37Rv (see figure 4.1b).

The four genes with the lower induction ratio *fmt*, *lexA*, Rv1956 and *sigG*, were examined more closely to reveal that all three of these genes other than *sigG* were expressed at a similar level following DNA-damage in the two strains, H37Rv and Δ*sigG* (see figure 4.1a); however, these genes were expressed at a higher level in the Δ*sigG* strain under uninduced conditions, resulting in a reduced induction ratio. The elevated level of expression observed under normal growth conditions might be attributed to the sigma factor competition, whereby the sigma factor responsible for the expression of these genes may be better able to compete for RNAP in the absence of SigG. In the case of SigG itself, expression was detected, as the probe overlaps with the retained 5′ region of SigG by approximately 48bp.

Of the 13 genes with significantly higher induction ratios, only 6 genes appear to be expressed at a higher level following DNA-damage when looking at the dissected uninduced and induced data; the other 7 genes appear to be expressed to a similar extent after DNA-damage in both the Δ*sigG* strain and H37Rv. Those genes which appear to be upregulated in Δ*sigG* strain to a greater extent than in H37Rv under induced conditions are: *dnaB* - a probable replicative DNA helicase, Rv2884 – a predicted transcriptional regulator and Rv0059, Rv2734, Rv3075c and Rv3467 which are all conserved hypothetical proteins. Further analysis revealed that only

Figure 4.1a

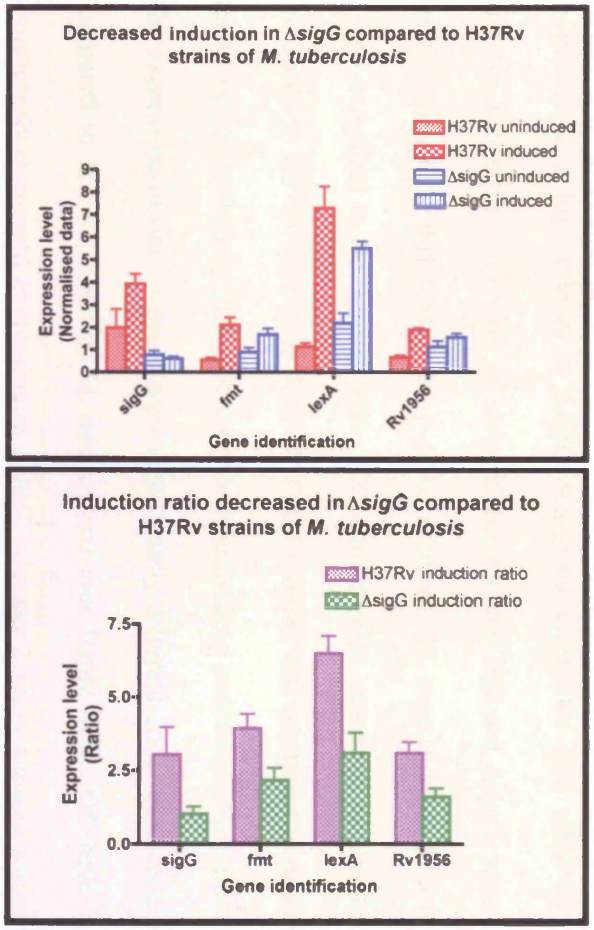

Figure 4.1b

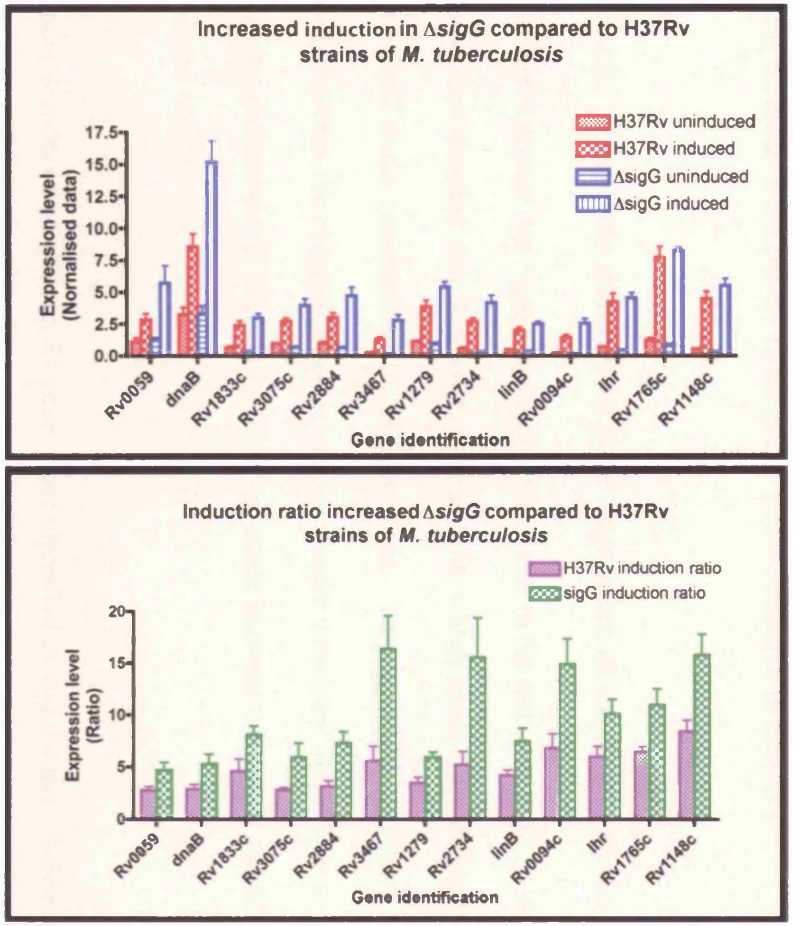

Figure 4.1a: Microarray data showing decrease in induction ratio of genes in Δ*sigG* strain, following in DNA damage. Four genes were identified that were 2-fold or more upregulated in H37Rv in response to DNA damage (mitomycin C stress), where the induction ratio in Δ*sigG* was decreased in comparison to H37Rv with $p<0.05$ (student t-test). The top graph shows the individual values under induced and uninduced conditions for each strain, whereas the bottom graph shows the induction ratio.

Figure 4.1a: Microarray data showing an increase in induction ratio of genes in Δ*sigG* strain, following in DNA damage. Thirteen genes were identified the were 2-fold or more upregulated in H37Rv in response to DNA damage (mitomycin C stress), where the induction ratio in Δ*sigG* was increased in comparison to H37Rv with $p<0.05$ (student t-test).The top graph shows the individual values under induced and uninduced conditions for each strain, whereas the bottom graph shows the induction ratio.

Rv2884 under uninduced and Rv3467 under induced conditions were significantly different using a Student t-test $p<0.01$ in the Δ*sigG* strain compared to H37Rv

4.1.2.2 Detecting differential gene expression in the Δ*sigG* strain

It does not appear that SigG plays a significant role in the response to DNA-damage. Therefore, the second question was addressed, to determine, which genes were differentially expressed in the Δ*sigG* strain compared to the H37Rv strain. To answer this question, a comparison was made between the expression levels of genes under uninduced conditions in each strain, then a separate comparison of expression level was made between the Δ*sigG* and H37Rv strains under induced conditions.

Under uninduced conditions, 81 genes were identified as significantly different between the two strains at the $P<0.01$ level, using a parametric Student's T-test (assume equal variance). Of these, 52 were expressed less in Δ*sigG* compared to H37Rv (see table 4.1), whereas 29 were expressed to a higher level in Δ*sigG* compared to H37Rv (see table 4.2). A comparison between the expression level of induced H37Rv and induced Δ*sigG*, revealed that 50 genes were significantly different at the $p<0.01$; of those, 15 were induced to a lesser extent in the Δ*sigG* compared to H37Rv (see table 4.3), and 35 were expressed to a higher degree in Δ*sigG* compared to H37Rv (see table 4.4). A Venn diagram was produced to determine if any of the genes were significantly different under both uninduced and induced conditions (see figure 4.2): The expression of only 7 genes were significantly different under both conditions in the Δ*sigG* compared to H37Rv strain of *M. tuberculosis* (see figure 4.2). Of these 7 genes, 5 showed significantly decreased expression in Δ*sigG*, whereas 2 genes showed a significant increase in expression for Δ*sigG* compared to the H37Rv wild-type (see figure 4.3a and 4.3b).

Table 4.1

		H37Rv uninduced		H37Rv induced		ΔsigG uninduced		ΔsigG induced	
Common name	Gene ID	Mean	SEM	Mean	SEM	Mean	SEM	Mean	SEM
Rv0040c	Rv0040c	2.839	± 0.317	0.692	± 0.072	1.299	± 0.136	0.495	± 0.023
fadD5	Rv0166	1.441	± 0.158	0.786	± 0.107	0.549	± 0.083	0.472	± 0.089
Rv0168	Rv0168	2.938	± 0.341	1.846	± 0.135	1.504	± 0.212	1.482	± 0.422
mce1	Rv0169	3.552	± 0.464	1.716	± 0.199	1.440	± 0.209	1.306	± 0.118
Rv0232	Rv0232	0.704	± 0.066	0.536	± 0.043	0.368	± 0.036	0.436	± 0.066
nrdB	Rv0233	0.976	± 0.099	0.603	± 0.044	0.516	± 0.026	0.471	± 0.055
Rv0312	**Rv0312**	**1.717**	**± 0.183**	**0.525**	**± 0.060**	**0.511**	**± 0.036**	**0.238**	**± 0.025**
murB	Rv0482	0.841	± 0.082	0.478	± 0.053	0.404	± 0.048	0.428	± 0.058
Rv0655	**Rv0655**	**8.305**	**± 1.261**	**3.409**	**± 0.192**	**2.552**	**± 0.392**	**1.747**	**± 0.186**
Rv0887c	Rv0887c	0.405	± 0.054	0.530	± 0.082	0.240	± 0.032	0.292	± 0.024
Rv0888	Rv0888	1.132	± 0.137	0.367	± 0.061	0.457	± 0.060	0.375	± 0.104
pks4	Rv1181	0.568	± 0.093	0.705	± 0.141	0.192	± 0.033	0.409	± 0.182
papA3	**Rv1182**	**2.713**	**± 0.354**	**1.793**	**± 0.234**	**0.244**	**± 0.024**	**0.302**	**± 0.018**
Rv1204c	Rv1204c	0.304	± 0.029	0.271	± 0.028	0.186	± 0.006	0.220	± 0.026
Rv1230c	Rv1230c	2.037	± 0.141	1.242	± 0.119	1.261	± 0.156	1.212	± 0.068
Rv1232c	Rv1232c	1.827	± 0.176	1.573	± 0.208	1.254	± 0.089	1.958	± 0.245
Rv1348	Rv1348	0.811	± 0.120	0.640	± 0.096	0.440	± 0.028	0.592	± 0.072
lprF	Rv1368	1.655	± 0.128	1.207	± 0.143	1.007	± 0.138	1.076	± 0.144
Rv1566c	Rv1566c	2.387	± 0.179	1.019	± 0.076	1.505	± 0.109	0.730	± 0.157
Rv1776c	Rv1776c	1.279	± 0.141	0.896	± 0.097	0.830	± 0.085	0.726	± 0.057
PPE	Rv1802	0.330	± 0.023	0.309	± 0.035	0.221	± 0.020	0.310	± 0.060
Rv1883c	Rv1883c	1.040	± 0.123	0.595	± 0.151	0.656	± 0.065	0.322	± 0.052
Rv1891	Rv1891	2.198	± 0.164	1.629	± 0.155	1.294	± 0.083	0.988	± 0.127
Rv1986	Rv1986	0.913	± 0.044	0.639	± 0.097	0.607	± 0.101	0.416	± 0.047
Rv1987	Rv1987	2.287	± 0.112	1.063	± 0.039	1.491	± 0.176	0.725	± 0.154
Rv2180c	Rv2180c	0.284	± 0.030	0.269	± 0.033	0.179	± 0.010	0.217	± 0.027
fabD	Rv2243	4.389	± 0.534	1.617	± 0.179	1.771	± 0.051	1.277	± 0.167
kasB	Rv2246	5.831	± 0.389	3.912	± 0.426	3.027	± 0.309	3.361	± 1.001
Rv2251	Rv2251	0.648	± 0.081	0.490	± 0.067	0.385	± 0.063	0.428	± 0.063
Rv2252	Rv2252	0.723	± 0.051	0.503	± 0.037	0.557	± 0.044	0.610	± 0.042
Rv2262c	Rv2262c	0.314	± 0.022	0.263	± 0.016	0.223	± 0.019	0.269	± 0.030
Rv2293c	Rv2293c	0.592	± 0.036	0.410	± 0.027	0.361	± 0.025	0.376	± 0.027
glyS	Rv2357	0.449	± 0.038	0.276	± 0.033	0.213	± 0.013	0.235	± 0.032
lipQ	Rv2485c	0.627	± 0.044	0.305	± 0.039	0.242	± 0.022	0.215	± 0.031
Rv2563	Rv2563	0.563	± 0.046	0.412	± 0.057	0.360	± 0.011	0.346	± 0.014
Rv2599	Rv2599	0.714	± 0.087	0.521	± 0.045	0.441	± 0.036	0.647	± 0.069
Rv2616	Rv2616	0.617	± 0.061	0.457	± 0.060	0.356	± 0.041	0.425	± 0.039
Rv2633c	Rv2633c	1.601	± 0.166	0.722	± 0.102	0.564	± 0.057	0.505	± 0.037
Rv2690c	Rv2690c	0.550	± 0.074	0.383	± 0.042	0.293	± 0.021	0.400	± 0.047
ald	Rv2780	2.855	± 0.178	1.897	± 0.313	1.744	± 0.203	1.521	± 0.112
efpA	Rv2846c	1.918	± 0.194	1.144	± 0.136	1.101	± 0.083	0.946	± 0.075
Rv2884	Rv2884	1.030	± 0.081	3.017	± 0.323	0.658	± 0.028	4.735	± 0.618
ppsE	**Rv2935**	**1.182**	**± 0.118**	**1.304**	**± 0.168**	**0.092**	**± 0.023**	**0.116**	**± 0.018**
Rv3050c	Rv3050c	1.732	± 0.215	1.445	± 0.256	0.837	± 0.134	1.137	± 0.166
Rv3083	Rv3083	0.460	± 0.055	0.356	± 0.053	0.278	± 0.013	0.267	± 0.024
nuoB	**Rv3146**	**2.343**	**± 0.650**	**1.366**	**± 0.081**	**1.058**	**± 0.112**	**0.831**	**± 0.065**
nuoL	Rv3156	2.356	± 0.215	1.953	± 0.128	1.426	± 0.144	1.416	± 0.224
Rv3402c	Rv3402c	4.299	± 0.372	2.138	± 0.217	2.141	± 0.117	1.865	± 0.223
Rv3616c	Rv3616c	3.978	± 0.697	3.148	± 0.614	1.428	± 0.087	2.025	± 0.309
Rv3633	Rv3633	5.762	± 0.310	3.511	± 0.482	3.684	± 0.345	3.312	± 0.466
Rv3719	Rv3719	2.672	± 0.169	3.148	± 0.690	1.858	± 0.085	2.838	± 0.193
Rv3764c	Rv3764c	2.513	± 0.454	1.522	± 0.138	1.313	± 0.144	1.031	± 0.112

Table 4.1: Gene list of genes showing decreased expression in uninduced conditions in Δ*sigG* compared to H37Rv wild-type. The gene list was produced in Gene spring, using a parametric t-test, with cut off p value <0.01, to determine which genes were significantly different in Δ*sigG* compared to H37Rv wild-type under uninduced conditions. The normalised expression levels were then exported into Excel, where the list was divided into genes significantly lower in the Δ*sigG* and genes significantly higher in Δ*sigG* (table 4.2) compared to H37Rv wild-type. The highlighted genes are significantly different in Δ*sigG* for both uninduced and induced (0.02μg/ml mitomycin C) conditions.

Table 4.2

		H37Rv uninduced		H37Rv induced		ΔsigG uninduced		ΔsigG induced	
Common name	Gene ID	Mean	SEM	Mean	SEM	Mean	SEM	Mean	SEM
fadE6	Rv0271c	1.455	± 0.320	1.876	± 1.004	2.706	± 0.343	2.080	± 0.510
Rv0540	Rv0540	0.362	± 0.039	0.747	± 0.209	0.888	± 0.164	0.531	± 0.073
Rv0997	Rv0997	0.982	± 0.061	1.917	± 0.229	1.544	± 0.208	1.733	± 0.092
Rv1057	Rv1057	0.509	± 0.152	0.595	± 0.088	1.208	± 0.120	0.959	± 0.052
sigE	Rv1221	2.723	± 0.438	3.138	± 0.412	5.521	± 0.358	3.231	± 0.199
Rv1261c	Rv1261c	1.438	± 0.145	2.333	± 0.798	3.078	± 0.594	1.474	± 0.097
Rv1265	Rv1265	1.706	± 0.216	2.932	± 0.805	2.695	± 0.294	1.564	± 0.155
Rv1288	Rv1288	0.520	± 0.098	0.823	± 0.191	1.316	± 0.208	1.118	± 0.082
Rv1457c	Rv1457c	0.370	± 0.025	0.506	± 0.035	0.688	± 0.118	0.466	± 0.089
PPE	Rv1809	0.674	± 0.051	0.706	± 0.070	0.947	± 0.080	0.911	± 0.077
Rv1813c	Rv1813c	0.474	± 0.137	0.392	± 0.036	1.170	± 0.116	0.951	± 0.123
ureD	Rv1853	0.533	± 0.067	0.637	± 0.043	0.876	± 0.085	0.871	± 0.083
aao	Rv1905c	0.556	± 0.049	1.145	± 0.202	1.028	± 0.154	0.879	± 0.095
rpmB2	Rv2058c	3.246	± 0.465	2.805	± 0.399	6.418	± 0.393	4.675	± 0.659
rpfE	**Rv2450c**	**0.904**	**± 0.136**	**1.115**	**± 0.062**	**1.755**	**± 0.175**	**1.844**	**± 0.119**
Rv2604c	Rv2604c	1.466	± 0.166	3.141	± 0.796	3.616	± 0.712	1.458	± 0.186
Rv2743c	Rv2743c	0.441	± 0.032	0.622	± 0.165	0.668	± 0.055	0.634	± 0.099
fadD26	Rv2930	2.185	± 0.267	4.592	± 1.114	4.129	± 0.399	6.616	± 0.980
ppsA	Rv2931	1.338	± 0.213	1.721	± 0.338	2.594	± 0.350	3.896	± 0.816
ppsD	**Rv2934**	**1.249**	**± 0.150**	**1.520**	**± 0.143**	**2.278**	**± 0.224**	**2.762**	**± 0.347**
Rv3123	Rv3123	0.485	± 0.053	0.865	± 0.206	1.074	± 0.198	0.709	± 0.085
Rv3133c	Rv3133c	0.658	± 0.049	0.978	± 0.192	1.108	± 0.095	1.110	± 0.118
Rv3482c	Rv3482c	0.792	± 0.052	0.851	± 0.052	1.239	± 0.107	1.006	± 0.089
cpsA	Rv3484	0.925	± 0.052	0.968	± 0.098	2.557	± 0.273	1.864	± 0.340
Rv3485c	Rv3485c	0.408	± 0.028	0.528	± 0.080	0.835	± 0.155	0.783	± 0.108
otsA	Rv3490	0.502	± 0.083	0.706	± 0.065	0.912	± 0.165	0.769	± 0.119
Rv3836	Rv3836	0.771	± 0.057	1.903	± 0.711	2.389	± 0.355	1.802	± 0.188
bfrB	Rv3841	1.030	± 0.172	2.603	± 1.213	2.070	± 0.330	2.571	± 0.539

Table 4.2: Gene list of genes showing increased expression under uninduced conditions in Δ*sigG* compared to H37Rv wild-type. The gene list was produced using Gene spring software, with a parametric t-test, using a cut off p value of <0.01, to determine which genes were significantly different in Δ*sigG* compared to H37Rv wild-type under uninduced condition. The normalised expression levels were then exported into Excel where the mean standard deviation and standard errors were calculated. The genes with increased mean expression levels in the Δ*sigG* strain compared to H37Rv are listed in the table, and the genes marked in bold are significantly different in Δ*sigG* compared to H37Rv under both uninduced and induced (0.02μg/ml mitomycin C) conditions.

Table 4.3

		H37Rv uninduced		H37Rv induced		ΔsigG uninduced		ΔsigG induced	
commen name	Gene ID	Mean	SEM	Mean	SEM	Mean	SEM	Mean	SEM
Rv0180c	Rv0180c	0.947	± 0.135	1.694	± 0.134	0.880	± 0.122	0.863	± 0.113
Rv0181c	Rv0181c	1.176	± 0.091	3.108	± 0.454	0.491	± 0.102	1.050	± 0.108
sigG	Rv0182c	1.985	± 0.813	3.924	± 0.401	0.785	± 0.182	0.616	± 0.096
Rv0312	**Rv0312**	**1.717**	**± 0.183**	**0.525**	**± 0.060**	**0.511**	**± 0.036**	**0.238**	**± 0.025**
Rv0655	**Rv0655**	**8.305**	**± 1.261**	**3.409**	**± 0.192**	**2.552**	**± 0.392**	**1.747**	**± 0.186**
galU	Rv0993	1.084	± 0.123	0.757	± 0.156	0.640	± 0.112	0.359	± 0.027
Rv1085c	Rv1085c	0.939	± 0.140	1.102	± 0.171	1.059	± 0.115	0.600	± 0.014
papA3	**Rv1182**	**2.713**	**± 0.354**	**1.793**	**± 0.234**	**0.244**	**± 0.024**	**0.302**	**± 0.018**
cobH	Rv2065	0.647	± 0.107	0.793	± 0.072	0.772	± 0.205	0.531	± 0.047
Rv2074	**Rv2074**	**4.866**	**± 0.524**	**4.619**	**± 0.707**	**5.101**	**± 0.306**	**2.275**	**± 0.231**
xerC	Rv2894c	1.169	± 0.126	0.665	± 0.085	0.867	± 0.044	0.317	± 0.016
ppsE	**Rv2935**	**1.182**	**± 0.118**	**1.304**	**± 0.168**	**0.092**	**± 0.023**	**0.116**	**± 0.018**
nuoB	**Rv3146**	**2.343**	**± 0.650**	**1.366**	**± 0.081**	**1.058**	**± 0.112**	**0.831**	**± 0.065**
nuoD	Rv3148	2.097	± 0.347	1.971	± 0.155	1.695	± 0.139	1.290	± 0.115
pirG	Rv3810	4.929	± 0.462	1.730	± 0.186	2.628	± 0.131	0.846	± 0.074

Table 4.3: Gene list of genes showing decreased expression under induced conditions in Δ*sigG* compared to H37Rv wild-type. The gene list was produced using Gene spring software, with a parametric t-test, using a cut off p value of <0.01, to determine which genes were significantly different in Δ*sigG* compared to H37Rv wild-type under induced (0.02μg/ml mitomycin C) conditions. The normalised expression values were then exported into Excel where the mean, standard deviation and standard errors were calculated. The genes with decreased expression under induced conditions in Δ*sigG strain* compared to H37Rv are listed above and the genes marked in bold are significantly different in Δ*sigG* compared to H37Rv under both uninduced and induced (0.02μg/ml mitomycin C) conditions.

Table 4.4

		H37Rv uninduced		H37Rv induced		ΔsigG uninduced		ΔsigG induced	
Common name	Gene ID	Mean	SEM	Mean	SEM	Mean	SEM	Mean	SEM
Rv0057	Rv0057	1.036	± 0.121	2.061	± 0.310	1.090	± 0.148	4.482	± 0.500
Rv0187	Rv0187	0.880	± 0.110	1.049	± 0.091	0.889	± 0.106	1.758	± 0.178
Rv0196	Rv0196	0.966	± 0.135	1.069	± 0.173	1.384	± 0.200	1.728	± 0.123
Rv0197	Rv0197	1.625	± 0.189	1.807	± 0.273	2.368	± 0.418	4.018	± 0.680
Rv0342	Rv0342	0.749	± 0.071	0.664	± 0.064	0.874	± 0.073	1.174	± 0.152
mgtE	Rv0362	0.406	± 0.050	0.370	± 0.024	0.461	± 0.051	0.689	± 0.070
aceA	Rv0467	1.227	± 0.145	1.259	± 0.240	2.126	± 0.283	2.106	± 0.182
atsA	Rv0711	0.788	± 0.089	0.711	± 0.064	1.387	± 0.184	1.270	± 0.166
cysM3	Rv0848	0.316	± 0.052	0.311	± 0.042	0.364	± 0.041	0.691	± 0.063
Rv0849	Rv0849	0.231	± 0.045	0.206	± 0.033	0.175	± 0.021	0.343	± 0.021
echA6	Rv0905	0.811	± 0.095	1.160	± 0.085	1.263	± 0.093	2.124	± 0.248
Rv0906	Rv0906	0.893	± 0.115	1.166	± 0.140	1.386	± 0.048	1.884	± 0.164
Rv0970	Rv0970	0.575	± 0.060	0.527	± 0.065	0.590	± 0.031	0.888	± 0.113
PPE	Rv1168c	0.387	± 0.049	0.450	± 0.053	0.363	± 0.029	0.760	± 0.053
cysN	Rv1286	0.404	± 0.035	0.262	± 0.026	0.415	± 0.054	0.428	± 0.056
Rv1393c	Rv1393c	0.423	± 0.071	0.350	± 0.031	0.516	± 0.059	0.540	± 0.035
Rv1804c	Rv1804c	0.218	± 0.057	0.197	± 0.075	0.138	± 0.059	0.618	± 0.041
Rv2011c	Rv2011c	0.550	± 0.206	0.412	± 0.090	0.755	± 0.192	1.005	± 0.002
rpmG	Rv2057c	4.921	± 1.063	3.161	± 0.482	15.091	± 5.847	6.290	± 0.409
rpfE	**Rv2450c**	**0.904**	**± 0.136**	**1.115**	**± 0.062**	**1.755**	**± 0.175**	**1.844**	**± 0.119**
Rv2566	Rv2566	0.469	± 0.062	0.329	± 0.020	0.459	± 0.075	0.433	± 0.024
Rv2862c	Rv2862c	1.348	± 0.330	0.436	± 0.055	0.629	± 0.111	0.980	± 0.032
ppsB	Rv2932	0.600	± 0.068	0.729	± 0.069	1.063	± 0.064	1.645	± 0.179
ppsD	**Rv2934**	**1.249**	**± 0.150**	**1.520**	**± 0.143**	**2.278**	**± 0.224**	**2.762**	**± 0.347**
lppX	Rv2945c	1.891	± 0.294	1.565	± 0.252	2.207	± 0.162	3.002	± 0.344
Rv2961	Rv2961	0.727	± 0.084	0.754	± 0.109	1.011	± 0.116	1.674	± 0.186
ilvB	Rv3003c	1.727	± 0.176	0.944	± 0.066	1.446	± 0.218	1.494	± 0.086
lpqA	Rv3016	0.561	± 0.050	0.695	± 0.032	0.867	± 0.139	1.169	± 0.124
Rv3467	Rv3467	0.273	± 0.036	1.313	± 0.201	0.180	± 0.017	2.797	± 0.409
Rv3522	Rv3522	0.964	± 0.263	0.582	± 0.040	0.996	± 0.180	0.928	± 0.087
acs	Rv3667	0.729	± 0.033	0.793	± 0.097	0.954	± 0.074	1.155	± 0.081
Rv3780	Rv3780	2.188	± 0.234	2.068	± 0.270	2.302	± 0.172	3.337	± 0.304
Rv3835	Rv3835	1.476	± 0.258	1.479	± 0.149	2.340	± 0.545	2.667	± 0.414
glpQ1	Rv3842c	6.158	± 1.244	5.464	± 0.631	5.492	± 0.704	9.239	± 0.961
serS	Rv3848c	0.218	± 0.021	0.205	± 0.024	0.247	± 0.033	0.293	± 0.026

Table 4.4: Gene list of genes showing increased expression under induced conditions in Δ*sigG* compared to H37Rv wild-type. The gene list was produced using Gene spring software, with a parametric t-test, using a cut off p value of <0.01, to determine which genes were significantly different in Δ*sigG* compared to H37Rv wild-type under induced (0.02μg/ml mitomycin C) condition. The normalised expression values were then exported into Excel where the mean, standard deviation and standard error were calculated. The genes with increased expression under induced conditions in the Δ*sigG* strain compared to H37Rv are listed above, and the genes marked in bold are significantly different in Δ*sigG* compared to H37Rv under both uninduced and induced (0.02μg/ml mitomycin C) conditions.

Figure 4.2

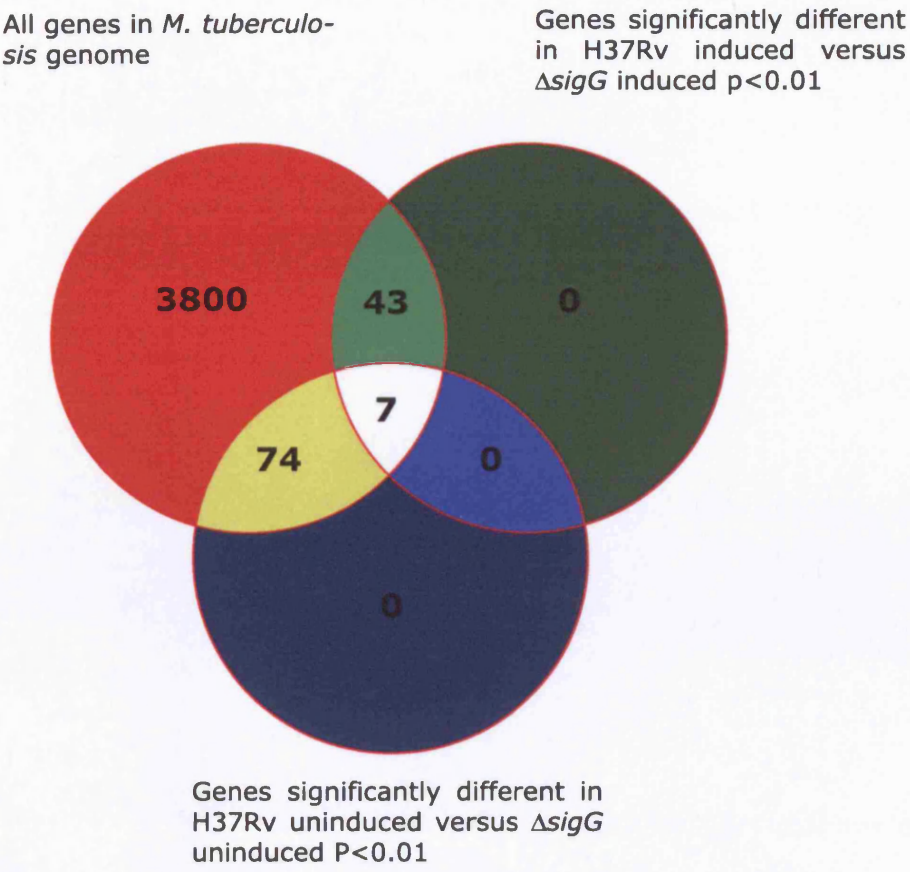

Figure 4.2: A Venn diagram of genes significantly different in H37Rv and Δ*sigG* under induced and uniduced conditions. Microarrays were perfomed with RNA extracted from H37Rv and ΔsigG strains under uninduced and induced (0.02μg/ml mitomycin C) conditiond. The Venn diagram was constructed in Gene Spring microarray analysis programme, using genes lists derrived by ANOVA statistical analysis. The Venn diargam illustrates that 7 genes are significantly different under both restrictions, whereas 43 genes are only significantly different between H37Rv and ΔsigG under induced conditions, and 74 genes are significantly different between H37Rv and ΔsigG under uninduced conditions.

Figure 4.3a

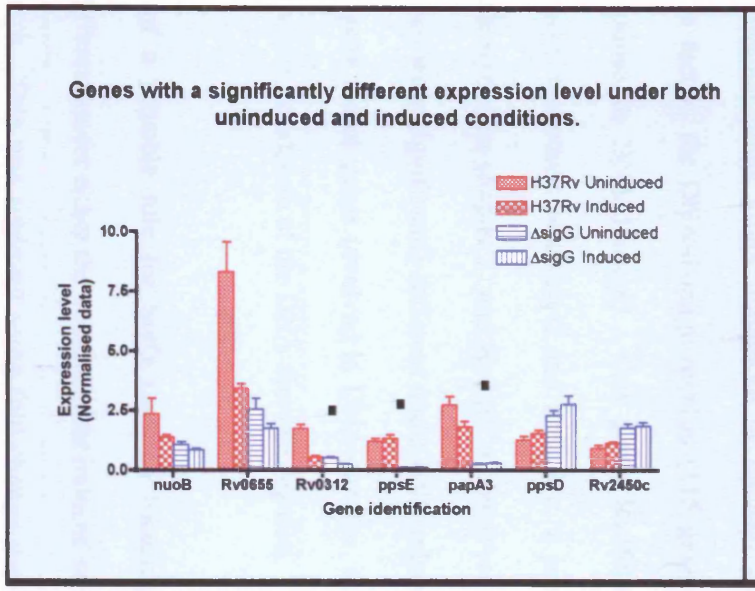

Figure 4.3b

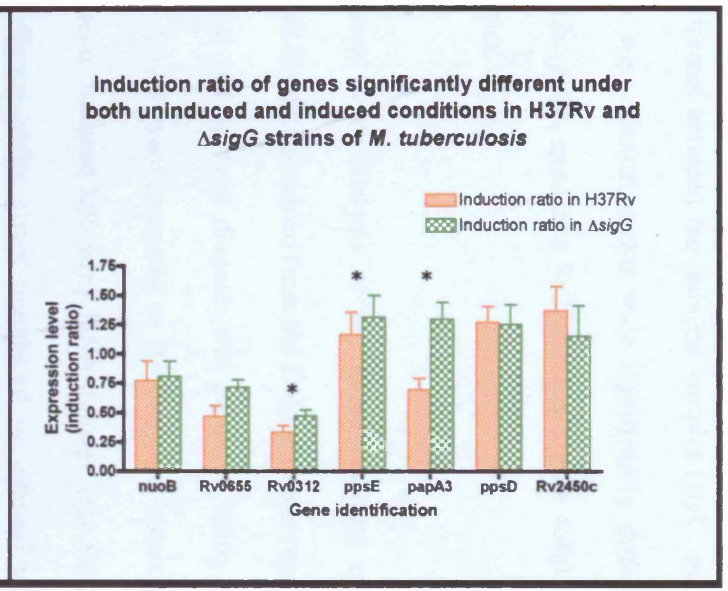

Figure 4.3a: Genes significantly different under both uninduced and induced conditions for ΔsigG compared to H37Rv wild-type. Data obtained from DNA vs RNA microarrays. Venn diagram was used to show which genes were significantly different with $p<0.01$ using a student t-test between ΔsigG and H37Rv. The normalised values of uninduced and induced expression were plotted for each strain. The first 5 genes show decreased expression in ΔsigG strain (*nuoB*, Rv0655, Rv0312, *ppsE* and *papA3*), whereas the last two genes (*ppsD* and Rv2450c) show increased expression in ΔsigG. The box indicates genes where the expression level is less than 1.

Figure 4.3b: Induction ratio of genes significantly different under both uninduced and induced conditions for DsigG compared to H37Rv wild-type. Data obtained from DNA vs RNA microarrays. Venn diagram was used to show which genes were significantly different with $p<0.01$ using a student t-test between ΔsigG and H37Rv, and individual induction ratios were calculated and plotted. The asterisk marks the induction ratios that are missleading due to very low levels of expression observed with individual normalised values (figure 4.3a).

When the strains were compared using a Student T-test, $p<0.05$, alongside a Benjamini and Hochberg false discovery rate (FDR) correction, only three genes were identified that were significantly different between the induced samples (*sigG*, *papA3* and *ppsE* (see figure 4.4a)), and five genes were identified that were significantly different under uninduced conditions (*papA3*, Rv2633c, *ppsE*, *cpsA* and Rv2293c (see figure 4.4b). The significance of these genes are discussed later.

The data obtained from analysis of the uninduced and induced conditions were used in conjunction with the data obtained from the DNA-damage regulon to determine if there was any overlap. To that end, a Venn diagram was produced using the genes that were significantly different in the Δ*sigG* strain compared to H37Rv under either uninduced or induced conditions, alongside the genes induced following DNA-damage (see figure 4.5). Only 4 genes that were significantly different under either uninduced or induced conditions for *sigG* compared to H37Rv were in fact in the DNA-damage regulon (115 genes, upregulated 2-fold or more in H37Rv in response to DNA-damage). One gene, Rv2884, is a predicted transcriptional regulatory protein, the others were *sigG* and Rv0181c, a predicted hypothetical protein, co-transcribed with *sigG* (see chapter 3) and Rv3467 a conserved hypothetical protein. However, none of the genes were significantly different under both induced and uninduced conditions and present in the gene list of genes involved in DNA-damage, thus adding more proof that SigG did not play a role in regulation of the DNA-damage regulon.

Identification of a possible role for SigG required focusing on the 131 genes, that were significantly different under either the uninduced or induced conditions, and assigning them into functional groups. This was achieved using fold change (Geiman *et al.*, 2004; Raman *et al.*, 2004) whereby Δ*sigG* gene expression was expressed as a proportion of H37Rv gene

Figure 4.4a

Figure 4.4b

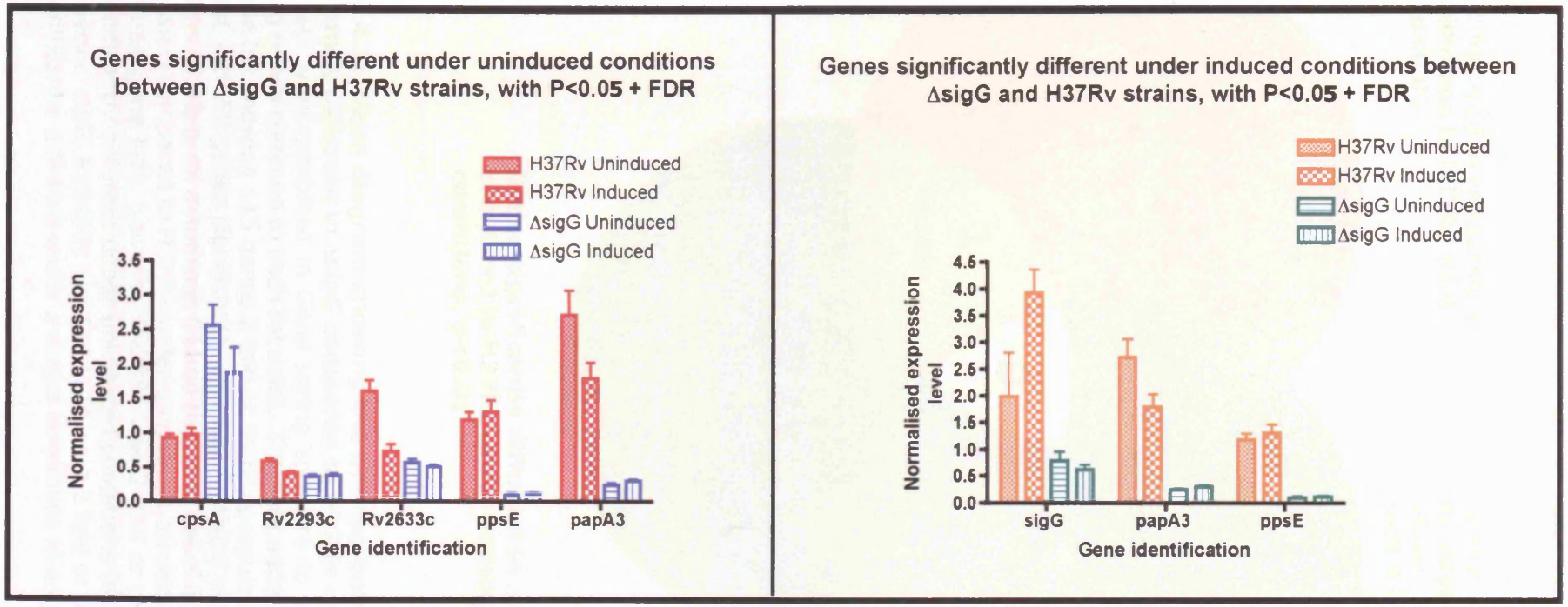

Figure 4.4a: Genes significantly different in the Δ*sigG* compared to H37Rv under uninduced conditions at P<0.05 with Benjamini false discovary rate correction. Genes were identified using Genes spring where there was a significant difference at p<0.05 between the normalised expression levels under uninduced conditions for Δ*sigG* compared to H37Rv, then a Benjamini and Hockberg false discovery rate correction was applied to the data.

Figure 4.4b: Genes significantly different in the Δ*sigG* compared to H37Rv under induced conditions at P<0.05 with Benjamini false discovary rate correction. Genes were identified using Genes spring where there was a significant difference at p<0.05 between the normalised expression levels under induced conditions (0.02μg/ml mitomycin C) for Δ*sigG* compared to H37Rv, then a Benjamini and Hockberg false discovery rate correction was applied to the data.

Figure 4.5

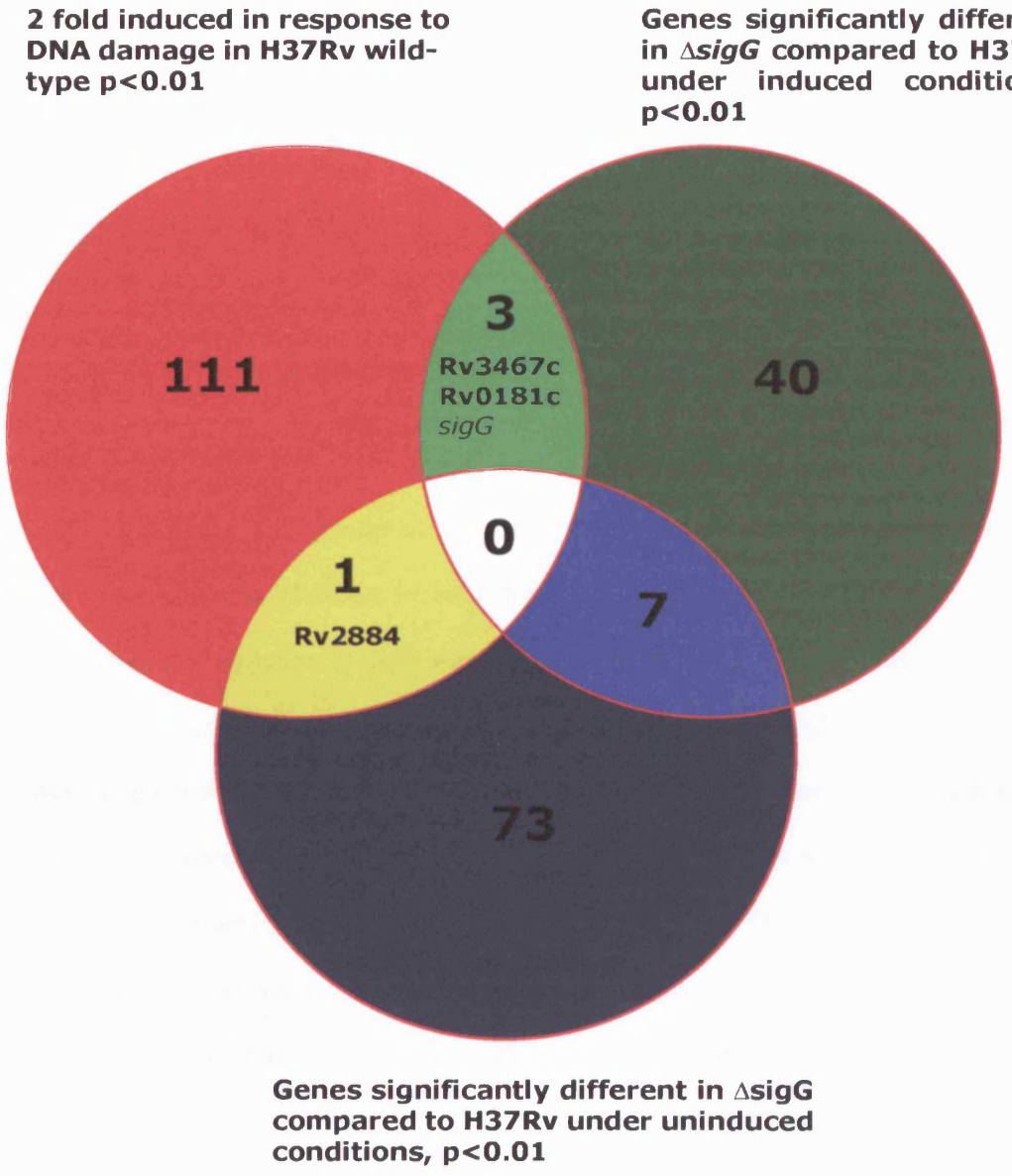

Figure 4.5: Venn diagram showing the overlap between genes found to be signifcantly different in Δ*sigG* compared to H37Rv under various conditions. Gene lists were combined in Gene spring software to produced a venn diagram, showing genes common to each list used. The data added to the venn diagram were the gene list showing 115 genes 2 fold or more upregulated in H37Rv ($p<0.01$), the gene list with 50 genes significantly different in Δ*sigG* versus H37Rv under induced condtions (0.02μg/ml mitomycin C) and the gene list of 81 genes significantly different in Δ*sigG* compared to H37Rv under uninduced condtions. No genes were present in all three gene lists, however, Rv2884 was 2 fold or more upregulated in H37Rv and significantly different under uninduced conditions in Δ*sigG* compared to H37Rv. Three genes, sigG, Rv3467c and Rv0181c were 2 fold or more upregulated in H37Rv and significantly different under induced conditions in Δ*sigG* compared to H37Rv.

expression. The cut-off values were set at >1.7 fold and <0.59 (1/1.7) fold. This revealed that 36 genes were expressed significantly less in the Δ*sigG* strain, with p<0.01, cut-off >1.7 (see table 4.5), and 16 genes, were significantly higher in Δ*sigG* strain with a fold change of <0.59 (see table 4.6). This data was then collated into functional groups, using the data available on the TubercuList website (see table 4.5 and 4.6).

4.2 Identification of *sigG* transcriptional start site(s)

Microarray analysis of Δ*recA* strain compared to H37Rv strain of *M. tuberculosis* had shown that SigG was the most highly induced sigma factor in response to DNA-damage (Rand *et al.*, 2003). with only a slight decrease in induction in the Δ*recA* strain compared to wild-type, suggesting that the regulation of *sigG* was not hindered by the absence of RecA. However, even though the microarray data presented in section 4.1 showed that SigG was not involved in regulation of genes involved in DNA-damage response, *sigG* was induced in H37Rv wild-type yet *sigG* did not appear to be induced in response to DNA-damage in the Δ*sigG* strain, which may have been a result of the position of the microarray probe,. Therefore, experiments were performed to determine the number and location of transcriptional start site(s), and to identify which were DNA-damage inducible, as well as to determine whether *sigG* is subject to autoregulation.

4.2.1 Primer extension of *sigG*

Primer extension reactions utilise radioactively end-labelled primers combined in a reaction with reverse transcriptase to produce cDNA from an RNA template, in order to determine the quantity and position of the 5′ end of the RNA molecule. Primer extension reactions were carried out using 50μg of RNA, extracted from uninduced and induced (mitomycin C, final

Table 4.5

Fold change ≥ 1.7			
Gene	Mean	SEM	Functions:
Lipid metabolism			
ppsE	19.21	± 5.71	PHENOLPTHIOCEROL SYNTHESIS TYPE-I POLYKETIDE SYNTHASE PPSE
papA3	11.69	± 1.73	PROBABLE CONSERVED POLYKETIDE SYNTHASE ASSOCIATED PROTEIN PAPA3
pks4	3.73	± 1.20	PROBABLE POLYKETIDE BETA-KETOACYL SYNTHASE PKS4
fadD5	3.19	± 0.50	PROBABLE FATTY-ACID-CoA LIGASE FADD5 (FATTY-ACID-CoA SYNTHETASE) (FATTY-ACID-CoA SYNTHASE)
fabD	2.52	± 0.34	MALONYL CoA-ACYL CARRIER PROTEIN TRANSACYLASE FABD (Malonyl CoA:AcpM acyltransferase) (MCT)
kasB	2.04	± 0.27	3-OXOACYL-[ACYL-CARRIER PROTEIN] SYNTHASE 2 KASB (BETA-KETOACYL-ACP SYNTHASE) (KAS I)
Virulence			
mce1A	2.90	± 0.36	MCE-FAMILY PROTEIN MCE1A
Cell wall and cell processes			
Rv0888	2.73	± 0.44	PROBABLE EXPORTED PROTEIN
murB	2.33	± 0.45	PROBABLE UDP-N-ACETYLENOLPYRUVOYLGLUCOSAMINE REDUCTASE MURB
Rv3402c	2.07	± 0.25	CONSERVED HYPOTHETICAL PROTEIN
Rv1348	2.06	± 0.24	PROBABLE DRUGS-TRANSPORT TRANSMEMBRANE ATP-BINDING PROTEIN ABC TRANSPORTER
lprF	1.93	± 0.46	PROBABLE CONSERVED LIPOPROTEIN LPRF
Rv2690c	1.93	± 0.30	PROBABLE CONSERVED INTEGRAL MEMBRANE ALANINE AND VALINE AND LEUCINE RICH PROTEIN
Rv1230c	1.76	± 0.28	POSSIBLE MEMBRANE PROTEIN
efpA	1.74	± 0.12	POSSIBLE INTEGRAL MEMBRANE EFFLUX PROTEIN EFPA
Intermediary metabolism and respiration			
lipQ	2.68	± 0.28	PROBABLE CARBOXYLESTERASE LIPQ
nuoB	2.30	± 0.55	PROBABLE NADH DEHYDROGENASE I (CHAIN B) NUOB (NADH-UBIQUINONE OXIDOREDUCTASE CHAIN B)
Rv2251	1.81	± 0.26	POSSIBLE FLAVOPROTEIN
nuoL	1.79	± 0.34	PROBABLE NADH DEHYDROGENASE I (CHAIN L) NUOL (NADH-UBIQUINONE OXIDOREDUCTASE CHAIN L)
Rv3083	1.75	± 0.21	PROBABLE MONOOXYGENASE (HYDROXYLASE)
ald	1.74	± 0.21	SECRETED L-ALANINE DEHYDROGENASE ALD (40 KDA ANTIGEN) (TB43)
Information pathways			
glyS	2.28	± 0.41	PROBABLE GLYCYL-tRNA SYNTHETASE GLYS (GLYCINE--tRNA LIGASE) (GLYRS)
nrdB	2.01	± 0.17	PROBABLE RIBONUCLEOSIDE-DIPHOSPHATE REDUCTASE (BETA CHAIN) NRDB
Regulatory proteins			
Rv3050c	2.29	± 0.38	PROBABLE TRANSCRIPTIONAL REGULATORY PROTEIN (PROBABLY ASNC-FAMILY)
Rv0232	2.06	± 0.30	PROBABLE TRANSCRIPTIONAL REGULATORY PROTEIN (PROBABLY TETR/ACRR-FAMILY)
Rv3764c	2.03	± 0.38	POSSIBLE TWO COMPONENT SENSOR KINASE TCRY
Conserved and hypothetical proteins			
Rv0655	3.79	± 0.40	POSSIBLE RIBONUCLEOTIDE-TRANSPORT ATP-BINDING PROTEIN ABC TRANSPORTER MKL
Rv0312	3.49	± 0.52	CONSERVED HYPOTHETICAL PROLINE AND THREONINE RICH PROTEIN
Rv2633c	3.04	± 0.49	HYPOTHETICAL PROTEIN
Rv3616c	2.88	± 0.52	CONSERVED HYPOTHETICAL ALANINE AND GLYCINE RICH PROTEIN
Rv0040c	2.28	± 0.31	SECRETED PROLINE RICH PROTEIN MTC28 (PROLINE RICH 28 KDA ANTIGEN)
Rv0168	2.28	± 0.45	CONSERVED HYPOTHETICAL INTEGRAL MEMBRANE PROTEIN YRBE1B
Rv2616	1.75	± 0.21	CONSERVED HYPOTHETICAL PROTEIN
Rv1883c	1.74	± 0.25	CONSERVED HYPOTHETICAL PROTEIN
Rv1891	1.73	± 0.17	PROBABLE MEMBRANE PROTEIN
Rv0887c	1.73	± 0.14	CONSERVED HYPOTHETICAL PROTEIN

Figure 4.5: Microarray data of genes with a fold change of greater than or equal to 1.7 for H37Rv compared to Δ*sigG* strains of *M. tuberculosis*. The normalised data for H37Rv was expressed as a proportion of Δ*sigG*, for uninduced cultures, giving a fold change, all data with a fold change of ≥ 1.7 were identified. This indicated that the expression level in H37Rv was ≥ 1.7 times the expression level in Δ*sigG* strain.

Table 4.6

Fold change >0.59			
Gene	**Mean**	**SEM**	**Function**
Lipid metabolism			
fadD26	0.58	± 0.03	FATTY-ACID-CoA LIGASE FADD26 (FATTY-ACID-COA SYNTHETASE)
ppsD	0.55	± 0.05	PHENOLPTHIOCEROL SYNTHESIS TYPE-I POLYKETIDE SYNTHASE PPSD
Information pathways			
rpmB2	0.52	± 0.10	PROBABLE 50S RIBOSOMAL PROTEIN L28 RPMB2
sigE	0.49	± 0.06	ALTERNATIVE RNA POLYMERASE SIGMA FACTOR SIGE
Cell wall and cell processes			
rpfE	0.54	± 0.10	PROBABLE RESUSCITATION-PROMOTING FACTOR RPFE
Intermediary metabolism			
Rv3485c	0.58	± 0.09	PROBABLE SHORT-CHAIN TYPE DEHYDROGENASE/REDUCTASE
bfrB	0.53	± 0.10	POSSIBLE BACTERIOFERRITIN BFRB
Rv2604c	0.50	± 0.07	PROBABLE GLUTAMINE AMIDOTRANSFERASE SNOP
Conserved and hypothetical proteins			
cpsA	0.40	± 0.08	CONSERVED HYPOTHETICAL PROTEIN
Rv0540	0.45	± 0.06	CONSERVED HYPOTHETICAL PROTEIN
Rv1057	0.39	± 0.07	CONSERVED HYPOTHETICAL PROTEIN
Rv1261c	0.54	± 0.10	CONSERVED HYPOTHETICAL PROTEIN
Rv1288	0.44	± 0.11	CONSERVED HYPOTHETICAL PROTEIN
Rv1813c	0.45	± 0.15	CONSERVED HYPOTHETICAL PROTEIN
Rv3123	0.57	± 0.14	HYPOTHETICAL PROTEIN
Rv3836	0.35	± 0.05	CONSERVED HYPOTHETICAL PROTEIN

Table 4.6: Microarray data of genes with a fold change of less than 0.59 for H37Rv compared to *ΔsigG* stain of *M. tuberculosis*. The normalised data for H37Rv was expressed as a proportion of *ΔsigG*, for uninduced samples, resulting in a fold change. The data above is therefore expressed 1.7 times higher in *ΔsigG* compared to H37Rv strains of *M. tuberculosis*

concentration 0.02μg/ml) cultures of wild-type H37Rv *M. tuberculosis*, alongside a no RNA control. Prior to the primer extension, the RNA samples were quantified using a spectrophotometer, and the primer extension was performed using a primer sigGmidH, designed from within the predicted coding region of *sigG* (see figure 4.6a and b), based on the predictions available on the TubercuList website. The primer extension reactions were run alongside manual sequencing reactions, where the template used for the sequencing reactions was a clone, constructed in pBluescript, containing the upstream region and predicted coding region of *sigG* (see table 2.2). The same primer was used in the primer extension and sequencing reactions so one could determine the exact transcriptional start site. A commercially available control (1.2kb kanamycin positive control RNA, Promega) was used which produced a band of 87bp. However, although the manual sequencing reactions with the *sigG* primer produced a clear manual sequencing trace, the primer extension reactions failed to produce a product (data not shown).

A test was performed whereby the radiolabelled primer was either ethanol precipitated after the labelling reaction, cleaned up using a G25 column, or left as they were. These were then run on a polyacrylamide gel, either undiluted or diluted 1/10 (data not shown). The G25 spin columns appeared to remove all the unincorporated label (usually present as a smear), but also appeared to remove the primer, despite the fact that the primer was larger than the cut off of the G25 spin columns. The unpurified primer, diluted 1/10 gave the least smearing, so, the remaining primer extension reactions were carried out using 1/10 diluted primer, as outlined in figure 4.6b.

The primer extension reactions were repeated using different quantities of RNA, 25, 45 and 85μg of RNA, the quantity of the RNA was increased, due to the low level of expression of *sigG* (Manganelli *et al.*, 1999). However, no transcriptional start sites were identified.

Figure 4.6a

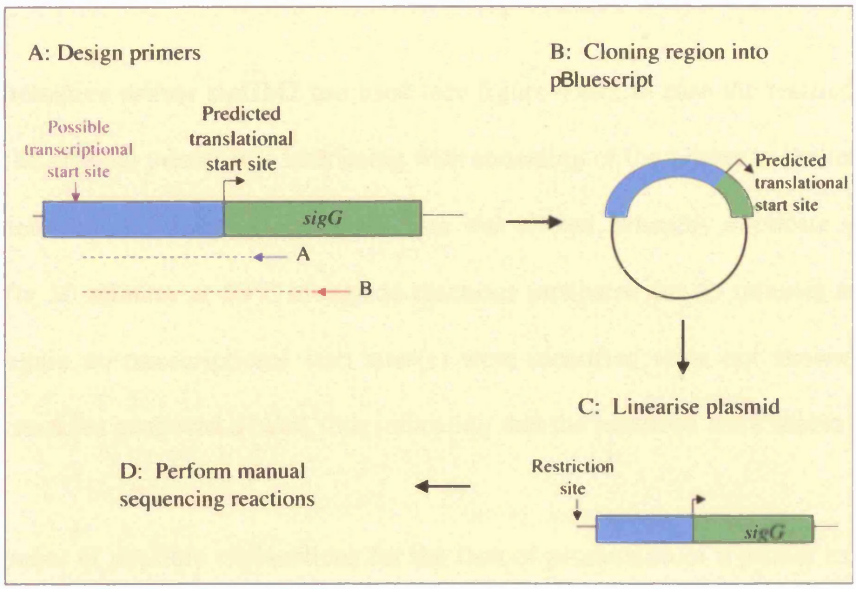

Figure 4.6b

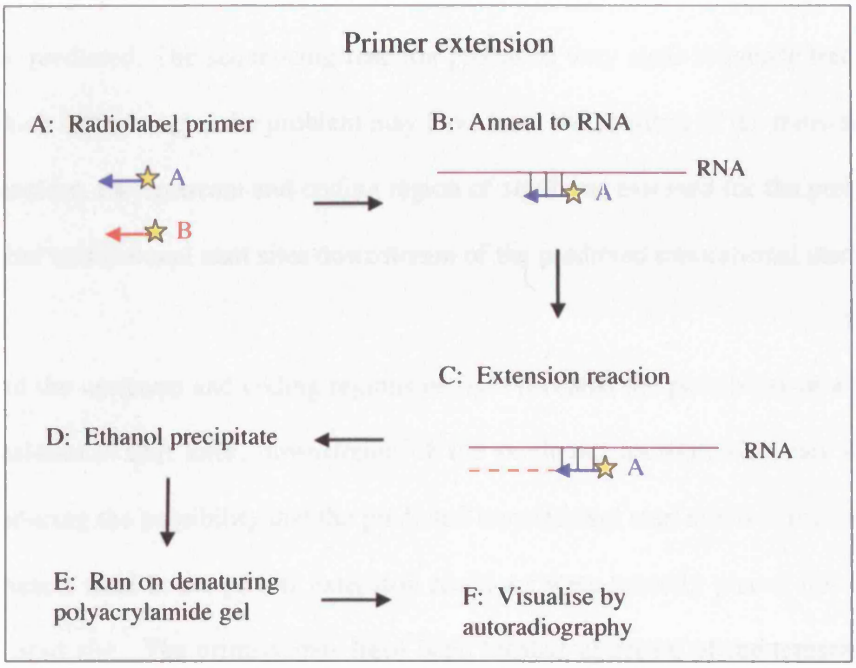

Figure 4.6a: Schematic representation of the primer designed to perform the primer extension assay and the manual sequencing reactions. Arrow A, corresponds to the primer extension primer sigGM2, located 47bp downstream, of the translational start site, and arrow B correponsed to primer extension primer sigGmidH, located 89bp downstream of the translational start site. The region of interest was cloned into pBluescript and the sequenced clone was used in the manual sequencing reactions.

Figure 4.6b: Schematic representation of the primer extension reactions. The primer extension primers A and B as outlined above, were end-labelled with γ32P-ATP. Primer A (or B) was then annealed to the total RNA from H37Rv wild-type *M. tuberculosis*. Extension reactions were carried out using AMV reverse transcriptase to produce cDNA, which was then ethanol precipitated, run on a denaturing polyacrylamide gel and visualised by autoradiography.

Therefore an alternative primer sigGM2 use used (see figure 4.6a), in case the restriction site on the 3′ end of the original primer was interfering with annealing of the primer to the template. In addition, the temperature of the extension reaction was altered, whereby duplicate samples were incubated for 30 minutes at 60°C alongside reactions incubated for 45 minutes at 54°C. However, once again no transcriptional start sites(s) were identified (data not shown). The positive control reactions produced a band, thus indicating that the reactions were successful.

There were a number of possible explanations for the lack of production of a primer extension product. Either both primers used were unable to bind effectively to the RNA template at the reaction temperatures tested, or the transcriptional start site(s) was further upstream or downstream than predicted. The sequencing reaction produced very clear sequence traces with both primers, which indicated that the problem may have been the position of the transcriptional start site(s). Therefore, the upstream and coding region of *sigG* was assessed for the presence of additional potential translational start sites downstream of the predicted translational start site.

Closer analysis of the upstream and coding regions of *sigG* revealed the possibility of a number of different translational start sites, downstream of the predicted translational start site (see figure 4.7), introducing the possibility that the predicted translational start site was incorrect and therefore, the primers used in the primer extension reactions were actually placed upstream of the translational start site. The primers may have been located upstream of the transcriptional start site(s), which would have resulted in no primer extension product, or if the primers were located in too close a proximity to the transcriptional start site(s), the resulting primer extension products would have been so small that they would not have been resolved from the unincorporated labelled primers. Due to these possibilities, an alternative method was sought, whereby the position of the predicted translational start site was not such a vital issue. RNase

Figure 4.7

Figure 4.7: Relative positions of primers used in Primer extension and the potential translational start sites. The primers indicated in yellow were used to clone the *sigG* region into pBluescript for manual sequencing. The green primer (sigGM2) and the yellow primer (sigGMidH) were used in both the sequencing and primer extension reactions. The predicted translational start site is marked in red with an arrow indicating the direction of translation. The alternative translational start sites are outlined with a pink box, and a potential ribosome binding site gtgaga is underlined in red.

protection was chosen as it enables production of a probe of approximately 500bp used to detect the transcriptional start site(s), which gives a larger region of the gene to use as a probe, thus relinquishing the need to know the exact position of the translation start site.

4.2.2 RNase protection of *sigG*

The possibility of a discrepancy between the predicted translational start site and the actual translational start site was taken into account in the design of the RNase protection assay for *sigG*. A region of 386bp was cloned into pCR4-Blunt, containing 311bp downstream of the predicted translational start site and 75bp upstream of the translational start site. This region was cloned between the T3 and T7 promoters of pCR4-Blunt, to be used in an *in-vitro* transcription reaction to produce a complementary radiolabelled RNA probe (see chapter 5, figure 5.4). An outline of the RNase protection assay can be found in chapter 5 (section 5.2.1). A number of optimisation steps were performed prior to the RNase protection assay, to determine the optimum conditions for the reaction (outlined in section 5.2.1, figures 5.5, 5.6, 5.7 and 5.8).

The RNase protection assay was performed using 40μg of total RNA extracted at mid-exponential phase (OD 0.35), from H37Rv wild-type, *ΔrecA* and *ΔsigG* strains, under both uninduced and induced (mitomycin C 0.02μg/ml) conditions. The assay in the Δ*sigG* strain indicated that *sigG* possesses 2 possible transcriptional start sites, indicated by arrows 1 and 2 (figure 4.8), both of which appeared to be inducible, whereas in the H37Rv and Δ*recA* strains, one of these was detected (see figure 4.8). Interestingly, the level of expression appeared to differ between strains, yet closer examination of the autoradiograph showed a band co-migrating with the probe control for the induced sample (track 2, figure 4.8), suggesting in this

Figure 4.8

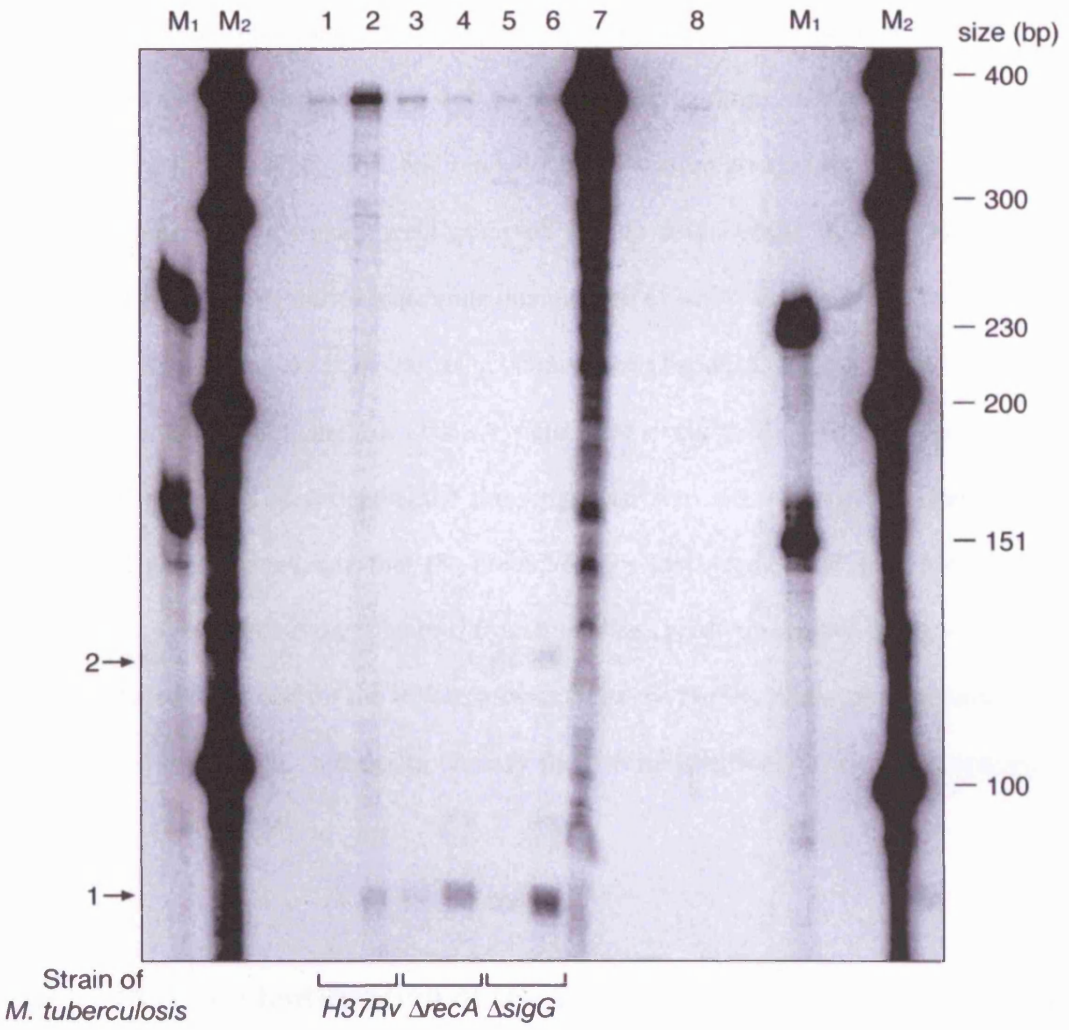

Figure 4.8: RNase protection assay to identify the *sigG* promoters in H37Rv, Δ*recA* and Δ*sigG* strains of *M. tuberculosis*. Assays were performed with 40μg of RNA, harvested at an optical density of 0.3, under uninduced and induced (0.02μg/ml mitomycin C) conditions for H37Rv (tracks 1 and 2), Δ*recA* (tracks 3 and 4) and Δ*sigG* (tracks 5 and 6) strains of *M. tuberculosis*. The strains are indicated below the tracks. The undigested probed was used as a positive control (track 7) and yeast RNA was used as a negative control (track 8). Samples were run alongside *in-vitro* transcribed markers (track M1 and M2), sizes are indicated. Two products are marked with arrows 1 and 2.

case that the RNase digestion may have been incomplete. Therefore, even though it appeared that the level of expression under induced conditions was greater in the *ΔrecA* strain, and greater still in the *ΔsigG* strain, in comparison to H37Rv, this result is not conclusive. It is also possible that this difference may be due to differential loading. However, the same RNA samples were also used in the *ruvC* and *recA* RNase protection assays (see section 5, figures 5.9 and 5.11), where weaker signals were observed for the *ΔsigG* strain than H37Rv, suggesting that if differential loading due to inaccurate quantitation of RNA were the case, one would have expected the level to be lower in the *ΔsigG* strain (see chapter 5, figures 5.9, 5.11 and 5.12). This indicates that equal quantities of RNA were most likely used in all the RNase protection assays. Identification of two potential transcriptional start sites of approximately 80bp and 120bp (see figure 4.8) indicate that the prediction for the translational start site is probably wrong. This approximate sizing obtained from the RNase protection assay, along with the clone used to produced the probe for the RNase protection assay, facilitated the performance of a new primer extension reaction, in order to identify the precise positions of the transcriptional start sites.

4.2.3 Precise identification of the *sigG* transcriptional start site(s)

The primer extension reactions were repeated, using the primers designed to produce the construct of *sigG* in pCR4-Blunt for the RNase protection assay. The clone constructed to produce the complementary RNA probe for the RNase protection assays was also used in the sequencing reactions, which were run alongside the primer extension reactions to determine the precise transcriptional start site(s) of *sigG*. The primer extension reactions were performed using 80μg of total RNA extracted at mid-exponential phase (OD 0.35), from H37Rv wild-type and *ΔsigG* strains of *M. tuberculosis*, under both uninduced and induced (mitomycin C

0.02μg/ml) conditions. In the H37Rv wild-type, three bands were visible, indicated with arrows 1,2 and 3 (figure 4.9). In the *ΔsigG* strain, only two bands were present, indicated with arrows 1 and 2 (figure 4.9). In both H37Rv wild-type and *ΔsigG* strains, one of the promoters P1, was clearly DNA-damage inducible (arrow 1, figure 4.9), whilst the P2 promoter may also be induced, but to a lesser extent (arrow 2, figure 4.9). The level of transcription and induction (where applicable) remains the same for both the P1 and P2 promoters, in both H37Rv wild-type and *ΔsigG* strains (arrows 1 and 2 respectively, figure 4.9). Interestingly there appeared to be no expression from the P3 promoter in the *ΔsigG* strain, suggesting that this promoter may be SigG dependent. It is also noteworthy that the level of expression from the P3 promoter is particularly low, especially when taking into account the amount of total RNA (80μg) used in the primer extension reaction.

4.2.4 Identification and analysis of promoter motifs

Analysis of the upstream region of *sigG* using the manual sequencing trace and the primer extension products, made it was possible to locate and identify the three transcriptional start sites (see figure 4.10). Closer analysis of the region enabled identification of potential σ^{70} consensus motifs at both the –10 and –35 sites for the P1 promoter (see figure 4.10), although there are two different possibilities for the location of the –35 site for the P1 promoter. One of these is highlighted in the green box, and shows homology to the consensus for *M. tuberculosis* σ^{70} -10 TA(G/T)(A/G)aT and -35 sites TtGaCa (Gomez M, 2000), the other potential –35 site identified is underlined in green (Gamulin *et al.*, 2004) (see figure 4.10). The motif defined by Gamlin *et al.*, (2004) tTGTCRgtg-N_8-TAnnnT (R indicates a G/A), was suggested to define a novel RecA/LexA independent promoter. The potential –10 site for the P2 promoter is indicated in blue (figure 4.10), with homology to the σ^{70} consensus, however, no consensus

Figure 4.9

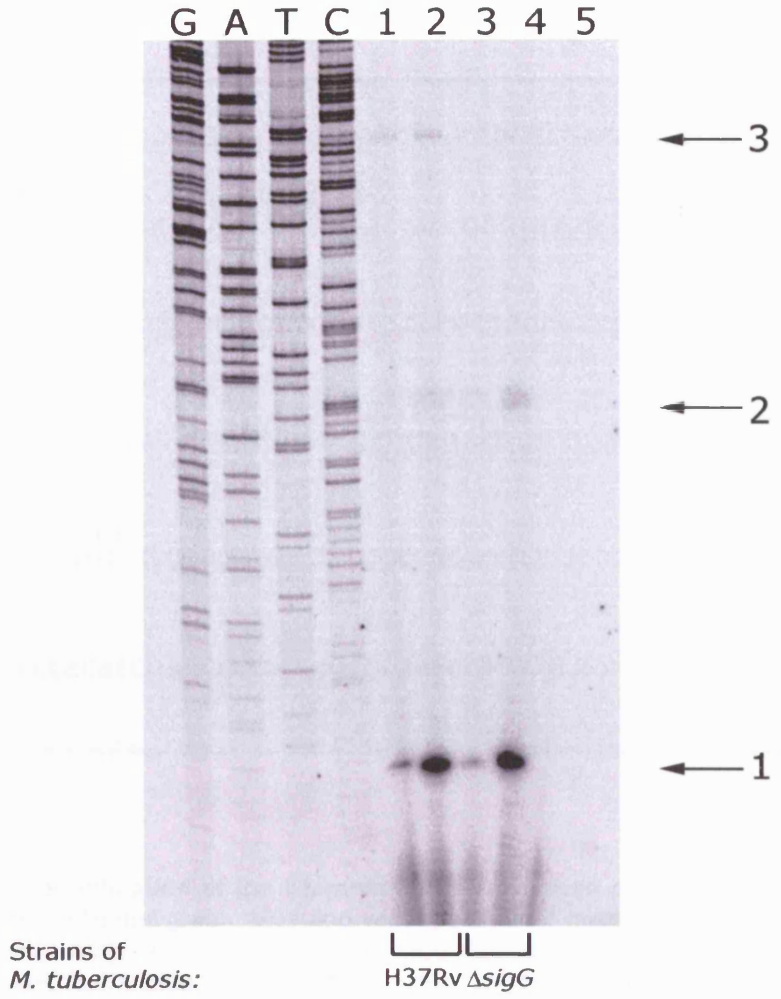

Figure 4.9: Primer extension of *sigG*. Assays were perfomed on 80µg of RNA under uninduced (track 1 and 3) and induced (0.02µg/ml mitomycin C) (tracks 2 and 4) conditions for H37Rv (tracks 1 and 2) and Δ*sigG* (tracks 3 and 4) strains of *M. tuberculosis*, alongside a negaitve control (track 5). Cultures were induced at an OD of 0.3, both uninduced and induced cultures were inbubated for a further 24 hours. The primer extension and sequencing reactions were carried out with the sigGRNaseR2 primer. Reactions were run on a denaturing polyacrylamide gel and visualised by autoradiography.

Figure 4.10

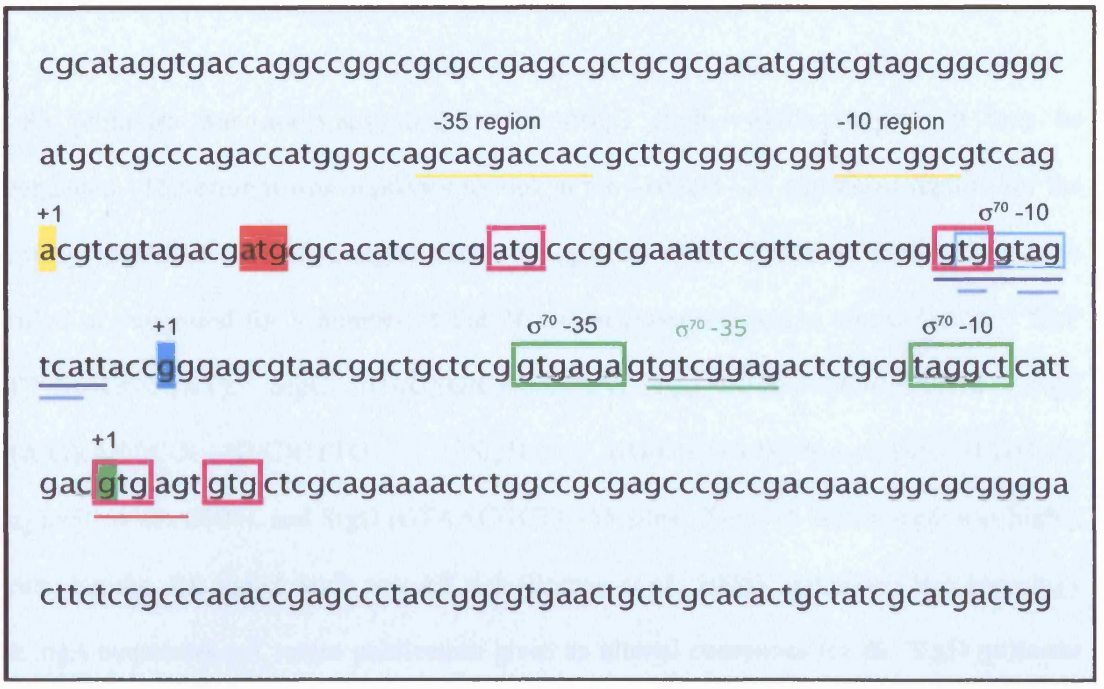

Figure 4.10: Identification of the transcriptional start sites of *sigG*. The transcriptional start sites are highlighted green, blue and yellow, with a +1 indication above. The promoter consensus sequences are indicated with a box, colour corresponding to the transcriptional start site. Therefore the potential -10 and -35 consensi for P1 are indicated in green and show homology to the *M. tuberculosis* σ^{70} consensus TA(G/T)(A/G)aT (-10) and TtGaCa (-35). The green underline and σ^{70} -35 label indicate an alternative prediction of the -35 promoter regions (Gamulin *et al.*, 2004). Regions of homology are underlined in black. The σ^{70} -10 denoted by the blue box representing P2, shows limited homology to the *M. tuberculosis* σ^{70} consensus TA(G/T)(A/G)aT (-10). The possible extended -10 is underlined in light blue. The dark blue line that extends under the σ^{70} -10 shows homology to the region between the -10 of the P2 promoter of *recA* and the transcriptional start site. The possible -10 and -35 regions of the P3 promoter are underlined in yellow. The potential ribosome binding site is underlined in red (GTGAG). The originally predicted translational start site is marked in red, and the alternative-potential translational start sites are outlined in pink.

motif was identified at the –35 site for the P2 promoter. There is an alternative possibility, that the position of the –10 sites is closer to the transcriptional start site, and therefore forms an extended –10 region (see figure 4.10, underlined in light blue).

The P3 promoter was not transcribed in the *ΔsigG* strain, which suggests it may be autoregulated. Therefore it was important to look at the –10 and –35 consensus regions for the previously identified alternative sigma factor recognition sites. Promoter motifs have been identified or suggested for a number of the *M. tuberculosis* alternative sigma factors: SigF (GTTT-N_{17}-GGGTAT), SigC ((G/C)(G/C)(G/C)AAT-$N_{16\text{-}20}$-CGT(G/C)(G/C)(G/C)), SigE (GG(A/G)(A/C)C-N_{18}-(G/C)GTTG), SigH ((G/C)GGAAC-$N_{17\text{-}22}$-((G/C)GTT(G/C)) (Manganelli *et al.*, 2004), and SigD (GTAACGCT) –35 sites. The –35 site of *sigD* was highly GC rich, but the –10 site of SigD was AT rich (Raman *et al.*, 2004), and shows less homology to the *sigA* consensus. A recent publication gives an altered consensus for the SigD promoter motif AGAAAG-$N_{16\text{-}20}$-CGTTAA (Calamita *et al.*, 2005). It appears that the consensus sequences identified for the alternative sigma factors differ somewhat from the general σ^{70} consensus of *M. tuberculosis* and appear to have a higher GC content that the σ^{70} consensus (*sigA*). Therefore, if *sigG* is autoregulated from the P3, the promoter consensus may differ somewhat from the general σ^{70} consensus of *M. tuberculosis*, which may indicate why it was not possible with only one promoter to define a –10 or –35 promoter consensus sequence. However GC rich regions were identified at both the –10 and –35 regions, underlined in yellow (see figure 4.10). It is clear that the SigG P3 promoter does not exhibit homology to any of the previously defined sigma factor consensus motifs. Without the upstream regions of other genes in the SigG regulon for comparison it is not possible to predict the promoter consensus for the SigG specific –10 and –35 regions. The microarray data presented in section 4.1 from the *ΔsigG* strain indicated there are a number of genes that appear to be regulated by SigG, such as

papA3 and *ppsE*. Primer extension studies could be performed on genes identified by the microarray analysis as part of the SigG regulon, with a view to identify their transcriptional start sites, and use this information to predict a potential consensus recognition site for SigG.

To determine if there was any homology between the P3 promoter region and the upstream region of genes thought to be in the SigG regulon, a 42bp region, upstream of and including the transcriptional start site (–41 to +1) of the P3 promoter of *sigG* was used in a MEME software (Bailey and Gribskov, 1998) motif search to identify any regions of homology. Sequences incorporating 150bp upstream and 100bp downstream of the predicted translational start sites for *nuoB*, Rv0655, Rv0312, *ppsE* and *papA3* were assembled in MEME, along with the 42bp region of the P3 promoter of *sigG*. A motif search was performed to identify a maximum number of 3 motifs, with the motif width limited to 4-11bp. For *nuoB* and Rv0655, both motif 1 and 2 were identified in relatively close proximity, in the correct orientation, whereas for Rv0312, both motifs were identified, but in the incorrect orientation (see figure 4.11). It is possible however, that one of these is correct. For *ppsE*, the motif 2 was identified upstream too far of the motif 1, however problems have been encountered with the predictions of the translational start sites as mentioned. For *papA3*, none of the motif searches revealed a possible homologous motif to the P3 promoter region of *sigG*. However, there appear to be some similarities, as indicated with the red boxes.

Interestingly further analysis using part of the predicted motif from MEME revealed that a potential SigG consensus of CGACC(W)(t/c)C-N_{13-22}-TGTCCG, where w is a/t/g, was present within 100bp of the predicted translational start sites, see below:

Figure 4.11

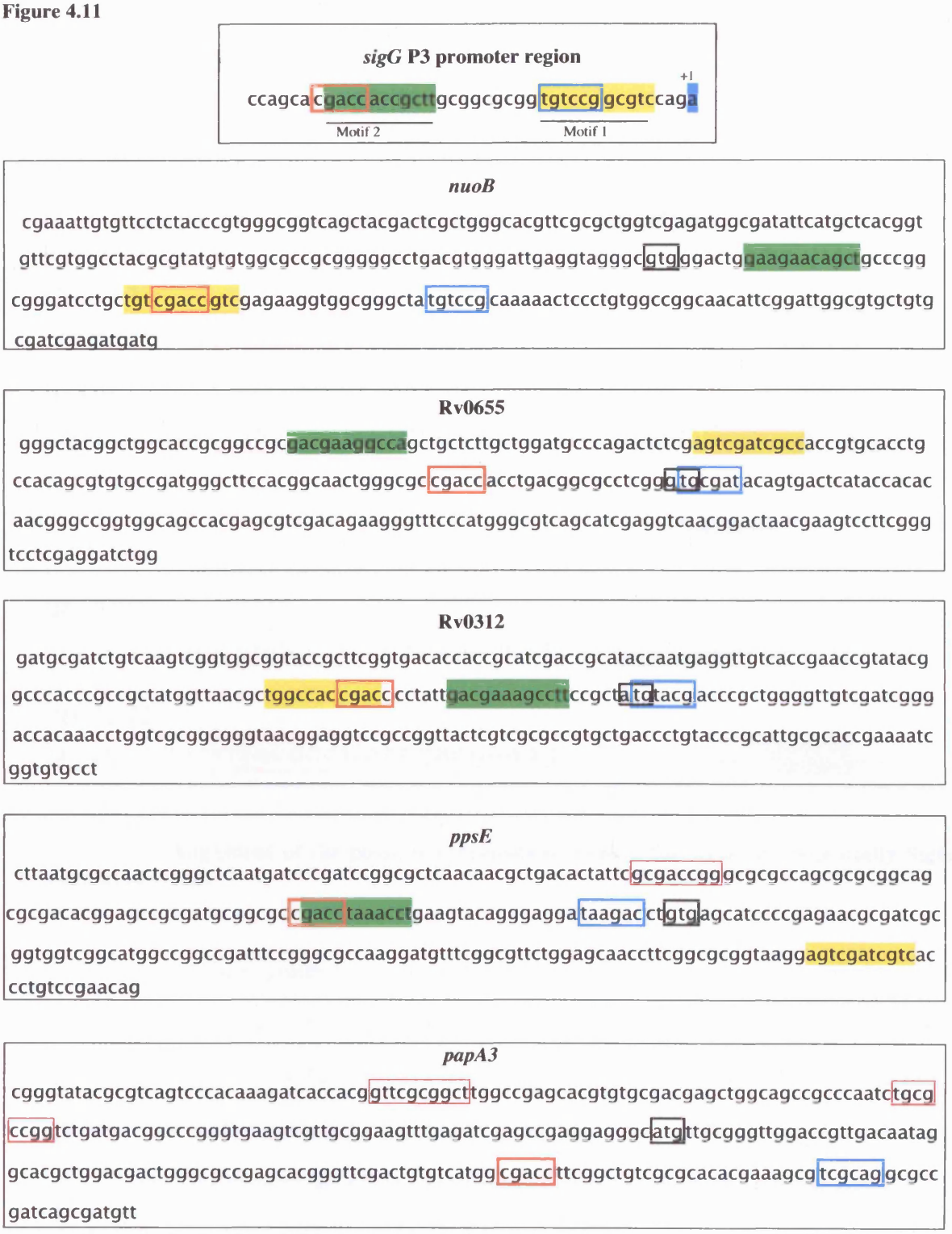

Figure 4.11: MEME motif search using the P3 promoter region of *sigG*. Motif 1 (yellow) represents a possible –10 region, and motif 2 (pink) represents a possible –35 site. The predicted translational start sites are highlighted with a box, and other potential –10/-35 sites are highlighted with a red box. Homology between part of the –35 motif and the MEME consensus revealed an alternative for the –35 site consensus CGACC, boxed in orange, and the corresponding –10 sites are boxed in light blue.

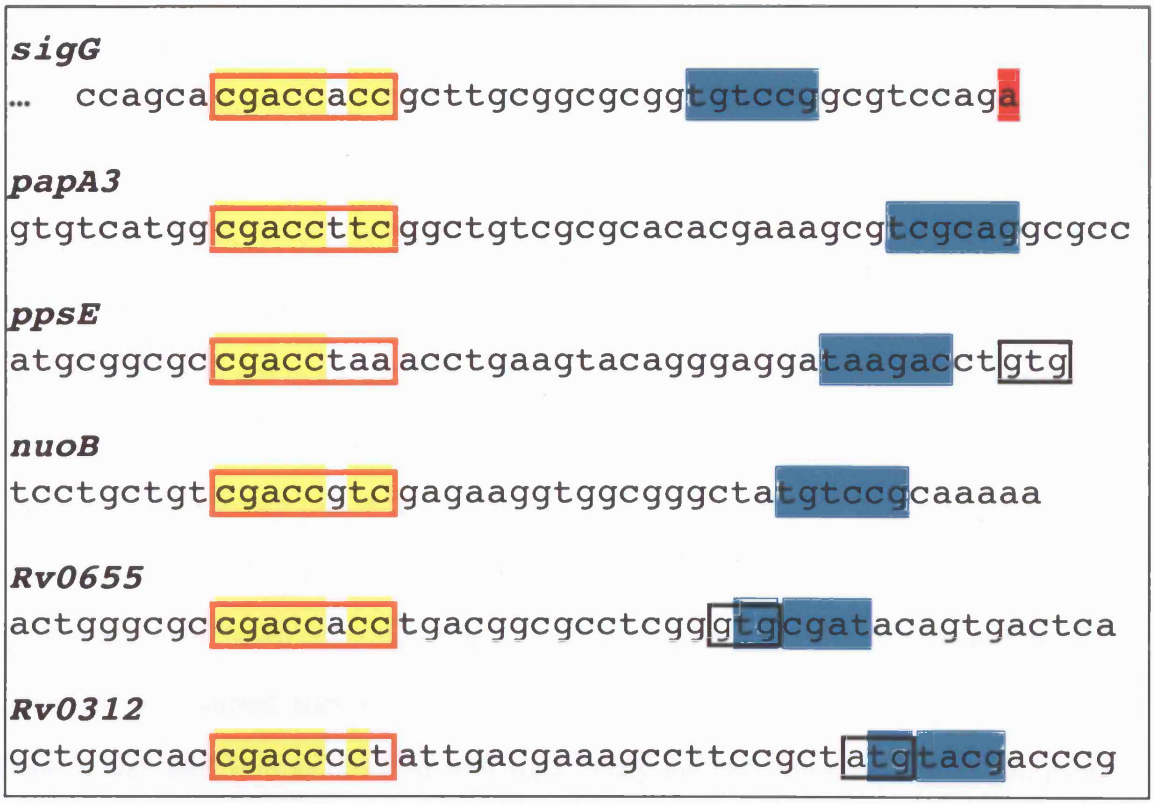

Table 4.7: Alignment of the possible consensus sequences for *sigG* and potentially SigG regulated genes.

There appears to be a greater degree of similarity at the –35 sites rather than the –10 site, which has been observed before with other ECF family sigma factor (Raman *et al.*, 2004). Interestingly, *nuoB*, Rv0655 and Rv0312 show a high degree of homology at both the –10 and –35 sites. The SigG consensus for *papA3* was 71bp downstream of the predicted translational start site and 37bp downstream of the predicted translational start site of *nuoB* (see figure 4.11). Conformation of the consensus would require either RNase protection or primer extension to identify the transcriptional start sites of the aforementioned genes, which could then be used in conjunction with the microarray findings to search for other genes regulated by SigG using the defined consensus.

An additional interesting feature was identified within the promoter region for *sigG*, upstream of the second transcriptional start site (figure 4.10, underlined in dark blue). The motif GTGGTagTCATT is also found with minor variation (GTGGTgaTCATT) upstream of the –10 site of the P2 promoter of *recA* (see chapter 5, figure 5.2c). The consensus sequence GTGGT-n_2-TCATT was used in the DNA pattern search tool, available on the TubercuList website, to determine whether this motif occurred upstream of the predicted translational start sites of other genes. The search was limited to allow 1bp mismatch in the first part of the consensus, and 1bp mismatch in the second part of the consensus, and a filter was applied to restrict the search to sequences between 150bp before and 100bp after the predicted translational start sites. These parameters were chosen rather than simple restricting the search to the upstream regions of the predicted translational start sites due to potential problems with mis-identification of the translational start sites as observed with *sigG*. Only the two genes *sigG* and *recA*, used to define the consensus were identified with no mismatches, while 24 genes were identified with 1 mismatch, and 207 genes were identified with 2 mismatches (see appendix III).

None of the 24 genes with the 1bp mismatch were significantly different in the Δ*sigG* microarrray data compared to H37Rv. However, 4 of the genes significantly different in uninduced Δ*sigG* compared to H37Rv were present in the list of genes with 2bp mismatch to the consensus: Rv1232c, Rv2616, Rv2743c and *ald* (see figure 4.12 and table 4.7). The expression level of Rv1232c, *ald* and Rv2616 is decreased in Δ*sigG* strain under uninduced conditions, whereas the expression level of Rv2743c is increased under uninduced conditions with $p<0.01$ (Student t-test, assume equal variance – see section 4.3.2). Curiously, Rv1232c appears to be induced in Δ*sigG* strain, but not in H37Rv; however, this difference is not significant at $p<0.01$ between the strains.

Figure 4.12

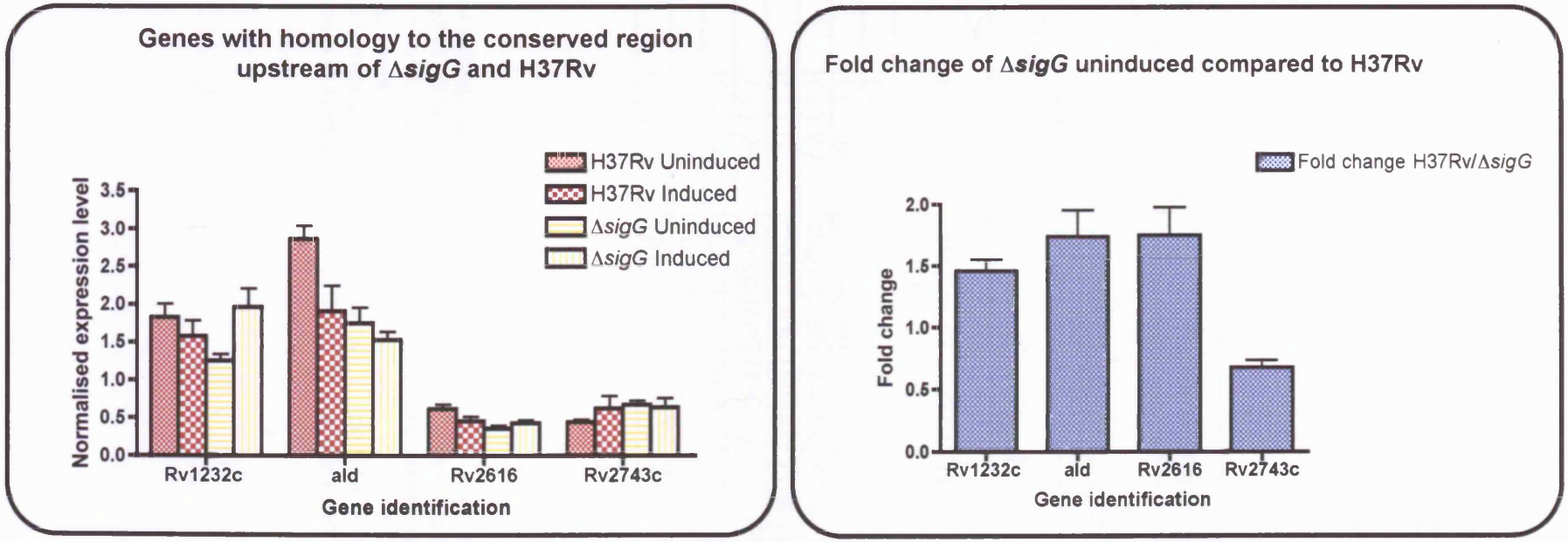

Figure 4.12: A comparison between genes identified with conserved upstream regions which are significantly different in ΔsigG strain and H37Rv. These regions of homology GTGGTn$_2$TCATT were defined by Gamulin *et al.*, (2004) as the RecA-NDP or RecA non dependent promoter, These regions were identified upstream of 4 genes which were significantly different in the Δ*sigG* strain under uninduced conditions. The fold change was calculated as H37Rv as a proportion of Δ*sigG* strain.

Table 4.8

Gene	Location	Pattern sequence
0 mismatches		
sigG	(+) 42	cagtccgg**GTGGT**ag**TCATT**accggga
recA	(-) 102	cggctact**GTGGT**ga**TCATT**cggagca
mismatch 1bp		
end	(+) 3	agacttgg**GTTGT**gc**TCATT**ggttcgc
mismatch 2bp		
ald	(-) 9	tatcgaga**GGGGT**aa**TCATG**cgcgtcg
dnaE1	(+) 17	tcatctgc**GGGGT**cc**TCCTT**cgtgcac
Rv1765c	(+) 27	ctggcgca**GCGGT**ag**TCAGT**cctgccg
Rv1232c	(+) 38	gcctggcg**GTGGC**cg**GCATT**gtgattg
Rv2015c	(+) 27	ctggcgca**GCGGT**ag**TCAGT**cctgccg
Rv2616	(+) 0	ctggccag**GTGGA**cc**TCAAT**gcgctgg
Rv2743c	(+) 29	cgccggcc**GTGGC**gt**TCGTT**gctgcag
Rv2792c	(-) 34	cgatcttg**CTGGT**ct**TCATC**gccttgc
uvrB	(+) 21	gtcacttc**GAGGT**gg**TCAGT**ccgcatg
uvrD2	(-)134	tgagcgca**GCGGT**ga**TCATG**acacgc

Table 4.8: Interesting genes with the *sigG/recA* consensus in close proximity to predicted translational start sites. Genes identified with the GTGGTn$_2$TCATT consensus within close proximity to predicted translational start sites. These genes were either significantly different in the ΔsigG strain compared to H37Rv in microarray analysis, or were identified as possessing a RecA-NDp as outlined in Gamulin *et al.*, (2004), or are involved in DNA damage repair.

The list of 47 genes identified with the RecA-NDp consensus (Gamulin *et al.*, 2004), were analysed for the presence of the potential conserved region, GTGGT-n_2-TCATT, with 1 or 2 mismatches. A total of 6 genes were identified that possessed both the RecA-NDp and the conserved region: *dnaE1*, *uvrB*, *uvrD2*, Rv1765c, Rv2015c and Rv2792c, with the conserved region located within a maximum of 34bp proximity of the predicted translational start sites, except for *uvrD2*, located 134bp upstream of the translational start site (see table 4.7). One other gene, *end*, involved in DNA repair, also possessed the conserved region (see table 4.7), in this case, with only a single mismatch. Thus, it is possible that this motif plays a role in the regulation of expression of a subset of genes following DNA-damage.

4.3 Discussion

4.3.1 Analysis of the *sigG* regulon

The initial hypothesis was that SigG was involved in regulation of genes involved in DNA-damage repair. This hypothesis was based on viability data (see chapter 3), which indicated that the Δ*sigG* strain was significantly more susceptible to the chemical DNA damaging agent mitomycin C, than the H37Rv wild-type strain. Previous microarray analysis has also revealed that *sigG* was the most highly induced sigma factor following DNA-damage (Rand *et al.*, 2003). Therefore, in order to determine whether SigG was responsible for regulating genes involved in DNA-damage repair, the induction ratios in the Δ*sigG* strain were compared with those in the wild-type strain. Of the 115 genes that were induced 2-fold or more in the wild-type, only 4 genes exhibited reduced induction ratios in the Δ*sigG* strain. However, closer analysis of the data revealed that discrimination by induction ratio was possibly not the best method of examining the data. The use of RNA vs DNA hybridizations in the microarray experiments

meant it was possible to determine whether there were any differences in expression under uninduced and induced conditions individually for the Δ*sigG* and H37Rv strains. This revealed that the apparent decrease in induction ratio was affected by an increase in the expression under uninduced conditions in the Δ*sigG* strain. This is highlighted with Rv1956, a predicted transcriptional regulatory protein. The induction ratio is 3.09 ± 0.37 in H37Rv, and only 1.59 ± 0.28 in Δ*sigG*, these are significantly different with a p=0.0093. Although, when one looks at the normalised data for the uninduced and the induced conditions individually, there appears to be little difference between the induced expression level in Δ*sigG* strain compared to H37Rv; rather the expression level of Rv1956 appears to be higher in the Δ*sigG* than in H37Rv under uninduced conditions, however, this difference was not significantly different at P<0.01. This disparity between the uninduced and induced comparisons compared to the induction ratio becomes particularly apparent when looking at genes whose expression is almost completely ablated, of which, *papA3* is a prime example. Using induction ratio, it appears that *papA3* expression is induced to a greater extent in the Δ*sigG* strain than in H37Rv; however, when looking at the uninduced and induced values separately, it became evident that the expression level of *papA3* under both uninduced and induced conditions is greatly reduced in Δ*sigG* compared to H37Rv. This difference in induction ratio could be the result of dividing by a small value; any ratio whereby a very small denominator is used results in a large ratio, thus skewing the data. This observation is particularly important when looking for genes whose expression in dramatically reduced in a mutant. Examining the induction ratio gives the impression that the induction levels of *lexA*, *fmt*, and Rv1956 are all decreased in Δ*sigG* compared to H37Rv; nevertheless, when dissecting the expression level under uninduced and induced conditions separately, it becomes clear that although expression varies slightly under uninduced and induced conditions between the strains, this difference is not significant.

Therefore, in spite of the induction ratio suggesting that *fmt*, Rv1956 and *lexA* are regulated by SigG, the individual evidence suggests this is unlikely to be the case.

This highlights the potential difficulties in analysing microarray data in determining which comparisons are meaningful. From the set of 17 genes with a significantly different induction ratio in the Δ*sigG* strain compared to H37Rv, only Rv2884 was also significantly different in the uninduced versus uninduced comparisons, and Rv0181c, *sigG* and Rv3467 were significantly different in the induced versus induced comparisons. Interestingly, *sigG* is co-transcribed with Rv0181c and Rv0180c (see chapter 3); however, only *sigG* and Rv0181c appear to be induced greater than 2-fold in response to DNA-damage in H37Rv wild-type, while Rv0180c is induced to a lesser extent (1.7-fold) in H37Rv. Even though *sigG*, Rv0181c and Rv0180c are all significantly different under induced conditions $P<0.01$, none of the 17 genes with significantly different induction ratios were significantly different under both uninduced and induced conditions $P<0.01$. Therefore, it would appear that SigG does not play a significant role in the control of gene expression following DNA-damage.

The differential expression observed in Rv0181c, one of the downstream co-transcribed genes of the *sigG* operon could show decreased expression in Δ*sigG* compared to H37Rv, due to the polar effects of the SigG deletion and insertion (hyg resistance cassette). The hygromycin resistance cassette may affect the stability of the mRNA, thus making it more prone to degradation.

The problems observed with examination of the data using the induction ratio lead to a different focus of analysis, whereby the uninduced samples were directly compared between strains, then the induced samples were also directly compared between strains, to determine whether the

expression of any genes were significantly different in the Δ*sigG* strain compared to H37Rv. This revealed that 7 genes were significantly different under both uninduced and induced conditions in the Δ*sigG* strain compared to H37Rv. These included genes involved in lipid metabolism (*papA3*, *ppsE*, *ppsD*), respiration (*nuoB*), transport across the membrane (Rv0655), a probable resuscitation promoting factor (*rpfE*/Rv2450c) and a hypothetical protein (Rv0312). Interestingly both *papA3* and Rv0312 were predicted to be essential by transposon mutagenesis (Sassetti *et al.*, 2003), suggesting that the low levels of expression observed in Δ*sigG* compared to H37Rv are sufficient for the knockout to remain viable. This residual level of expression may be explained by compensation by an alternative sigma factor, which may be able to initiate sub-optimal levels of transcription from *papA3* and Rv0312, in the absence of SigG. The residual level of expression of Rv0655 in the Δ*sigG* strain is higher than that of the other 4 genes whose expression is decreased in the Δ*sigG* strain compared to H37Rv. This may be because these genes are expressed from multiple promoters, one or more of which is recognised by a different sigma factor, conversely, it may be that more than one sigma factor can recognise a single promoter. An alternative possibility is that SigG may regulate a repressor of Rv0655.

There appear to be conflicting results regarding the expression of genes in the *pps* operon. The expression level of *ppsE* is all but abolished in the Δ*sigG* strain, while the upstream, co-transcribed gene *ppsD* appears to be upregulated in Δ*sigG* compared to H37Rv. In previous dye-swap RNA vs RNA *M. tuberculosis* arrays, problems have been observed with incorporation of the fluorescent labels cy3/cy5 with *ppsE*, resulting in an apparent decrease in expression, when in reality this decrease was due to differential labelling with cy3/cy5 (Roger Buxton- personal communication). However, the design of the DNA vs RNA arrays discounts any preferential labelling with either cy3/cy5, by using DNA as the normalising control, always labelled with cy3. Therefore it is unlikely that the almost complete abolition of expression of

ppsE in Δ*sigG* occurred as a result of preferential labelling with cy3/cy5. The validity of the data values for *ppsE* are even more convincing taking into account that *ppsE* was also significantly different in the Δ*sigG* strain compared to H37Rv, under the increased stringency of the Benjamini and Hockberg false discovery rate correction. Nevertheless it is surprising, that the level of *ppsD* should be increased and the level of *ppsE* decreased, given that they have been demonstrated experimentally to be co-transcribed (Camacho *et al.*, 2001), However, these are huge genes; *ppsE* is 4.467kb and *ppsD* is 5.484kb. It is possible therefore, that either the microarray probes are not specific for the genes, due to their size, or the RT-PCR may be flawed. Closer analysis of the predicted co-transcribed region revealed that not only *ppsA*, *ppsB*, *ppsC*, *ppsD* and *ppsE* were predicted to form an operon, based on RT-PCR data between adjacent pairs of genes (Camacho *et al.*, 2001), but that *fadD26* upstream of the *pps* operon was shown to also be co-transcribed with *ppsA*, as were *ppsE* and *drrA*, therefore suggesting that the predicted polycistronic region includes; *fadD26*, *ppsA-E*, *drrA-C* and *papA5* . The RT-PCR results visually do not seem conclusive, yet they are reported to have been sequenced. However, it seems unlikely that an operon as large as 32.4kb could be transcribed from a single promoter. It may, therefore, be possible that *ppsE* is transcribed independently from *ppsD*. It could be that *ppsE* is transcribed from an alternative promoter located in the coding region of *ppsD*, which is regulated directly or indirectly by SigG.

Potentially, the most interesting set of genes are those that are expressed to a lesser extent in Δ*sigG* strain, as these may be directly or indirectly regulated by SigG. Examination of the data obtained in the absence of DNA-damage, revealed that 52 genes showed reduced expression in the Δ*sigG* strain. These include 6 genes involved in lipid metabolism and 8 genes in cell wall and cellular processes. The reduced expression of these genes may account for the increased susceptibility of *M. tuberculosis* Δ*sigG* strain to mitomycin C. Lipids comprise a large

proportion of the cell wall of *M. tuberculosis*, which provides a protective layer to help defend the bacterium against the hostile external environment and the components of this barrier may be altered by as a consequence of the changes in gene expression observed. In addition, the cell wall and cell processes genes downregulated in Δ*sigG* strain include two genes involved in membrane transport: Rv1348 is thought to be an ABC transporter most likely involved in drug transport and *epfA* is an integral membrane protein, involved in efflux. Therefore, a decrease in the expression of membrane transporters may increase the levels of damaging agents in the cell, or may prevent agents such as mitomycin C being removed from the cell.

Among the genes with decreased expression in Δ*sigG* strain are four transcriptional regulators, Rv3050c, Rv0232, which are annotated to be AsnC family and TetR family respectively, Rv3764c a sensor of a two component regulatory system and Rv2884 which is predicted to contain a response regulator receiver domain. TetR family of transcriptional represssors respond to tetracycline, whereby in the absence of tetracycline, the TetR repressor binds to the operator and suppresses transcription (Yan *et al.*, 2001). The AsnC family, often referred to as the Lrp/AsnC family of transcriptional regulators respond to leucine/asparagine synthase C (Shrivastava *et al.*, 2004). It is possible, that *sigG* could regulate the genes described directly or indirectly via any one of the four transcriptional regulators identified in the *sigG* regulon.

Another interesting gene shown to decrease in expression level in Δ*sigG* strain, is *mceIA*, which is involved in host cell invasion and is thought to be involved in entry and survival in macrophages. This may suggest why preliminary mouse *in-vivo* data has indicated a decrease in virulence of Δ*sigG* strain compared to H37Rv (see chapter 3).

Although the main focus has so far been on genes whose expression is deceased in the *ΔsigG* strain, one gene in particular was of interest that showed increased expression in *ΔsigG* strain, the stress response sigma factor *sigE*. The increased expression of *sigE*, might be expected to result in increased expression of genes in the SigE regulon, although there was no overlap in the set of genes showing increased expression in uninduced *ΔsigG* strain here, and those reported to be reduced in expression in exponential growth in *ΔsigE* strain (Manganelli *et al.*, 2001). Alternatively, one could speculate that SigE may be able to partially compensate for the lack of SigG. Interestingly two of the genes whose expression is increased in *ΔsigG* strain to greater than 1.7 fold are involved in lipid metabolism, *fadD26* and *ppsD* with *ppsA* increased to a lesser extent in *ΔsigG* strain. These are of particular interest as they have been suggested to be co-transcribed as part of the *pps* gene cluster (Camacho *et al.*, 2001). Another interesting genes is the resuscitation promotion factor *rpfE* whose expression was increased under both uninduced and induced conditions in the *ΔsigG* strain, suggesting SigG may directly or indirectly regulate, *rpfE*, possibly via a repressor, which potentially may be emergence from dormancy.

To confirm the possibility that the genes identified by microarray analysis did belong to the SigG regulon, the expression of these genes could be validated using Taqman real-time PCR in both the *ΔsigG* strain and H37Rv wild-type. The upstream regions of these genes could then be used to identify a consensus motif for the recognition site of SigG, initially by alignment, then using primer extension assay to determine the precise transcriptional start site(s). Since the level of *sigG* expression decreased, but was not abolished in the *ΔsigG* strain, it is possible that *sigG* may be subject to autoregulation. However, due to the detection of expression of *sigG* in the *ΔsigG* strain it is likely that *sigG* is transcribed from multiple promoters, one of which may be subject to autoregulation.

4.3.2 Dissection of the upstream region of *sigG*

Identification of the transcriptional start sites of *sigG* proved difficult initially due to the incorrect prediction of the translational start site, in the TubercuList database. Both primer extension and RNase protection have revealed that the major transcriptional start sites are in fact downstream of the originally predicted translational start site, indicating that the actual translational start site is further downstream than initially thought.

Primer extension is a useful assay for the precise identification of the transcriptional start site(s) of a gene to the nucleotide, due to the ability to run a manual sequence alongside the primer extension reactions using the same primer, thus enabling a direct comparison between the band(s) produced in the primer extension reactions and the manual sequence.

The initial primer extension reactions performed on *sigG* were unsuccessful, although the positive control yielded a band, indicating the technique was working. A number of possibilities were checked out to determine the cause of the primer extension reaction failing for *sigG*. The primer used in the *sigG* primer extension worked in the sequencing reactions, so it was not that the primer was not annealing to the template (RNA). It has been suggested by Manganelli (1999) that the level of *sigG* expression is very low during exponential phase, therefore, it was thought that more template RNA was required for the primer extension, but, even after increasing the template to 85μg, no product was observed.

A closer look at the *sigG* translational start site revealed there were a number of other possible translational start sites further into the coding region of *sigG*. Therefore, another technique was employed, whereby a 500bp RNA probe was used in an RNase protection assay. This assay is

more quantitative than the primer extension assay, nevertheless, it does not allow such accurate location of the transcriptional start site. Markers used along side the RNase protection assay enable the approximate sizing, but the size range of the makers is such that only an approximation can be made, thus necessitating a subsequent primer extension assay to define the transcriptional start sites to the nucleotide. This meant that both assays were used sequentially to firstly identify if the transcriptional start site(s) were in fact downstream of the predicted translational start site, then secondly to identify precisely the transcriptional start sites based on this information.

The primer extension reaction showed the presence of two inducible promoters in both the Δ*sigG* strain and H37Rv strain, as observed in the RNase protection assay. In addition, there appeared to be a constitutively expressed promoter in the H37Rv strain, that was potentially autoregulated, as indicated by the absence of a corresponding band in the Δ*sigG* strain in the primer extension assay. Intriguingly, the finding from the primer extension and RNase protection do not tie up with the microarray data, in which it appeared that *sigG* was not induced in response to DNA-damage in the Δ*sigG* strain, yet the primer extension and RNase protection assays clearly show that *sigG* possesses two DNA-damage inducible promoters, regulated independently of SigG, due to their induction in Δ*sigG* strain.

As expression of *sigG* from the P1 and P2 promoters increased following DNA-damage, if the P3 promoter is autoregulated, one would have expected its level of expression to also increase. However, the RNase protection and primer extension showed that *sigG* possesses three promoters, two of which are DNA-damage inducible, and a third which does not appear to be DNA-damage inducible, but may potentially be autoregulated. Therefore, the data indicates that SigG is not required for the induction of expression from the two inducible promoters,

which begs the question, why was the level of *sigG* transcription decreased in the knockout. The answer may lie in the position of the *sigG* probe for the microarray analysis. The probe appears to overlap with the deletion of the *sigG* coding region, but also overlaps by approximately 48bp with the remaining region of *sigG*, therefore the binding of the probe to the *sigG* message may be transient, or unstable. However, it is perhaps more likely that the decreased induction of *sigG* in the Δ*sigG* strain, is due to the decreased stability of the transcript brought about by the insertion of the hygromycin resistance gene, which may have made the mRNA more prone to digestion with RNase.

Analysis of the upstream region of *sigG* revealed that there were a number of potential promoter recognition sites upstream of the three transcriptional start sites identified by the primer extension. Interestingly, the P1 promoter was the most highly induced, and showed the greatest homology to a σ^{70} consensus for the –10 and –35 regions. However, there appear to be two potential sites of the –35 region, that show a similar degree of homology to the σ^{70} consensus. One in particular was of interest, as it was identified by Gamulin *et al.*, (2004) and is similar to a promoter motif upstream of DNA repair genes, such as *recA*, *ruvC* and *uvrA/B*, along with some mobile genetic elements, such as Rv1148c. This motif, termed the RecA-NDp (RecA non-dependent promoter) has been suggested to be involved in an alternative mechanism of regulation, in a RecA/LexA independent fashion, thought to be by sigma factor specificity (Gamulin *et al.*, 2004).

There are two main hypotheses, which have been put forward to explain how the RecA-NDp is regulated. The first hypothesis is that an undefined sigma factor is responsible for regulating transcription from this motif, and the other is that this motif is recognised by a major sigma factor, through interactions of the –35 site with a positive regulatory protein (activator),

whereby the activator protein modifies the preference of the sigma factor for the –35 region (Gamulin *et al.*, 2004).

The RecA-NDp motif was identified upstream of two ECF family sigma factors, *sigG* and *sigH*. Many ECF sigma factors have been shown to be autoregulated, suggesting that this motif may be regulated by either SigG or SigH. RNase protection experiments performed in chapter 5 demonstrate that SigG is not responsible for the expression from the *recA* P1 promoter. The primer extension data for *sigG* shows that the P1 promoter, which contains the aforementioned motif, is induced in response to DNA-damage in the Δ*sigG* strain, thus indicating that SigG is not involved in regulation of gene expression from the P1 promoter. Microarray data for the Δ*sigG* strain revealed that SigG does not regulate expression from any of the genes with this identified motif, thus suggesting that SigG does not recognise promoters with the previously described RecA-NDp motif. Therefore, current literature was surveyed for the possibility that SigH regulates expression of DNA-damage inducible genes possessing this upstream motif. Analysis of a *sigH* knockout strain of *M. tuberculosis* revealed that it was more susceptible to heat shock and oxidative stress (diamide) than H37Rv. Furthermore, transcriptional profiling using microarray technology revealed that SigH directly or indirectly regulated 39 genes, some of which were involved in heat shock and others were predicted to be involved in thiol metabolism. Interestingly two other sigma factors showed decreased induction (5mM diamide) in the Δ*sigH* strain, SigE and SigB (Manganelli *et al.*, 2002). It was later hypothesised that SigH was a central regulator in the response to oxidative stress and heat shock in *M. tuberculosis*, and that SigH was responsible for regulation of these two sigma factors, *sigE* and *sigB* (Song *et al.*, 2003). Although SigH is involved in the response to oxidative stress, it appears that RecA-NDp genes, some of which fall under the DNA-damage repair system, are not regulated directly by SigH, or indirectly by SigE or SigB based on currently available

microarray data describing the regulons of these sigma factors. Microarray analysis of Δ*sigE* strain identified genes regulated by SigE under untreated conditions during exponential phase, and after SDS treatment. This showed that *sigB* was not upregulated during exponential growth in the Δ*sigE* strain, thus indicating *sigB* is part of the SigE regulon (Manganelli *et al.*, 2001). It has been shown that *sigE* is regulated by SigH and *sigB* is dependent on both SigE and SigH for both basal and inducible expression. The analysis of these mutants lead to the identification of possible –35 and –10 recognition sites for these sigma factors, none of which match the motif consensus defined by Gamulin *et al.*, (2004). Interestingly the oxidative stress response genes *sodA* and *sodC* were induced to a lesser extent in the Δ*sigH* strain, but no SigH promoter consensus was observed upstream of *sodA*, *sodC* or *ahpC* (Raman *et al.*, 2001), suggesting that *sigH* may indirectly affect expression of these genes, or may be able to recognise more than one promoter motif. Although the RecA-NDp motif was identified upstream of *sigG* and *sigH* it does not appear that these motifs are recognised by either SigG or SigH.

Another noteworthy observation was made during the analysis of the upstream regions of *sigG* (figure 5.4), and *recA* (see chapter 5, figure 5.2c): There is a conserved motif GTGGT-N_2-TCATT (SigRec motif), which overlaps with the P2 promoter of *sigG* and is located downstream of the –10 site of the distal P2 promoter of *recA*. This conserved region may act as a binding site for a repressor or activator protein, which may be involved in regulation of transcription from these promoters. The close proximity of the RecA-NDp motif and SigRec motif, to the P2 promoter of *recA* and the P1 promoter of *sigG*, suggests they may be involved in regulation. However, it was shown by Gopaul et al., (2003) that the region containing the SigRec motif was not essential for induction of the RecA P1 promoter. Therefore, SigRec motif could represent an activator binding site, the presence of which, merely enhances transcription rather than being a pre-requisite for transcription. As mentioned in the results, 24 genes were

identified with 1bp mismatch to the consensus outlined above, and 207 genes were identified with 2 mismatches. None of the 24 genes with the 1bp mismatch were uncovered in the Δ*sigG* microarrray data as significantly different in the Δ*sigG* strain compared to H37Rv. Nevertheless, a total of 5 genes were identified that possessed both the RecA-NDp and the conserved region, comprised of the potential DNA repair genes; *uvrB* helicase, subunit B, *uvrD2* ATP dependent DNA helicase II, Rv2792c a possible resolvase, *dnaE1* a DNA polymerase III, and Rv1765c and Rv2015c, conserved hypothetical proteins. In addition, one DNA repair gene without a RecA-NDp was identified as possessing the conserved region, *end*, an endonuclease involved in base excision repair. It does not appear that the SigRec motif identified upstream of *recA* and *sigG* is required for regulation of DNA-damage repair genes that are induced independently of the RecA/LexA system, nor does it appear that the RecA-NDp is solely responsible for regulation of these genes, as the motif is not present in all cases. Therefore, it appears that there is a complex network of interconnected regulation of genes responding to DNA-damage, including those predicted to be dual regulated.

Although sigma factors often autoregulate, the primer extension and RNase protection assays performed on the Δ*sigG* strain have revealed they may possess more than one promoter and that only one of the promoters may in fact be autoregulated, as is the case of *sigG*. In the case of *sigG*, this could be tested using *lacZ*-promoter fusion assays, whereby the three promoters of *sigG* could be cloned upstream of a *lacZ* reporter gene, and various mutations could be introduced to define the regions of importance in the potential -10 and -35 promoter sites. These could then be assayed in both the H37Rv wild-type (as a control) and Δ*sigG* strain, to address the hypothesis that the P3 promoter is regulated by SigG and therefore would not be expressed in the Δ*sigG* strain. If SigG regulated expression from the P3 promoter by recognising and binding to the motif outlined above, then there would be either abolition of

expression or decreased expression (due to compensation) in the Δ*sigG* strain compared to H37Rv.

The SigG dependent promoter, identified upstream of *sigG*, P3, reveals potential -10 and -35 motifs that do not resemble any of the previously described sigma factor motifs. Motif searches using MEME database (Bailey and Gribskov, 1998), with the 5 genes though to be regulated by SigG, under both induced and uninduced conditions did not reveal any concrete consensus for the consensus motif of SigG, but when the smaller –35 region CGACC (from the MEME search) was used to search the sequences, potential –10 and –35 sites were identified upstream of the predicted translational start sites for all of the genes except *nuoB* and *papA3*, where the consensus was identified downstream of the predicted translational start site. This revealed the potential consensus CGACC(R)(t/c)C-$N_{13\text{-}22}$-TGTCCG (R represents g/c/a). There was less homology observed at the –10 site than the –35 site for all genes, except *nuoB* which was identical to the P3 promoter of *sigG* at the –10 sites. Therefore, the best course of action would be to perform primer extension assays on the 5 genes predicted to be downregulated in Δ*sigG* strain under both induced and uninduced conditions, to identify the transcriptional start site(s), thus enabling an alignment to be produced to define a consensus for the recognition motif of SigG. This could then be tested using the wild-type sequence and mutated sequences upstream of a *lacZ* reporter gene to determine which of the residues are vital from the recognition of the sigma factor SigG.

5 Detailed analysis of *ruvC*

The RecA/LexA system coordinating expression of the DNA-damage regulon has been extensively studied in *E. coli*, whereby the majority of genes induced following DNA-damage appear to be regulated by the RecA/LexA system (Walker 1984). The same appears to hold true for a number of different species (Eisen and Hanawalt, 1999). However, the DNA-damage regulon is not controlled by the RecA/LexA system in all bacterial species. A number of bacteria whose annotated genome sequence is complete lack a *lexA* homologue, including; *Aquifex aeolicus*, *Borrelia burgdorferi*, *Campylobacter jejuni*, *Chlamidia pneunomiae*, *Helicobacter pylori*, *Mycoplasma pneumoniae* and *Porphyromonas gingivalis* (Fernandez de Henestrosa *et al.*, 2002), and even those that possess *lexA/recA* homologues, such as the plant pathogen *Xylella fastidiosa*, show independent induction of some genes involved in the DNA-damage regulon (Campoy *et al.*, 2002).

Analysis of the DNA-damage repair regulon in H37Rv wild-type compared to Δ*recA* strain of *M. tuberculosis* showed that although a proportion of DNA-damage repair genes were regulated by the classical RecA/LexA system, some DNA-damage inducible genes were regulated independently of the RecA/LexA system. In H37Rv wild-type, 112 genes were induced greater than or equal to 3 fold in the wild-type in response to DNA-damage (Rand *et al.*, 2003). Of those 112, 21 genes were not expressed in the Δ*recA* strain, suggesting they are solely regulated by RecA/LexA system. However, 28 genes were expressed less in the Δ*recA* strain, suggesting these genes were partially regulated by RecA/LexA system, and partially by an alternative mechanism. Interestingly 50 genes were expressed to the same extent in the Δ*recA* strain, suggesting these genes are solely regulated by an alternative mechanism (Rand *et al.*, 2003). Some of the genes shown to be partially induced in the Δ*recA* strain have been shown to possess

LexA binding sites (Brooks *et al.*, 2001; Davis *et al.*, 2002): *ruvC* and *recA* were among the genes partially induced in the Δ*recA* strain of *M. tuberculosis*, in response to DNA-damage by mitomycin C (Rand *et al.*, 2003), which possess a LexA binding site. It has been determined that *recA* has two promoters, both of which are DNA-damage inducible, but only one possesses a LexA binding site (Davis *et al.*, 2002b). Therefore, the similar pattern of expression of both *ruvC* and *recA* in the Δ*recA* strain and the presence of the LexA binding sites upstream of both *ruvC* and *recA* suggests that an analogous mechanism regulates expression of these two genes. In order to dissect the possibility of an alternative method of regulation, the upstream region of *ruvC* was analysed to look for the presence of two inducible promoters in *ruvC* with *recA* as a control. The expression of *ruvC* and *recA* were analysed in the Δ*sigG* and Δ*recA* strains of *M. tuberculosis* in comparison with the wild-type H37Rv, to assess any role of SigG in control of an individual promoter and compare it with that of RecA.

5.1 Identification of *ruvC* transcriptional start site(s) by primer extension

Preliminary RNA verses RNA microarray data from the Δ*sigG* strain of *M. tuberculosis* compared to the wild-type H37Rv, had suggested a significant decrease (at the 2% level) in induction of *ruvC* in the Δ*sigG* strain compared to the wild-type in response to DNA-damage (mitomycin C 0.2μg/ml) (data not shown). Therefore, the expression level of *ruvC* appeared to be decreased in Δ*recA* and Δ*sigG* strains, which suggests that *ruvC* may be dual regulated by RecA/LexA and SigG. One could hypothesise, that this dual regulation takes place via two promoters, one regulated by LexA/RecA and the other by SigG. It has been demonstrated that *ruvC* has a DNA-damage inducible promoter, which contains a palindromic LexA binding site (Brooks *et al.*, 2001). Consequently, to test the theory that two promoters drive *ruvC*

expression and to investigate their dependence on RecA and SigG, RNA was extracted from induced (mitomycin C, final concentration 0.02μg/ml) and uninduced cultures of wild-type H37Rv, Δ*recA*, and Δ*sigG* strains of *M. tuberculosis*. The RNA samples were quantified using a spectrophotometer, and primer extension reactions were performed using a primer designed from within the coding region of *ruvC* (see figure 5.1a). The primer extension reactions were run alongside manual sequencing reactions, where a clone containing the upstream region and coding region of *ruvC* in pBluescript (see table 2.2) was used as a template. The same primer was used in the primer extension and sequencing reactions so one could determine the exact transcriptional start site. However, the sequencing reaction failed and sizing could not be performed. In the uninduced isolates of H37Rv wild-type, Δ*recA*, and Δ*sigG* strains, two bands were visible (see figure 5.1b), suggesting that *ruvC* possesses two transcriptional start sites. The P1 promoter (indicated with arrow A, figure 5.1b) possesses a LexA binding site (Brooks *et al.*, 2001), and was clearly DNA-damage inducible in the H37Rv wild-type. However, this induction was not apparent with the P2 promoter (indicated with arrow B, figure 5.1b). Nevertheless, the P2 promoter may be DNA-damage inducible, as the P2 promoter of *recA* did not appear to be induced by mitomycin C when samples were used in primer extension reactions (Movahedzadeh et al., 1997), although induction of the P2 promoter was observed using a transcriptional fusion to *lacZ* (Davis *et al.*, 2002b). The apparent lack of induction of the P2 promoter of *ruvC* in the primer extension reactions may have been a result of poor levels of quantitation available by primer extension. Surprisingly, in the Δ*recA* strain, the P1 promoter (labelled A, figure 5.1b), regulated by LexA, remained partially inducible; suggesting the repression of *ruvC* by LexA may be partially overcome by an alternative mode of regulation. In the Δ*sigG* strain, the promoter P1 was induced, but to a lesser extent than in the H37Rv wild-type and Δ*recA* strain. In contrast, the P2 promoter was not induced in any of the three strains

Figure 5.1a

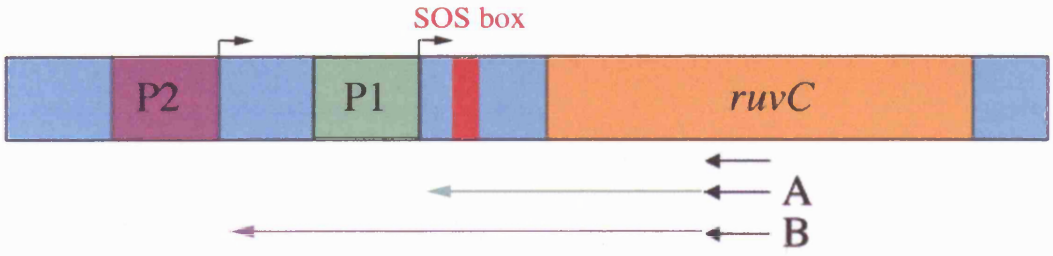

Figure 5.1b

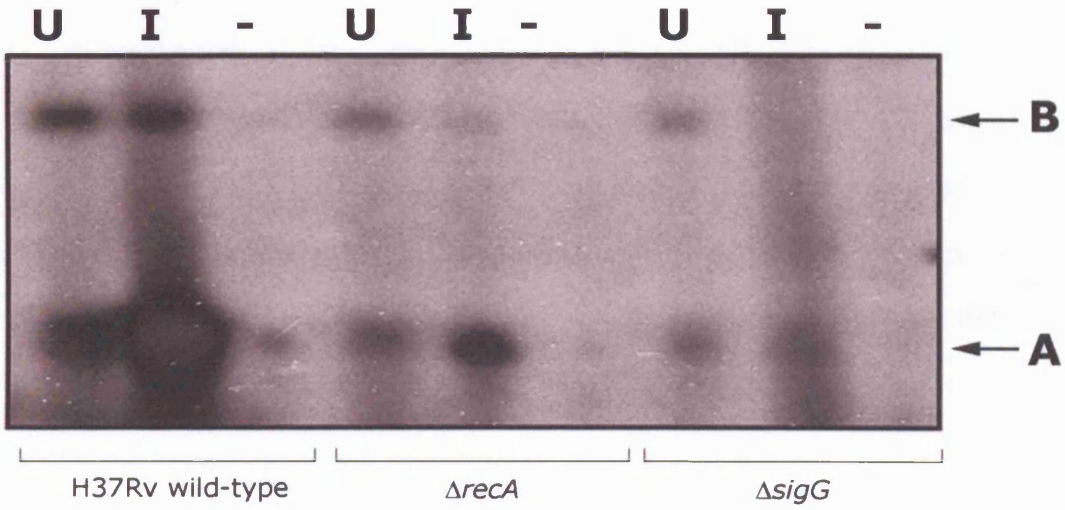

Figure 5.1a: A schematic representation of the position of *ruvC* and potential transcriptional start sites. The arrow below *ruvC* indicates the primer designed in the coding region of *ruvC* for the primer extension reaction to detect the transcriptional start sites, indicated by A and B. The P1 promoter contains a putative LexA binding site, defined in red and labelled the SOS box.

Figure 5.1b: An autoradiograph showing the transcriptional start sites of *ruvC* in H37Rv wild type, Δ*recA* and Δ*sigG* strains of *M. tuberculosis*. Two cultures of each strain were grown to mid exponential phase (0.3-0.4) in a rolling incubator at 37°C. These were pooled and split, one remained untreated, while the other was induced with 0.02μg/ml mitomycin C, all cultures were incubated for a further 24hours in a rolling incubator at 37°C. RNA was then extracted form the cultures, and primer extension reactions were carried out with 100μg of RNA from uninduced (track U), induced (track I), and a negative control with no RNA,(track -). The strains of *M. tuberculosis* used in the primer extension are indicated below the autoradiograph.

tested and the level of transcription from the P2 promoter appeared to be less under induced rather than uninduced conditions (see figure 5.1b).

The original primer extension (figure 5.1) had indicated that *ruvC* possesses two transcriptional start sites; however, technical problems encountered with the manual sequencing run along side the primer extension meant the exact transcriptional start sites were not identified. The sequencing reactions were repeated using an increased quantity of template. Half of the sequencing reactions were run on a polyacrylamide gel and visualised by autoradiography (data not included). The remaining halves were stored at –20°C overnight before being run alongside the primer extension reactions. The same primer used in the sequencing reactions was used for the primer extension reactions. The primer extension was repeated using uninduced and induced (0.02μg/ml mitomycin C) H37Rv wild-type RNA, from a duplicate culture, alongside a sequencing reaction (see figure 5.2a), enabling precise positioning of the transcriptional start sites (see figure 5.2b). This revealed that the LexA binding site overlaps the P1 transcriptional start site, suggesting that LexA binding would interfere with transcription initiation (see figure 5.2b).

5.1.1 Potential promoter motifs upstream region of *ruvC*

Primer extension analysis showed that *ruvC* is expressed from two promoters (see figure 5.2a). Analysis of the upstream sequence revealed that the P1 promoter exhibits some similarity to sigma 70 (σ^{70}) –10 and –35 promoter elements (see figure 5.2b), with the *E. coli* consensus TATAAT and TTGACA respectively (Gross *et al.*, 1992). Interestingly there is a high degree of similarity between the P1 promoter regions of *recA* and *ruvC*: the –10 region of the P1 promoter of *ruvC* (pink box, figure 5.2b) CTAGcGT exhibits similarity to the –10 region

Figure 5.2a

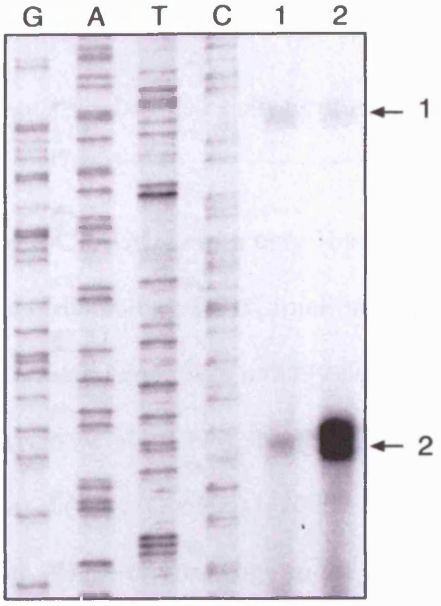

Figure 5.2b

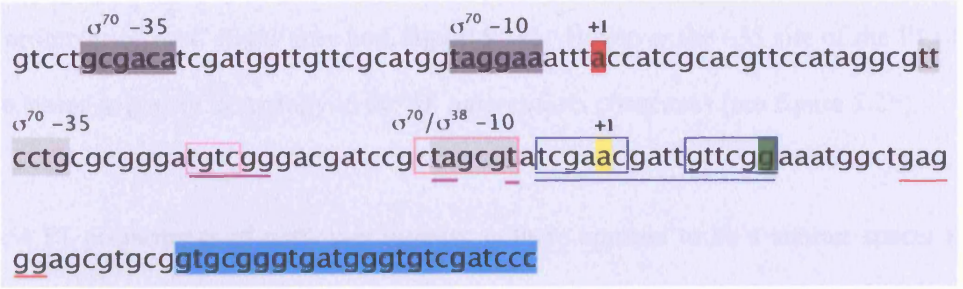

Figure 5.2c

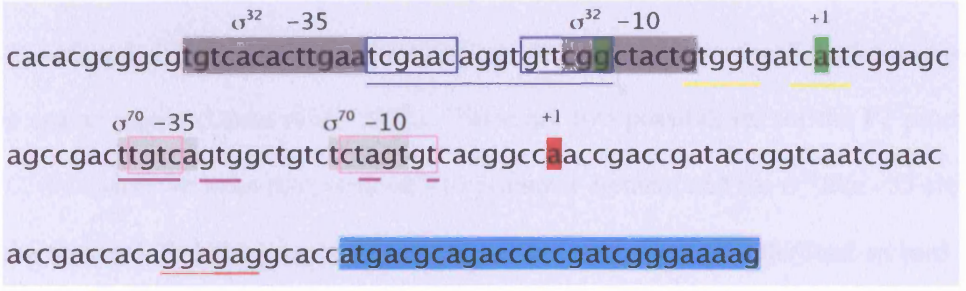

Figure 5.2a: Primer extension of *ruvC*. Primer extension reactions were carried out using 80µg of RNA from H37Rv uninduced and induced (0.02µg/ml mitomycin C) cultures. These were run alongside manual sequencing reactions.

Figure 5.2b: Transcriptional start sites of *ruvC*. The first transcriptional start site (+1) indicated in yellow, and the second is indicated in red (+1). The blue box and line indicate the position of the LexA binding site, with the consensus TCGAACN$_4$GTTCGA. The green highlighted base in the LexA binding site indicates the deviation from the LexA binding site consensus. The potential ribosome binding site GAGGG is underlined in red. The light blue box indicates the coding region of *ruvC*. The potential σ^{70} –10 and –35 sites are indicated with light grey boxes, and the underlined regions indicate regions of homology to the *M. tuberculosis lexA* σ^{70} promoter at –10 (TACATT) and –35 (TTGGTC). The regions of homology to the RecA-NP promoter Gamulin *et al.*, (2004) are underlined in purple. Homology to the *recA* P1 promoter is boxed in pink.

Figure 5.2c: Transcriptional start sites of *recA*. Amended from Movahedzadeh 1996. The first transcriptional start site (+1) is indicated in red and the second is indicated in green (+1). The blue box and line indicates the position of the LexA binding site, with the consensus TCGAACN$_4$GTTCGA. The green highlighted base in the LexA binding site indicates the deviation from the LexA binding site consensus. The potential ribosome binding site GGAGAG is underlined in red. The light blue box indicates the coding region of *recA*. The potential σ^{70} –10 and –35 sites are indicated with light grey boxes, with the consensus –10 (TATAAT) and –35 (TTGACA) for *E. coli*. Regions of homology to the RecA-NP promoter Gamulin *et al.*, (2004) are underlined in purple. The potential σ^{32} -10 and -35 sties are indicated in dark grey, with the *E. coli* consensus -10 (CCCCATNTA) and -35 (TCTCNCCCTTGAA). Homology with the *ruvC* P1 promoter is boxed in pink. The SigRec motif is underlined in yellow.

upstream of the P1 promoter of *recA* CTAGtGT, with only 1bp mismatch, which is separated by an 11bp spacer from a 4bp region of homology TGTC (pink box figure 5.2b) at the –35 site of *recA* P1. The σ^{70} consensus of *M. tuberculosis* was initially outlined as TAYgAT (-10), where Y indicates a pyrimidine (Bashyam et al., 1996), however, that was slightly modified to TA(G/T)(A/G)aT (–10) and TtGaCa (–35) (Gomez M, 2000). The –10 and –35 regions of the P2 promoter of *ruvC*, show a high degree of homology to the *M. tuberculosis* consensus for a σ^{70} promoter (dark grey box, figure 5.2b), this homology is also observed at the –10 region of the P1 promoter of *ruvC* (light grey box, figure 5.2b). However the –35 site of the P1 promoter shows a lesser degree of homology to the *M. tuberculosis* consensus (see figure 5.2b).

The *recA* P1 promoter is of particular interest as there appears to be a shorter spacer between the –10 and –35 sites (see figure 5.2c) than observed in *E. coli* (Movahedzadeh et al., 1997), which has been noted for a few promoters regulated by σ^{70}, although the spacer between the proposed –10 and –35 sites for the P2 promoter of *ruvC* may follow the *E. coli* consensus of a 16-19bp spacer region (Gross et al., 1992). There are two possibilities for the P1 promoter of the *ruvC*, the spacer between the proposed –10 promoter element and the σ^{70} like –35 element is 23bp (see figure 5.2b light grey boxes), whereas the other option, underlined in pink (figure 5.2b) pertains to the RecA non-dependent promoter (RecA-NP) consensus defined by Gamulin et al., (2004). The similarity of the –10 regions indicated the possibility that the P1 promoters of *recA* and *ruvC* may be transcribed by the same sigma factor.

The LexA binding sites for both *ruvC* and *recA* differ from the consensus TCGAAC$(N)_4$GTTCGA (Davis *et al.*, 2002a) by 1bp, indicated in green (see figures 5.2b and 5.2c). The sequence of the spacer region between the palindromic sites are different for *recA* and *ruvC*, which may play a role in regulation/strength of repression. Interestingly the LexA

regulated promoters of *recA* (P2) and *ruvC* (P1) appear to be transcribed by different RNAP-σ complexes (according to sequence homology at the –10 and –35 sites). The P2 promoter of *recA*, regulated by LexA shows a high degree of homology to the σ^{32} promoter consensus (see figure 5.2c), whereas the P1 promoter of *ruvC*, regulated by LexA shows homology to the σ^{70} promoter consensus (see figure 5.2b).

5.2 Quantitative analysis of the transcriptional start sites of *ruvC* compared to *recA* by RNase protection

To address the differential expression observed from the P1 and P2 promoters of *ruvC* in the three different experimental strains of *M. tuberculosis*, a complementary method, RNase protection was utilised, which enables quantitation of the transcript from multiple promoters. RNase protection is a method by which the level of transcription can be quantified from a number of individual promoters of the same gene. The method involves *in-vitro* transcription of a complementary RNA probe, which is then incubated with the RNA sample of interest. The homologous regions of the probe and transcript bind to form dsRNA, any ssRNA probe not bound to the sample RNA is digested using RNaseA/T1, resulting in a protected fragment which can be run on a polyacrylamide gel and visualised by autography.

The RNA used in the RNase protection assays was quantified using an Agilent bioanalyser (see figure 5.3), this accurate quantitation of the RNA prior to the RNase protection enabled greater precision in quantitation of the RNase protection assay, due to equal loading of RNA for all the different samples. As outlined in section 5.1, the RNA was extracted from exponential phase (OD 0.3) for H37Rv wild-type, Δ*recA* strain and Δ*sigG* strain, under both induced (mitomycin C 0.02μg/ml) and uninduced conditions. RNA was also extracted for H37Rv wild-type and

Figure 5.3

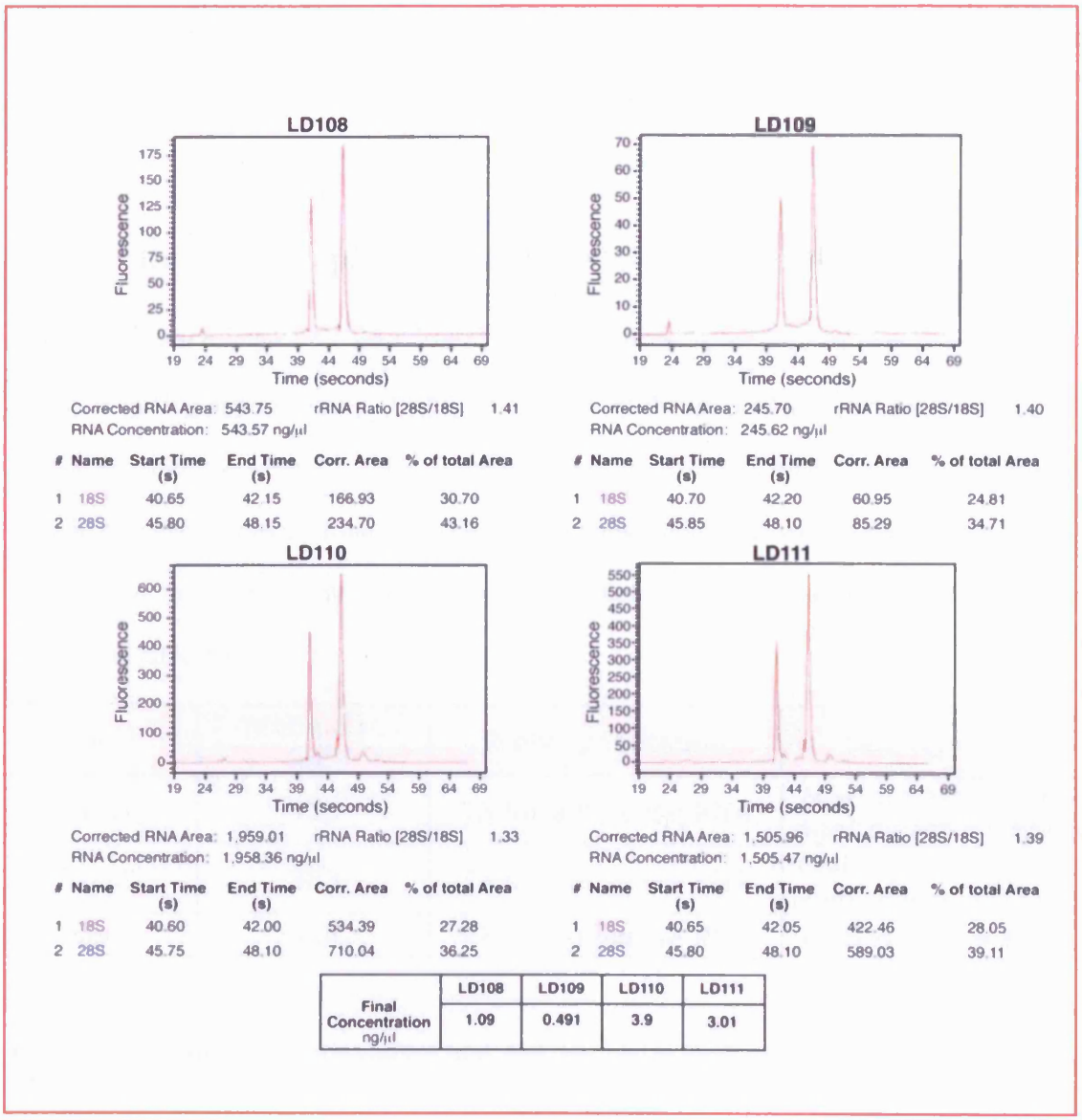

	LD108	LD109	LD110	LD111
Final Concentration ng/µl	1.09	0.491	3.9	3.01

Figure 5.3: Bioanalyser data from RNA extractions. RNA samples were quantified using the Bioanalyser (Agilent Technologies). Quantification of the RNA samples is indicated in the table above.

Δ*sigG* strain, under both induced (mitomycin C 0.02μg/ml) and uninduced conditions, at early exponential phase (OD 0.15) due to the preliminary Taqman data suggesting that *sigG* may be preferentially expressed early on in growth.

5.2.1 Design and optimisation of the RNase protection assay.

Constructs were designed for *recA*, *sigG* and *ruvC* containing a region of approximately 322-358bp, including approximately 151-271bp upstream of the translational start site, were cloned into pCR4 blunt, between T3 and T7 promoters (see table 2.2). Clones were then sequenced and the orientation was determined. The *in-vitro* transcription was carried out on a linearised template, in the reverse orientation to produce radiolabelled complementary RNA (section 2.9.7.1 and table 5.1).

Gene	probe size (bp)	Probe Orientation	Test template
recA	423	T3 for antisense RNA	*NheI* digest = 44bp *AgeI* digest = 265bp
ruvC	383	T3 for antisense RNA	*ClaI* digest = 152bp *NheI* digest = 231bp
sigG	404	T7 for antisense RNA	*EagI* digest = 68bp

Table 5.1: Probe size, orientation and test templates designed for the three genes of interest

The sizes were determined using Map Draw (DNAstar) to predict the restriction sites in the cloned regions of interest. The orientation for probe transcription was derived from the sequencing data on the orientation of the insert of the gene in the plasmid. The test templates are linearized with the listed enzymes and transcribed from the opposite promoter to the probe. For *ruvC*, two separate digests were performed (*ClaI* and *NheI*), which were then pooled to determine if more than one in-vitro transcription product could be detected, and sized reasonably accurately.

The complementary RNA probe would then bind to the homologous transcript in the total RNA from the strain of interest. Digestion of single stranded RNA (ssRNA) was performed using

RNase A/T1, the resultant protected dsRNA product was then separated on a polyacrylamide gel, and visualised by autoradiography. In order for the experiment to be quantitative, the probe must be in excess, and has to be a clear single band (see figure 5.4).

Prior to performing the RNase protection assay, a number of optimization steps were performed, including increasing the quantity of template in the *in-vitro* transcription reaction (data not included), altering the ratio of radiolabelled to unlabelled UTP, decreasing the temperature of the transcription reaction, as well as varying the type and quantity of RNase used in the digestion.

The quantity of unlabelled UTP was altered to limit premature termination of the probe, and therefore produce a pure probe for the RNase protection assay. An *in-vitro* transcription of the *ruvC* probe was performed using increasing concentration of unlabelled UTP, alongside the radiolabelled UTP (see figure 5.5). A size marker was also produced by linearizing the template construct at different sites along the upstream region of *ruvC*, these fragments were then pooled and used in an *in-vitro* transcription reaction, thus producing radiolabelled transcription products of known size (see figure 5.5). Figure 5.5 shows that whilst weighing up purity against quantity, the probe synthesised with 0.5mM unlabelled UTP yielded the optimum probe.

The effect of altering the temperature of the *in-vitro* transcription reaction was tested for *ruvC* and *recA*, to determine whether this had an effect on the purity of the probe; figure 5.6 shows that the *in-vitro* transcription reaction produced a probe of greater purity when the reaction was performed at 37°C rather than 15°C.

Figure 5.4

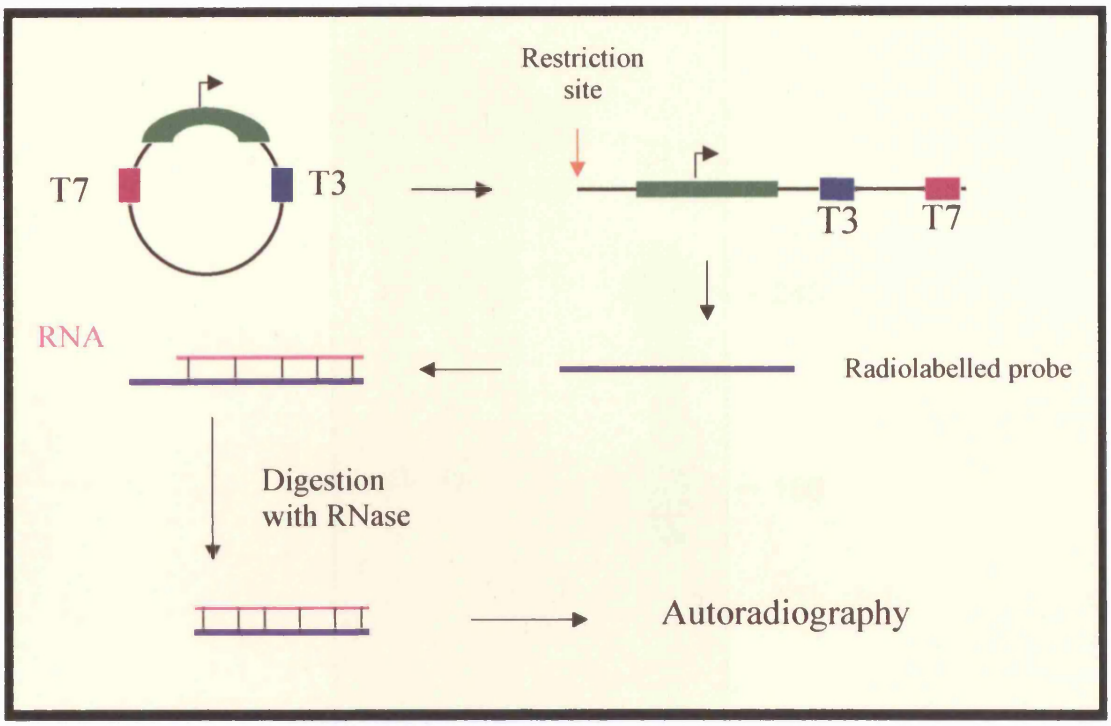

Figure 5.4: Schematic of an RNase protection assay. The region of interest, including a minimum of 150bp upstream of the predicted translational start site (green) was cloned into pCR4-blunt between the T7 and T3 promoters. The construct was linearised using a restriction site, and *in-vitro* transcription was performed in the opposite direction to transcription *in-vivo*. This resulted in the production of a complementary radiolabelled probe (purple), which was quantified using a scintillation counter, and combined with total RNA. The probe annealed to complementary regions of RNA, and following digestion using RNase A/T1, the resultant protected fragment was visualised by autoradiography.

Figure 5.5

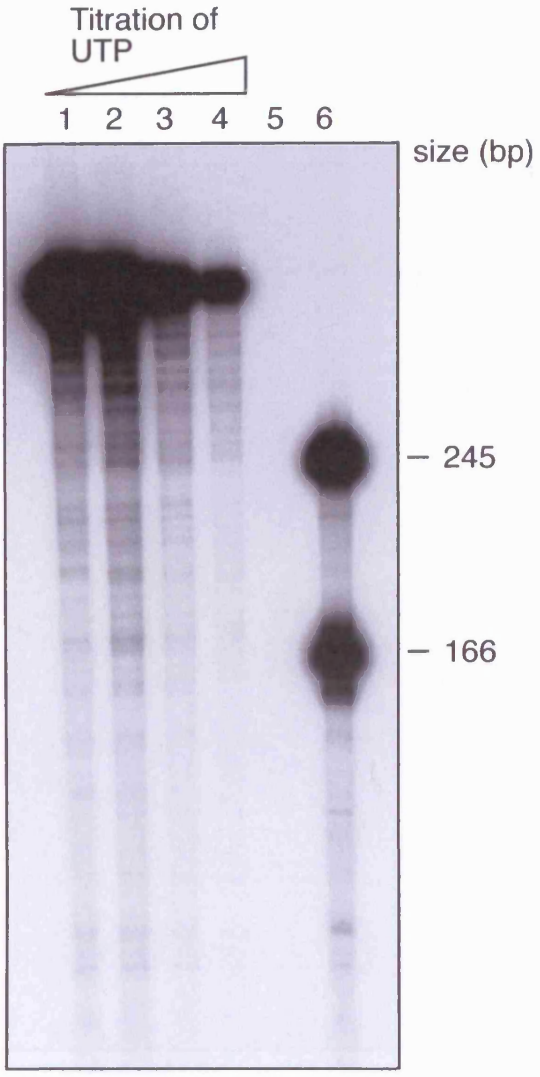

Figure 5.5: *In-vitro* transcription of the *ruvC* probe with varying concentrations of unlabelled UTP. The transcription reaction was performed on the linearised (*Not1* digest) *ruvC* template DNA, using T3 RNA polymerase. The transcription reaction was set up using increasing concentrations of unlabelled UTP; 0.125mM (track 1), 0.25mM (track 2), 0.5mM (track 3), and 2.5mM (track 4). The *ruvC* template was digested with *NheI* and *ClaI*, these were then combined in an *in-vitro* transcription reaction to produce a marker of known size. These products were then run on a polyacrylamide gel and visualised by autoradiograpgy.

Figure 5.6

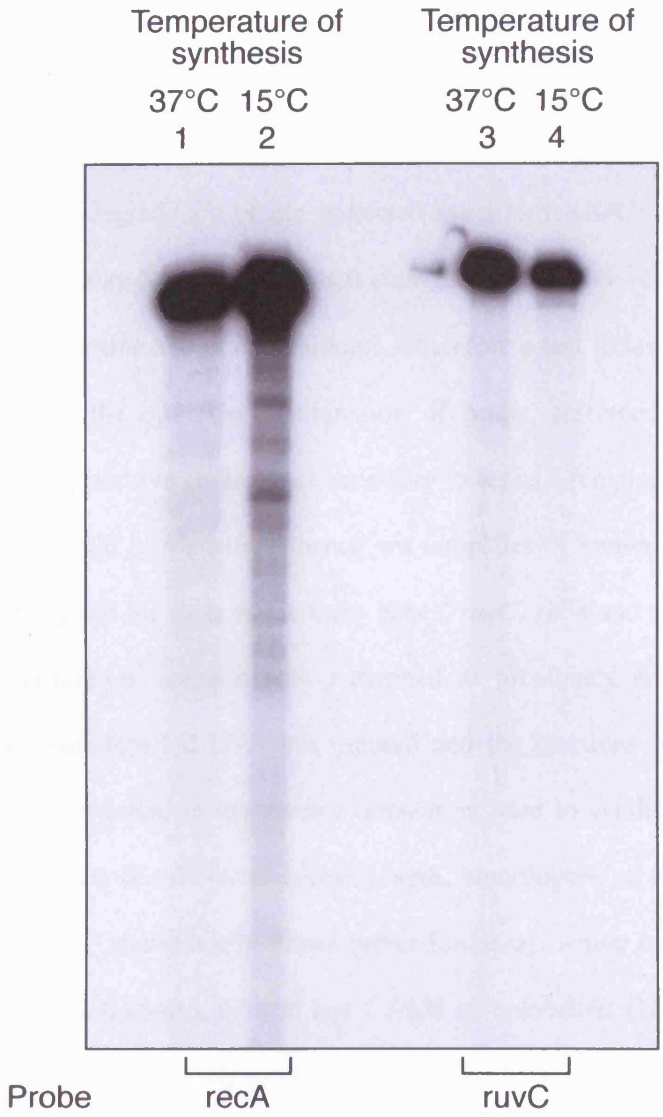

Figure 5.6: *In-vitro* transcription of the *ruvC* and *recA* probes at altered temperature. The *in-vitro* transcription reactions to produce the probes were carried out using 0.5mM unlabelled UTP, at either 37°C or 15°C. The radiolabelled probes were then run on a polyacrylamide gel, and visualised using autoradiography.

Finally, it is important to determine the quantity and type of RNase used in the protection assay to optimise the signal-to-noise ratio, whereby the RNase will remove any background (non-specific hybridization), but will not degrade the protected fragment. Degradation of the protected fragment appears as a smear on the autoradiograph, and can occur when dsRNA breathes or locally denatures, usually at regions of high uracil content. In a protection assay, this could result in the degradation of the protected specific dsRNA. To minimise incorrect degradation, RNase T1 may be used alone, as it cleaves 3′ of guanine residues, whereas RNase A cleaves 3′ of both cytosine and uracil residues. Therefore a test RNase protection assay was designed to determine the optimum combination of probe, test template(s) and digestion enzyme(s) and ratio. A positive control was necessary to act as a template for the probe, so that a protected fragment could be visualised, hence test templates of known size were synthesised using *in-vitro* transcription for each of the three genes, *ruvC*, *recA* and *sigG* (see table 5.1). A similar *in-vitro* transcription reaction was performed as previously described for the probe synthesis, however, radiolabelled UTP was omitted and the reactions were performed in the forward orientation as opposed to the reverse orientation used to synthesise the probes. This resulted in the production of ssRNA of known length, homologous to the *in-vitro* transcribed cRNA probe. Figure 5.7 shows a test RNase protection assay, where the *ruvC* probe, *in-vitro* transcribed at 0.125mM, 0.25mM, 0.5mM and 2.5mM of unlabelled UTP, were used with the test templates for *ruvC*, which clearly produced two bands at 152bp and 231bp, from the pooled *ClaI* and *NheI* digests used to form the test templates. The test RNase protection (figure 5.7) also shows the different digestions with a combination of RNase A/T1 mix, and T1 only. It is clear that probe 2 (0.5mM cold UTP) produced the most crisp band for both the probe and test template, when the digestion was performed with 1:100 ratio of RNaseA/T1 mix to reaction mix (see figure 5.7). Therefore the remaining RNase protection assays were performed with probe

Figure 5.7

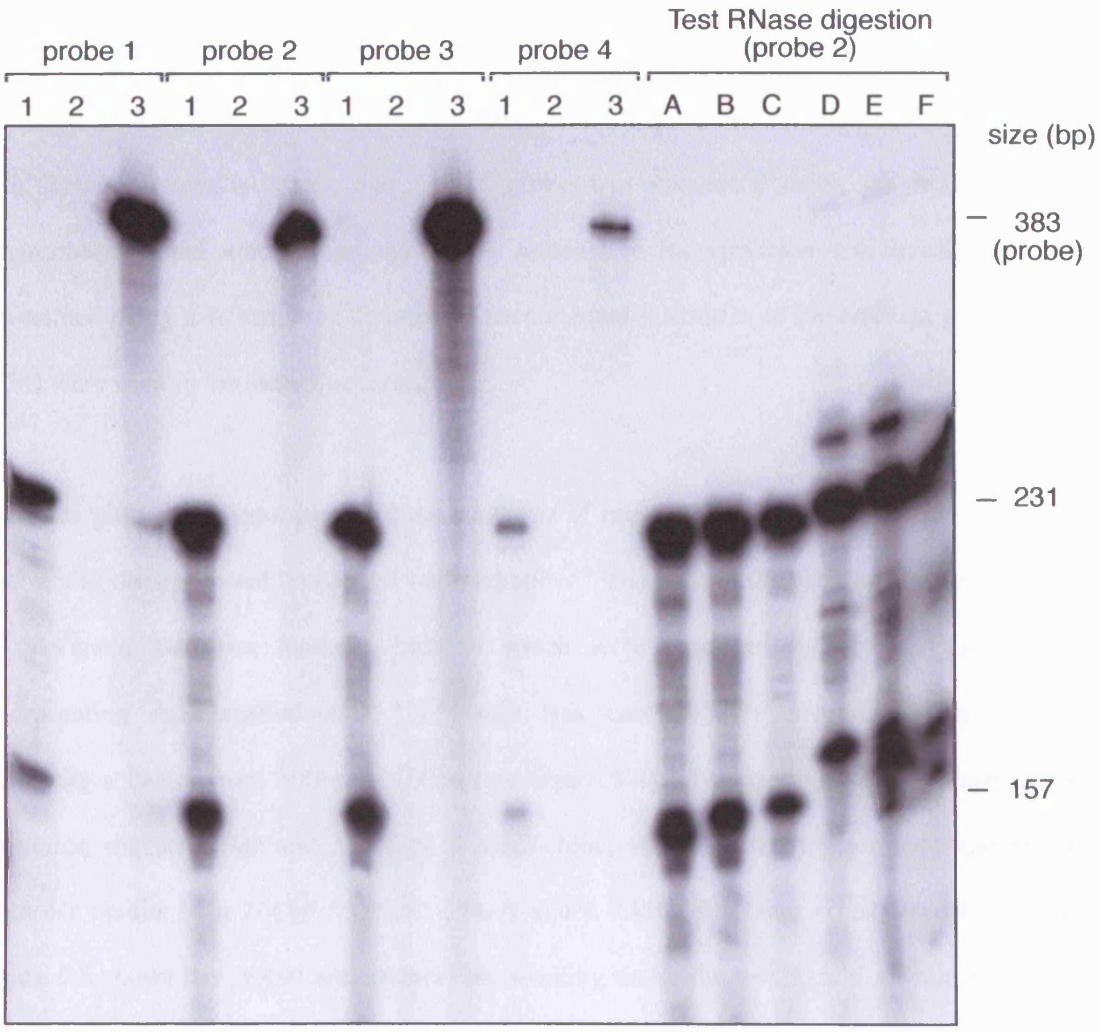

Figure 5.7: Optimisation of the RNase protection. In-vitro transcription reactions were carried out as outlined in figure 5.4, with varying concentrations of unlabelled UTP, probe 1 was synthesised with 0.125mM, probe 2 with 0.25mM, probe 3 with 0.5mM and finally probe 4 with 5mM (track 4). These probes were then used in a test RNase protection assay with an in-vitro transcribed test template. The test templates and negative control were incubated with the probe and digested with 1:100 ratio of RNase A:T1 (track 1 test template, track 2, negative control). Non-specific yeast RNA was used as a negative control. Track 3 contains the undigested probe. A test RNase digestion was performed whereby different ratios of RNaseA/T1 mix were used; 1:50 (track A), 1:100 (track B), 1:500 (track C). RNase T1 was also used alone, 1:50 (track D), 1:100 (track E), 1:500 (track F).

transcribed with the additional 0.5mM cold UTP, and the RNase digestion was performed with a ratio of 1:100 RNaseA/T1 mix to reaction mix. To enable accurate quantitation to take place, the radiolabelled probe must be in excess, therefore the probes were synthesised fresh, prior to each RNase protection assay, and 1µl of probe was visualised using polyacrylamide gel electrophoresis and autoradiography. The radioactive incorporation and quantitation was determined using a scintillation counter, to ensure equal quantities of the relevant probe ($5x10^4$ CPM) were used in the subsequent reactions.

The final pilot experiment involved the synthesis of each of the three probes, *ruvC*, *recA* and *sigG* under the optimised conditions outlined above. These were then run on a polyacrylamide gel alongside two size markers, both of which were produced by *in-vitro* transcription, incorporating radiolabelled α^{32}P UTP; one was commercially available from Ambion, producing a ladder from 500bp to 100bp (see figure 5.8). The second was produced by two restriction digests (*ClaI* and *NheI*) of a *ruvC* clone, which, when transcribed from the T3 promoter results in a 166bp fragment (*NheI*) and a 245bp fragment (*ClaI*) (see figure 5.8). Figure 5.8 shows the probes and markers are working under the test conditions outlined above, and that the test-templates and the markers can be distinguished by size, thus indicating the power of resolution of the system.

5.2.2 RNase protection of *ruvC*

The RNase protection for *ruvC* was performed using 40µg of total RNA from H37Rv wild-type, *ΔrecA* and *ΔsigG* strains, under both uninduced and induced (mitomycin C 0.02µg/ml) conditions at an OD of 0.3. The probe was used undigested as a positive control, and the *NheI* test template (see table 5.1) was used a positive control after RNase A/T1 digestion. These samples were run alongside the marker and the ladder produced by *in-vitro* transcription from

Figure 5.8

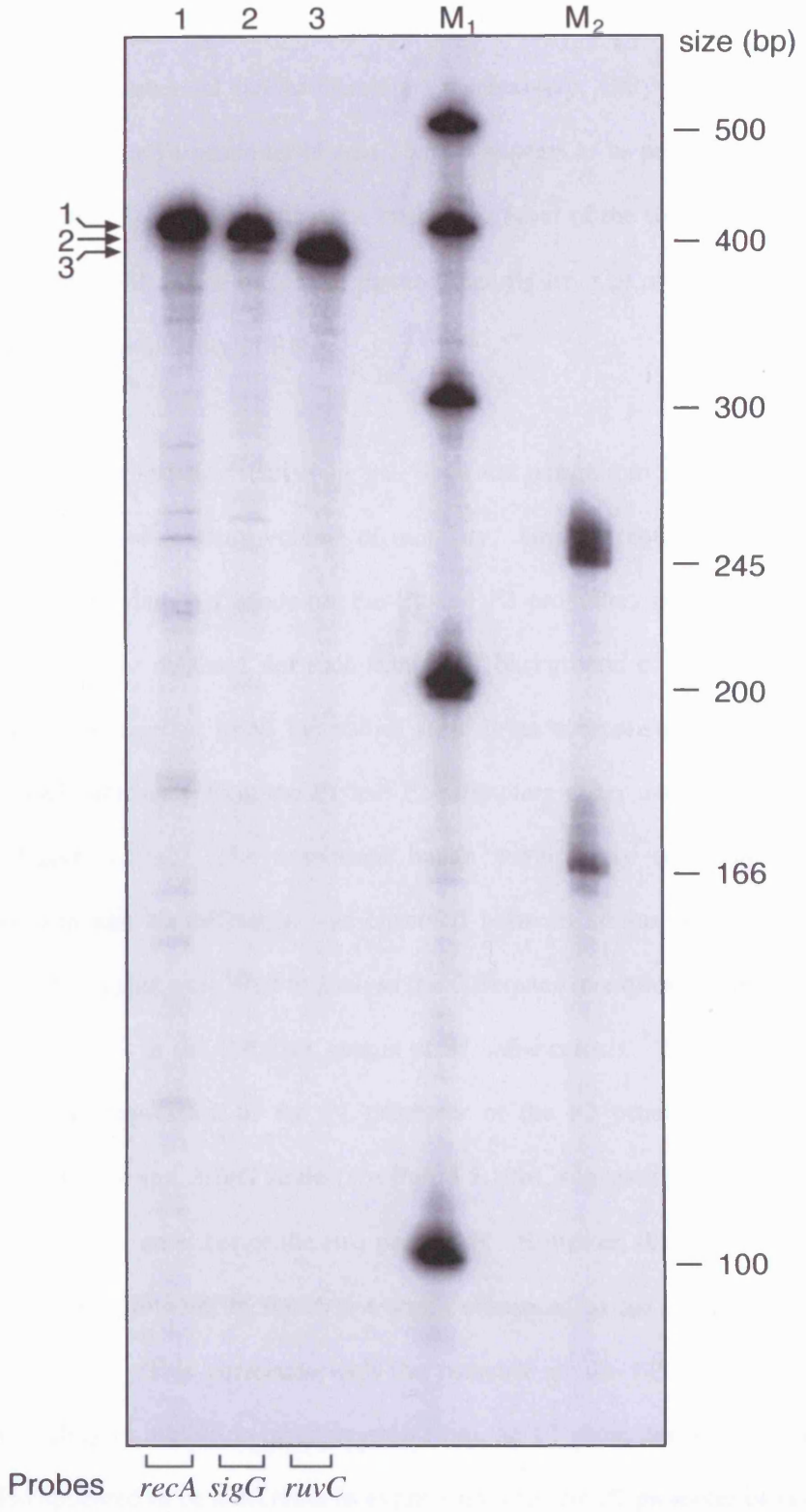

Figure 5.8: Synthesis and sizing of the *ruvC*, *recA* and *sigG* probes under optimised conditions. The *in-vitro* transcription reactions were performed with 0.5mM unlabelled UTP at 37°C. The probes were run alongside an *in-vitro* transcribed commercial ladder M1 (Ambion) and a constructed marker M2, sizes are indicated. The *recA* probe (track 1), the *sigG* probe (track 2) and the *ruvC* probe (track 3) all appear as clean bands.

the *ruvC* clone and a commercial ladder (Ambion) respectively. Only one clear band was present, corresponding to the P1 promoter of *ruvC*, which appears to be partially induced in the Δ*recA* strain (see figure 5.9). It appears that the expression level of the second promoter P2 of *ruvC* is close to the limit of detection for the method (see figure 5.9), which may have been improved by using a greater quantity of RNA.

A phosphorimager was utilised to visualise the gel, so it was possible to quantify the levels of expression from each promoter using volume of intensity. Grids of equal sizes were placed around the uninduced and induced bands for the P1 and P2 promoters individually, enabling volume measurements to be obtained, for each sample. A background correction (background value) for each grid was applied to all the values so a direct comparison could be obtained between the levels of expression from the P1 and P2 promoters under uninduced and induced conditions (see figure 5.10a). The uninduced bands were barely detectable above the background correction and no difference was observed between strains (data not included), therefore the induced samples were used to analyse the difference in expression between the P1 and P2 promoters of *ruvC* in the different strains of *M. tuberculosis*. There was clearly no difference between the expression of the P1 promoter or the P2 promoter, under induced conditions for both H37Rv and Δ*sigG* strain (see figure 5.10b), suggesting that SigG does not play a role in expression from either of the two promoters. However, there was a decrease in the expression of the P1 promoter in the Δ*recA* strain compared to the wild-type and Δ*sigG* strains (see figure 5.10b). This correlates with the presence of the SOS box and therefore implicates LexA binding in inhibition of expression from the P1 promoter of *ruvC* (see figure 5.10b). There also appeared to be a decrease in expression from the P2 promoter of *ruvC* in the Δ*recA* strain compared to the wild-type and Δ*sigG* strains, but the low level of expression from

Figure 5.9

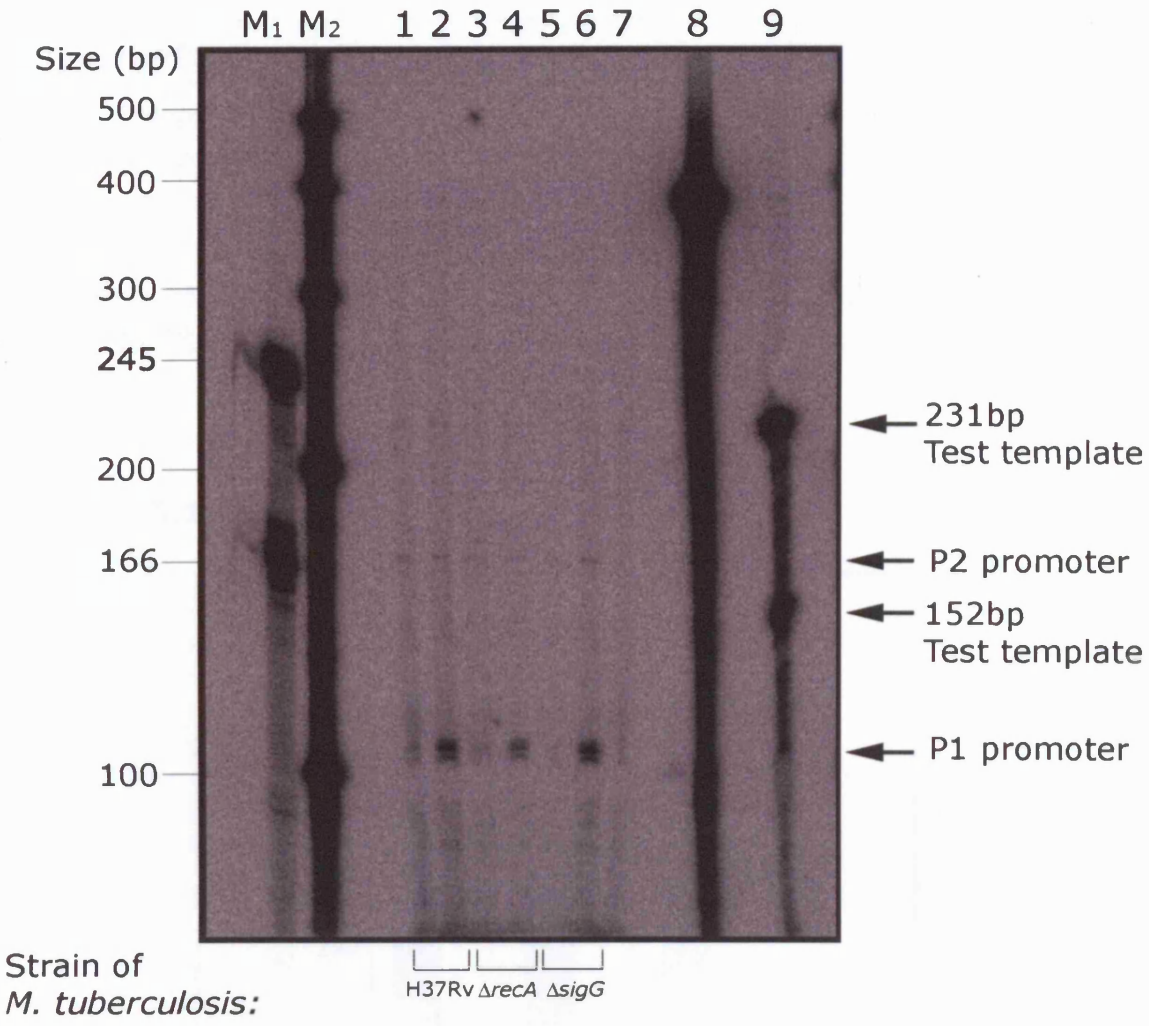

Figure 5.9: RNase protection assay to identify *ruvC* promoters in H37Rv, Δ*recA* and Δ*sigG* strains of *M. tuberculosis*. Assays were performed on 40μg of RNA, under uninduced and induced conditions (0.02μg/ml mitomycin C), at an OD of 0.3, tracks 1-6. Yeast RNA was used as the negative control (track 7), two positive controls were the undigested probe (track 8) and the test template (track 9). The *ruvC* test template was produced by non-radiolabelled *in-vitro* transcription in the forward orientation of the probe construct, and yields products of 152bp and 231bp, when protected by the *ruvC* probe. The hybridization reaction of the template/RNA and probe was carried out over night at 42°C. Digestion was carried out with a ratio of 1:100 RNase A:T1. Samples were run alongside *in-vitro* transcribed markers (track M_1 and M_2), sizes are indicated above. Samples were then visualised by polyacrylamide gel electrophoresis and autoradiography. The position of the two *ruvC* promoters and the test template are marked with arrows.

Figure 5.10a

Grid Name	Grid Area	Volume	Background Value	Corrected volume
H37Rv Induced P1	600	8181.6	12.24	8169.36
ΔrecA Induced P1	600	4137.67	6.607	4131.063
ΔsigG Induced P1	600	7876.67	14.095	7862.575
H37Rv Induced P2	600	582.34	3.207	579.133
ΔrecA Induced P2	600	41.3	2.372	38.928
ΔsigG Induced P2	600	651.65	3.102	648.548

Figure 5.10b

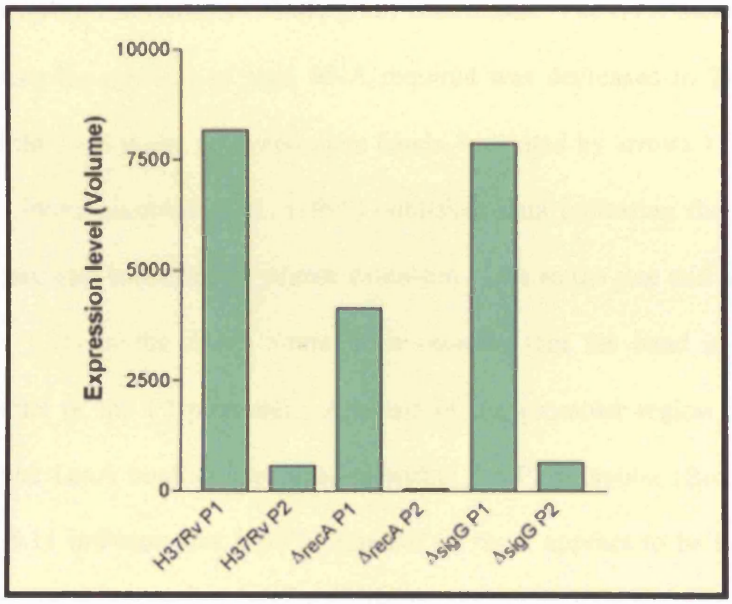

Figure 5.10a: The expression level of P1 and P2 promoters of *ruvC*, under induced conditions in H37Rv wild type, Δ*recA* and Δ*sigG* strains of *M. tuberculosis*. An RNase protection assay was performed on uninduced and induced RNA form H37Rv wild type, Δ*recA* and Δ*sigG* strains to detect the *ruvC* promoters P1 and P2. Using the phosphorimager software, grids of equal size were placed over the bands produced from an RNase protection assay, to determine the level of transcript for each promoter from each strain. The levels of expression from the uninduced samples were below the level of detection above background, therefore volume and background measurements were taken from only the induced bands. The area of each grid is listed, alongside the volume inside the grid, and the background correction (Local/average).

Figure 5.10b: A graph showing the differences in expression level of the P1 and P2 promoters of *ruvC* as determined using the phosphorimager. The corrected volume data was used to create the graph in Graphpad programme, Prism 4.

the P2 promoter hindered accurate quantification of the transcript, so the reliability of this observation is uncertain.

5.2.3 RNase protection of *recA*

In view of the partial induction of *ruvC* observed by both RNase protection and primer extension in the Δ*recA* strains of *M. tuberculosis*, it was of interest to assess the expression of *recA*. The RNase protection for *recA* was performed using 20μg of total RNA extracted at mid-exponential phase (OD 0.3), from H37Rv wild-type, Δ*recA* and Δ*sigG* strains, under both uninduced and induced (mitomycin C 0.02μg/ml) conditions. The *recA* transcript is relatively abundant; therefore the quantity of total RNA required was decreased to 20μg. The RNase protection using the *recA* probe produced three bands, indicated by arrows 1, 2 and 3 in figure 5.11. However, Movahedzadeh *et al.*, (1997) published data indicating there were only two transcriptional start sites identified by primer extension. Due to the size and absence of band 2 (arrow 2, figure 5.11) in the Δ*recA* strain, it is possible that the band is merely a partial degradation product of the P2 promoter. Analysis of the promoter region of *recA* indicated there was only one LexA binding site, situated within the P2 promoter (Brooks *et al.*, 2001). Arrow 3, figure 5.11 indicates that the P1 promoter of *recA*, appears to be induced in H37Rv wild-type, Δ*recA* and Δ*sigG* strains. However, the level of induction appears to be decreased in the Δ*sigG* strain. In contrast, the P1 promoter in the Δ*recA* strain gave an undiminished band, further confirming that the P1 promoter is DNA-damage inducible independently of RecA. The P2 promoter, indicated with arrow 3 (figure 5.11) appears to be induced in both the H37Rv and Δ*sigG* strains, but there is no induction of the P2 promoter in the Δ*recA* strain (figure 5.11). The P2 promoter possesses a putative LexA binding site and therefore the LexA repressor

Figure 5.11

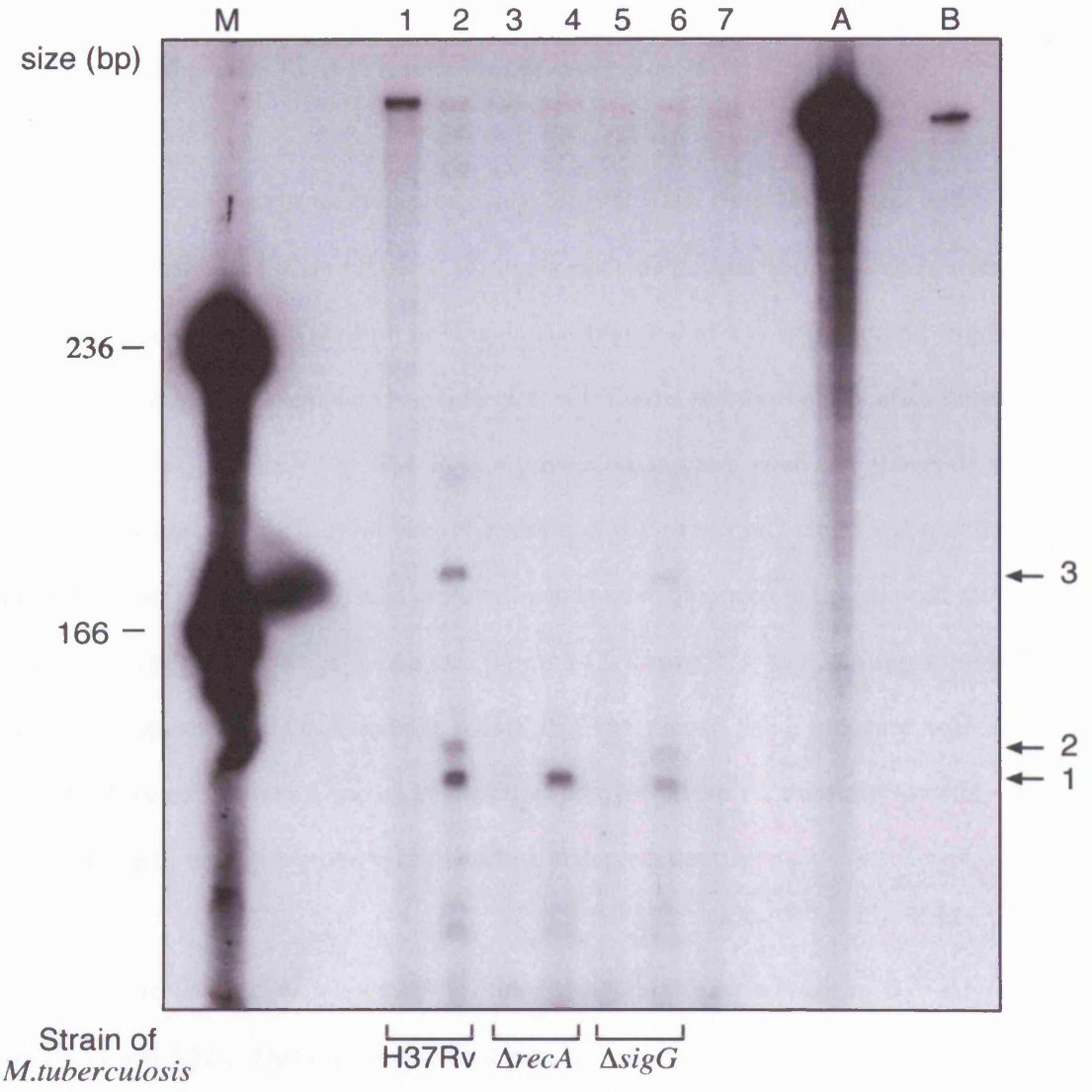

Figure 5.11: RNase protection assay to identify *recA* promoters in H37Rv, Δ*recA* and Δ*sigG* strains of *M. tuberculosis*. Assays were performed on 20μg of RNA, under uninduced and induced conditions (0.02μg/ml mitomycin C), for H37Rv, Δ*recA* and Δ*sigG* strains of *M. tuberculosis* induced at an OD of 0.3, tracks 1-6 respectively. The strains are marked under the tracks. Yeast RNA was used as the negative control (track 7), two positive controls were the undigested probe (track A) and the test template (track B). The *recA* test template was produced by non-radiolabelled *in-vitro* transcription in the forward orientation of the probe construct. The hybridization reaction of the template/RNA and probe was carried out over night at 42°C. Digestion was carried out with a ratio of 1:100 RNase A:T1. Samples were run alongside *in-vitro* transcribed marker (track M), sizes are indicated. Samples were then visualised by polyacrylamide gel electrophoresis and autoradiography. The position of the three *recA* products are marked with arrows.

appears to abolish expression from the P2 promoter in the Δ*recA* strain, indicating, as previously published, that RecA is required for de-repression of the P2 promoter.

The RNase protection assay was repeated using 20μg of RNA from H37Rv and Δ*sigG* strains. The RNA was harvested at an OD of 0.15, under both uninduced and induced (mitomycin C 0.02μg/ml) conditions. The *recA* probe was used undigested as a positive control (figure 5.12, track 6), and the *NheI* test template (see table 5.1) was used a positive control after RNase A/T1 digestion (figure 5.12, track 7). The RNase protection samples were run alongside the size marker and ladder produced by *in-vitro* transcription from the *ruvC* clone and a commercial ladder (Ambion) respectively. Three protected bands were produced in the induced samples of H37Rv wild-type and the Δ*sigG* strain (see figure 5.12, arrows 1, 2 and 3), suggesting both the P1 and P2 promoters are DNA-damage inducible. The second band, indicated with arrow 2 (figure 5.12) is most likely a partial degradation product of the P2 transcript possibly due to local breathing of the RNA-probe hybrid, leading to degredation.

Intriguingly the level of expression of all three bands appeared weaker in the Δ*sigG* strain (figure 5.11 and 5.12). This may simply be due to differential loading of RNA; however, this is unlikely as the samples of RNA were quantified using a bioanalyser, which produces accurate quantitations, particularly in light of the fact that two biological replicates of the Δ*sigG* strain produced similar results. This might indicate that SigG may directly or indirectly partially regulate expression from both the P1 and P2 promoters of *recA*, however, this possibility would need to be tested, potentially using *lacZ* fusion assays in the Δ*sigG* strain compared to H37Rv.

Figure 5.12

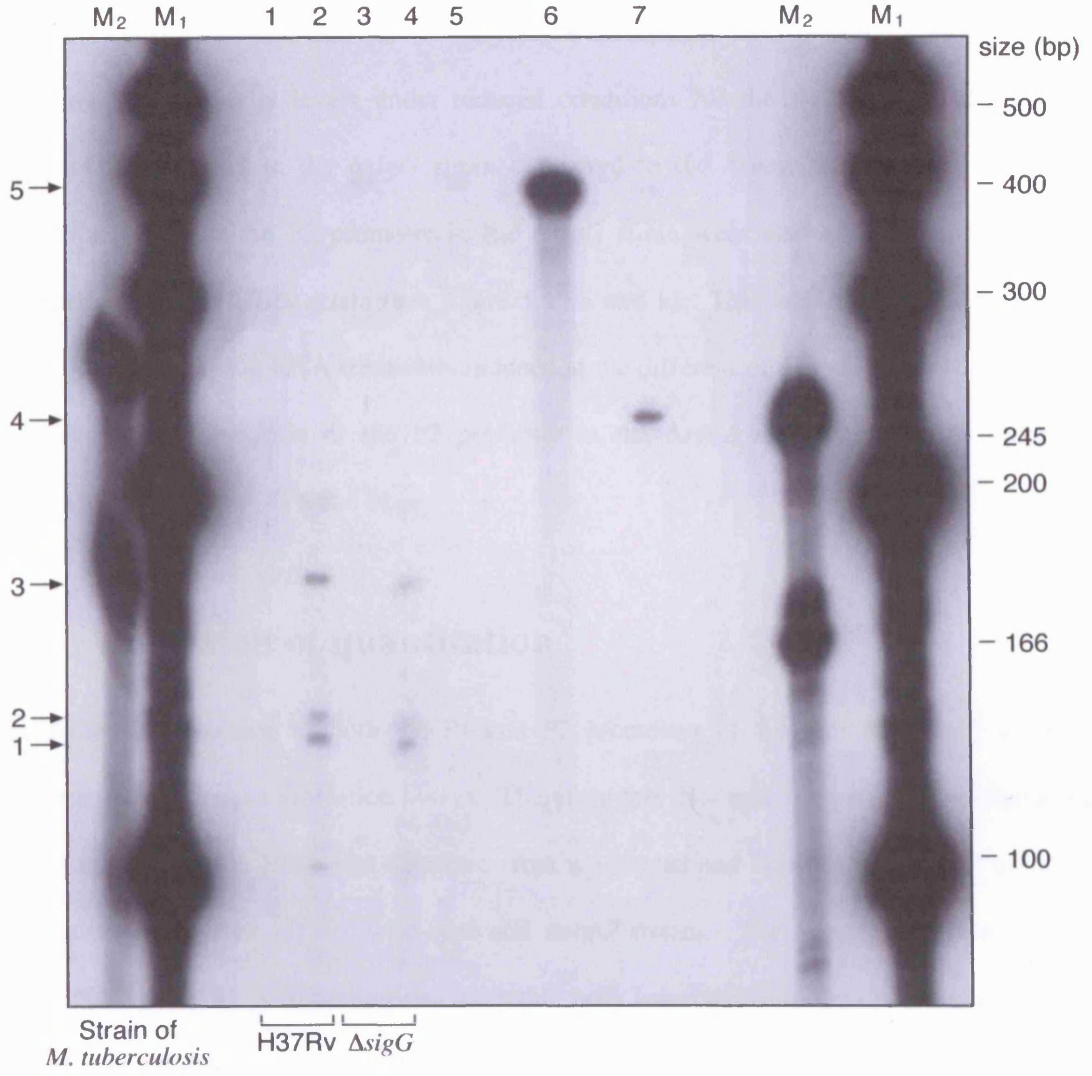

Figure 5.12: RNase protection assay to identify *recA* promoters in H37Rv and *sigG* strains of *M. tuberculosis*. Assays were performed on 20μg of RNA, under uninduced and induced conditions (0.02μg/ml mitomycin C), for H37Rv and *sigG* strains of *M. tuberculosis* induced at an OD of 0.15, tracks 1-4 respectively. The strains are marked under the tracks. Yeast RNA was used as the negative control (track 5), two positive controls were the undigested probe (track 6) and the test template (track 7). The *recA* test template was produced by non-radiolabelled *in-vitro* transcription in the forward orientation of the probe construct. The hybridization reaction of the template/RNA and probe was carried out over night at 42°C. Digestion was carried out with a ratio of 1:100 RNase A:T1. Samples were run alongside *in-vitro* transcribed markers (track M1 and M2), sizes are indicated. Samples were then visualised by polyacrylamide gel electrophoresis and autoradiography. The position of the three *recA* promoters are marked with arrows 1, 2 and 3. The probe and test template are marked with arrows 5 and 4 respectively.

In order to quantify the difference in expression observed in figures 5.11 and 5.12, grids were placed around the bands of both RNase protection assays on the phosphorimager, and corrected volume calculations were derived to analyse the differences in expression (see figure 5.13); revealing that transcript levels under induced conditions for the P1 promoter of *recA* were approximately halved in the Δ*sigG* strain compared to the Δ*recA* and H37Rv strains. The transcript levels for the P2 promoter in the Δ*sigG* strain were also approximately halved in comparison to the H37Rv strain (see figure 5.13 a and b). This was observed in both RNase protection assays using RNA from cells induced at the different optical densities (0.3 and 0.15). The level of transcription of the P2 promoter in the Δ*recA* strain was almost completely abolished (see figure 5.13 a and b).

5.3 Validation of quantitation

The reduced expression of both the P1 and P2 promoters of *recA* in the Δ*sigG* strain was observed in both RNase protection assays. Therefore this data was compared to microarray data (see chapter 4), where RNA was extracted from uninduced and induced (0.02ug/ml mitomycin C) conditions for both H37Rv wild-type and Δ*sigG* strains. The microarrays were designed with DNA versus RNA hybridisations to enable both inter- and intra-strain comparisons. The normalisations carried out are outlined in chapter 4. There were no significant differences at the 1% confidence interval between the expression of *recA* or *ruvC* under uninduced and induced conditions for H37Rv wild-type and Δ*sigG* strain (see figure 5.14), although as expected the expression of *sigG* was clearly reduced in the Δ*sigG* strain.

Figure 5.13a

Grid name	Area	Volume	Background Value	Corrected volume
H37Rv 0.35 Ind P2 (SOS Box)	975	34485.91	12.579	34473.331
ΔrecA 0.35 Ind P2 (SOS box)	975	3026.73	5.911	3020.819
ΔsigG 0.35 Ind P2 (SOS Box)	975	14365.75	10.099	14355.651
H37Rv 0.35 Ind P1	975	53332.96	19.834	53313.126
ΔrecA 0.35 Ind P1	975	54802.28	20.266	54782.014
ΔsigG 0.35 Ind P1	975	25271.22	20.354	25250.866
H37Rv 0.15 Ind P2 (SOS box)	975	118412.42	24.678	118387.742
ΔsigG 0.15 Ind P2 (SOS box)	975	63609.18	20.592	63588.588
H37Rv 0.15 Ind P1	975	112971.87	47.096	112924.774
ΔsigG 0.15 Ind P1	975	80674.5	39.962	80634.538

Figure 5.13b

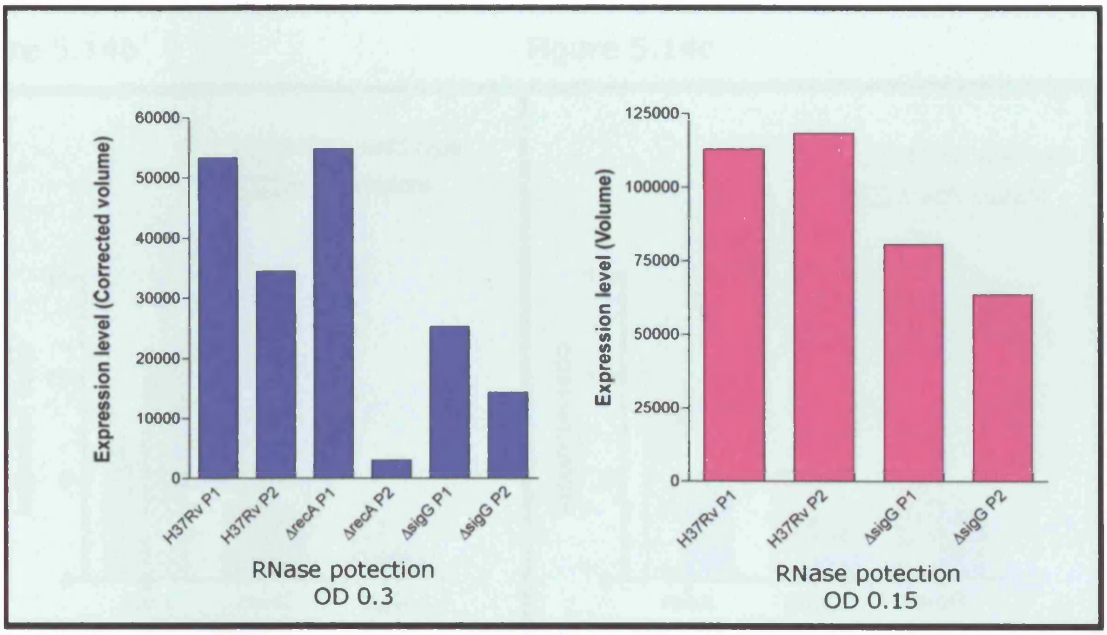

Figure 5.13a: The expression level of P1 and P2 promoters of *recA*, under induced conditions in H37Rv wild type, Δ*recA* and Δ*sigG* strains of *M. tuberculosis*. An RNase protection assay was performed on uninduced and induced RNA form H37Rv wild type, Δ*recA* and Δ*sigG* strains to detect the *ruvC* promoters P1 and P2. Using the phosophorimager software, grids of equal size were placed over the bands produced from an RNase protection assay, to determine the level of transcript for each promoter from each strain. The levels of expression from the uninduced samples were below the level of detection above background, therefore volume and background measurements were taken from only the induced bands. The area of each grid is listed, alongside the volume inside the grid, and the background correction (Local/average).

Figure 5.13b: A graph showing the differences in expression level of the P1 and P2 promoters of *recA* as determined using the phosphorimager. The corrected volume data was used to create the graph in the Graphpad programme, Prism 4.

Figure 5.14a

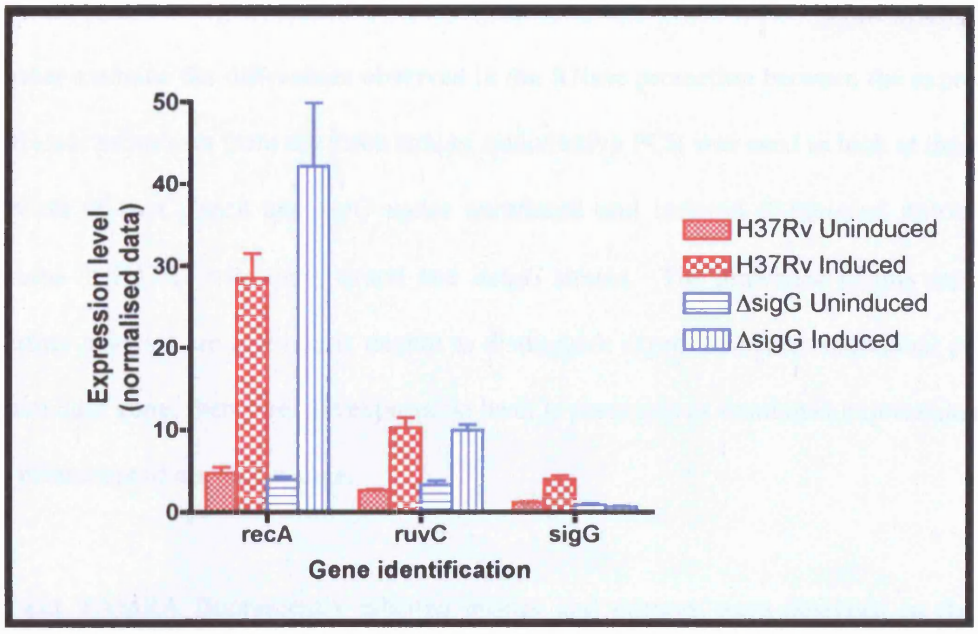

Figure 5.14b

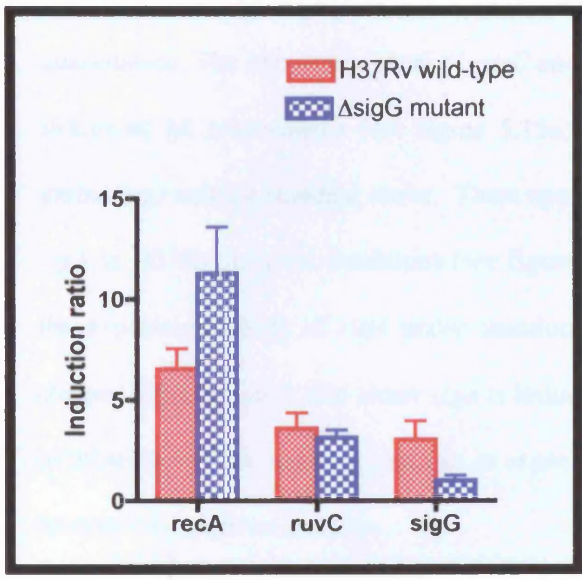

Figure 5.14c

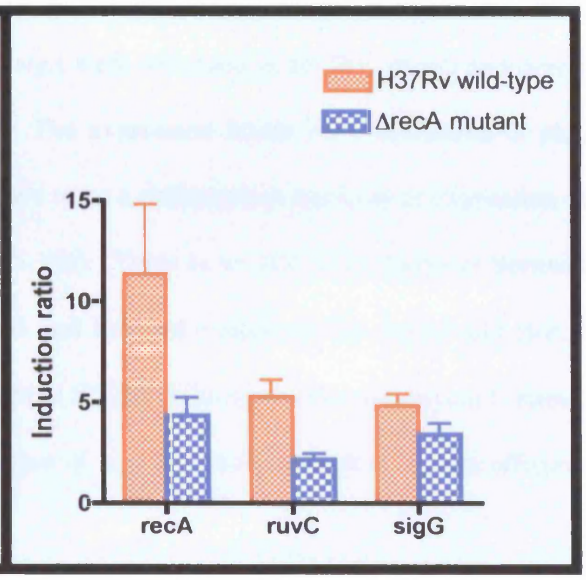

Figure 5.14a: A comparison between the expression level of *recA*, *ruvC* and *sigG* in the wild-type H37Rv and Δ*sigG* mutant of *M. tuberculosis*. The data were obtained from micro-array experiments outlined in chapter 4. The graph shows a comparison between the gene expression level, under both uninduced and induced conditions (0.02μg/ml mitomycin C) at an OD of 0.15.

Figure 5.14b: A comparison between induction ratio of *recA*, *ruvC* and *sigG* in the wild-type H37Rv and Δ*sigG* mutant of *M. tuberculosis*. Induction ratios were calculated using the normalised values for uninduced and induced data outlined above.

Figure 5.14c: A comparison between the expression level of *recA*, *ruvC* and *sigG* in the wild-type H37Rv and Δ*recA* mutant of *M. tuberculosis*. Data was modified from Rand *et al.*, 2003.

To further examine the differences observed in the RNase protection between the expression of the different promoters from the three strains, quantitative PCR was used to look at the levels of expression of *ruvC*, *recA* and *sigG* under uninduced and induced (0.02μg/ml mitomycin C) conditions in H37Rv wild-type, *ΔrecA* and *ΔsigG* strains. The drawback of this method and microarray analysis are that one is unable to distinguish expression from individual promoters of a particular gene; therefore, the expression level is presented as combined expression from all of the promoters of a specific gene.

FAM and TAMRA fluorescently labelled probes and primers were designed in the coding region for *recA*, *ruvC* and *sigG*. These were used along side an internal standard control *sigA* and were also run alongside a standard curve of known concentrations of DNA, to enable quantitation. The expression level of *ruvC* and *sigA* were measured in H37Rv, *ΔsigG* and *ΔrecA* strains of *M. tuberculosis* (see figure 5.15a). The expression levels were calculated in pico grams (pg) using a standard curve. There appears to be a difference in the level of expression of *sigA* in H37Rv induced conditions (see figure 5.15a). There is no difference however between the expression levels of *sigA* under uninduced and induced conditions for *ΔsigG* and *ΔrecA* strains. This indicates that either *sigA* is induced in H37Rv wild-type under mitomycin C stress, or more likely, the apparent increase in expression of *sigA* is merely a result of a more efficient reverse transcription reaction.

In figure 5.15b, the expression of *ruvC* is expressed as a proportion of internal standard, *sigA*. The expression level of *ruvC* in uninduced conditions is higher in the *ΔsigG* strain than the H37Rv and *ΔrecA* strains (figure 5.15b). Despite this, there is no difference in the induced level of expression of *ruvC* between H37Rv and *ΔsigG* strains. A decrease in the level of induction of *ruvC* in the *ΔrecA* strain was observed, although this decrease was not as marked as the

Figure 5.15a

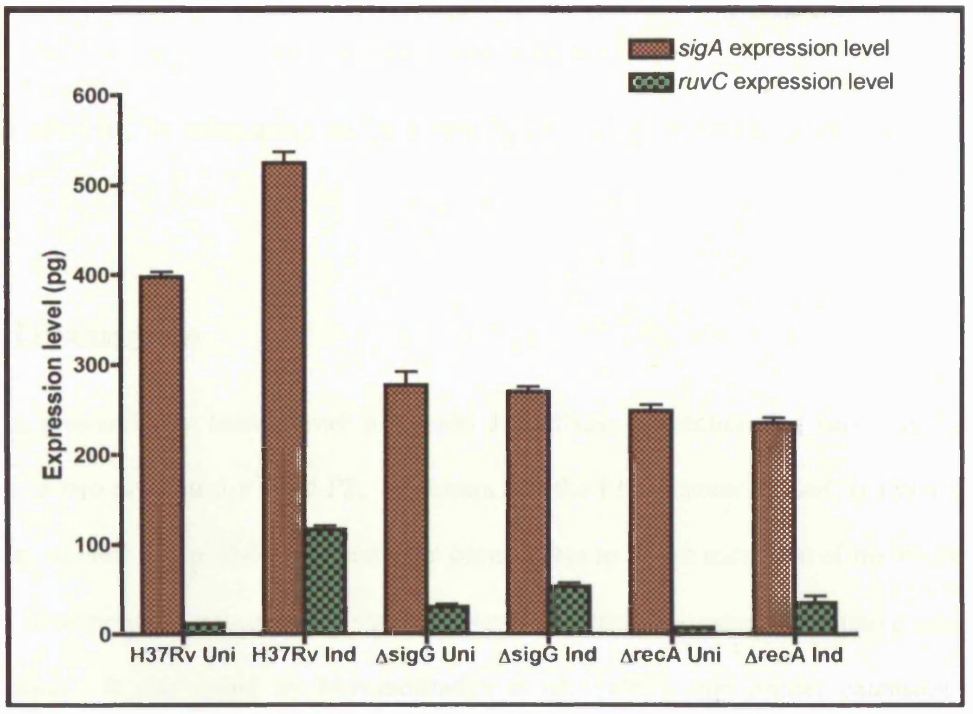

Figure 5.15b

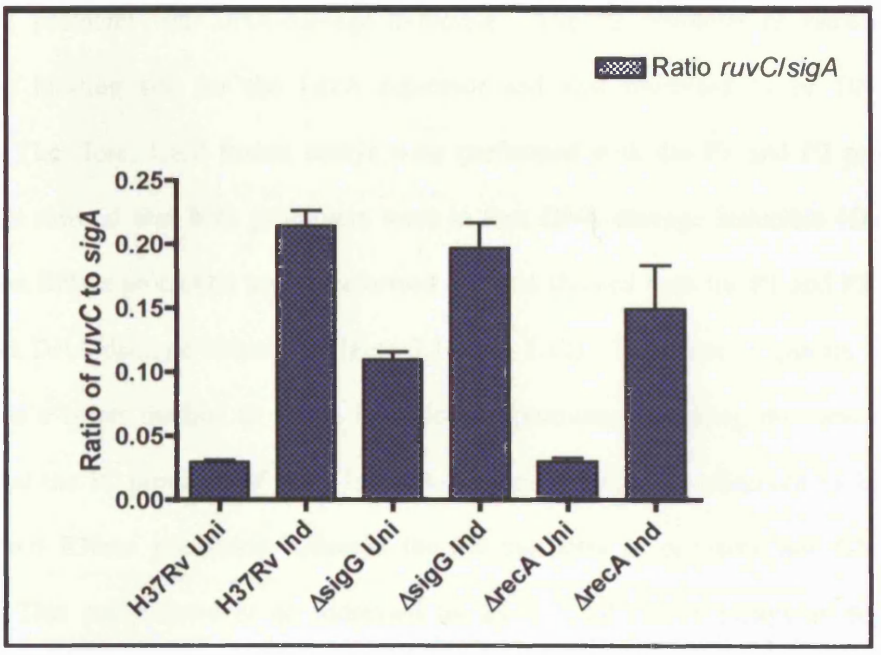

Figure 5.15a: Taqman expression levels of *ruvC* in H37Rv wild-type, Δ*recA* and Δ*sigG* strains of *M. tuberculosis*. 1μg of RNA for each strain under both uninduced and induced (0.02μg/ml mitomycinC) conditions were used in a cDNA synthesis reaction, using random primers (RT+), a negative control ommitting reverse transcriptase was also used (RT-). The resultant cDNA was diluted 1:20 with DEPC dH_2O, and 5μl were used in the Taqman real time PCR. The *sigA* and *ruvC* probes used were FAM/TAMRA labelled. *sigA* was used as an internal standard and known concentrations of DNA were used to produce a standard curve to determine the concentration (pg). Both RT+ and RT- reactions were used in triplicate. The expression level obtained from each sample for both probes was used in Graph Pad Prism to create a graph.

Figure 5.15b: Taqman expression level of *ruvC* expressed as a proportion of *sigA*. The data obtained for *ruvC* from the above Taqman was expressed as a proportion of the internal control *sigA*.

decrease observed by microarray analysis (see figure 5.15c), or RNase protection (see figure 5.9).

5.4 Discussion

The data presented by both primer extension and RNase protection for *ruvC* indicates the presence of two promoters P1 and P2. It appears that the P1 promoter of *ruvC* is DNA-damage inducible, whereas the methods utilised have been unable to detect induction of the P2 promoter of *ruvC*, in response to mitomycin C stress. RNase protection is a more quantitative measure of transcription. It was noted by Movahedzadeh *et al.*, (1997) that primer extension assays performed on *recA* showed the P1 promoter was DNA-damage inducible, but it did not appear that the P2 promoter was DNA-damage inducible. The P2 promoter of *recA* contains a palindromic binding site for the LexA repressor and was predicted to be DNA-damage inducible. Therefore, LacZ fusion assays were performed with the P1 and P2 promoters of *recA*, which showed that both promoters were in fact DNA-damage inducible (Davis *et al.*, 2002b). The RNase protection assay performed on *recA* showed both the P1 and P2 promoters were in fact DNA-damage inducible (figure 5.11 and 5.12). Therefore it appears that RNase protection is a better method to detect induction of promoters. Taking this into account, it indicates that the P1 promoter of *ruvC* is DNA-damage inducible as observed by both primer extension and RNase protection, whereas the P2 promoter is probably not DNA-damage inducible. This could however be addressed by using LacZ fusion assays as described by (Davis *et al.*, 2002b)

It is particularly interesting to note that the P1 promoter of *ruvC*, remains partially DNA-damage inducible in the Δ*recA* strain of *M. tuberculosis*, which indicates that the P1 promoter

may be dual regulated, especially as the P2 promoter of *recA* in the Δ*recA* strain shows no induction. This indicates that the P2 promoter of *recA* is regulated by the RecA/LexA system: ablation of expression of the *recA* P2 promoter in the Δ*recA* strain indicates dependence of the P2 promoter on RecA for de-repression. Conversely the P1 promoter of *ruvC* is able to partially overcome the repression by LexA, even in the absence of RecA. There are a number of different mechanisms by which the P1 promoter of *ruvC* may be able to partially overcome repression by LexA: These include the promoter recognition site, which may affect sigma factor specificity and competition for the core RNAP, along with the possibility that transcription factors play a role by either affecting sigma factor binding or RNAP stability. Possible transcription factors include ppGpp, H-NS, Fis and other architectural proteins, which also affect local DNA topology and may therefore influence repression by LexA. The other possibility is that the relative position of the LexA binding site may enable binding of the RNAP to the –10 and –35 regions, which may destabilize and overcome the repression of the LexA, or the RNAP may initiate transcription during equilibrium maintenance, discussed below.

To address the possibility that these differences in repression were a result of sigma factor specificity, promoter consensi were analysed. There have been a number of promoter consensus sequences identified, including *E. coli* sigma S, encoded by RpoS; the stress response sigma factor for *E. coli* (Lee and Gralla, 2001). This sigma factor is particularly interesting as it drives transcription from approximately 100 genes, involved in the stress response regulon, including those involved in oxidative stress, such as *sodC* (superoxide dismutase), *katE* and *katD* (catalases), *xthA* (endonuclease) and *ada* (methyl transferase), as well as virulence factors, *csgBA* (curli) (Lacour and Landini, 2004). SigS is a member of the σ^{38} family and the consensus sequence for σ^{38} at –10 is CTAcacT (Lee and Gralla, 2001), which was refined

further by Lacour and Landini, (2004) to $TGN_{0-2}C(C/T)ATA(C/A)T$. The underline indicates where this sequence is nearly identical to the consensus of sigma 70 in *E. coli* (TATAAT) –10 and (TTGACA) –35 (Lisser and Margalit, 1993). The –35 site of RpoS is identical to the sigma 70 site. This is particularly interesting, as it suggests two sigma factors are able to recognise similar –10 and -35 promoter elements. It has been shown *in-vitro* that σ^s/σ^{38} is able to initiate transcription from some σ^{70} promoters. The promoters all had similar –10 regions, and were divided into three categories, type I were recognised by both σ^{70} and σ^{38}, type II were recognised by mainly σ^{70} whereas type III were recognised by only σ^{38} (Tanaka et al., 1993). Therefore these sigma factors could compete to initiate transcription. However, RpoS is expressed at low levels in the cell, until stationary phase, when the level gradually increases. Conversely the levels of σ^{70} appear to remain relatively constant (Tanaka et al., 1993). This is particularly relevant, as the P1 promoter region of *ruvC* appears to show homology to both the σ^{70} and σ^{38} – 10 promoter consensus sequences, suggesting the possibility that transcription of *ruvC* from P1 may be regulated by two sigma factors.

It is noteworthy that *in-vitro* transcription levels do not always conform with the *in-vivo* findings, suggesting that different transcription factor(s) and/or specific transcription conditions may be necessary for transcription by σ^{38} in preference to σ^{70} (Tanaka et al., 1995). Interestingly, the *csgA* promoter of *E. coli* is transcribed by both σ^{38} and σ^{70}, yet the histone like protein H-NS selectively inhibits transcription of the *csgA* promoter by σ^{70}, thus indicating the importance of DNA structure in transcriptional initiation (Tanaka et al., 1995). Other structural proteins including Lrp, CRP, IHF and Fis have been implicated in determining whether expression from a given promoter is driven by σ^{38} or σ^{70} (Hengge-Aronis, 1999). Transcriptional analysis of genes transcribed in *E. coli* by σ^{38} revealed that the region

downstream of –17 (including the –10 hexamer) is important for recognition, by σ^{38} (Tanaka et al., 1995). Transcription of a single promoter may be subject to differential regulation by two sigma factors. This has been observed with genes involved in osmoregulation, *osmB* and *osmY* in *E. coli*. Under normal conditions, transcription is driven equally by σ^{38} and σ^{70}; however under elevated concentrations of glutamate or acetate the level of transcription by σ^{38} increased by approximately 20 fold (Tanaka et al., 1995). It has been shown that the –10 regions for *E. coli* and *M. tuberculosis* housekeeping promoters are highly conserved, but there are differences at the –35 sites (Lee and Gralla, 2001).

Another factor affecting transcription of genes dual regulated by σ^{S} and σ^{70} is alarmone guanosine tetraphosphate (ppGpp), which can act as a positive or negative regulator of transcription. ppGpp can bind to the β or β′ subunits of RNA polymerase, which reduces the ability of the RNAP-σ complex to form an open complex, necessary for elongation during transcription. However ppGpp can also work an a positive regulator of transcription, by destabilising the RNAP-σ complex bound to *rrnP1* promoters, thus increasing the amount of free RNAP-σ complex, which is then able to drive transcription of promoters which are less well adapted to recruiting RNAP-σ complex (Jishage et al., 2002). Interestingly regulators of alternative sigma factors require elevated concentrations of ppGpp for transcription. Po and Pu inducers of σ^{54} promoters require ppGpp for transcription. ppGpp has been shown to affect sigma factor competition for core RNAP, favouring interactions with alternative sigma factors rather than σ^{70} (Gralla, 2005).

It has been shown that sigma factors compete to bind with core RNAP and initiate transcription of their regulon. As previously mentioned, σ^{S} encoded by *rpoS* is a stress response sigma factor

in *E. coli*, responding to a number of environmental stresses including oxidative stress. In a σ^S mutant strain of *E. coli*, super induction of genes regulated by σ^{70} was observed. This was thought to be due to the quantity of σ^{70} binding to core RNAP, brought about by the absence of competition for the core RNAP by σ^S (Nystrom, 2004a). Interestingly, over-expression of σ^A, results in a decrease in the expression of genes transcribed by other sigma factors, suggesting the levels of competing sigma factors provide an additional layer to the regulation of transcription at different stages during growth. However, it is not known whether this competition is a direct result of the relative concentrations of specific sigma factors, or their relative affinities for the core RNAP (Nystrom, 2004a). The current hypothesis states that there is a transcriptional trade off between stress defence and growth and proliferation. SpoT and RelA affect levels of ppGpp in the cell, by affecting production and hydrolysis of ppGpp, which in turn affects the affinity of the RNAP for the alternative sigma factors involved in the stress response. However, to complicate matters, DskA is a polymerase binding protein, which is attracted to the active site of the RNAP, like ppGpp and nucleotides. In the presence of the co-regulator, significantly less ppGpp is required to inhibit transcription (Gralla, 2005). Interestingly Hengge-Aronis, (1999) suggested that σ^{70} and σ^S recognise almost identical promoter regions, and that the stress response genes transcribed by σ^S, were actually transcribed by the interactions of the holoenzymes containing σ^{70} and σ^S, along with other factors, such as H-HS, Lrp, CRP, IHF or Fis. These additional factors were key in determining whether transcription was initiated by σ^{70} or σ^S (Hengge-Aronis, 1999). It was also suggested that the local difference in DNA structure may play a role in the differential choice between σ^{70} and σ^S (Hengge-Aronis, 1999).

The proximity of the +1, -10 and –35 sites may also have an effect on transcription. Closer analysis of the promoter regions upstream of the *E. coli* rRNA P1 revealed that there is an unusually short spacer between the –10 and –35 sites (this is also observed with the P1 promoter of *M. tuberculosis recA*), as well as a CG rich sequence upstream of the +1, and a long spacer between the –10 and the +1. A reduction of supercoiling with the rRNA promoter has been shown to significantly decrease transcription (Lew and Gralla, 2004).

Another alternative mechanism for regulation of transcription of a particular gene has been observed with the heat shock induced *dnaK* in *Clostridium acetobutylicum*, whereby there is an 11bp inverted repeat (GCACTC) present between the transcriptional and translational start site, which forms a hairpin loop structure, and may be involved in regulation of expression (Narberhaus et al., 1992). Thus further indicating the importance of DNA topology in regulation of gene expression in response to environmental stress.

The sequence and the position of the LexA binding site may play a role in the efficacy of repression. However, taking into account that both *recA* and *ruvC* show the same mismatch to the SOS box consensus, it is more likely that the position of the SOS box plays a role in differential repression of *recA* and *ruvC*. The relative position of repressor binding sites has been shown to be of importance in regulation by TrpR, a repressor protein. Genes regulated by the TrpR repressor have either weak or strong TrpR boxes, which show weak or strong binding of the TrpR repressor respectively (Pittard *et al.*, 2005). The level of repression is dependent on the binding site (TrpR box) and the relative position of the TrpR box to the –10 and –35 promoter elements as well as to the transcriptional start site. The formation of the repressor is also important, as the TrpR repressor can form both dimers and hexamers, dimers bind to strong

TrpR boxes, whereas hexamers of TrpR bind to weak TrpR boxes. TrpR is a dimer in solution, but in the presence of ATP and tyrosine can form a hexamer (Pittard et al., 2005). It has also been demonstrated that weak TrpR box overlaps with the promoter. This is of interest as it has been shown that LexA *in-vitro* is present in dimers (Chattopadhyaya and Pal, 2004).

These weak TrpR boxes are recognised and repressed by the hexamers, which bind to the TrpR boxes with the low affinity. The dimers usually bind strong TrpR boxes, but can bind to weak TrpR boxes with low affinity. The binding of the different repressors if further complicated by the involvement of co-factors, such as phenylalanine, which either enables binding of the RNAP, or TrpR dimer to a weak adjacent TrpR Box. Therefore the TrpR repressor is able to not only repress, but also activate transcription of the Trp regulon, by coordination with aromatic amino acids and co-factors. An additional note is that although the sequence between the palindromic binding sites of the repressor is not thought to be significant, a particularly strong TrpR box, upstream of *aroG*, contains the palindromic binding consensus with a GC rich region between the palindromic sites (Pittard et al., 2005).

Under certain circumstances, when the binding site of the repressor is upstream of the promoter, it can actually initiate transcription, for example, when the TrpR repressor is bound upstream of the promoter, in the presence of co-factors such as phenylalanine, tyrosine or tryptophan the Trp protein interacts with the α subunit of RNAP to initiate transcription (Pittard et al., 2005). Therefore the positioning of the repressor is vital to the mechanism by which the repressor affects transcription.

The relative positions of the repressor binding sites and promoter recognition sites are important for the repression of transcription, as this can alter the mode of repression. One mechanism of

repression involves the exclusion of RNAP from the promoter, thus preventing the RNAP forming a contact between the –10 and –35 sites of the promoter, while the other involves the repressor interfering with the bound RNAP, inhibiting isomerisation, which inhibits the formation of an open complex (Neidhardt, 1996); this prevents the RNAP from exiting the promoter and thereby entering elongation phase of transcription (Pittard et al., 2005). In the second case, the RNAP is able to bind to the –10 and –35 sites of the promoter, but the repressor prevents the RNAP from forming a stable open complex and moving into elongation phase of transcription. The other possibility is that a stable elongation complex is formed, but the elongation is halted by the presence of the repressor, which acts as a road block, as observed in the *lac* operon (Neidhardt, 1996). The DNA template sequence can also cause lateral oscillation of the ternary RNAP complex, either slowing down elongation of RNA, pausing, or even causing cessation of transcription. Cis-acting antisense RNA can act to stabilise the RNA polymerase when bound to a segment of the transcript behind the RNAP, thus preventing backward translocation of the ternary complex (Toulme et al., 1999). Therefore regulation, either activation or inhibition of transcription can take place during all three stages of transcription: initiation, elongation and termination.

The site of the operator, can result in competition, whereby, the operator/DNA binding regions overlap with promoters, therefore causing the repressor protein and the RNAP to compete for binding to the operator or promoter respectively. In this case, they are unable to bind simultaneously and therefore compete either kinetically or thermodynamically for the promoter-operator region. The bound repressor decreases the amount of free promoter, so decreasing the rate of formation of an open complex and thus decreasing transcription (Neidhardt, 1996).

The Lac operator overlaps with the transcriptional start site (+1); therefore the position of the repressor is thought to be important in regulation of transcription, possibly by preventing elongation phase of transcription. However, repression may still be overcome, as RNA polymerase has the ability to oscillate back or forward at each template position (Toulme et al., 1999), which could result in destabilisation of a repressor protein to enable read-through transcription. During transcription the RNAP covers approximately a 35bp region of DNA; 12-15bp of this region are unwound, thus forming the transcription bubble. Inside the melted region the template forms a constant heteroduplex with the 3′ region of the transcript, covering approximately 8-9bp. Where the RNA-DNA hybrid is weak, the ternary RNAP complex moves backwards (backtracking) rather than forming the next phosphodiester bond, therefore stabilising the complex before re-initiating the elongation process. Site-specific repressor proteins and chromosomal proteins can block transcription elongation. However transcriptional fusions assays have implied that these road blocks are overcome to a certain extent by RNAP, thus enabling some transcription (Toulme et al., 1999). Although repressors form transcriptional road blocks, analysis of the *lac* repressor revealed that transcriptional read through was increased when the elongation complex was able to extend the RNA chain by an additional nucleotide, which destabilises the repressor-operator complex, and allows increased transcriptional read through (Mosrin-Huaman et al., 2004). The frequency of chain extension by an additional nucleotide is increased when intracellular NTP concentrations are elevated, thus suggesting that NTP concentrations may play a key role in regulation of transcriptional elongation.

Finally, it has been suggested that the lateral stability of the complex can be altered by cis and trans acting RNA sequences, which adds another method of regulation of gene expression into the complex pot of activator/repressor proteins, co-factors, DNA topology, Histone like

architectural proteins, NTP concentrations, and backtracking of RNAP. In order for transcription to be efficient, the RNAP has to overcome a number of different obstacles. Therefore one could hypothesise that the regulation of the *ruvC* P1 promoter is far more complicated that the mere presence of the LexA repressor. The position of the LexA binding site, downstream of the promoter recognition site indicates the possibility that RNAP and LexA may be able to bind simultaneously; therefore the LexA repressor may act as a roadblock to the RNAP. The laws of equilibrium suggest that the LexA repressor is not constantly bound to the SOS box, so therefore during dissociation and re-association, the RNAP would no longer be blocked by the repressor and would therefore be able to transcribe *ruvC*. The fact that no induction is observed from the P2 promoter of *recA* in the Δ*recA* strain suggests the LexA repressor binding site obscures the promoter binding region as they have been shown to overlap (Movahedzadeh et al., 1997). This would most likely prevent binding of the RNAP, and therefore prevent transcription.

It has been shown that the P1 promoter of *ruvC* is DNA-damage inducible (figure 5.1b, 5.2a, and 5.9). Therefore if the promoter were transcribed by two sigma factors, the level of the stress response sigma factor, would increase under stress conditions. This would result in elevated levels of the stress response sigma factor, which would compete with σ^{70} for the core-RNAP. This competition would increase the concentrations of the relevant RNAP-σ complex in the cell, and may therefore have a downstream effect on the competition balance between the RNAP and the repressor for the P1 promoter of *ruvC*. Interestingly these two promoters, P1 of *ruvC* and P2 of *recA* appear to have different recognition sequences for σ factors, and therefore are probably recognised by different σ factors. One could hypothesise that sigma factor specificity and affinity for particular recognition sequences may explain some of the differential

expression observed. However as previously mentioned regulation of transcription is a multifactorial process, which would need to be further dissected.

The primer extension technique is useful for the ability to determine the exact transcriptional start site of a gene, due to the advantage of running a manual sequence alongside the primer extension reaction. However, this method in less quantitative than RNase protection, which, does not allow exact identification, down to the nucleotide of the transcriptional start site(s), but does allow approximate identification of the position of the transcriptional start site(s) using RNA markers, and more importantly allows accurate quantitation of the level of transcription from multiple transcriptional starts sites. Problems can arise using primer extensions when relying on the predictions of translational start sites, from which to design primers to perform the primer extension assay. The primer has to be within the coding region of the gene of interest, to enable the extension reaction to be carried out to detect the transcriptional start site(s). The potential difficulties of primer extension were observed in chapter 4, whereby the primer extension reactions carried out to find the transcriptional start site of *sigG* were unsuccessful due to the in-correct prediction of the translational start site. This incorrect prediction meant the primer used in the primer extension reactions, was in actual fact, upstream of the transcriptional start site, therefore no product was detected. This problem was overcome using RNase protection, which allows the use of a large region as a probe, thus taking into account any discrepancies between the predicted translational start site and the actual transcriptional start site.

Taqman is a method by which transcription can be quantified; however the limitations of the procedure are such that one cannot distinguish expression levels from different promoters of a given gene, but rather measures the overall combined expression. Therefore it does not provide

the ability to dissect transcription from different start sites for a particular gene. If the Taqman results are accurate, then there is a significant increase in expression of *ruvC* under uninduced conditions in the Δ*sigG* strain compared to H37Rv and Δ*recA* strains, and a slight decrease in induction of *ruvC* in Δ*recA* strain. This does not correspond with the results obtained by primer extension, RNase protection, and microarray analysis, where all methods show a significant decrease in the expression of *ruvC* in the Δ*recA* strain; indicating there may be problems with quantitation of the Taqman RT-PCR.

There were a number of concerns about the suitability of *sigA* as an internal control. Data available in the current literature is expressed as a proportion of the internal standard (*sigA*), therefore one cannot determine whether any differences have been observed in the expression levels of the internal standard *sigA*. Data from myself (data not shown), as well as from other members of the laboratory have raised concerns about the validity of using *sigA* as an internal control, due to differences observed in the expression level of *sigA*, particularly at different temporal levels, as seen when assessing the temporal expression levels of *sigG* (data not shown). The purpose of an internal control is to distinguish between differences in efficacy of the cDNA synthesis reaction; however, this cannot be achieved if the internal control varies under different conditions. For this reason, Taqman analysis was not performed for *sigG* or *recA* in the H37Rv Δ*sigG* and Δ*recA* strains of *M. tuberculosis*.

The RNase protection assays show no difference in the induction of *ruvC* from the P1 promoter in the Δ*sigG* strain compared to wild-type strain. This observation was also made using microarray and Taqman; however there appeared to be a decrease in induction of the P1 promoter in the Δ*sigG* strain when analysed by primer extension. Due to the limited

quantitative ability of the primer extension assay, alongside the conflicting data obtained by the RNase protection, microarray and Taqman, the collective conclusion is that *ruvC* P1 is most likely not regulated by *sigG*.

In the case of the P2 promoter of *ruvC*, the RNase protection and primer extension assays both indicate that *ruvC* P2 is not induced in response to DNA-damage. However, this hypothesis should be confirmed, using promoter fusion assays with *lacZ*, under uninduced and induced conditions.

Closer analysis of the expression level of *ruvC* in the Δ*recA* strain revealed that the P1 promoter, despite processing a LexA binding site, was partially induced. This was compared to data obtained by RNase protection for *recA*, which clearly showed the P2 promoter, regulated by LexA was not induced in the Δ*recA* strain. This indicates that RecA is required for removal of the repressor LexA, and therefore required for the expression of the P2 promoter of *recA*. However, it appears that RecA is required to return the induction level of the P1 promoter of *ruvC* back to full level, although in the absence of RecA, the promoter remained induced by DNA-damage to approximately half the magnitude. Taqman data showed that *ruvC* was expressed to a lesser extent in the Δ*recA* strain, but the expression level was not decreased by half, as was also observed in the microarray data (Rand et al., 2003). Therefore, as previously discussed, there appears to be another level of regulation, enabling transcription from the P1 promoter of *ruvC* in the absence of RecA. As mentioned, this difference in expression level may be due to the RNAP being able to read through the road-block produced by the LexA repressor, and the positions of the LexA binding sites for the P2 promoter of *recA* and the P1 promoter of *ruvC* differ. Alternatively as noted, the promoters appear to have different binding sites for different sigma factors, which may play a role in their regulation along with other

transcriptional regulatory proteins, architectural proteins and cellular concentrations of NTP. It is also of interest to note that *recA* expression in not completely abolished in Δ*recA* strain, as shown by microarray (Rand et al., 2003) and LacZ promoter fusion assays (Davis *et al.*, 2002b). Induction was observed from the P1 promoter of *recA*, to the same extent in the wild-type, and Δ*recA* strains, thus agreeing with previously published data, that the expression level of P1 promoter of *recA* is not regulated by the RecA/LexA system. However, the RNase protection assay, microarray data and Taqman indicate that the sigma factor regulating expression of *recA* P1 is not SigG. It may be that the same mechanism regulates transcription from the P1 promoters of *recA* and *ruvC*; however the decreased induction of the P1 promoter in *ruvC* may be assigned to the fact that the alternative mechanism is only able to partially overcome repression of the promoter by LexA.

The *recA* data was not quantified using Taqman due to the difference observed when using *sigA* as a standard control. Therefore this could be performed using a different internal standard such as 16s rRNA; however the problem of using 16s rRNA is one of relative abundance. The level of *sigG* is very low and the level of 16s rRNA is considerably higher, so using 16s rRNA as the normaliser may be unsuitable. Another alternative is *gnd*, which has been previously used as an internal standard control (Brooks *et al.*, 2001). It may be more beneficial to use a combination of these to determine if the levels of these alter consistently with the cDNA preparations, thus indicating that the differences observed are actually due to the efficiency of the cDNA synthesis rather than differences in levels of the normaliser. The difference in expression observed in the RNase protection assay could be addressed in a similar way, but using an additional probe in the reactions to quantify whether the differences in expression are due to an effect of the knockout strain, or due to different levels of RNA. It would therefore be vital to choose a gene, whose expression level remained constant in H37Rv as well as Δ*recA* and Δ*sigG* strain.

In conclusion, *ruvC* possesses two promoters, only one of which appears DNA-damage inducible. The P1 promoter, repressed by LexA, is induced, but to a decreased level in the absence of RecA. The P2 promoter of *ruvC* is expressed to lower levels than the P1 promoter and does not appear under these conditions to be DNA-damage inducible. The P2 promoter of *recA* is not expressed in the absence of RecA, however the P1 promoter remains DNA-damage inducible. It does not appear that SigG plays a role in regulating transcription of *recA* or *ruvC* in response to DNA-damage. It appears that there is an alternative mechanism regulating expression of both *recA* and *ruvC* in response to DNA-damage; however it is unclear what this mechanism is. There may be a clue in the DNA sequence analysis, as it appears that there is a high degree if homology between the –10 promoter elements of the P1 promoters of *recA* and *ruvC*. *lacZ* fusion assays along side site directed mutagenesis could be used to identify the important residues in the –10 and –35 regions.

6 Regulation of gene expression from the P1 promoter of *recA*

As outlined in the previous chapters, the *recA* gene is part of the SOS regulon in *M. tuberculosis*. The mechanism of action of the SOS response has been well defined in *E. coli*, where *recA* has been shown to be under the control of LexA (Little, 1982) a transcriptional repressor, which binds to a specific region (SOS box) located in the promoter of the SOS response genes.

Some proteins have been identified that are DNA-damage inducible, but are regulated independently of the LexA/RecA system (Kleinsteuber and Quinones, 1995); which has also been observed in *M. tuberculosis*, where a number of genes have been shown to be DNA-damage inducible independently of the LexA/RecA system, including *recA* itself (Rand *et al.*, 2003). Microarray data showed that the DNA-damage regulon is comprised of 112 genes upregulated 3-fold or more in response to DNA-damage by mitomycin C (0.2μg/ml), whereby the vast majority of genes are regulated in a RecA independent manor, as they exhibit either full or partial induction of expression in response to DNA-damage in the Δ*recA* strain (Rand *et al.*, 2003). This observation suggests that there may be an alternative mode of regulation of some DNA-damage inducible genes.

The possibility that SigG played a role in regulation of the DNA-damage regulon, in response to DNA-damage, was assessed in chapters 3 and 4. The data revealed that SigG did not play a major role in regulation of the DNA-damage response; therefore other options were explored to elucidate the alternative mode of regulation of the DNA-damage regulon. One possibility was that another sigma factor was responsible for regulation of the DNA-damage response.

Alternatively, a regulatory protein could bind to the promoter regions of some of these DNA-damage inducible genes and act to either repress or activate transcription. To address the possibility that regulation of the RecA independent DNA-damage response was controlled by a regulatory protein, the *recA* promoters were analysed by gel-shift assay to look for binding of potential regulatory proteins. The *recA* promoters were chosen for this experiment, as the P1 and P2 promoters of *recA* are DNA-damage inducible, the P2 promoter is regulated by LexA, and it has been shown by RNase protection assay that the P2 promoter is not expressed in the Δ*recA* strain (see chapter 5), suggesting the expression of this promoter is entirely dependent on RecA for de-repression. The P1 promoter remains DNA-damage inducible in the Δ*recA* strain, suggesting its regulation is independent of RecA.

6.1 Gel retardation assays

A method designed to detect DNA-protein interactions is the gel retardation or 'bandshift' assay. A radiolabelled DNA probe, is incubated with protein extracts, and electrophoresed through a non-denaturing polyacrylamide gel; any interactions between a protein from the cell free extracts (CFE) and the labelled probe result in the formation of a complex, which leads to a reduction in the electrophoretic mobility of the fragment in the non-denaturing polyacrylamide gel (Lane *et al.*, 1992), resulting in a bandshift.

6.2 Bandshifts using large P1 and P2 probes.

Two double-stranded oligonucleotide probes were designed to each cover a 60bp region of the P1 or P2 promoter regions of *recA* (see figure 6.1A), as these were enough to show induction of P1 in response to DNA-damage in a *lacZ* fusion assay (Davis *et al.*, 2002b). These probes were then used in bandshift experiments with induced (mitomycin C, 0.2μg/ml) and uninduced cell

Figure 6.1 A

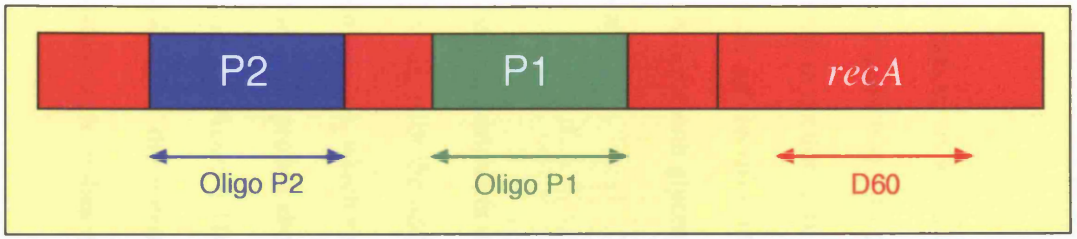

Figure 6.1 B

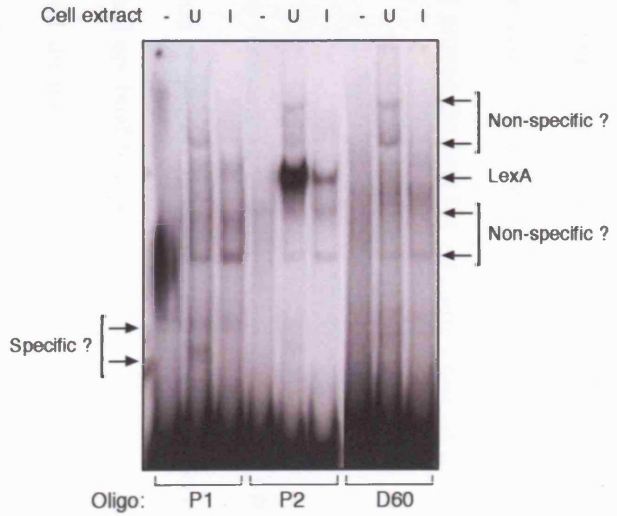

Figure 6.1A: A schematic representation of P1 and P2 promoter region of *recA*. The 60mer oligonucleotide probes used in gel retardation cover either the P1 or P2 promoters, or part of the internal coding region of *recA*.

Figure 6.1B: A gel retardation using 60mer oligonucleotide probes. Two cultures of H37Rv were grown to an OD of 0.3-0.4. These were then pooled and split. One was untreated, the other was induced with 0.2mg/ml mitomycin C and both were incubated in a rolling incubator for 24hrs at 37°C. Cell free extract was obtained from both uninduced and induced cultures and used in a gel retardation assay (track U and I respectively) with either P1 oligo, P2 oligo or internal *recA* oligo D60. A negative control containing no protein was used for all of the oligos (track -).

free extracts (CFEs). Binding reactions using purified LexA protein with labelled P2 probe, were used as a positive control. The labelled P2 probe bound to LexA in both the purified LexA protein preparation and the CFE, resulting in a visible shift or retardation (data not shown and figure 6.1B). The labelled P1 probe showed a range of retarded bands (see figure 6.1B), demanding optimisation of the conditions to aid specific binding and maintenance of a stable complex during electrophoresis.

Optimisation steps were carried out to decrease non-specific binding, and increase specific binding particularly to the P1 region of *recA*. Different binding buffer recipes were used as outlined in section 2.10.3. The most effective buffer was buffer 11 (see figure 6.3B). Two different gel recipies were also tested, one containing glycerol, and the other without: the EMSA mix (with glycerol) proved the best for resolution and separation of retardation (data not shown).

Bandshift experiments were repeated using the radiolabelled P1 and P2 probes, under optimised conditions, with the addition of another labelled oligo D60, designed from the internal coding region of *recA*, which should not bind to a potential activator or repressor protein. The labelled D60 and P1 probes showed different retardation patterns, suggesting the binding to P1 was specific (see figure 6.1B). However, there were several faint retardations visible. Therefore to narrow down the potential binding site, and get a clearer single retardation, shorter 30mer oligonucleotide probes were designed (see figure 6.2A)

Figure 6.2A

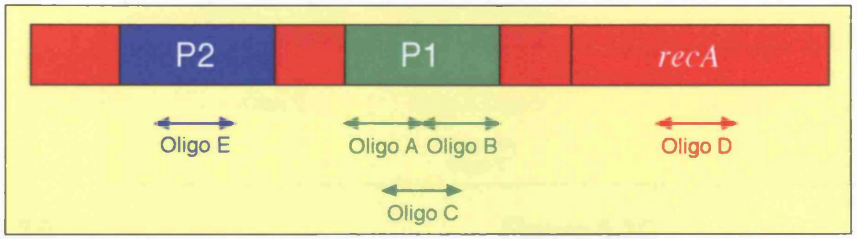

Figure 6.2B

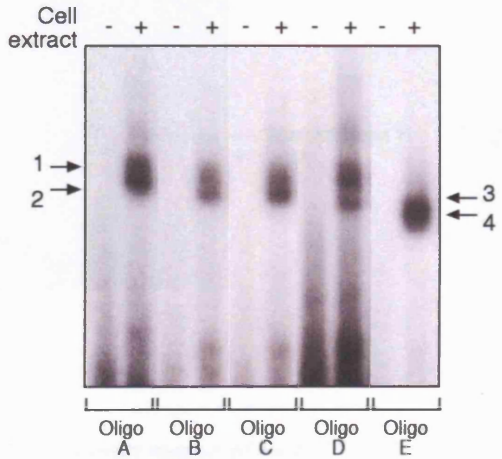

Figure 6.2A: A schematic representation of P1 and P2 promoter region of *recA*. The 30mer oligonucleotide probes used in gel retardation cover either the P1 or P2 promoters, or part of the internal coding region of *recA*

Figure 6.2B: A gel retardation using the 30mer oligonucleotide probes. Uninduced H37Rv CFE was used in a gel retardation assay (track +) with either P1 oligo A, B, C, the P2 oligo E, or the internal *recA* oligo D. A negative control, omitting the protein was used for all of the oligos (track -). Arrow 1 indicates possible non-specific band for oligos A, B and C, whereas arrow 2 indicates a potential specific band for P1 oligos A, B and C. Arrow 3 indicates the non-specific band produced by the internal *recA* oligo D and arrow 4 indicates LexA bound to P2 oligo E.

Figure 6.3A

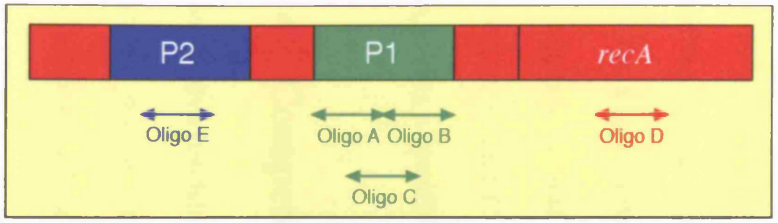

Figure 6.3B

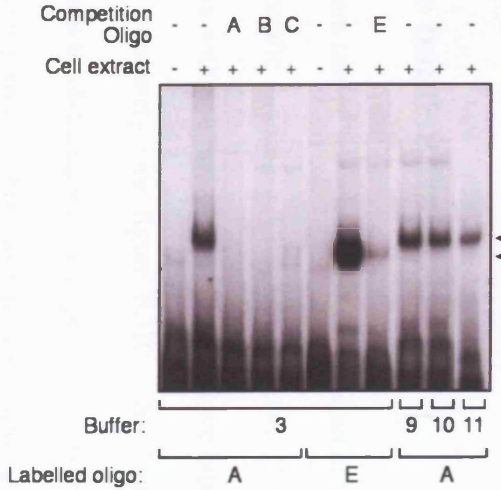

Figure 6.3C

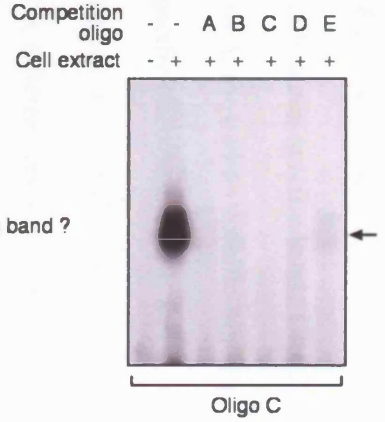

Figure 6.3A: A schematic representation of P1 and P2 promoter region of *recA*. The 30mer oligonucleotide probes used in gel retardation cover either the P1 or P2 promoters, or part of the internal coding region of *recA*

Figure 6.3B: A gel retardation comparing binding buffers using the 30mer oligonucleotide probes. Uninduced H37Rv CFE was used in a gel retardation assay (track +) with either P1 oligo A, or the P2 oligo E. A negative control, omitting the protein was used for all of the oligos (track -). Oligo A was used in reactions with uninduced CFE with different binding buffers, as indicated. Competition experiments were also carried out, where 100-fold excess of unlabelled P1 competition oligos, A, B and C, were included in the binding reaction along with labelled oligo A.

Figure 6.3C: A competeitive gel retardation using the 30mer oligonucleotide probes. Uninduced CFE H37Rv CFE was used in a gel retardation assay (track +) with P1 oligo C. A negative control, omitting the protein was used (track -). Binding of labelled oligo C was competed with 100-fold excess of unlabelled P1 A, B and C, P2 E and *recA* internal oligo D. The arrow indicates the retardation product using the oligo C probe.

6.3 Bandshifts using small P1 and P2 probes.

Bandshifts were carried out using the optimised conditions outlined in section 6.2. The positive control oligo E, designed to contain the LexA binding site of the P2 promoter, produced a retardation with LexA (see figure 6.2B and 6.3B). Oligos A, B and C produced two distinct retarded bands (see figure 6.2B), with one potential due to an activator/repressor protein, and the other retardation potentially a non-specific band. Oligo probe D (see figure 6.3B), designed from the coding region of *recA*, showed no specific binding. The top retarded band present in both binding with the P1 specific oligo probes A, B and C, and the negative control oligo probe D, suggested it was the result of non-specific binding. The bottom retarded band visible with oligos A, B and C ran at a different level to the oligo D retarded band (see figure 6.2B), suggesting a specific retardation.

6.4 Competitive bandshifts

Competitive bandshifts were carried out with a 100-fold excess of unlabelled probe designed to compete out any non-specific binding. Oligos A, B and C were labelled and used in competitive binding assays with unlabelled A, B and C, where labelled oligo A was competed with Oligo A, B and C separately (see figure 6.3B). No binding was seen under these conditions, suggesting either the binding was non-specific, or there were two potential binding sites for a repressor/activator protein. This was repeated, using labelled oligo B, then labelled oligo C. Again, no binding was observed under these conditions (data not shown).

To determine if there were two potential binding sites, or the initial binding was non-specific, labelled oligo C was competed with oligos A, B, C, D (*recA* internal oligo) and E (LexA

specific oligo). The binding observed with labelled oligo C was removed in all the competition reactions (see figure 6.3C), suggesting the binding observed under these conditions was non-specific.

One difficulty in detecting binding by gel retardation is the necessity for the protein-DNA interactions to form a stable complex during electrophoresis. Therefore, a method of cross-linking the complexes to aid stability was employed. Gluteraldehyde was added to the competitive bandshift reactions prior to electrophoresis, but still no specific shifts were visualised, i.e. the competitors A, B, C, D and E all removed binding observed with oligo C alone.

6.5 Discussion

Close analysis of the different DNA-damage repair systems in *E. coli* and *B. subtilis* have shown that they have a common regulatory system, which responds to DNA-damage, the SOS response (Cheo *et al.*, 1993; Raivio and Silhavy, 2001). This regulatory system is also present in *M. tuberculosis*. However, unlike *E. coli* and *B. subtilis*, *M. tuberculosis* has two promoters regulating DNA-damage inducible gene expression of *recA*. Only one of those promoters, P2, is regulated by the SOS response, and the other, P1, remains DNA-damage inducible independently of LexA/RecA (Davis et al., 2002b). Therefore, an alternative mechanism of regulation probably regulates DNA-damage inducible gene expression of the P1 promoter.

The gel retardation experiments were carried out to determine if double-stranded oligonucleotides covering the P1 or P2 regions of *recA* could bind to a protein from a CFE of *M. tuberculosis* and produce a visible retardation when electrophoresed in a non-denaturing

polyacrylamide gel. Detection of protein-DNA interactions by gel retardation depends on two critical factors, resolution from uncomplexed DNA, and maintenance of a stable protein-DNA complex (Lane *et al.*, 1992). The P2 promoter region was used as a positive control, and the formation of a retarded band confirmed the integrity of the CFE. However, the ideal conditions for the maintenance of a stable complex between P2 and LexA will not necessarily be ideal for binding of a repressor/activator protein to the P1 region. Although binding was detected to the P1 probe, competition bandshifts revealed that this binding was not specific. A specific binding complex was not detected even following cross-linking of complexes prior to electrophoresis.

The lack of formation of a specific complex with CFE might have been due to there being insufficient quantities of the regulatory protein in the extract. However, this may also have been due to the conditions of the experiment. It is possible that too little probe was used in the experiment, therefore a titration of the probe with the CFE could enhance the possibility of detecting a stable interaction. The competition experiments may also have been too stringent, therefore alongside the titration of probe, a titration of competitor could also be used. Another potential pitfall of using the A, B and C oligos to compete for binding, is that the potential binding site may cover a large region of the DNA, which could be looped in the presence of the repressor/activator, as observed with *dnaK*, in *Clostridium acetobutlicum*, in which a hairpin loop structure which is thought to play a role in regulation of expression (Narberhaus *et al.*, 1992). If this were the case, then the overlapping oligos would not be a good choice for the competitive oligo, as the binding site of a potential repressor/activator protein may overlap these oligos: hence the use of the non-specific oligo designed for and used in the assays (oligo D). This result does not indicate that a protein does not bind to the P1 region of *recA*, just that it was not detectable by this method. For this reason, an alternative approach was taken in which a gene inactivation knockout was produced in a predicted regulatory protein, which may

potentially be involved in regulation of the RecA independent DNA-damage regulon (see chapter 7).

7 Construction of a knockout in a predicted regulatory protein

7.1 Introduction

A wide variety of different environmental signals can alter gene expression, both temporally and spatially. Regulation of gene expression in response to these environmental cues requires different response regulators. As well as sigma factors, there are many families of response regulators, which either activate or repress expression of a specific regulon (Withey and DiRita, 2005). Activator or repressor proteins can also be used in-conjunction with sigma factors, which form the specific interaction between RNA polymerase and the promoter (Gomez *et al.*, 2000). Microarray experiments carried out by another member of the laboratory identified 5 predicted transcriptional regulatory proteins that were upregulated in response to DNA-damage (Rand *et al.*, 2003): Rv0586, Rv1956, Rv1985c, Rv2017 and Rv2884 (see Table 7.1).

Gene	Induction ratio in Wild type	Induction ratio in recA mutant	Literature
Rv0586	2.16± 0.16	2.20 ± 0.42	Non-essential (Sassetti *et al.*, 2003)
Rv1956	6.95 ± 0.34	9.43 ± 0.86	Non-essential (Sassetti *et al.*, 2003), induced by heat shock (Stewart *et al.*, 2002)
Rv1985c	2.86 ± 0.43	5.23 ± 1.01	Non-essential (Sassetti *et al.*, 2003)
Rv2017	3.36 ± 0.65	4.37 ± 1.21	Induced by heat shock (Stewart *et al.*, 2002)
Rv2884	4.62 ± 0.97	6.20 ± 1.43	Non-essential (Sassetti *et al.*, 2003)

Table 7.1: Relative induction ratio in response to mitomycin C induction of 5 predicted regulatory genes in both wild-type and Δ*recA* strains of *M. tuberculosis*

A recent transposon mutagenesis study performed by Sassetti *et al.*, (2003) showed mutations in certain genes were recoverable *in-vitro*, and were therefore classified as non-essential. Data for induction ratios was obtained from supplementary data tables (Rand *et al.*, 2003).

One or more of these transcriptional regulators could be involved in a novel mechanism regulating DNA-damage inducible gene expression.

7.2 Analysis of homology of the predicted regulatory proteins.

In order to assess the potential of the regulatory proteins to regulate gene expression of part of the DNA-damage regulon, and to further elucidate their possible relationships to other known regulatory proteins, homology studies were performed using BLAST, EMBOSS and pFAM, and domain searches were performed using NCBI conserved domain search (RPS-BLAST).

RPS-BLAST using the NCBI website revealed that Rv0586 showed homology to the GntR family of transcriptional regulators (see figure 7.1). An example is, *yhcF*, a repressor of the gluconate operon in *Bacillus cereus*. This homology covered a 60 residue region, which formed the helix-turn-helix motif, with which Rv0586 shared 100% homology (3e-11). At the N-terminal region, it shows homology to the GntR family of transcriptional regulator, pfam00392 *Bacillus cereus* (96.9% identity, 9e-12). The GntR family can be sub-divided depending on the C-terminal effector domains. In this case Rv0586 shows homology to a FadR transcriptional regulator, COG2186. BLASTP shows Rv0586 has homology to MAP4081 in *M. avium subsp. papatuberculosis*, and YP-116369 of *Nocardia farcinicia* with 67% and 60% identity respectively. Homology searches using FASTA (nucleotide search) showed Rv0586 shares homology (E=9.3e-08) with the regulatory protein P33233 of the L-lactate dehydrogenase operon from *Escherichia coli*, and to other GntR family of transcriptional regulators in *M. tuberculosis* e.g. Rv3060c and Rv0792c.

Figure 7.1

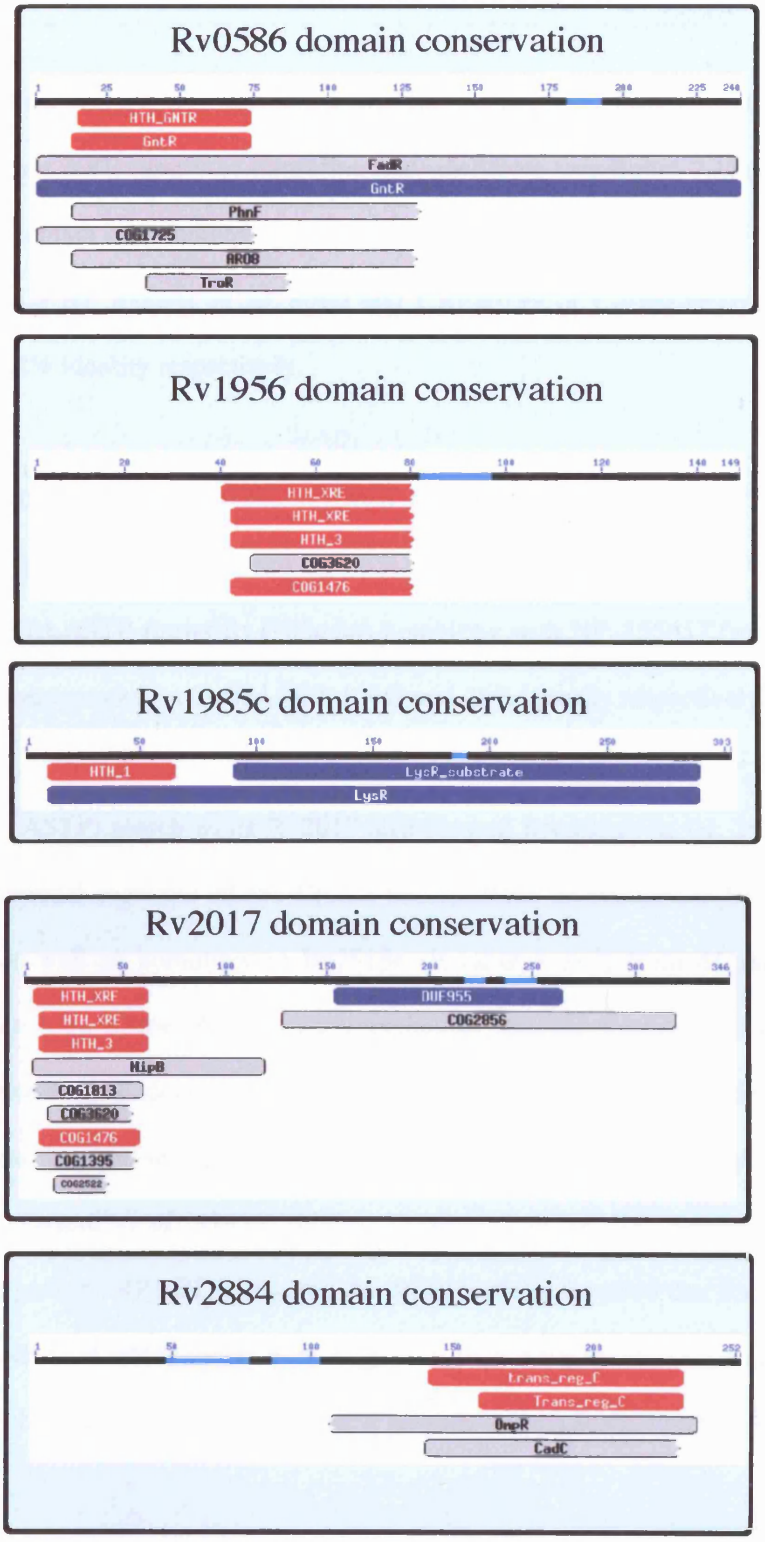

Figure 7.1: Conserved domains present in the 5 predicted regulatory proteins. Protein sequences available from the TubercuList website were used in the NCBI conserved domain search to detect any homology to known domains. The light blue represents regions of low complexity and the homology to specific domains is indicated below each protein.

RPS-BLAST using the NCBI website revealed that Rv1956 shared similarity with the xenobiotic response XRE family of transcriptional regulators (see figure 7.1) (cd00093). The helix-turn-helix domain also showed homology to Cro and Ci family. BLASTP shows Rv1956 has homology with NP_855641 of *M. bovis* and CAF20199 of *Corynebacterium glutamicun* with 100% and 52% identity respectively.

RPS-BLAST using the NCBI website revealed that Rv1985c shared homology with LysR family of transcriptional regulators (see figure 7.1)(Pfam00126 gnl/CDD/25406)), with a 95% alignment 2e-10. BLASTP shows Rv1985c has homology with NP_855657 from *M. bovis* and CAB93745 of *Streptomyces coelicolor*, with 100% and 48% identity respectively.

Protein blast (BLASTP) search using Rv2017 also showed homology to GI: 29345183, a zinc binding transcriptional regulator of the Cro/CI family, from *Enterococcus faecalis* V583 (E-value = $3e^{-83}$), as well as homology to Rv2515c (E-value = $3e^{-8}$) from *M. tuberculosis* and Mb2040 (E-value = $5e^{-7}$) from *M. bovis*, a hypothetical regulatory protein to which, Rv2017 showed a 100% nucleotide identity (FASTA). Rv2515c is particularly interesting, as it is listed as a hypothetical protein in TubercuList, and was shown to be essential by transposon mutagenesis by Sassetti *et al.*, (1999); it too contains a neutral zinc metallopeptidase, zinc binding region signature. RPS-BLAST using the NCBI website revealed that Rv2017 contains a Helix-turn-helix domain which shares homology with both XRE family of xenobiotic response regulators, and pbsX family; it also contains a domain of unknown function (DUF955) (see figure 7.1).

As previously stated by (Earl *et al.*, 2002), *irrE* of *D. radiodurans* shows homology to Rv2017 of *M. tuberculosis*. However homology blast searches using both nucleotide (FASTA) and

protein (BLASTP) sequences of Rv2017 downloaded from TubercuList failed to detect homology to *irrE* within the standard default cut-off. When the BLASTP was repeated using *irrE* protein sequence as the query, homology was detected with Rv2017 (E-value of $5e^{-7}$) (Figure 7.2a and b). An alignment of the regions of homology between IrrE and Rv2017 was also assessed using the protein alignment database EMBOSS (figure 7.2a). The alignments produced by both EMSOSS (figure 7.2a) and BLASTP (figure 7.2b) show a region of 31 residues of similarity, which is contained within the domain of unknown function (DUF 955). Pfam analysis showed that Rv2017 contains a predicted helix-turn-helix (HTH 3) DNA binding domain from residue 6 to 59, and a domain of unknown function (DUF 955), which contains a H-E-X-X-H motif. This motif is consistent with the presence of a catalytic active site, which has similarity to Peptidase M48, a metalloprotease.

RPS-BLAST using the NCBI website revealed that Rv2884 shared homology with the effector domain of response regulators (trans_reg_C) (see figure 7.1), present in two-component signal transduction systems. BLASTP for Rv2884 revealed homology to NP_855641 of *M. bovis* and CAF20199 of *Corynebacterium glutamicum* with an identity of 100% and 52% respectively. Interestingly, Rv2884 exhibits homology (E=3e-15) to Q55733, a regulatory component of a sensory transduction system, from *Synechocystis* sp. strain PCC 6803.

Rv2017 and Rv2884 were selected for further study based on their levels of induction in response to mitomycin C (see table 7.1), taking into account the fact that a mutant of Rv1956 was already under construction by another member of the laboratory. Rv2017 was particularly interesting due to sequence homology with *irrE* from *Deinococcus radiodurans* (*D. radiodurans*) (see figure 7.2a and b), a radio-resistant bacterium (Earl *et al.*, 2002). IrrE has been shown to positively regulate gene expression of *recA* (Earl *et al.*, 2002). Although *recA* is

Figure 7.2a

Search method	EMBOSS-align water
Aligned sequence 1	Rv2017 *Mycobacterium tuberculosis*
Aligned sequence 2	*irrE Deinococcus radiodurnas*
Martix	EBLOSUM62
Gap penalty	10
Extended penalty	0.5

```
Rv2017          114 SQQH--TPAFDPEFTAAEDAARLVHAWR----------------------    140
                    |:.|  :|...| |..|.||....:|:.|
irrE             28 SIPHPQTPVKLP-FVTAPDALAAAEAIMRDLAAAYVAALPGRDTHSLMAG     76

Rv2017          141 --------MPLGPVVNLTRWMLAAGCLVFLEDFATQRIDGLSQWVDDTPV    182
                            ||:|        |.:.|    |:                .:::.|
irrE             77 VPGVDLKFMPLG-------WRLGA----FL---------------PHNV    100

Rv2017          183 ELINLNAAPERRLTLAHELGHLVL----------HSTNPTENL----ET    218
                    :|||:.|.|:|:|.|||||:||.:|          |.....|.:    ||
irrE            101 ELINLAARPERRFTLAHEIGHAVLLGDDDLLSDIHDAYEGERLEQVIET    150

Rv2017          219 EATAFAAEFLMPESEIRPELRRLDLGKLLELKREGVEMLALLARAYRMG    268
                    .....||..||||..|...|.|              :|.:.:||...|.|
irrE            151 LCNVAAAAILMPEPVIAEMLER------------DGPTGLALAELAKR--    186

Rv2017          269 LVSAEARTKLYKAMNARGWETKEPGIELTV------REPPLPAHIG---    309
                        |.....|:.|...:|..|.|.::.      ||:.:.....|
irrE            187 -----AEVSASSALYALTEGTPVPVIYNVCAPGKPPREDALSDEDAGPST    231

Rv2017          310 ---PTLRIRGFTDQQAAALA-GYANPADEP    335
                       :|:|:...|......:|  |...|||:|
irrE            232 EKVLTTRLSSSTRGVKYTLASGTPVPADEP    261

 Length: 280
 Identity: 68/280 (24.3%),  Similarity: 98/280 (35.0%),  Gaps: 104/280 (37.1%),
 Score: 134.5
```

Figure 7.2b

Seach method	BLASTP
Query	*irrE Deinococcus radiodurans* (328 letters)
Database	PROTEIN: UniProt/Swiss-Prot + DAD + PDBSH + PRF protein sequence database (Last update May/03/2005)
Results	|BX842578-187|CAA17231.1|346|*Mycobacterium tuberculosis* H37Rv POSSIBLE TRANSCRIPTIONAL REGULATORY PROTEIN protein. (Rv2017) Length = 346

```
Query: 96  PLHNVELINLAARPERRFTLAHEIGHALLGDDDLLSDIHDAYEGERLEQVIETLCNVA 155
           ++ V+LIN+ A P+R+R TLAHE+GH +L                  + +ET
Sbjct: 178 DQTPVELINLNAAPDRRLTLAHELGHLVLHST--------------NPTLNLETEATAF 223

Query: 156 AAAILMPEPVIAEMLER 172
           AA  LMPE  I   L R
Sbjct: 224 AAEFLMPESEIRPELRR 240

Score = 57.4 bits (137), Expect = 5e-07
Identities = 27/77 (35%), Positives = 37/77 (48%), Gaps = 14/77 (18%)
```

Figure 7.2a: An alignment of IrrE from *D. radiodurans* with Rv2017 from *M. tuberculosis*. Alignments were performed using EMBOSS-align, with water alignment, designed to align local regions of homology. Homologous amino acids are indicated with yellow shading, while similar amino acids are indicated with green shading.

Figure 7.2b: Results of a blast search using IrrE from *D. radiodurans*. The blast search was performed using IrrE as the query. The results included Rv2017 from *M. tuberculosis*. Regions of homology are indicated in yellow, regions of similarity are indicated in green.

DNA-damage inducible in *D. radiodurans*, it does not appear to be negatively regulated by LexA (Narumi *et al.*, 2001) as in *E. coli* (Little, 1982), despite the fact that LexA, present in *D. radiodurans*, negatively regulates gene expression and undergoes autocatalytic cleavage in the presence of activated RecA (Narumi *et al.*, 2001), as extensively described in *E. coli.*

In order to address the possibility that a repressor or activator protein was responsible for regulating gene expression of some DNA-damage inducible genes, the approach chosen was to construction *M. tuberculosis* knockouts for Rv2884 and Rv2017, to assess the phenotypic effects and the effects of the knockout on gene expression.

7.3 Construction of Gene inactivation knockouts

Gene inactivation knockouts were planned for Rv2017 and Rv2884, to elucidate the function of the predicted regulatory genes and to identify their regulons.

7.3.1 Chromosomal location of Rv2017 and Rv2884

Firstly positional analysis of Rv2017 and Rv2884 was carried out using Tuberculist, to determine the orientation of the genes and the direction and orientation of surrounding genes (see figure 7.3a and b). This suggested that Rv2884 is mono-cistronic, whereas Rv2017 appears to be poly-cistronic. This hypothesis for Rv2017 was tested using RT-PCR. Forward and reverse primers were designed in adjacent genes to amplify the intergenic region separating the genes of interest (see figure 7.4a). If the genes were co-transcribed, forming a polycistron, these primers would produce a product from cDNA; however if the genes were mono-cistronic the intergenic regions would not be transcribed, and therefore a PCR would not produce any

Figure 7.3a

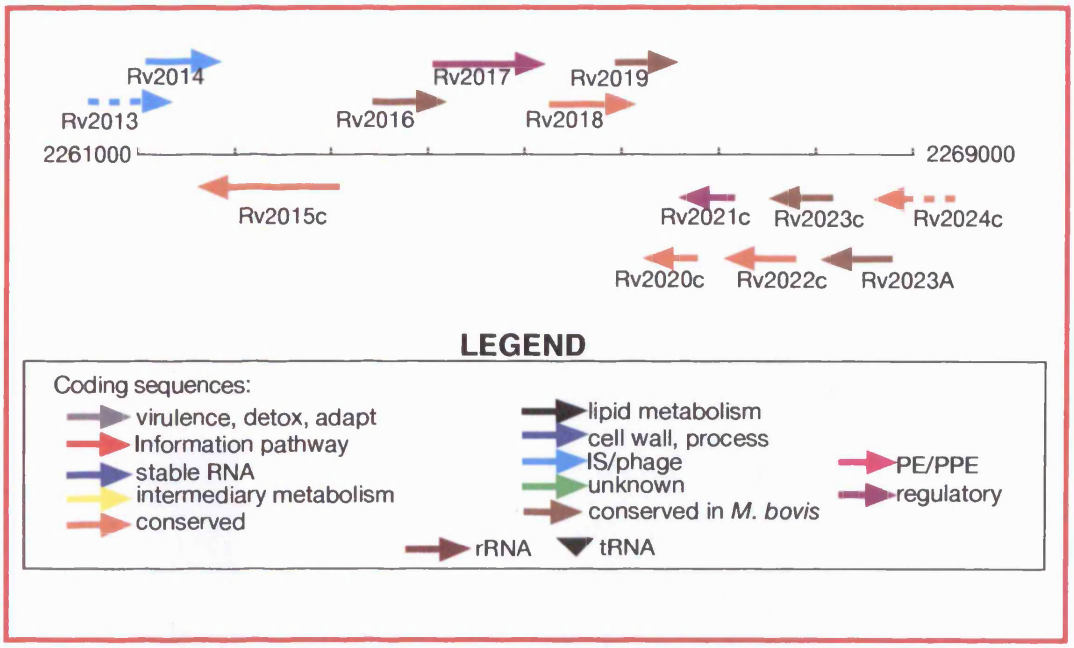

Figure 7.3b

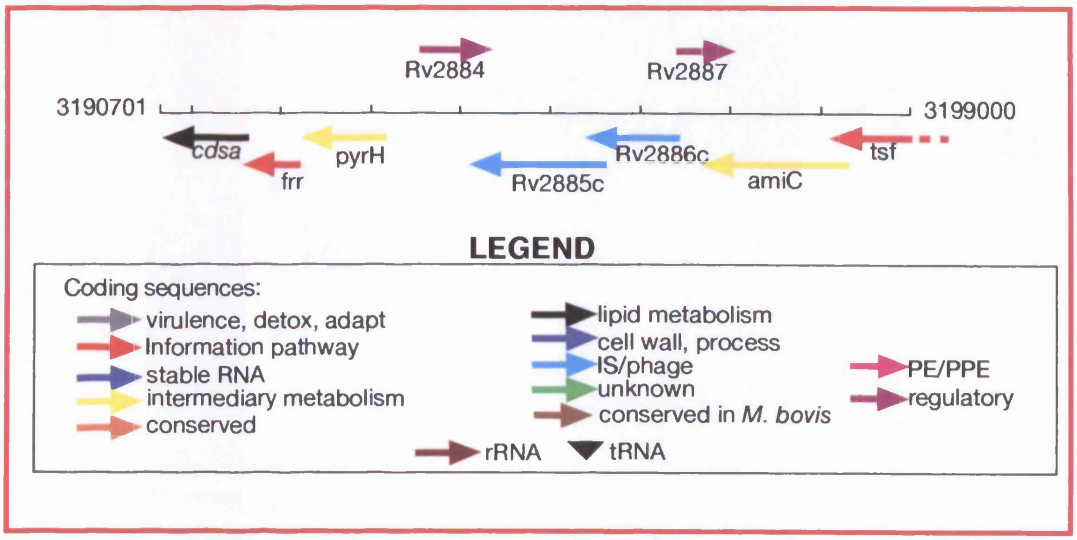

Figure 7.3a: Chromosomal location of Rv2017. The data was downloaded from the *M. tuberculosis* genome website, TubercuList. Arrows indicate the direction of transcription and are colour coded depending on their predicted functions.

Figure 7.3b: Chromosomal location of Rv2884. The data was downloaded from the *M. tuberculosis* genome website, TubercuList. Arrows indicate the direction of transcription and are colour coded depending on their predicted functions.

Figure 7.4a

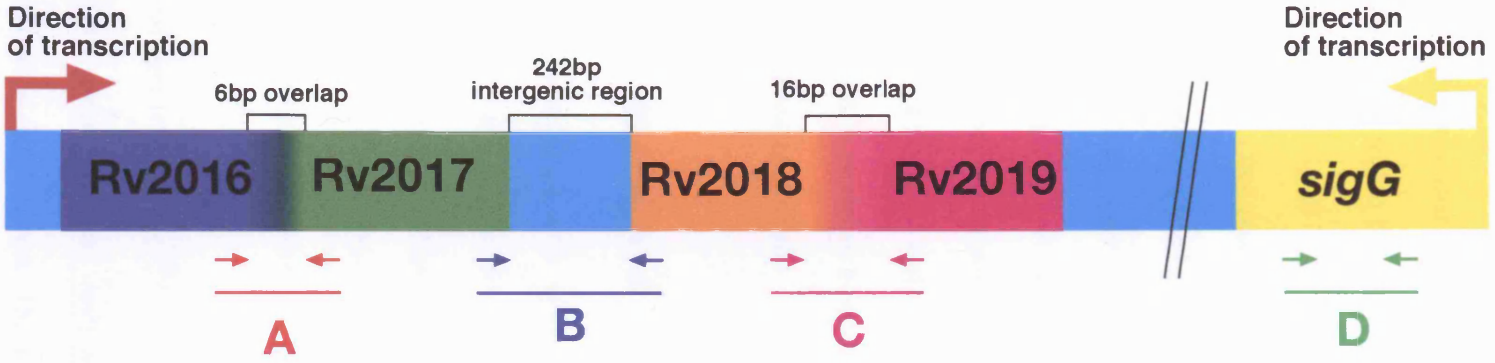

Figure 7.4b

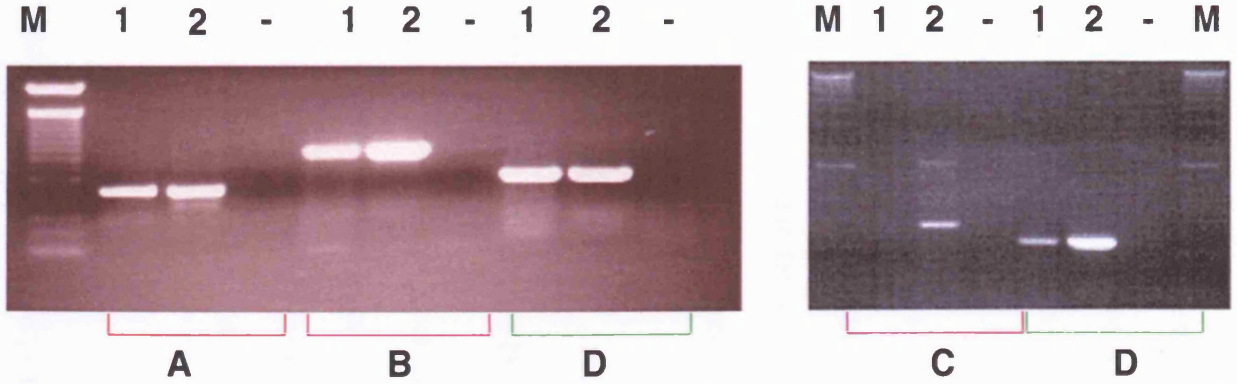

Figure 7.4a: A schematic representation of the relative position of the predicted transcriptional regulatory protein, Rv2017. The orientation and relative positioning of Rv2017 is depicted with arrows and overlap/intergenic distances between upstream and downstream genes are marked. The primers used in co-transcription studies are indicated; A (Rv2016-Rv2017), B (Rv2017-Rv2018), C (Rv2018-Rv2019), and the internal control D (*sigG*).

Figure 7.4b: An agarose gel showing co-transcription of Rv2017 operon. PCR reactions were carried out using cDNA (track 1), a positive DNA control (track 2), and a negative control RT- (Track -). The A, B, C and D label underneath, are equivalent to the primer pairs described in figure 7.4a, and the sizes were as expected A (492bp), B (849bp), C (715bp) and D (571bp).

product (see figure 7.4b). RNA that had not been reverse transcribed to form cDNA was used as a negative control (RT-) to determine if there was any DNA contamination in the RNA sample. DNA was used as a positive control (see figure 7.4b). Primers were designed to PCR the intervening region between Rv2016 and Rv2017, Rv2017 and Rv2018, then also Rv2018 and Rv2019 (see figure 7.4a). Internal *sigG* primers were used as a positive control to check the integrity of the cDNA (see figure 7.4b). The size of the intergenic regions suggests Rv2016 and Rv2017 are co-transcribed (see figure 7.4a) and that Rv2018 and Rv2019 are co-transcribed (see figure 7.4a), however the intergenic distance between Rv2017 and Rv2018 make prediction difficult (see figure 7.4a). Initial RT-PCR results suggested that Rv2016, Rv2017 and Rv2018 are co-transcribed (see figure 7.4b), whereas Rv2019 is not part of the same operon. The lower level of signal from the Rv2018 to Rv2019 primers on genomic DNA may explain why RT-PCR appeared to produced no band. Due to the overlap between these genes, it is highly likely that they are co-transcribed.

7.4 Designing and testing of knockout constructs

In brief, the approach used employed the design and construction of a non-integrating plasmid containing a deletion in the coding region, replaced by a hygromycin antibiotic resistance cassette. This was electroporated into H37Rv, where homologous recombination resulted in the replacement of the functional chromosomal copy of the relevant gene with the inactivated copy present on the plasmid, as outlined in (Parish *et al.*, 1999).

PCR primers were designed to amplify the 5′ and the 3′ coding region of Rv2017 and Rv2884, including some upstream and downstream flanking region to enable the homologous recombination to take place. These regions were cloned sequentially into pBackbone, with part

of the coding region between the 5′ and 3′ regions forming an internal deletion of 208bp for Rv2017 and 214bp for Rv2884. A hygromycin resistance cassette was inserted between the 5′ and 3′ coding regions to enable selection for the knockout. During the cloning stage, numerous problems occurred with Rv2884, including, obtaining a PCR product of the correct sequence for the 3′ region of Rv2884, and later on, insert the *sacB/lacZ* cassette. As Rv2017 was the most interesting gene and time was a limiting factor, Rv2884 was abandoned and the study focused on Rv2017.

A *sacB/lacZ* cassette was cloned into the *Pac*I site of the targeting construct to enable blue-white screening from the *lacZ* gene and sucrose counter-selection from the sucrose sensitivity gene *sacB* in *M. tuberculosis*. This construct (pLD2) was then electroporated into *M. tuberculosis*, H37Rv strain.

The selection and counter selection process was carried out as outlined in section 2.11.3, to detect potential knockouts, exhibiting Km^S and Hyg^R phenotypes. Screening of potential knockout colonies proved particularly difficult; in the first round of selections 50 colonies were screened and 16 were Km^S and Hyg^R. Of the 16 potential knockouts, 4 colonies were contaminated, the other 12 were DNA extracted (section 2.6.1) and screened by PCR using primers from the deleted region and Southern blot. The PCR using primers from the deletion gave bands for each of the 12 colonies screened (data not included), suggesting an intact copy of Rv2017 was present. The design of the Southern blot was such that 3′ and 5′ single crossovers were theoretically distinguishable from double crossovers by size difference (see figure 7.5). The PCR result was confirmed by the Southern blot, which produced two bands of different sizes, suggesting none of the colonies were double crossovers (see figure 7.6a).

Figure 7.5

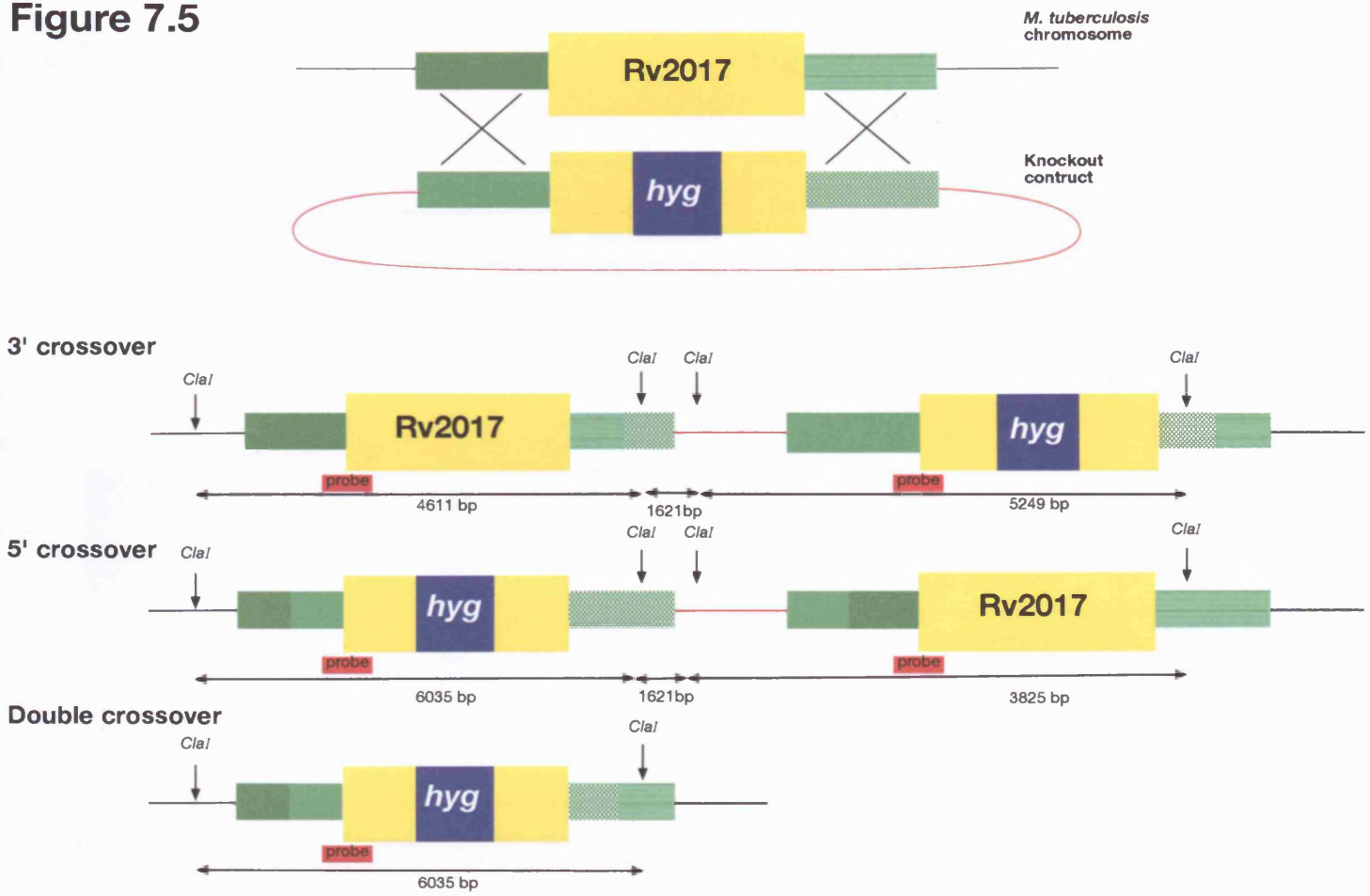

Figure 7.5: A schematic representation of formation of single and double crossovers for the Rv2017 knockout. The sizes produced after a *ClaI* digest, for a 3' or 5' single crossover and a double crossover event are indicated below the arrows. The positions of the probe in a Southern blot are marked, indicating both 3' and 5' single crossovers produce two bands in a Southern blot, whereas double crossover produces a single band.

Figure 7.6a

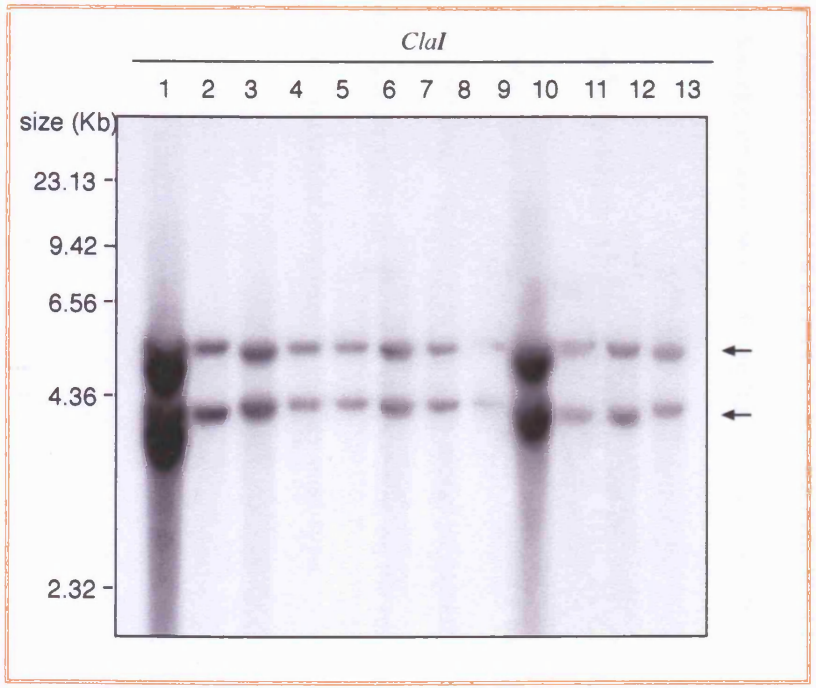

Figure 7.6b

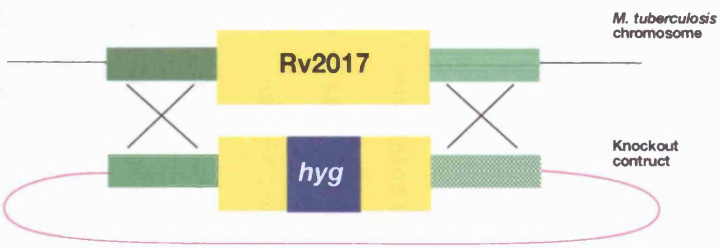

	Size of fragments (bp)	
5' single crossover	6035	3824
3' single crossover	5249	4611
Wild type	4611	—
Mutant	6035	—

Figure 7.6a: Southern blot to detect potential knockouts of Rv2017. DNA was extracted from potential knockout colonies, with the Km^S, Hyg^R phenotype. *ClaI* restriction digests were performed, separated using agarose gel electrophoresis, and Southern blot was performed.

Figure 7.6b: A schematic representation of the size of fragments produced in a Southern blot with *ClaI* digest. Size calculations for 3' and 5' single crossover events, double crossover (mutant) events and wild -type were derived from figure 8.6a.

crossovers (see figure 7.6a and b). A further 60 white colonies were replica plated onto Km and Hyg to screen for potential knockouts; however, none were Km^S and Hyg^R.

After going back to the original transformation, 6 blue colonies were picked and used to allow double crossovers to take place (see section 2.11.3). After serial dilutions, plates were left for 8 weeks before 100 colonies were taken and replica plated onto Km and Hyg + X-gal (to confirm loss of *lacZ*). A mixture of small and large colonies were tested as potential double crossovers on the Km^S and Hyg^R selection. Out of the 100 colonies screened only 5 were Km^S and Hyg^R. PCR using primers from the deletion was carried out to determine if there were any potential knockouts of Rv2017; the PCR showed 2 out of 5 colonies did not produce a product (data not included), therefore, Southern blots were performed using a *ClaI* digest (see figures 7.7a and 7.7b) and an *XhoI/HpaI* digest (see figures 7.8a and 7.8b), with one of the single crossover colonies from the previous Southern used as a control along with Wild-type H37Rv (see figure 7.7b and 7.8b). Two knockouts were detected (see figure 7.7b and 7.8b).

7.5 *in-vitro* and *in-vivo* phenotyping of the Rv2017 knockout

To assess whether Rv2017, as a predicted regulatory gene, regulates expression of the DNA-damage regulon, and/or regulates virulence in a mouse model of infection, *in-vitro* and *in-vivo* phenotyping was employed to study the effects of the mutation on the response to DNA-damage and on infection in the mouse model compared to H37Rv wild-type.

Figure 7.7a

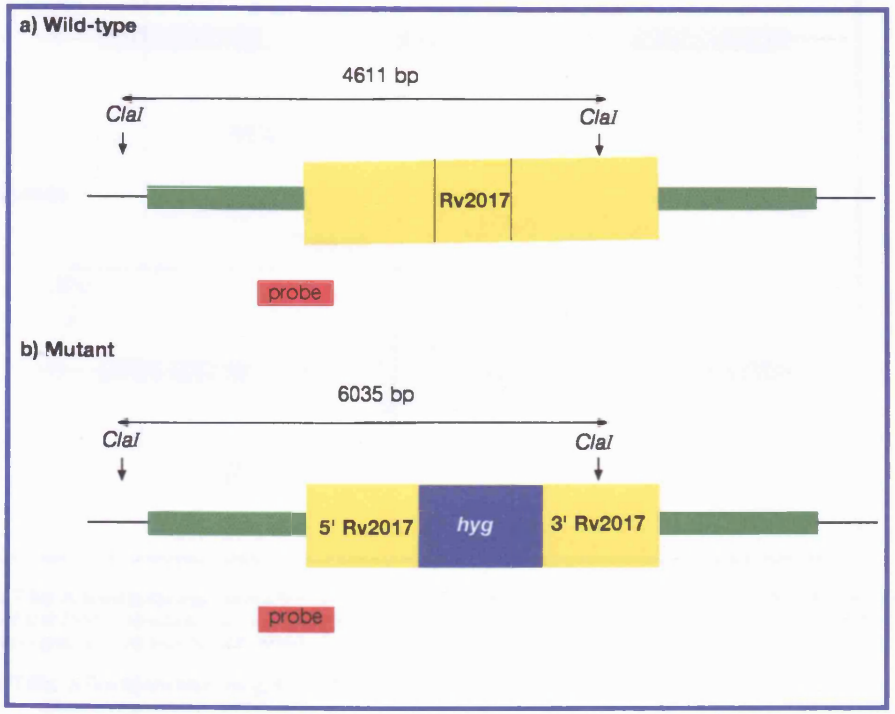

Figure 7.7b

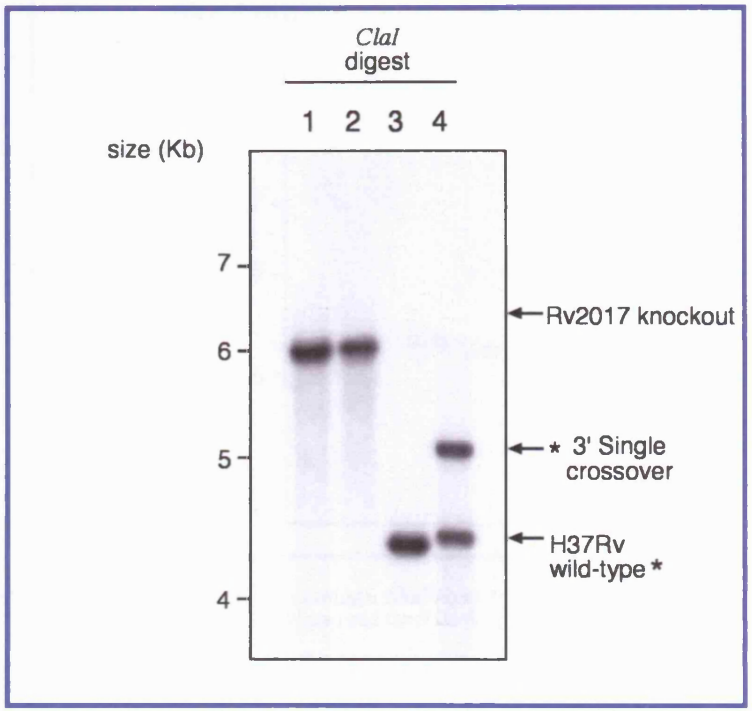

Figure 7.7a: A schematic representation of the size of the product produced by a Southern blot for both Rv2017 knockout and wild-type, following a *ClaI* digest. The positions of the *ClaI* restriction sites are indicated with the relative size products. The probe binding site overlaps the 5' coding region of Rv2017 (yellow) and the 5' flanking region of the Rv2017 construct (green). Genomic region outside the construct is black.

Figure 7.7b: A Southern blot using *ClaI* digest to detect potential Rv2017 knockout. Arrows indicate Rv2017 knockout, H37Rv wild-type and Rv2017 3' single crossover.

Figure 7.8a

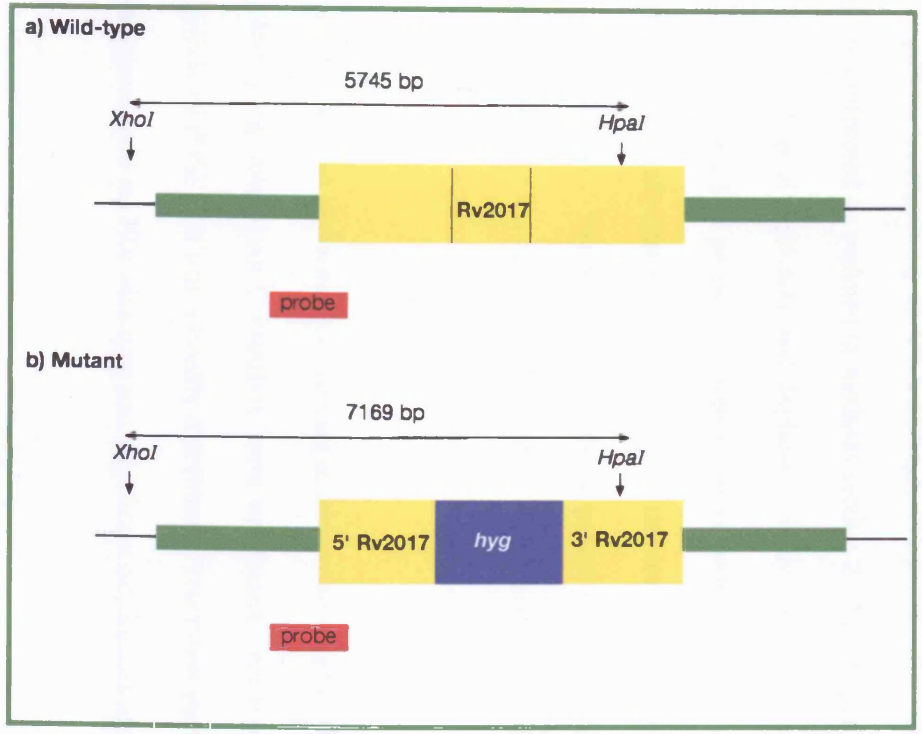

Figure 7.8b

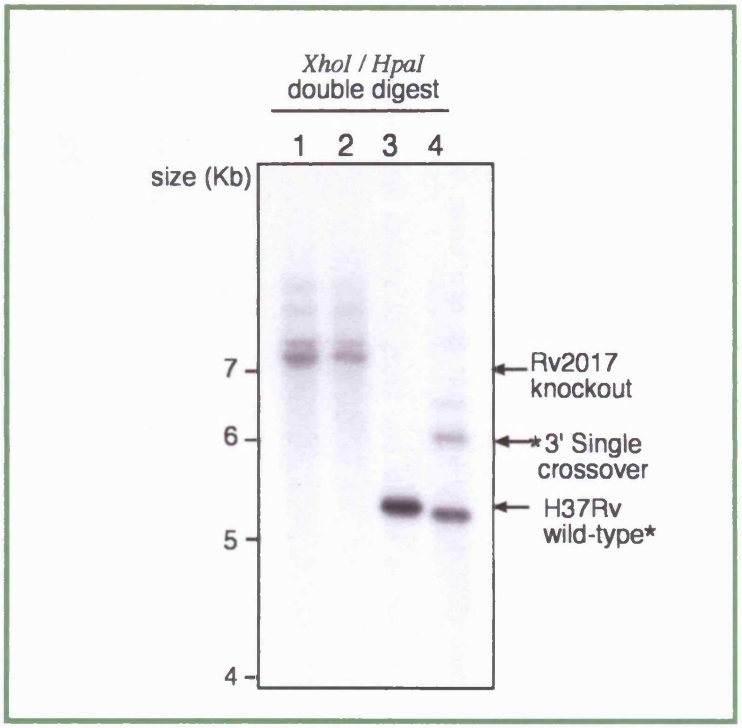

Figure 7.8a: A schematic representation of the size of the product produced by a Southern blot for both Rv2017 knockout and wild-type, following a *XhoI/HpaI* double digest. The positions of the *XhoI* and *HpaI* restriction sites are indicated with the relative size products. The probe binding site overlaps the 5' coding region of Rv2017 (yellow) and the 5' flanking region of the Rv2017 construct (green). Genomic region outside the construct is black.

Figure 7.8b: A Southern blot using *XhoI/HpaI* double digest to detect potential Rv2017 knockout. Arrows indicate Rv2017 knockout, H37Rv wild-type and Rv2017 3' single crossover.

7.5.1 Growth curve

Growth curves for the Rv2017 knockout and wild-type H37Rv were produced *in-vitro* under normal growth conditions, in a rolling incubator, as outlined in section (2.12.1). The Rv2017 knockout grew at the same rate as the wild-type H37Rv (see figure 7.9), suggesting the knockout has the same ability to grow and divide as the wild-type under normal growth conditions.

7.5.2 Susceptibility of the Rv2017 knockout and wild-type to DNA-damage

The DNA damaging agent mitomycin C was used to determine whether the Rv2017 knockout exhibited altered susceptibility to DNA-damage, compared with wild-type H37Rv. Viability assays were performed as outlined in methods section 2.12.2. Experiments were performed on two distinct biological replicates and duplicate colony counts were recorded for each. The viability was presented as percentage viable counts, with treated viable counts expressed as a proportion of mean untreated viable counts. The data for Rv2017 knockout was then compared with wild-type H37Rv. The Rv2017 knockout appeared to be less susceptible to mitomycin C than H37Rv wild-type, on each concentration of mitomycin C tested (see table 7.2 and figure 7.10).

Statistical analysis was performed on the data to determine whether the differences observed in viability following mitomycin C exposure were significant. An F-test was performed on the data to determine if the data was normally distributed. The F-test showed that both sets of data, Rv2017 knockout and H37Rv wild-type had significant differences in the variance at all

Figure 7.9

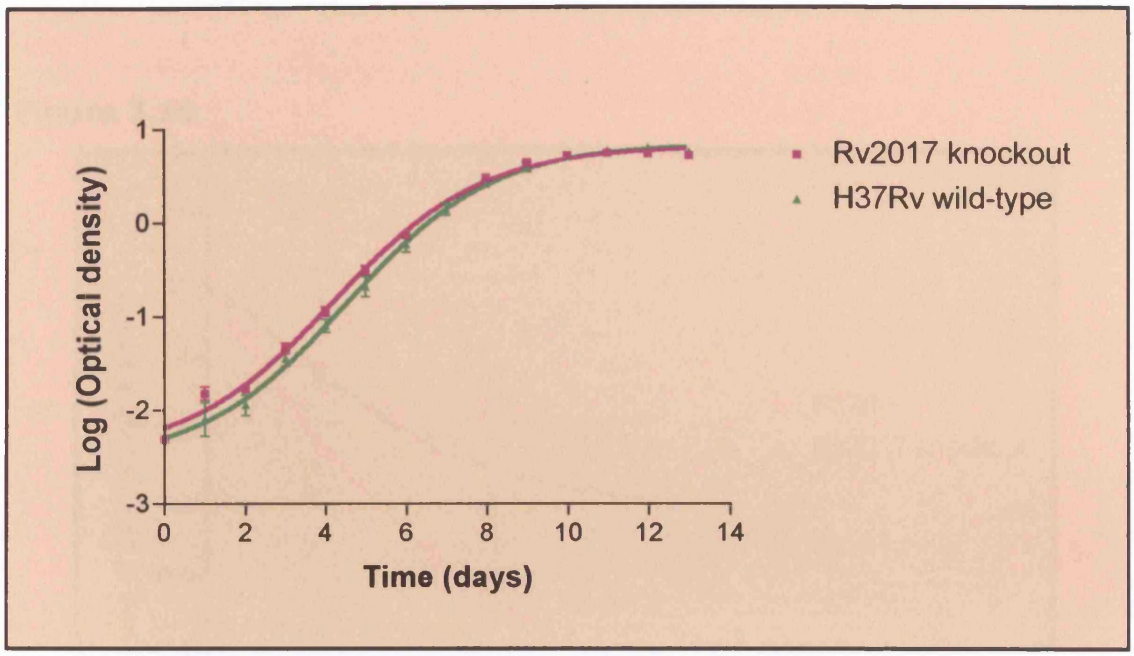

Figure 7.9: The *in-vitro* growth curve of ΔRv2017 strain compared to wild-type H37Rv. For each strain, single colonies were inoculated into 5ml of Dubos plus albumin in triplicate and incubated in static culture for 10 days at 37°C. Static cultures were then used to inoculate a 100ml rollingcultures in Dubos plus albumin, to an OD of 0.005 (approx 1ml). Triplicate cultures were returned to the rolling incubator for a total of 14 days. Optical density readings were taken at the same time daily, and dilutions were made in Dubos + albumin after an OD of 0.4 to enable accurate reading by the spectrophotometer.

Table 7.2

Mitomycin C (μg/ml)	H37Rv		Rv2017 knockout	
	Mean	Standard error	Mean	Standard error
Untreated	100.00	± 12.74	100.00	± 10.01
0.02	41.16	± 6.89	72.49	± 16.83
0.05	7.70	± 0.98	25.54	± 4.51
0.1	1.74	±0.46	8.68	±0.90
0.2	0.23	± 0.03	3.38	± 0.42

Figure 7.10

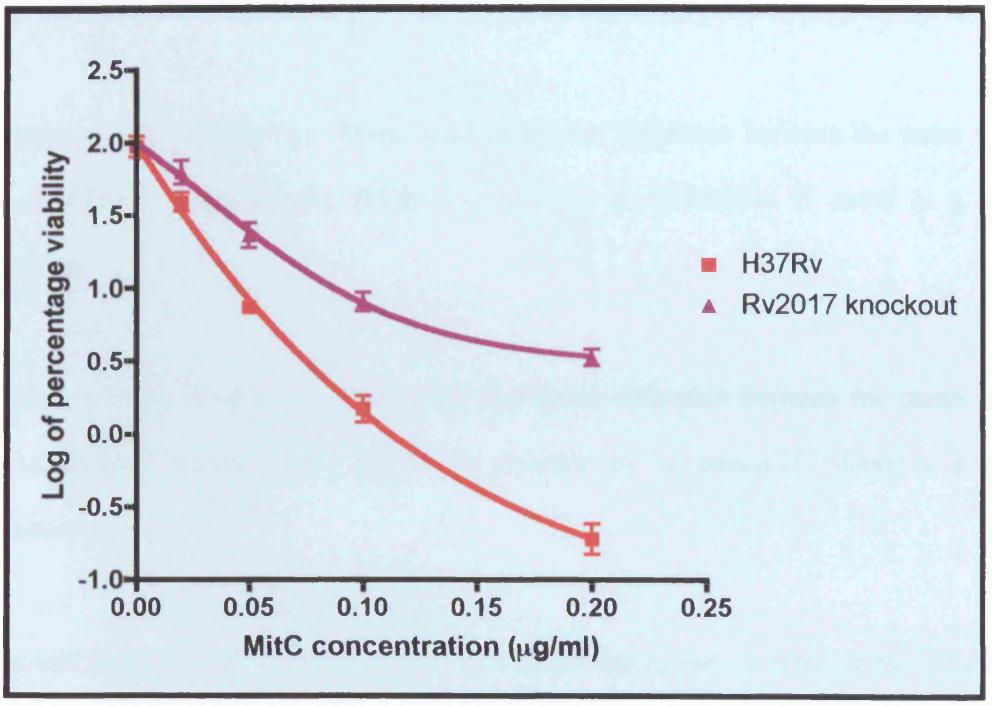

Table 7.2: Percentage viability of ΔRv2017 strain compared to H37Rv wild-type in response to Mitomycin C stress. Duplicate cultures were grown to exponential phase (0.3 to 0.4 OD), 40ml aliquots were incubated for 24 hours untreated or with the relevant concentration of Mitomycin C. After 24 hours the cultures were serial diluted and plated on 7H11 plates in duplicate and incubated at 37°C for 16-18 days. Colony counts were taken of at least 2 dilutions. The viable CFU was then expressed as a percentage of the untreated for each sample, and the mean and standard error was calculated.

Figure 7.10: A graph comparing the of viability of the ΔRv2017 strain with H37Rv wild-type to Mitomycin C stress. In Graphpad Prism 4, the percentage viability data as outlined above was transformed using log10, and plotted on a linear scale. A non-linear regression sigmoidal dose response curve was fitted to the data.

concentrations of Mitomycin C. This therefore meant the data were not normally distributed. The data were therefore transformed to approximate a normal distribution by a $\log_{10}$ transformation. The F-test was then performed again and this time showed no significant difference between the variances of the H37Rv data and the Rv2017 data, at the 95% confidence interval (see table 7.3), thus suggesting the data approximated a normal distribution. A student t-test was performed on the transformed data to determine whether there was a significant difference between the means when directly comparing data for H37Rv and Rv2017 knockout. Student T-tests were performed with the following hypotheses:

H_0: P value > 0.05. Accept H_0: There is no significant difference between the mean viable counts of Rv2017 knockout and H37Rv in response to mitomycin C stress at a given concentration.

H_1: P value < 0.05. Accept H_1: There is a significant difference between the mean viable counts of Rv2017 knockout and H37Rv in response to mitomycin C stress at a given concentration.

A two-tailed, unpaired T-test revealed there was a significant difference between the viability of H37Rv and Rv2017 knockout for mitomycin C stress at 0.05, 0.1 and 0.2μg/ml mitomycin C (95% confidence interval) see table 7.3. No significant difference was observed at the 95% confidence interval (student t-test) between wild-type and Rv2017 knockout for untreated and 0.02μg/ml mitomycin C.

Table 7.3

	Untreated	0.02μg/ml MitC	0.05μg/ml MitC	0.1μg/ml MitC	0.2μg/ml MitC
Table Analyzed	Transformed log10	Transformed log10	Transformed log10	Transformed log10	Transformed log10
H37Rv wild-type	H37Rv U	H37Rv 0.02	H367Rv 0.05	H37Rv 0.1	H37Rv 0.2
vs	vs	vs	vs	vs	vs
Rv2017 Knockout	Rv2017 U	Rv2017 0.02	Rv2017 0.05	Rv2017 0.1	Rv2017 0.2
Unpaired t test					
P value	**0.8767**	**0.0913**	**0.0001**	**P<0.0001**	**P<0.0001**
P value summary	ns	ns	***	***	***
Significant difference at (P < 0.05)	**No**	**No**	**Yes**	**Yes**	**Yes**
One- or two-tailed P value?	Two-tailed	Two-tailed	Two-tailed	Two-tailed	Two-tailed
t, df	t=0.1585 df=12	t=1.836 df=12	t=5.325 df=13	t=6.812 df=16	t=6.943 df=9
F test to compare variances					
F,DFn, Dfd	2.648, 5, 7	2.332, 7, 5	3.174, 6, 7	1.650, 7, 9	9.568, 7, 2
P value	**0.2366**	**0.3682**	**0.1564**	**0.4749**	**0.1957**
P value summary	ns	ns	ns	ns	ns
Are variances significantly different	**No**	**No**	**No**	**No**	**No**

Table 7.3: Statistical analysis of the response to Mitomycin C stress of the Rv2017 knockout compared to H37Rv wild-type. The percentage viability for ΔRv2017 and H37Rv was transformed using $\log_{10}$. An F-test was performed to determine if both samples had equal variance (H_0) (a requirement for parametric tests), when the p-value >0.05, H_0 is accepted, the populations have equal variance and a t-test is appropriate. Then unpaired, two-tailed t-tests were performed between each sample for both ΔRv2017 and H37Rv wild-type, under each stress condition individually, to determine if the means for each sample were the same (H_0) or the means of ΔRv2017 and H37Rv were different (H_1). Where the p-values <0.05, H_0 is rejected and H_1 is accepted: there is a significant difference between the means.

7.5.3 *in-vivo* phenotyping of the Rv2017 knockout compared to wild-type H37Rv

A mouse model of infection was used to determine the *in-vivo* phenotype of the Rv2017 knockout in comparison to wild-type H37Rv. Three month old female mice were injected intravenously in the tail vain with 200µl of each strain of bacteria by a trained animal technician (see section 2.12.3). Initial infection colony counts (CFU) were determined from the inoculum, by serial dilution and plating of the inoculum (see table 7.4); the CFU varied slightly, even though each strain was grown to an optical density (OD) of 0.3-0.4, then diluted to an OD of 0.02 in DAG (Dubos + albumin + glycerol).

Strain	Viable counts
H37Rv Wild-type	3.18E+05
Rv2017 Knockout	2.38E+05

Table 7.4: Viable CFU counts of H37Rv wild-type and Rv2017 knockout
The infection inoculum was serial diluted in saline in duplicate, and plated onto 7H11 plates. Viable colony counts were taken after 13-18 days.

Pathology of the infection was monitored using bacterial load calculated from harvested lungs and spleen obtained from 4 mice at days 1, 34, 68, 103 and 146 (see figure 7.11a and 7.11b). There was no difference observed between the H37Rv wild-type and the ΔRv2017 strain at day 1 or day 34; however, after this there is a significant increase in CFU in the lung in the ΔRv2017 strain compared to H37Rv wild-type (see figure 7.11a). There were problems with the initial plating of the 103 day time point, in that there were no colonies observed; therefore

Figure 7.11a

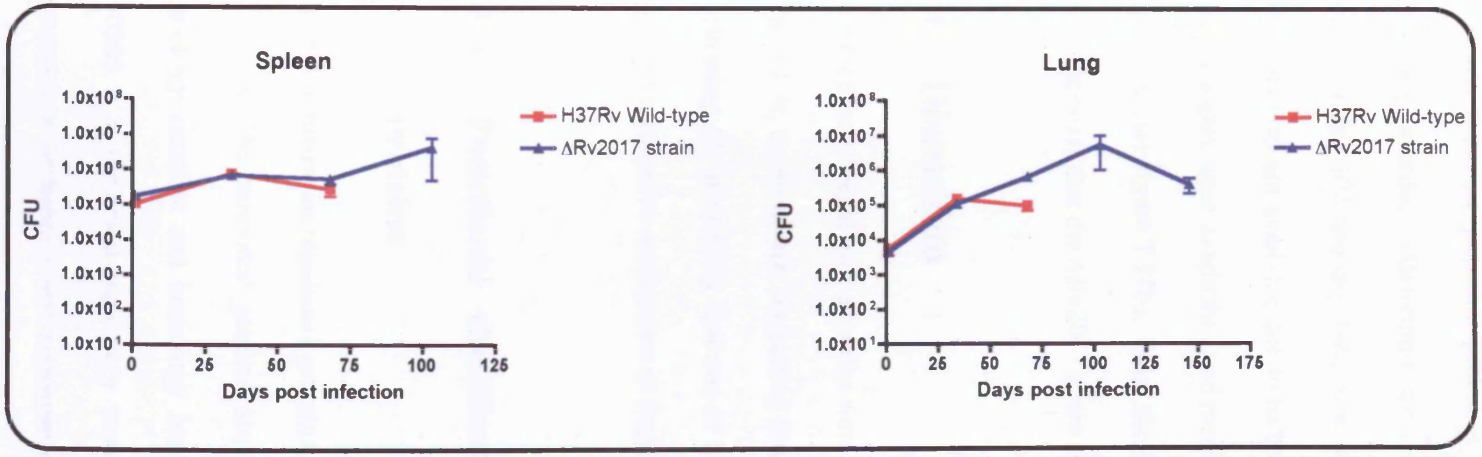

Figure 7.11b

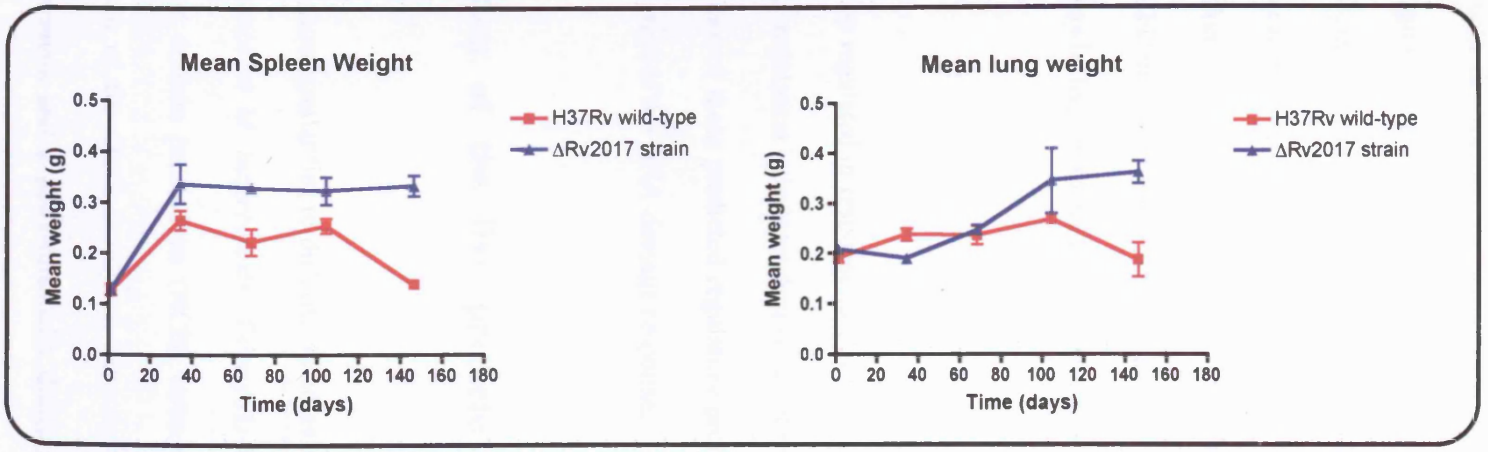

Figure 7.11a: *In-vivo* mouse data comparing ΔRv2017 strain with H37Rv. The data was obtained from intravenous infections of 3 month old BALBC female mice with the ΔRv2017 strain and H37Rv wild-type of *M. tuberculosis*. The lung and spleen were harvested from 4 mice at day 1, 34, 68, 103 and 146, after infection, and colony forming units (CFU) were counted, however there were problems with CFU counts for the wild-type, after day 34, and for the ΔRv2017 strain in the lung on day 148.

Figure 7.11b: *In-vivo* mouse data comparing mean spleen and lung weights for the ΔRv2017 strain and H37Rv, without re-spotted wild-type.

the organ stock for the H37Rv wild-type was re-plated and colony counts were obtained. However, there are potential problems with the viability of frozen and re-streaked samples. Therefore, in order to determine the magnitude of the loss of viability, the lung and spleen counts for day 103 and day 146, were re-plated for both ΔRv2017 strain and H37Rv, however CFU data was not available due to technical problems in the animal facility. Nevertheless, the organ weights were available , and therefore were plotted for both the lung and spleen at each time point (see figure 7.11b). From the CFU data from initial time points, and the organ weight data, it appears that the ΔRv2017 strain may be hypervirulent in the mouse model of infection.

7.6 Discussion

Five predicated regulatory proteins were up regulated in response to DNA-damage in the Δ*recA* strain of *M. tuberculosis*, suggesting their regulation is independent of the RecA/LexA system, implicating the possibility that one or more of these predicted regulatory proteins may play a role in an alternative mechanism of regulation of the DNA-damage response.

7.6.1 Functional classification of the five predicted regulatory proteins

These five predicted regulatory proteins show similarities to different families of transcriptional regulators. The annotated genome sequence of *M. tuberculosis* (TubercuList), together with homology searches and homology based domain predictions (NCBI website), suggests that Rv0586 is a predicted regulatory protein of the GntR family of transcriptional regulators, possessing a probable GntR signature domain and a helix-turn-helix domain. For Rv1956, Tuberculist did not indicate homology to a specific family of transcriptional regulators, yet,

Rv1956 contains a probable helix-turn-helix domain, which shows homology to the XRE family of transcriptional regulators, that respond to xenobiotics and is reported to be upregulated in response to starvation. Rv1985c is predicted to be part of the LysR family of transcriptional regulators, possessing a LysR signature domain and a helix-turn-helix domain. Rv2017 is not assigned to a particular family of transcriptional regulator, but, shows N-terminal similarity to a number of transcriptional regulators belonging to the XRE family and shows C-terminal homology to a zinc binding domain, suggesting a role as a metalloprotease. The N-terminal region of Rv2884 shows similarity to transcriptional regulators of sensory transduction systems, which exhibits some homology to OmpR, a stress response regulator present in *E. coli*; interestingly *M. tuberculosis* lacks an OmpR homologue.

Although (Earl *et al.*, 2002) suggested Rv2017 from *M. tuberculosis* and *irrE D. radiodurans* share homology, blast searches using Rv2017 protein as the query failed to detect IrrE, whereas blast searches using IrrE sequence as the query pulled out Rv2017 (E-value of $5e^{-7}$) (figure 7.2a and b). The alignments produced by both EMSOSS (Figure 7.2a) and BLASTP (Figure 7.2b) show a region of 31 residues of homology, which corresponds to the DUF955 conserved region. Protein blast (BLASTP) search using Rv2017 also showed homology to GI: 29345183, a zinc binding transcriptional regulator of the Cro/CI family, from *Enterococcus faecalis* V583 (E-value = $3e^{-83}$), as well as homology to Rv2515c (E-value = $3e^{-8}$) from *M. tuberculosis* and Mb2040 (E-value = $5e^{-7}$) from *M. bovis*. Rv2515c is particularly interesting, it is listed as a hypothetical protein in TubercuList, and was shown to be essential by transposon mutagenesis by (Sassetti *et al.*, 2001) it too contains a neutral zinc metallopeptidase, zinc binding region signature.

7.6.2 Analysis of the Rv2017 gene inactivation knockout

The gene inactivation knockout of the predicted regulatory proteins (Rv2017) was used to study the effect of the mutation on gene expression and phenotype, to determine whether it was involved in regulation of DNA-damage repair, or pathogenesis. Prior to the construction of the gene inactivation knockout in Rv2017, chromosomal locational and transcriptional analysis revealed that Rv2017 was part of a polycistron (Figure 7.3a and Figure 7.4a and b). This is important information in designing and constructing a knockout, as within polycistrons, inactivation via deletion and insertion may have polar effects on any downstream genes. In order to determine whether any phenotypic effects are solely due to the gene inactivation, a complementing construct should be analysed alongside the knockout. Complementation with a construct re-instating only the inactivated (Rv2017) gene will determine whether the effects observed are due to the gene inactivation, or as a result of the polar effects on the downstream genes. To assess any potential polar effects, RT-PCR can be performed using RNA from both the mutant and wild-type strains to determine if there are any differences in gene expression of other genes in the polycistron. The 3′ region of Rv2017 was retained in the knockout construct to help limit the potential for polar effects: the reason being the post-transcriptional modification of the mRNA should remain intact if the regions recognized by the post-translational modification process remain intact. Due to time constraints, a complementing construct was not produced for ΔRv2017 strain, but is vital for checking the effects of the Rv2017 gene inactivation knockout.

The first round of screening for an Rv2017 knockout revealed only single crossover events (figure 7.6a). Successful knockout strains of Rv2017 were not detected until the length of incubation for the double crossover stage of selection had been allowed to proceed for 8 weeks.

This may suggest the knockout has attenuated growth; however, later growth curves produced suggest that in liquid culture there was no difference between the H37Rv wild-type and the ΔRv2017 strain (Figure 7.9). This discrepancy is difficult to explain.

The design of the Southern blot used in detection of the ΔRv2017 strain enabled one to distinguish between single crossover events, random integrations, and the required double crossover events. However, due to the nature of the Southern blot, there are slight discrepancies between predicted and observed sizes for both wild-type and knockout strains. The Southern blot size estimation relies on the DNA marker run along side digested DNA samples, on an agarose gel. The gel is photographed under UV illumination with a fluorescent ruler, which is used to estimate sizes after autoradiography. Therefore the slight discrepancies in size are most likely due to human error when measuring the distance on the autoradiograph and comparing this to the gel picture. Nevertheless, two different digests show a continuous pattern for the Rv2017 knockout strains marked 1 and 2 on figures 7.7b and 7.8b, indicating that a knockout has been successfully obtained.

As previously stated there appears to be no difference between the *in-vitro* growth of the ΔRv2017 strain compared to H37Rv wild-type, suggesting the deletion of Rv2017 does not affect the ability to divide and replicate under normal *in-vitro* growth conditions. However the ΔRv2017 strain is hyposensitive to treatment with the chemical DNA damaging agent mitomycin C, compared to wild-type H37Rv. This difference in sensitivity is significant with treatment of greater than or equal to 0.05μg/ml mitomycin C. This may suggest that Rv2017 acts as a repressor protein of genes involved in the repair of interstrand cross links, such as those produced by mitomycin C. Possible candidates would include genes involved in NER, as NER mutants (*uvrA*, *uvrD*) show increased susceptibility to mitomycin C (Rand, 2003),

therefore in the absence of the repressor, these genes may be constitutively produced and so may act more quickly to repair such interstrand cross links between alkylated bases.

An alternative hypothesis is that Rv2017 may regulate genes involved in permeability, such as protein channels. Thus, knocking out Rv2017 could make the mutant strain less permeable to exogenous protein/chemicals. The hyposensitivity of Rv2017 to mitomycin C could be due to the regulon of Rv2017.

Rand, (2003) observed that mutants in base excision repair (BER) pathways showed decreased susceptiblity to mitomycin C; however, there was no significant difference between the susceptibility of the BER knockouts and the wild-type H37Rv, suggesting that inter-strand cross links were not repaired via BER. Mutants in nucleotide excision repair were more susceptible to mitomycin C than wild-type H37Rv. There are three main processes by which damaged DNA is repaired, depending on the type of DNA-damage. BER and NER removed damaged bases directly, using a different mechanism, and DNA-damage across DNA strands is repaired by homologous recombination. BER removes oxidised and alkylated bases (Mizrahi and Andersen 1998), whereas NER, studied in *E. coli* is performed by the exinucleases *uvr*ABC and D, which function to excise pyrimidine dimers in damaged DNA (Freidberg *et al.*, 1994).

Due to the apparent insusceptibility of ΔRv2017 strain to mitomycin C stress, it would be interesting to look at the effects of other DNA damaging agents, which target specific DNA repair pathways in the ΔRv2017 strain. During the infection process, *M. tuberculosis* is phagocytosed by macrophages, which develop into granulomas, producing a hostile environment for the bacterium. The macrophages produce reactive oxygen and nitrogen intermediates, known to damage DNA and the granuloma provides an hypoxic environment,

lacking in nutrients. Hydrogen peroxide and cumene hydroperoxide are reduced to superoxide radicals, known to damage DNA. Therefore, these could be used to determine the viability of ΔRv2017 strain. The bacteria are also subject to nitrosative stress in macrophages, which could be mimicked using sodium nitrite at acidic pH, to determine susceptibility of the ΔRv2017 strain.

An alternative approach to looking at the *in-vitro* susceptibility of the ΔRv2017 strain to stresses in liquid culture would be to look at the viability of the ΔRv2017 strain in *in-vitro* macrophage infections. Graham et al., (1999) showed that genes involved in DNA repair and virulence are induced in macrophages, to potentially cope with the hostile environment. The heat shock induced protein α-crystalin is upregulated under low oxygen tension, and is required for growth in macrophages. Therefore, activated bone marrow derived macrophages produce a number of DNA damaging agents, which would better mimic the intracellular environment that *M. tuberculosis* is exposed to during infection.

Animal models have been developed to mimic the effects of *in-vivo* infection. After 3 time points there appears to be no difference between H37Rv wild-type and ΔRv2017 strain in the spleen, yet there was a significant difference in CFU in the lung at day 68 in ΔRv2017 strain compared to H37Rv (t-test $p<0.05$). The log difference in CFU observed between the lung and the spleen can be accounted for due to the method of infection: intravenous injection results in an initially higher CFU in the spleen than the lungs. In a human infection, the aerosol route of infection determines that the CFU is highest in the lungs; therefore the only way to mimic this would be to use an aerosol route of infection, which is currently not available at our animal facility.

8 Identification of the Rv2017 regulon by microarray analysis

8.1 Introduction

Microarray analysis performed on Δ*recA* strain of *M. tuberculosis* revealed that the majority of genes in the DNA-damage regulon were regulated in a RecA/LexA independent manner (Rand *et al.*, 2003). It was hypothesised that another regulatory protein, such as an activator/repressor may be involved in regulation of expression of some of the genes in the DNA-damage regulon. Rv2017 appeared to be a potential candidate, due to the higher levels of induction observed in Δ*recA* strain compared to H37Rv (Rand *et al.*, 2003) and the homology of Rv2017 to IrrE of *Deinococcus radiodurans* (*D. radiodurans*), shown to positively regulate *recA* (Earl *et al.*, 2002).

Microarray experiments were designed to address the possibility that Rv2017 was involved in regulation of genes in the DNA-damage regulon. The experimental design was such that inter- and intra-strain comparisons could be made between the level of gene expression under uninduced and induced (0.02μg/ml mitomycin C) conditions. The advantages of using RNA versus DNA arrays are outlined in chapter 4.

The microarray slides used, were PCR spotted whole genome *M. tuberculosis* arrays, produced by the BμGS microarray unit at St. George's Hospital Medical School. Triplicate RNA samples were harvested from H37Rv and ΔRv2017 strains of *M tuberculosis*, that were either uninduced or induced with 0.02μg/ml mitomycin C in exponential phase (OD 0.15). Both the uninduced and induced cultures were incubated for a further 24 hours after the addition of the chemical

DNA damaging agent mitomycin C. DNA contamination was removed by DNase treatment for the H37Rv strain; however problems occurred with the DNase treatment of the ΔRv2017 strain, resulting in degradation of the RNA. Therefore the small amount of sample retained, that was not DNase treated was analysed for the presence of DNA contamination using PCR. A PCR was performed on all the ΔRv2017 strain RNA samples alongside a DNA control to detect any potential DNA contamination. The PCR showed that the ΔRv2017 RNA samples were not contaminated with DNA (see figure 8.1). The RNA samples for both H37Rv wild-type and ΔRv2017 strain were then analysed using a Bioanalyser (Agilent Technologies) to determine the quantity and quality of the RNA preparation (data not shown).

8.2 Analysis and input of the microarray slides

For the microarray experiments, each triplicate biological sample was used in duplicate for both the uninduced and induced (mitomycin C 0.02μg/ml) cultures of H37Rv wild-type and the ΔRv2017 strain, resulting in a minimum of 6 slides per strain, per treatment. (Slides were repeated where either problems with scratching of the slide or background fluorescence occurred).

The slides were scanned and analysed as outlined in the methods. The spread of the data was determined using Genespring to produce a graph of the normalised data plotted against the strain, and induction (-/+ mitC), to enable a comparison to be made between H37Rv and the ΔRv2017 strain (see figure 8.2). The spread of the data determines the type of statistical analysis performed on the data. Therefore the unequal spread of the data suggests the variances are not equal for H37Rv and ΔRv2017 strains, therefore the assumption was used that the

Figure 8.1

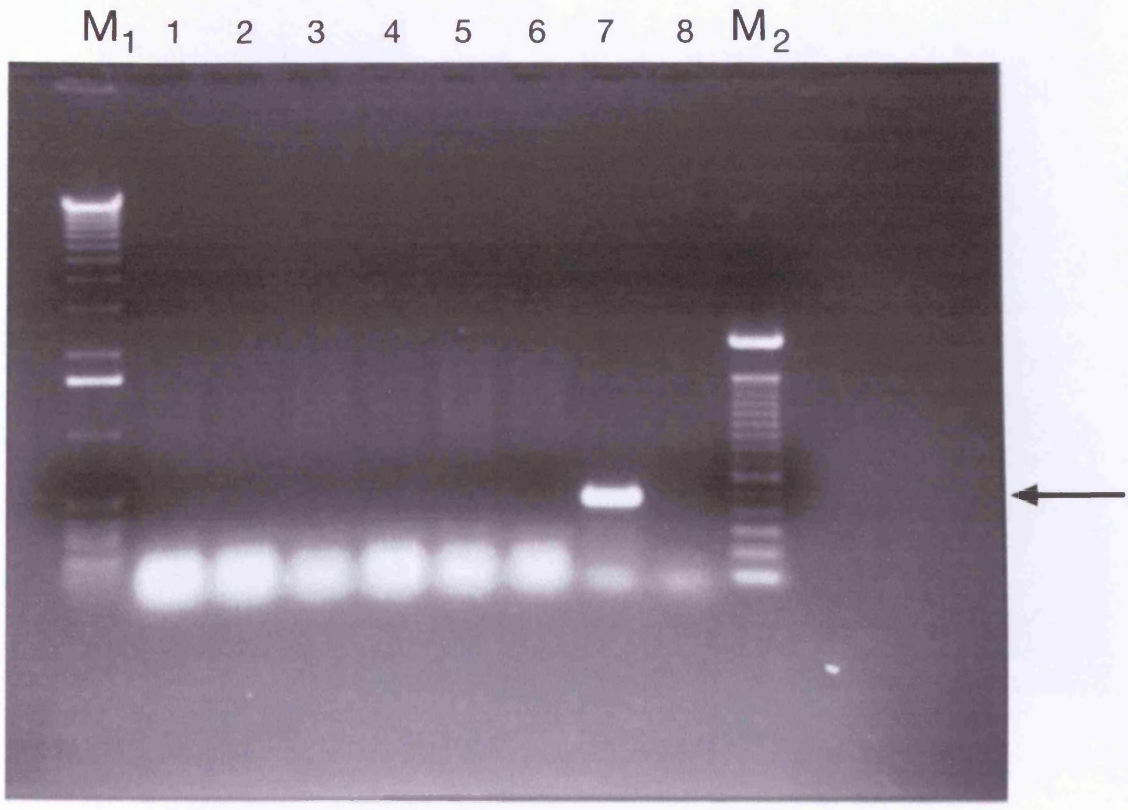

Figure 8.1: PCR to detect DNA contamination in ΔRv2017 RNA extractions. 1μg of RNA was used in the PCR reaction, for each of the biological replicates (1-3) of uninduced (tracks 1,3 and 5) and induced (0.02μg/ml mitomycin C) (tracks 2,4 and 6) samples from ΔRv2017 strain of *M. tuberculosis*. Genomic *M. tuberculosis* DNA was used as a positive control (track 7), negative control (track 8). The samples were run alongside commercial markers M1 (1kb ladder) and M2 (100bp ladder).

Figure 8.2

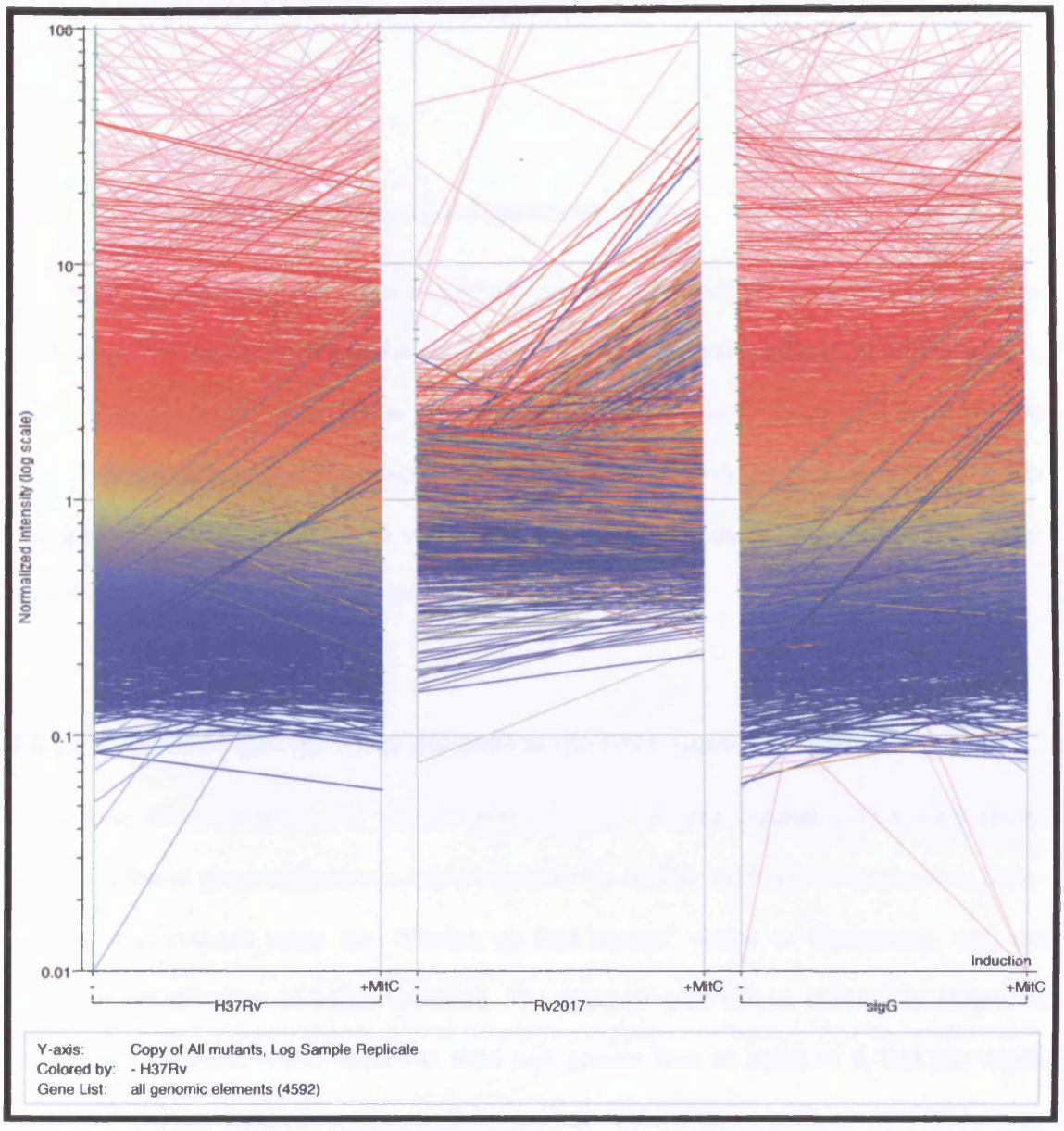

Figure 8.2: Schematic representation of the spread of microarray data for H37Rv, Δ*sigG* and ΔRv2017 strains of *M. tuberculosis*. PCR spotted M. tuberculosis whole genome microarrays (Bμgs Unit, St. Georges Hospital) were perfomed to compare expression of genes in H37Rv, Δ*sigG* and ΔRv2017 strains of *M. tuberculosis*. Arrays were performed as two colour experiments cy3/cy5 arrays, using DNA versus RNA respectively. The strain is marked under each of the three figures, and the data goes from uninduced (-) on the left, to the induced (+MitC) 0.02μg/ml mitomycin C, on the right. The data shown is comprised of three biological replicates each with two technical replicates for each strain under each condition.

variances of the data were unequal, which required the use of the Welsh's approximation to the Student T-test.

8.2.1 Statistical analysis of microarray data

The microarray data was analysed in two ways, to answer two different questions. The first was to identify whether Rv2017 played a role in the regulation of genes induced by DNA-damage, identified in the H37Rv wild-type as genes that were 2-fold or more up-regulated in response to DNA-damage (mitomycin C stress). The second strategy was to look globally at genes regulated by Rv2017 under either uninduced or induced conditions, and determine whether there was any overlap between the two groups.

8.2.1.1 Rv2017 and the genes involved in the DNA-damage response

To address the possibility that Rv2017 was involved in gene regulation following DNA-damage, a list of genes induced two fold or more in the H37Rv wild-type in response to DNA-damage, was collated using the 'filtering on fold change' option in Genespring, with the minimum cut off value of 2-fold induction. The resultant gene list, as outlined in chapter 4, contained 118 genes, whose induction ratio was greater than or equal to 2, and for which expression in the induced conditions compared to uninduced conditions in H37Rv was significantly different, with a p value $P<0.01$ (Student T-test).

The normalised data for both H37Rv and ΔRv2017 from the list of 118 DNA-damage inducible genes were exported into Excel, where calculations were performed to determine the mean, standard deviation and standard error for both the uninduced and induced values for each strain

individually. Any standard errors greater than 3 were highlighted, and the individual values were assessed. In some cases, spurious data spots had not been effectively removed in Gene Pix, which could be seen as huge numbers, usually in one out of the 6 replicates. When the data for 5 out of the 6 biological and technical replicates were within one standard deviation of the mean, and the last replicate was greater than 3 standard deviations away from the mean, these data points were removed as errors.

After the removal of the outliers, the induction ratios were calculated for all 118 genes, using induced/uninduced for all the individual biological and technical replicates. The mean, standard deviation and standard error were then calculated for the induction ratios of both H37Rv and ΔRv2017 strains. The induction ratios were transformed using $\log_{10}$, before a two-tailed Welsh's approximation to a T-test was used with a p value $p<0.01$, to calculate whether there was a significant difference between the induction ratio of H37Rv compared to ΔRv2017 strain. A total of 59 genes were identified with significantly different induction ratios, all of which were decreased in ΔRv2017 compared to H37Rv (see figure 8.3); therefore 59 genes were also identified whereby there was no significant difference in induction ratio between ΔRv2017 strain and H37Rv. However, potential pitfalls of using the induction ratio alone were identified in chapter 4. Therefore the data were further analysed to determine which genes were significantly different in ΔRv2017 strain compared to H37Rv under uninduced conditions and then induced conditions, using a two-tailed Welsh's approximation to a T-test, with a p value $p<0.01$, performed using transformed uninduced and induced data ($\log_{10}$).

There are 30 genes with a significantly different induction ratio, which are also significantly different under induced conditions (see figure 8.3 and 8.4). The induction ratios are all significantly lower ($p<0.01$), as are the induced values; the normalised data in the bottom graphs

Figure 8.3 Analysis of the DNA damage regulon

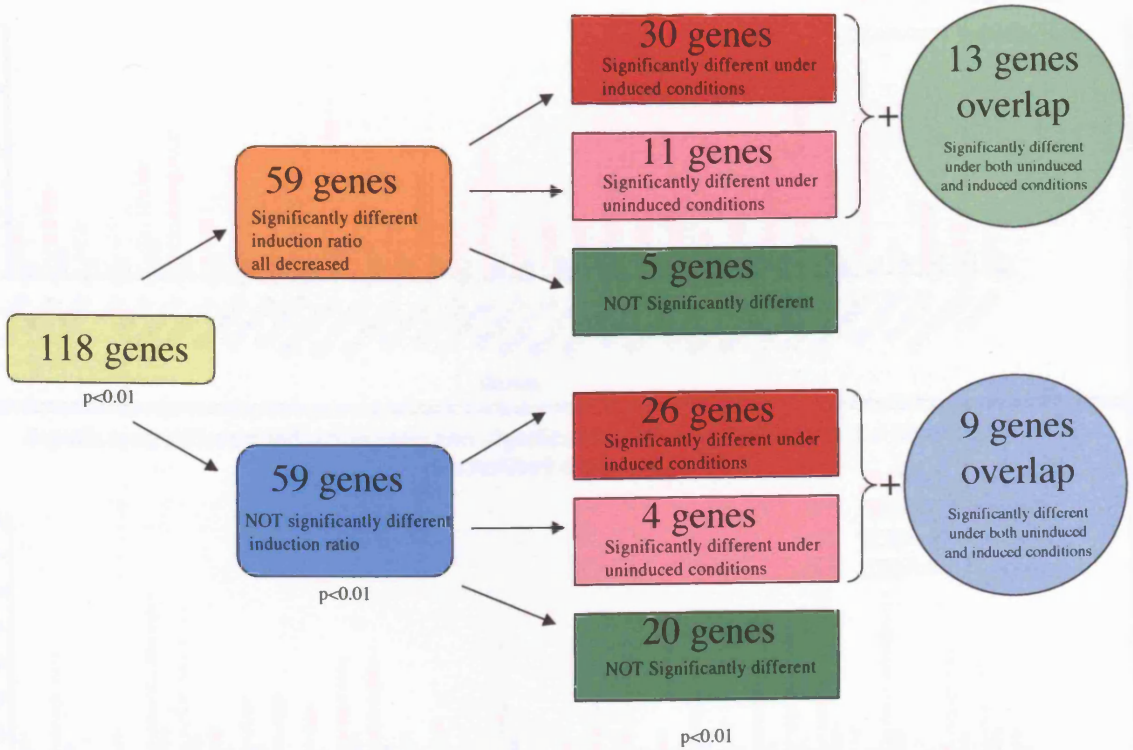

Figure 8.3: Schematic representation of the analysis of genes in the DNA damage regulon. The DNA damage regulon was defined by those genes that were regulated 2-fold or more in response to DNA damage (mitomycin C stress 0.02μg/ml) in H37Rv wild-type, with a $p<0.01$ (Students T-test). This data was then compared to the ΔRv2017 strain. The induction ratio was calculated (induced/uninduced) for both H37Rv and ΔRv2017 strains, a T-test was then performed $p<0.01$ to determine which genes had a significantly different induction ratio in ΔRv2017 compared to H37Rv. These were then further analyzed to determine which genes were significantly different under induced conditions between H37Rv and ΔRv2017, then under uninduced conditions using a Student T-test $p<0.01$. The overlap between the induced and uninduced comparisons is also shown.

Figure 8.4

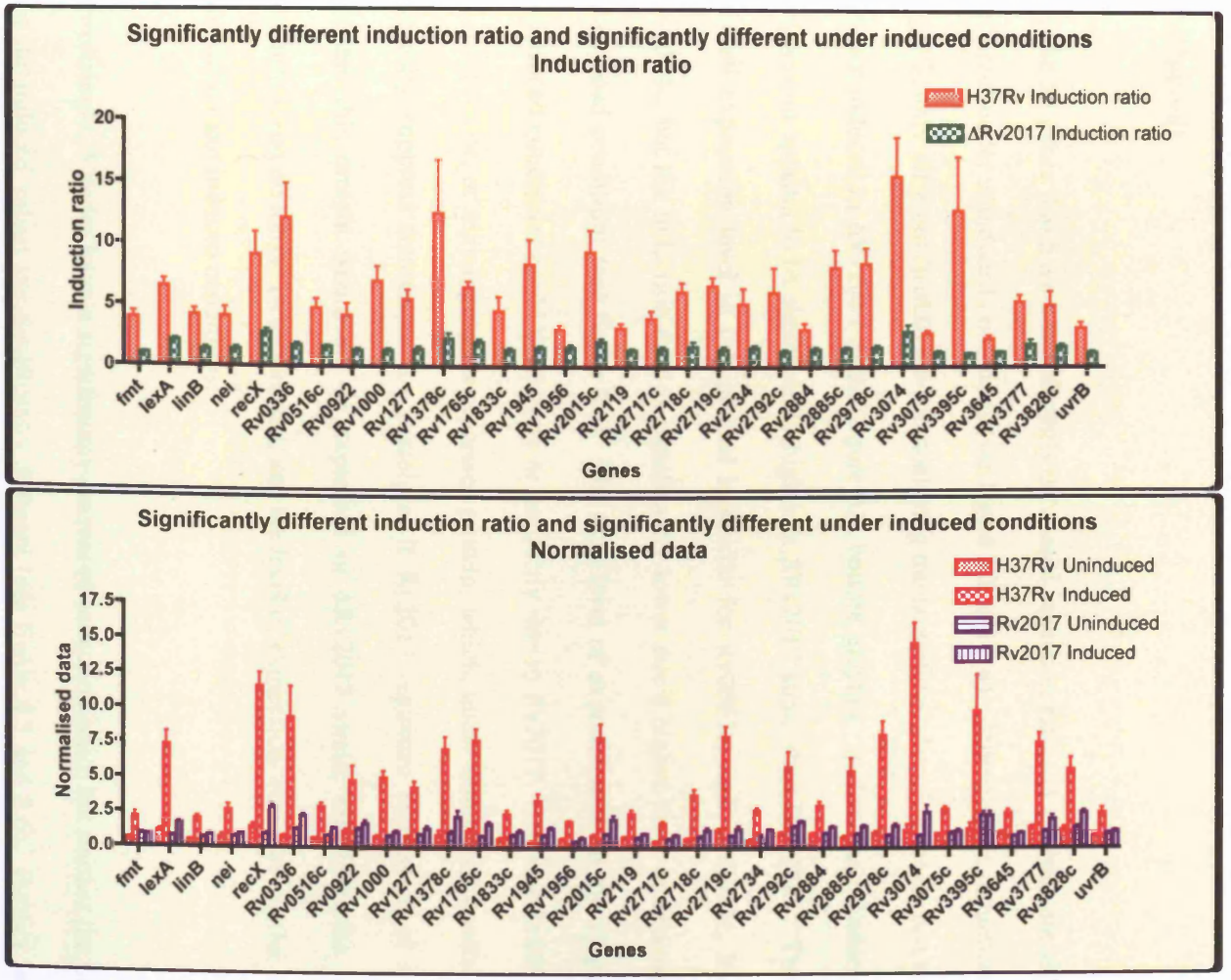

Figure 8.4: 30 genes with significantly different induction ratios, also significantly different under induced conditions. The data were obtained from DNA versus RNS microarrays with H37Rv and ΔRv2017 strain of *M. tuberculosis* under both uninduced and induced (0.02μg/ml mitomycin C) conditions. The induction ratios were calculated for both H37Rv and ΔRv2017, as induced/uninduced, a Student T-test was performed $p<0.01$, top graphs. The induced values for each strain were also significantly different using Student T-test $p<0.01$, bottom graphs.

shows the induced levels are significantly lower in ΔRv2017 strain compared to H37Rv. In this case, the induction ratios and the normalised data tie in together, and show a significant difference in expression under induced conditions, suggesting that these genes are directly or indirectly regulated by Rv2017, in response to the DNA damaging agent mitomycin C (0.02μg/ml).

Of the 59 genes that have a significantly decreased induction ratio, 11 of these are significantly different under uninduced conditions (see figure 8.3 and 8.4). Although the induction ratios are significantly different ($p<0.01$), when analysing the normalised data, it appears that these genes are not induced in ΔRv2017 strain (figure 8.5, bottom graphs). Rather, the uninduced level of expression appears to be significantly higher in ΔRv2017 strain than in H37Rv. Therefore the overall expression level in the induced is similar for Rv0861c, *ligB*, Rv2413c, Rv3517 and Rv0094c, but the induction ratio is significantly lower due a higher level of expression under uninduced conditions (see figure 8.5). The high level of expression of all the 11 genes under uninduced conditions could be directly or indirectly due to Rv2017, whereby Rv2017 may act as a repressor, or may regulate a repressor protein, which, under uninduced conditions would normally suppress transcription. Therefore, if Rv2017 regulates expression of a repressor protein, this protein would not be expressed in ΔRv2017 strain, therefore, the repressors' regulon would no longer be suppressed, and the level of expression would be similar under both uninduced and induced conditions.

Surprisingly, 5 genes have a significantly decreased induction ratio, but neither the uninduced, nor the induced values are significantly different (see figure 8.3 and 8.6). Further analysis of the induced conditions for the ΔRv2017 and H37Rv strains, revealed that although the induced values are not significantly different at $p<0.01$, they are significantly different at $p<0.05$ (see

Figure 8.5

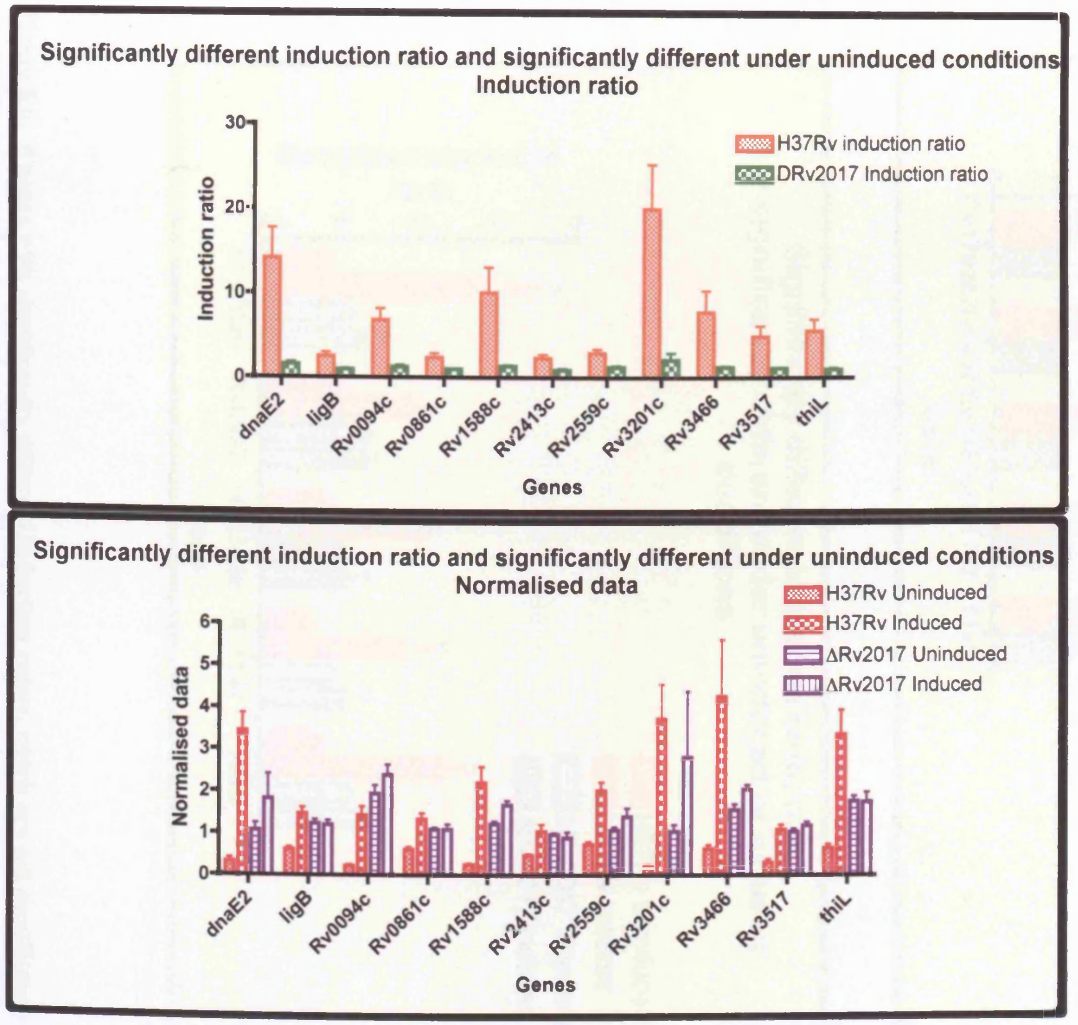

Figure 8.5: 11 genes with significantly different induction ratios, also significantly different under uninduced conditions. The data were obtained from DNA versus RNA microarrays with H37Rv and ΔRv2017 strain of *M. tuberculosis* under both uninduced and induced (0.02μg/ml mitomycin C) conditions. The induction ratios were calculated for both H37Rv and ΔRv2017, as induced/uninduced, a Student T-test was performed $p<0.01$, top graph. The uninduced values for each strain were also significantly different using Student T-test $p<0.01$, bottom graph.

Figure 8.6

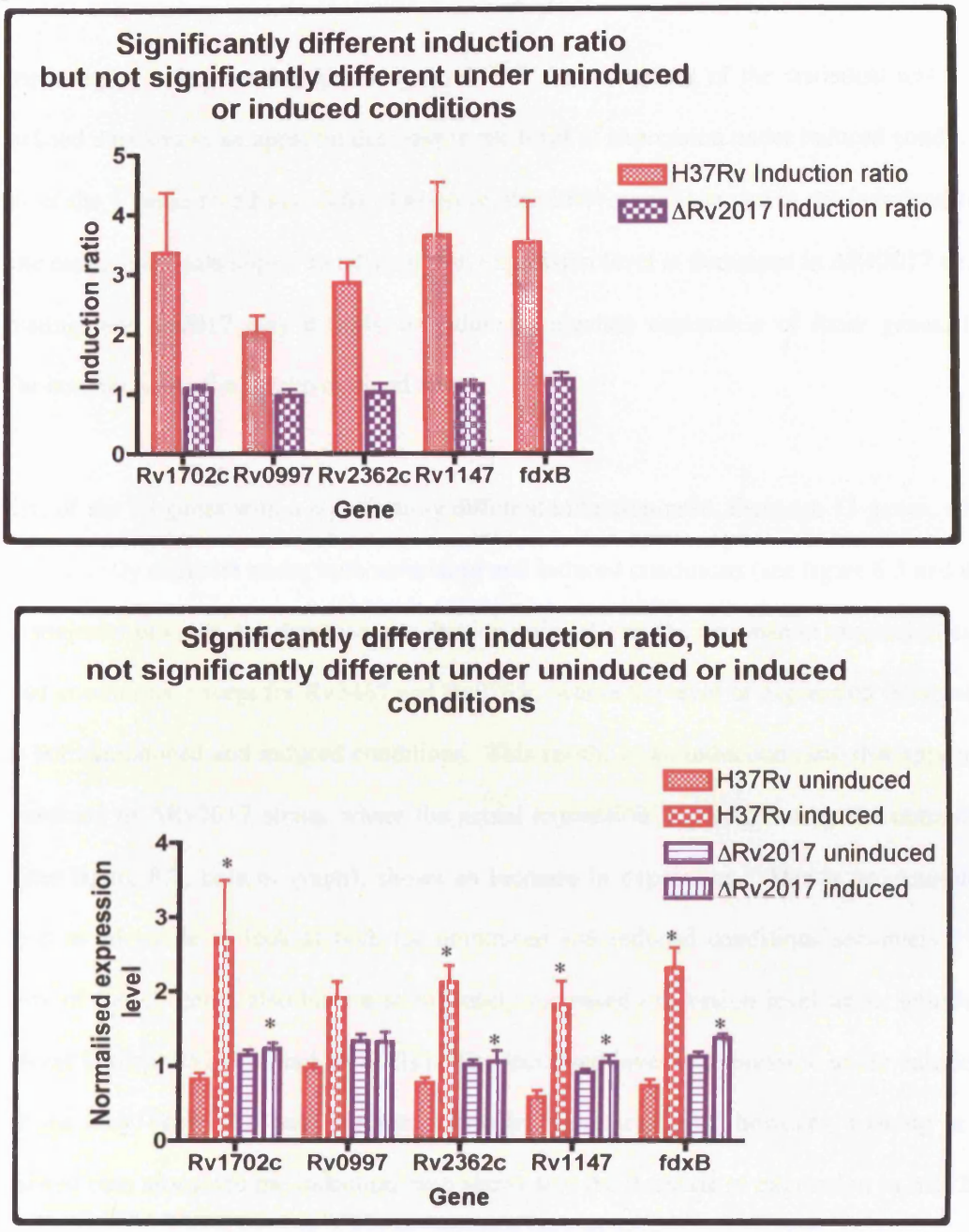

Figure 8.6: 5 genes with significantly different induction ratios, which are not significantly different under uninduced or induced conditions. The data were obtained from DNA versus RNA microarrays with H37Rv and ΔRv2017 strain of *M. tuberculosis* under both uninduced and induced (0.02μg/ml mitomycin C) conditions. The induction ratios were calculated for both H37Rv and ΔRv2017, as induced/uninduced, a Student T-test was performed $p<0.01$, top graph. The uninduced values for each strain were not significantly different using Student T-test $p<0.01$, bottom graph. Asterists mark the induced values that are significantly different in ΔRv2017 compared to H37Rv, with $p<0.05$. The uninduced values are all significantly different at $p<0.05$.

asterisks figure 8.6); therefore this may be due to the stringency of the statistical test. The normalised data shows an apparent decrease in the level of expression under induced conditions for all of the 5 genes (see figure 8.6). Therefore, the differences observed in the induction ratio and the normalised data appear to tally, in that, expression level is decreased in ΔRv2017 strain, suggesting that Rv2017 may directly or indirectly regulate expression of these genes, in a similar manner to the first group outlined above.

Finally, of the 59 genes with a significantly different induction ratio, there are 13 genes, which are significantly different under both uninduced and induced conditions (see figure 8.3 and 8.7). In the majority of cases, the decrease in induction ratio reflects the decrease in expression under induced conditions, except for Rv3467 and Rv0765c, where the level of expression is increased under both uninduced and induced conditions. This results in an induction ratio that appears to be decreased in ΔRv2017 strain, where the actual expression levels, given by the normalised data (see figure 8.7, bottom graph), shows an increase in expression. This is an example of where it is advisable to look at both the uninduced and induced conditions separately. The majority of the 13 genes also have a significantly increased expression level under uninduced conditions (except Rv2979c and Rv2791c). The increased level of expression under uninduced conditions may skew that data towards a smaller induction ratio; however, looking at the normalised data alongside the induction ratio shows that the decrease in expression in ΔRv2017 strain is consistent with the decreased induction ratio, in every case, except Rv3467 and Rv0765c.

Interestingly, there are a large proportion of genes that do not have a significantly different induction ratio, but are significantly different under induced and uninduced conditions (see figure 8.3). Of the 59 genes without a significantly different induction ratio, 26 are significantly

Figure 8.7

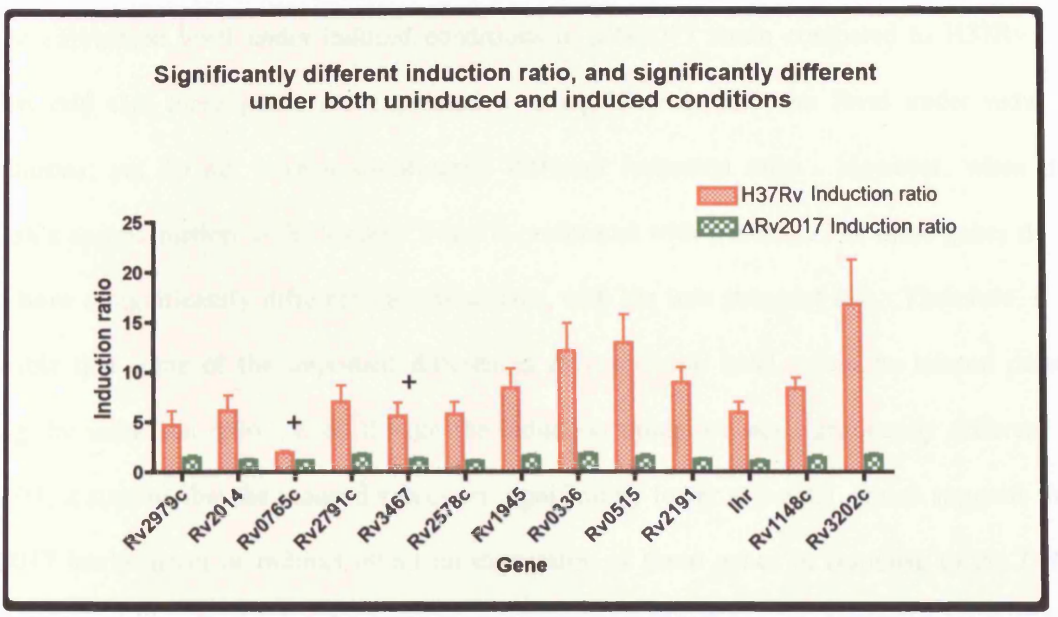

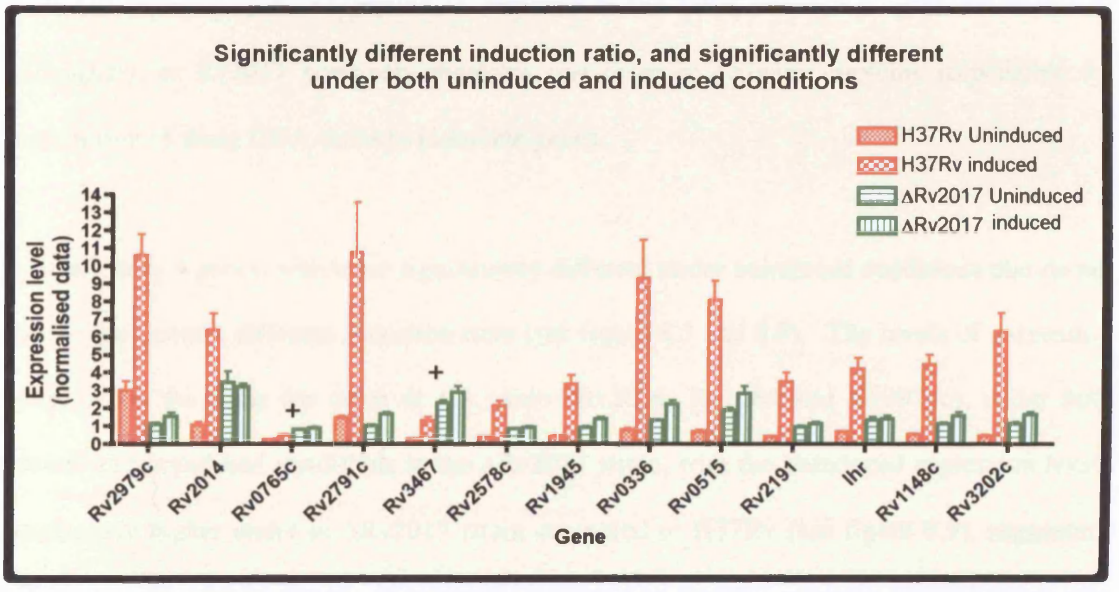

Figure 8.7: 13 genes with significantly different induction ratios, also significantly different under both induced and uninduced conditions. The data were obtained from DNA versus RNA microarrays with H37Rv and ΔRv2017 strain of *M. tuberculosis* under both uninduced and induced (0.02μg/ml mitomycin C) conditions. The induction ratios were calculated for both H37Rv and ΔRv2017, as induced/uninduced, a Student T-test was performed $p<0.01$, top graph. The induced and uninduced values for each strain were also significantly different using Student T-test $p<0.01$, bottom graph. The + symbol indicates genes expressed to a higher level in the ΔRv2017 strain.

different under induced conditions (see figure 8.8). All of these genes have a significantly lower expression level under induced conditions in ΔRv2017 strain compared to H37Rv. It seems odd that these genes are expressed to a significantly different level under induced conditions; yet do not have a significantly different induction ratio. However, when the Welsh's approximation to the Student T-test is performed with $p<0.05$, 11 of these genes do in fact have a significantly different induction ratio, with the less stringent test. Therefore, it is possible that some of the important differences in expression level would be missed purely using the induction ratio. Even though the induction ratios are not significantly different at $p<0.01$, it appears that the induced values are significantly lower at $p<0.01$, which suggests that Rv2017 has a direct or indirect effect on expression of these genes in response to the DNA damaging agent mitomycin C (0.02μg/ml). Either Rv2017 is an activator protein, that positively regulates gene expression in response to the DNA damaging agent mitomycin C (0.02μg/ml), or Rv2017 positively regulates one or more activator proteins responsible for transcription of these DNA-damage inducible genes.

There are only 4 genes, which are significantly different under uninduced conditions that do not have a significantly different induction ratio (see figure 8.3 and 8.9). The levels of expression appear to be the same for three of the genes (Rv3836, Rv1084 and Rv2974c), under both induced and uninduced conditions in the ΔRv2017 strain, with the uninduced expression levels significantly higher under in ΔRv2017 strain compared to H37Rv (see figure 8.9), suggesting that these genes may be directly or indirectly regulated by Rv2017, whereby Rv2017 either acts as a repressor protein, to suppress transcription, or activates one or more repressor proteins, to suppress transcription under uninduced conditions.

Figure 8.8

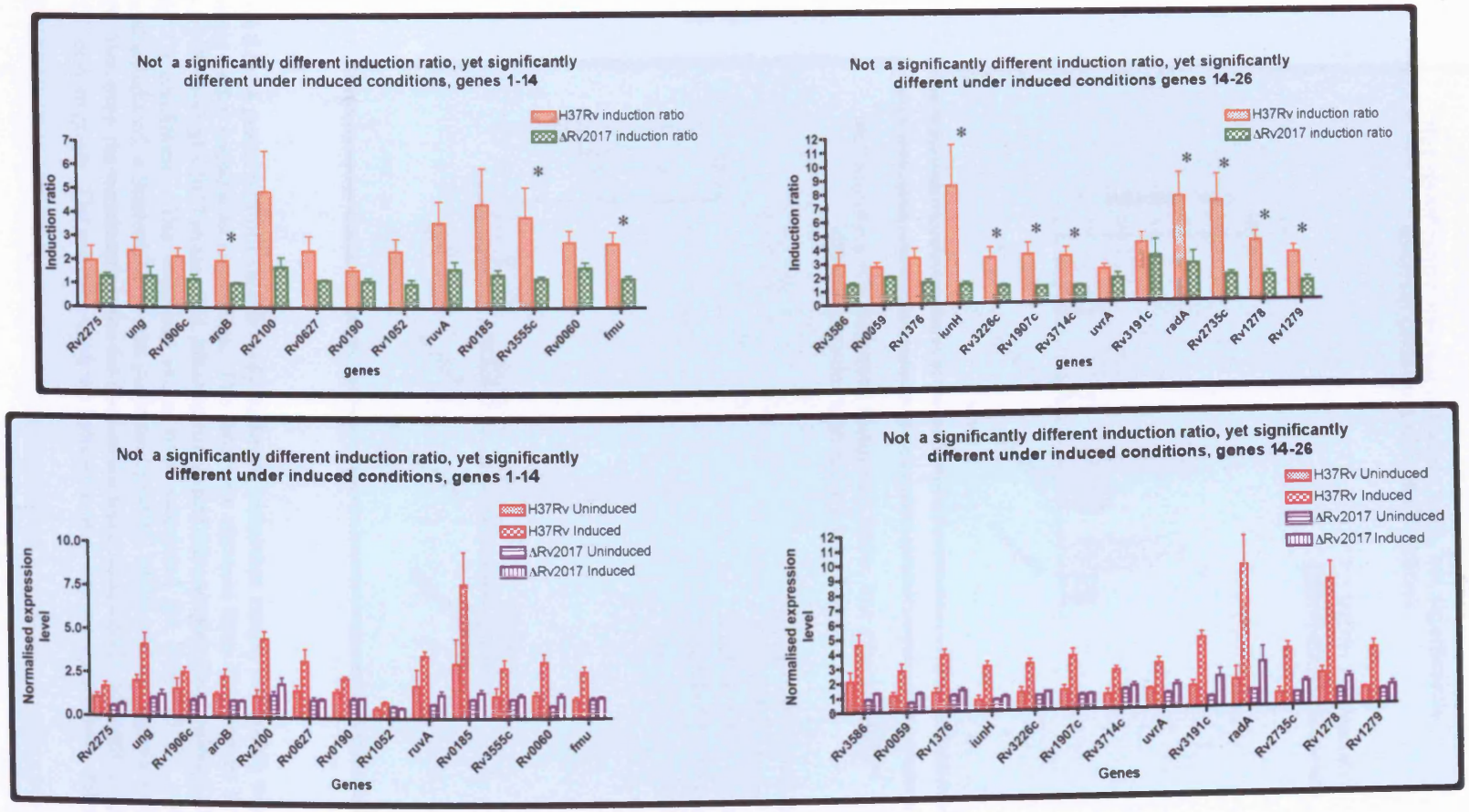

Figure 8.8: 26 genes without significantly different induction ratios, but which were significantly different under induced conditions. The data were obtained from DNA versus RNA microarrays with H37Rv and ΔRv2017 strain of *M. tuberculosis* under both uninduced and induced (0.02mg/ml mitomycin C) conditions. The induction ratios were calculated for both H37Rv and ΔRv2017, as induced/uninduced, a Student T-test was performed $p<0.01$ and none were significantly different, top graph. However the induced values for each strain were significantly different using Student T-test $p<0.01$, bottom graph. Asterisks mark the induction ratios that are significantly different at $p<0.05$.

Figure 8.9

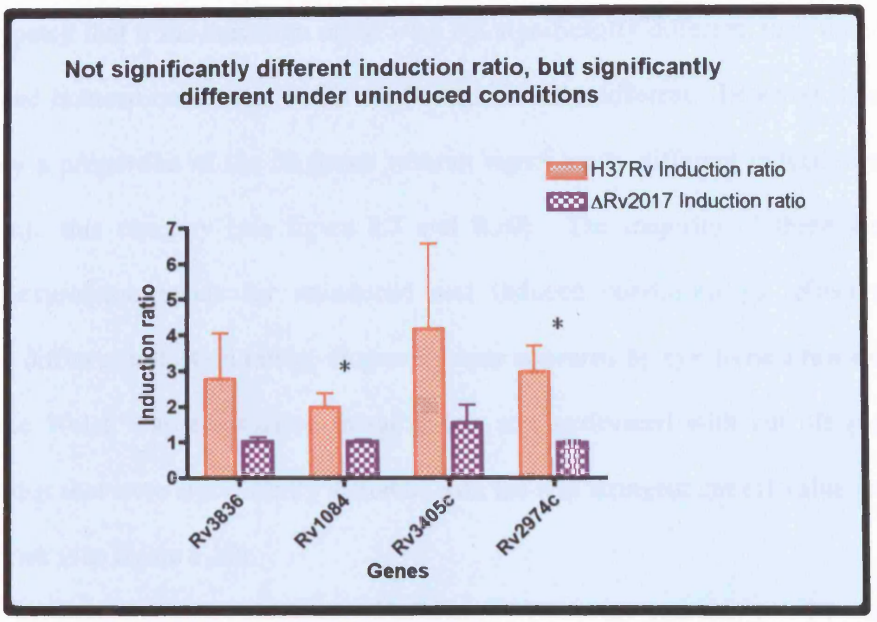

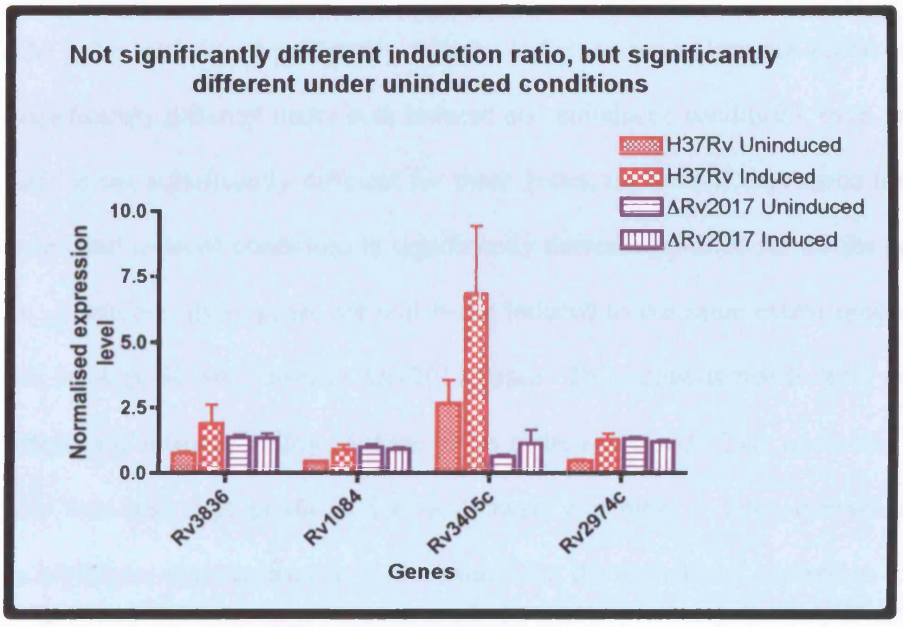

Figure 8.9: 4 genes without significantly different induction ratios, but which were significantly different under uninduced conditions. The data were obtained from DNA versus RNA microarrays with H37Rv and ΔRv2017 strain of *M. tuberculosis* under both uninduced and induced (0.02μg/ml mitomycin C) conditions. The induction ratios were calculated for both H37Rv and ΔRv2017, as induced/uninduced, a Student T-test was performed $p<0.01$, which was not significantly different, top graph. However, the uninduced values for each strain were significantly different using Student T-test $p<0.01$, bottom graph. The asterisks mark the induction ratios that are significantly different at $p<0.05$.

It was anticipated that if the induction ratios were not significantly different, then the individual uninduced and induced conditions would not be significantly different. However, this was the case for only a proportion of the 59 genes without significantly different induction ratios: 20 genes fell into this category (see figure 8.3 and 8.10). The majority of these genes have normalised expression levels for uninduced and induced conditions to reflect the non-significantly different induction ratios. However, there appeared by eye, to be a few exceptions; therefore, the Welsh's approximation to the T-test was performed with cut off $p<0.05$, the induction ratios that were significantly different with the less stringent cut off value are marked with an asterisk (see figure 8.10).

Finally for the genes without a significantly different induction ratio, there are a total of 9 genes which are significantly different under both induced and uninduced conditions, even though the induction ratio is not significantly different for these genes, the overall expression level under both uninduced and induced conditions is significantly decreased $p<0.01$ for all the genes (see figure 8.11). Therefore, these genes are still being induced to the same extent proportionally, but the levels are significantly lower in ΔRv2017 strain. This suggests that Rv2017 directly or indirectly affects the intrinsic ability of these genes to be expressed. This means that there is proportionally less transcript produced for *recA*, *ruvC* and other 7 DNA-damage inducible genes. This highlights that importance of analysing both the normalised expression levels and the induction ratios simultaneously.

8.2.1.2 Analysis of the Rv2017 regulon

To determine whether Rv2017 directly or indirectly regulates expression of genes besides those in the DNA-damage regulon, statistical analysis in Genespring was used to generate genes lists

Figure 8.10

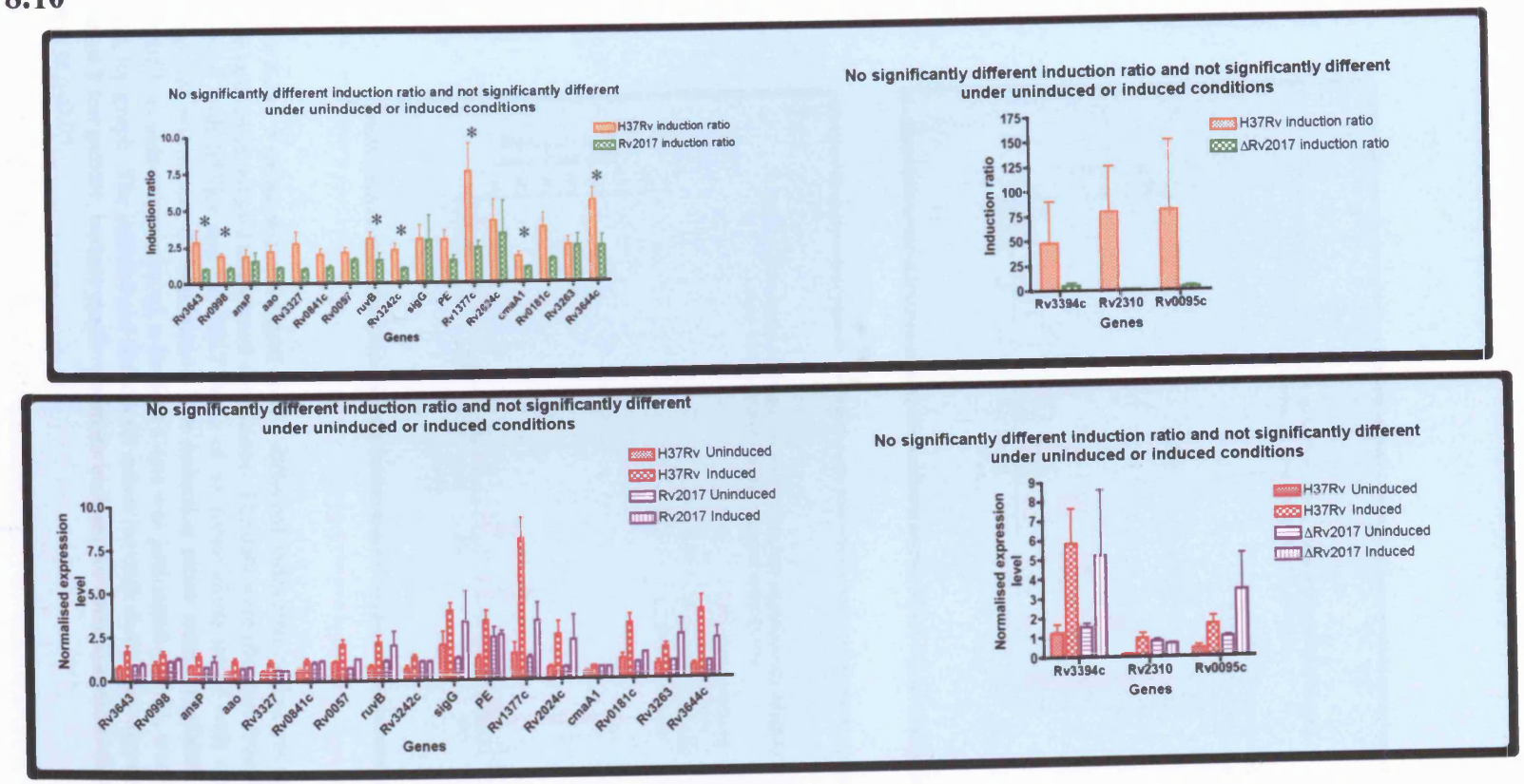

Figure 8.10: 20 genes without significantly different induction ratios, which are not significantly different under uninduced or induced conditions. The data were obtained from DNA versus RNA microarrays with H37Rv and ΔRv2017 strain of *M. tuberculosis* under both uninduced and induced (0.02μg/ml mitomycin C) conditions. In the top figure the large standard errors required a different scale. The induction ratios were calculated for both H37Rv and ΔRv2017, as induced/uninduced, a Student T-test was performed $p<0.01$, which was not significantly different, top graph. When a student T-test was performed for both the uninduced and induced conditions separately, there was no significant difference. Asterisks mark the induction ratios were the t-test was significant at $p<0.05$.

Figure 8.11

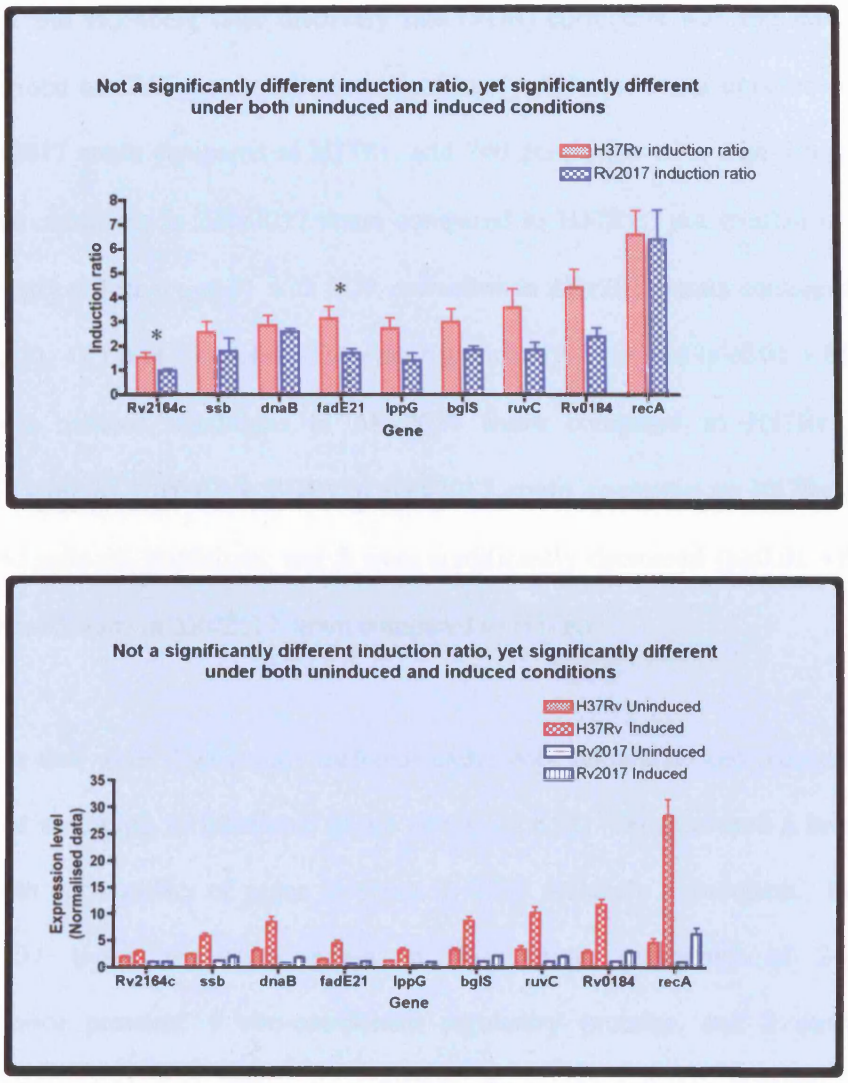

Figure 8.11: 9 genes without significantly different induction ratios, yet significantly different under both induced and uninduced conditions. The data were obtained from DNA versus RNA microarrays with H37Rv and ΔRv2017 strain of *M. tuberculosis* under both uninduced and induced (0.02μg/ml mitomycin C) conditions. The induction ratios were calculated for both H37Rv and ΔRv2017, as induced/uninduced, a Student T-test was performed $p<0.01$, were not significantly different, top graph. The induced and uninduced values for each strain were significantly different using Student T-test $p<0.01$, bottom graph. Asterisks indicate the induction ratios that are significantly different at $p<0.05$.

to determine whether there was any significant difference between the expression level of the genes in ΔRv2017 strain compared to H37Rv under uninduced conditions and induced conditions separately. The Welsh's approximation to a T-test was performed using $p<0.01$, and the Benjamini and Hochberg false discovery rate (FDR) correction was applied to the data. There were a total of 1347 genes that were significantly different under uninduced conditions between ΔRv2017 strain compared to H37Rv, and 740 genes that were significantly different under induced conditions in ΔRv2017 strain compared to H37Rv. An overlap of 595 genes were significantly different $p<0.01$ with FDR correction in ΔRv2017 strain compared to H37Rv (see figure 8.12). Of these 595 genes, 224 were significantly decreased ($p<0.01$ + FDR) in both uninduced and induced conditions in ΔRv2017 strain compared to H37Rv, 366 were significantly increased ($p<0.01$ + FDR) in ΔRv2017 strain compared to H37Rv under both uninduced and induced conditions, and 5 were significantly decreased ($p<0.01$ +FDR) under only induced conditions in ΔRv2017 strain compared to H37Rv.

The 595 genes that were significantly different under both uninduced and induced conditions were classified according to functional group (see table 8.1). They covered a broad range of categories, with the majority of genes involved in small molecule metabolism. Interestingly, there were 31 broad regulatory genes in this group, comprised of 24 predicted activator/repressor proteins, 5 two-component regulatory proteins, and 2 serine-thrionine protein kinases (see table 8.1). These are potentially the most interesting, therefore, these were further grouped into those that were decreased in the ΔRv2017 strain compared to H37Rv (see figure 8.13a), and those that were increased in ΔRv2017 strain compared to H37Rv (see figure 8.13b). The level of expression of these regulatory genes appears to be the same in uninduced

Figure 8.12

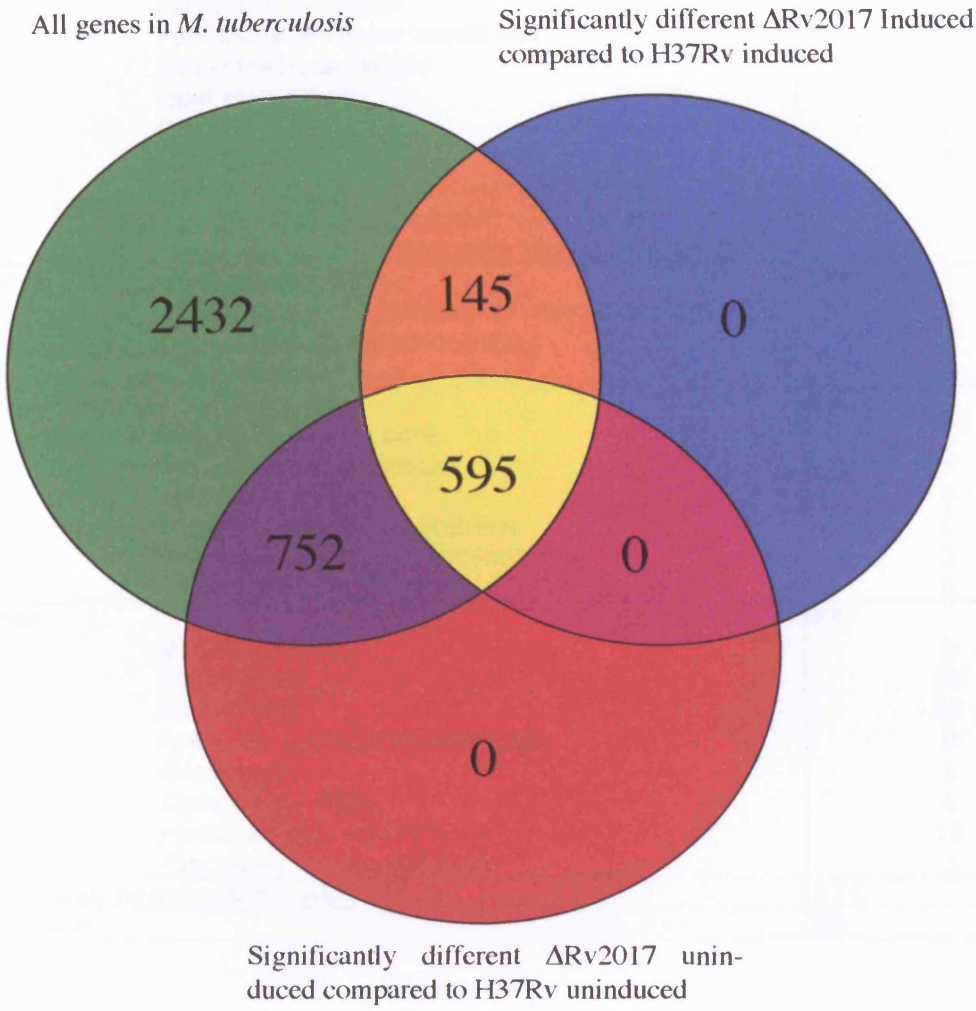

Figure 8.12: Venn diagram showing the genes significantly different in ΔRv2017 strain compared to H37Rv wild-type. The diagram was produced in Genespring using the microarray data for the DNA versus RNA arrays from ΔRv2017 and H37Rv strains of *M. tuberculosis*, under uninduced and induced (0.02μg/ml mitomycin C) conditions. Gene lists were produced to identify genes that were significantly different in ΔRv2017 compared to H37Rv under uninduced conditons, then separately under induced conditions. The significant differences were determied using a Student's T-test, performed with cut off $p<0.01$, with the Bengamini and Hochberg false discovery rate correction.

Table 8.1

Category	Number of genes
Small molecule metabolism	**197**
Degradation	27
Energy metabolism	75
Central intermediary metabolism	8
Amino acid biosynthesis	16
Polyamine synthesis	0
Purines/pyrimidines/nucleotides	9
Biosynthetic co-factors	14
Lipid biosynthesis	9
Polyketide	8
Broad regulatory function	31
Activator/repressors (24)	
Two component systems (5)	
Serine-threonine protein kinases (2)	
Macromolecular metabolism	**119**
Synthesis and modification of macromolecules	51
Degredation of macromolecules	9
Cell envelope	59
Cell processes	**44**
Transport/binding sites	27
Chaperones/heat shock	4
Cell division	4
Protein and peptide synthesis	1
Adaptation and atypical conditions	2
Detoxification	6
Other	**71**
Virulence	9
IS elements	22
PE and PPE	12
Antibiotic production/resistance	0
Bacteriocin	1
Cytochrome P450	6
Miscellaneous transferases	12
Miscellaneous phosphatases	3
Conserved hypothetical proteins	**114**
Unknown	**50**

Table 8.1: Functional classification of 595 genes significantly different under uninduced and induced conditions in ΔRv2017 compared to H37Rv. The gene list of those genes significantly different under both uninduced and induced (0.02μg/ml mitomycin C) conditions from the Rv2017 strain compared to H37Rv wild-type , were classified using the classification genes lists in Genespring, obtained from the annotated genome sequence of *M. tuberculosis*, Cole *et al.*, 1998.

Figure 8.13

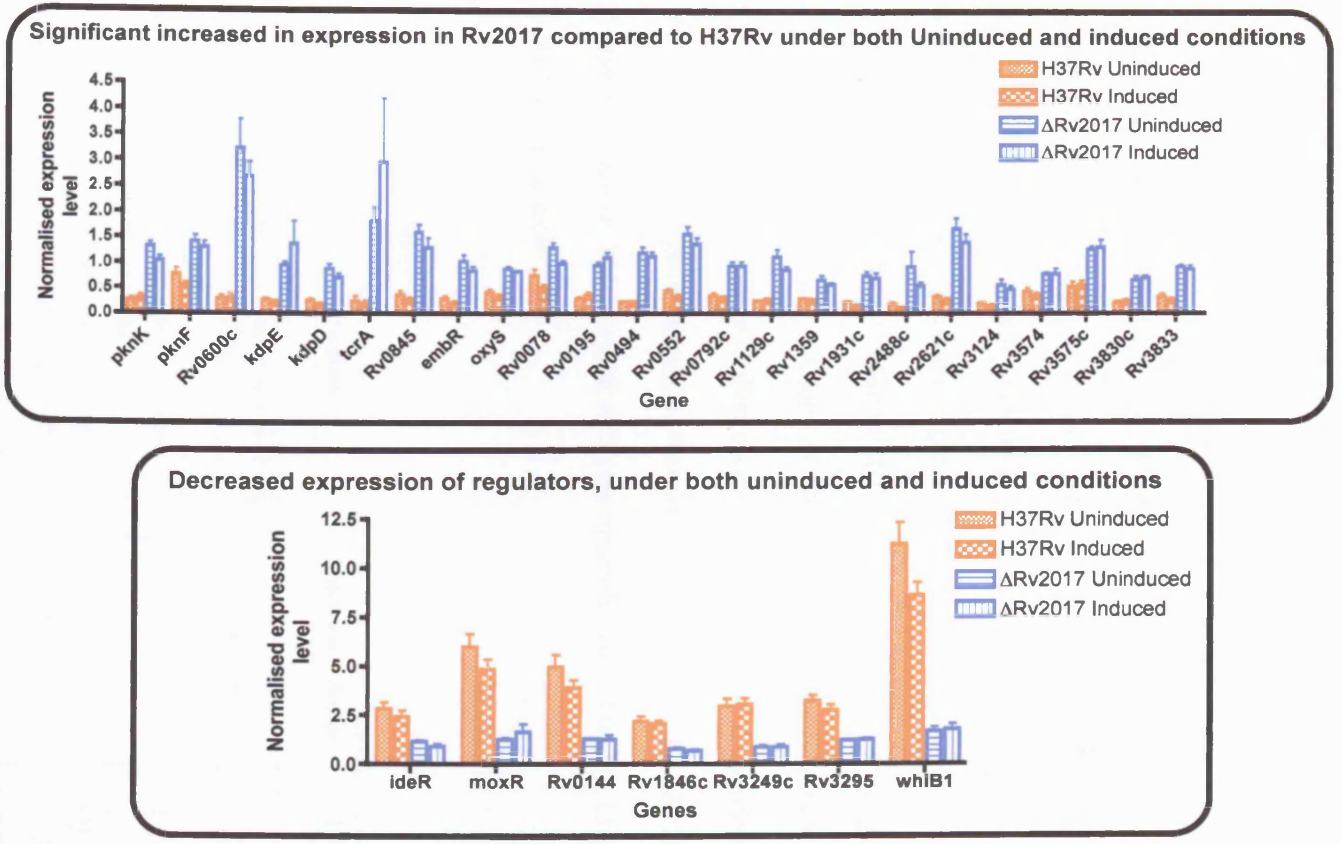

Figure 8.13: Transcriptional regulators with altered expression in ΔRv2017 compared to H37Rv under both uninduced and induced conditions. The data was obtained from the gene list of 595 genes significantly different under both induced and uninduced conditions in ΔRv2017 strain compared to H37Rv, at $p<0.01$ with False discovary rate correction (Benjamini and Hochberg). The top graph indictates genes with increased expression in ΔRv2017 strain and the bottom graph indictaes genes with decreased expression in ΔRv2017 strain compared to H37Rv.

and induced conditions, suggesting they are not induced in response to mitomycin C stress in either H37Rv or ΔRv2017 strain.

In order to determine which genes were the most severely affected in the ΔRv2017 strain, all 1347 genes that were significantly different in ΔRv2017 strain compared to H37Rv under uninduced conditions $p<0.01$ + FDR correction were imported into Excel, and the fold change was calculated with Rv2017 expression level as a proportion of H37Rv. A list was derived whereby genes with differential expression of greater than or equal to 5 fold were collated (cut-off 0.2 for genes expressed to a lesser extent in ΔRv2017 strain and 5 for those genes expressed to a greater extent in ΔRv2017 strain). A total of 100 genes were identified with cut-off of less than or equal to 0.2, the reciprocal was then taken, and displayed as a negative number (see appendix III). There were 90 genes identified that were upregulated in the ΔRv2017 strain, i.e. their fold change was greater than or equal to 5 (see appendix III). The top 15 genes with the greatest fold are listed (see table 8.2).

Table 8.2: (continued over-page)

Gene name	Function	Mean Fold change	SEM	Gene ID
Virulence				
groEL2	Prevents mis-folding/aids refolding of proteins	-13.3119	1.14E-02	Rv0440
Lipid metabolism				
kasA	Fatty acid biosynthesis	-9.9907	5.43E-03	Rv2245
Cell wall and cell processes				
Rv1892	Probable membrane protein	-9.3952	2.95E-02	Rv1892
Rv0584	Conserved export protein	8.7677	1.72E+00	Rv0584
IS and phage				
Rv3827c	Possible transposase for IS1537	-10.4465	1.99E-02	Rv3827c
Rv2648	Probable transposase IS6110	9.9949	3.21E+00	Rv2648
PE/PPE				
PE	PE	-15.7004	1.25E-02	Rv3477
Intermediary metabolism and respiration				

ctaB	Cytochrome oxidase	-15.0068	6.24E-03	Rv1451
Rv1516c	Sugar transferase	-13.0203	2.73E-02	Rv1516c
Rv1245c	Dehydrogenase	-9.3264	3.84E-02	Rv0287
Rv0648	Alpha-mannosidase	15.0447	5.86E+00	Rv0648
adhE	Zinc type alcohol dehydrogenase	9.0267	5.02E+00	Rv0162c
Regulatory proteins				
Rv3583c	Possible transcription factor	-10.3212	2.55E-02	Rv3583c
Rv0600c	Two component sensor kinase	12.0134	1.71E+00	Rv0600c
tcrA	Two component DNA -binding transcriptional regulator	11.4503	3.00E+00	Rv0602c
Conserved hypothetical proteins				
Rv3489	Conserved hypothetical protein	-16.3821	1.84E-02	Rv3489
Rv0893c	Conserved hypothetical protein	-12.1760	2.64E-02	Rv0893c
Rv0289	Conserved hypothetical protein	-11.6996	1.14E-02	Rv0289
Rv3384c	Conserved hypothetical protein	-11.5391	2.10E-02	Rv3384c
Rv3745c	Conserved hypothetical protein	-10.4280	3.12E-02	Rv3745c
Rv1519	Conserved hypothetical protein	-9.3690	4.70E-02	Rv1519
Rv2624c	Conserved hypothetical protein	10.5286	2.13E+00	Rv2624c
Rv2407	Conserved hypothetical protein	10.4178	4.68E+00	Rv2407
Rv2897c	Conserved hypothetical protein	10.3820	3.48E+00	Rv2897c
Rv3467	Conserved hypothetical protein	9.2535	1.45E+00	Rv3467
Rv2205c	Conserved hypothetical protein	9.1427	2.86E+00	Rv2205c
Rv2415c	Conserved hypothetical protein	9.0786	2.65E+00	Rv2415c
Rv1259	Conserved hypothetical protein	8.8608	1.72E+00	Rv1259
Rv0094c	Conserved hypothetical protein	8.6473	7.49E-01	Rv0094c
Rv2624c	Conserved hypothetical protein	10.5286	2.13E+00	Rv2624c

Table 8.2: Genes with the highest fold change in ΔRv2017 strain compared to H37Rv

The top 15 genes with the highest and lowest fold changes were classified according to function. The fold changes indicated were calculated using ΔRv2017/H37Rv, the reciprocal was taken and expressed as a -, indicating the gene expression was less in the ΔRv2017 strain. The standard error (SEM) for the fold change is indicated along with the gene identification.

GroEL2 is involved in the general stress response, and is upregulated in response to heat shock, however these uninduced conditions were standard growth conditions at 37°C, without the addition of chemical or physiological stresses to either the ΔRv2017 strain or the H37Rv wild-type, which suggests the deletion of Rv2017 may affect the general stress level of the bacterium. Interestingly a two component sensor kinase (Rv0600c) and a two-component transcriptional regulator (Rv0602c) were both upregulated by 12 and 11 fold respectively, and

are located in close proximity, separated by Rv0601c, the first part of a probable two component sensor kinase. Rv0600c and Rv0602c are significantly different under both uninduced and induced conditions in ΔRv2017 strain compared to H37Rv. Surprisingly, Rv0601c is not significantly different in ΔRv2017 strain compared to H37Rv under either uninduced or induced conditions at $P<0.01$, but this may be due to the stringency of the statistical test.

There appear to be a large number of genes, which are present in operons where the expression levels are altered in the ΔRv2017 strain compared to H37Rv. An example is *gyrB* (Rv0005) and *gyrA* (Rv0006), DNA gyrase subunits, which form an operon; their fold changes are -4.3 and -3.8 respectively (down regulated in ΔRv2017 strain). There are a lot of ribosomal proteins which appear to have significantly decreased expression in ΔRv2017 strain compared to H37Rv, including those located in close proximity: *rpsF* (Rv0053) a conserved 30S ribosomal protein, *ssb* (Rv0054) – a single stranded binding protein, *rpsRI* (Rv0055) – a probable 30S ribosomal protein and *rplL* (Rv0056) – a probable 50S ribosomal protein as well as Rv0700 through to Rv0709, which are also ribosomal proteins. There are also genes involved in heat shock that are down-regulated in ΔRv2017 strain compared to H37Rv, which appear to form an operon; *dnaK* (Rv0350) a chaperone, *grpE* (Rv0351) which stimulates *dnaK* with DnaJ, *dnaJ* (Rv0352) a co-chaperone and *hspR* (Rv0353) a heat shock transcriptional repressor which negatively regulates *dnaJ*.

8.3 Discussion

The analysis of the genes involved in DNA-damage repair revealed many of the same genes that were identified as up-regulated in response to DNA-damage in Rand *et al* (2003) were also

identified in the ΔRv2017 and H37Rv comparison, even though there were differences in the experimental design. Rand *et al* (2003) used a 3-fold induction ratio cut off for the DNA-damage regulon genes, following induction with the mitomycin C at a higher concentration (0.2 μg/ml) and also used RNA versus RNA arrays. The difference in experimental design explains the subtle differences observed in the gene lists of the DNA-damage repair regulon. However, the majority of genes identified in this study correspond with the published DNA-damage regulon (Rand *et al.*, 2003).

Analysis of genes involved in DNA-damage repair revealed that 59 genes were significantly decreased ($p<0.01$) in their induction ratio, in ΔRv2017 strain compared to H37Rv. However, analysis of the individual values for the induced and uninduced conditions revealed that additional genes that were significantly different under one or both conditions, that were not detected by the induction ratio analysis, suggesting that this data need to be used in conjunction with the induction ratio to determine whether genes are being missed or overlooked that were actually significantly different.

A significantly decreased induction ratio was observed for just over half of the genes that were significantly different under induced conditions (figures 8.4 and 8.8) in ΔRv2017 strain compared to H37Rv. This draws our attention to 26 genes that were significantly decreased ($p<0.01$) under induced conditions in ΔRv2017 strain compared to H37Rv, yet the induction ratios were not significantly different (figure 8.8). Repeating the statistical test with a less stringent p value ($p<0.05$) still does not account for all the genes that appear to be induced to a lesser extent in ΔRv2017 strain, but do not have a significantly different induction ratio. Consequently, it is important to look at both the induction ratio, and the separate conditions, otherwise genes would be over looked that are not induced to the same level in the ΔRv2017

strain compared to H37Rv. In some cases the standard errors may account for the lack of significant difference in induction ratio, when the genes are significantly different under induced conditions. In calculating the induction ratio, one has to compound standard errors for both the uninduced and induced values, making this data less reliable overall.

Examining that data for the uninduced and induced conditions separately can also give clues as to whether genes are being regulated by a repressor or an activator, which the induction ratio alone does not reveal. For example, if the level of expression in the uninduced condition is similar to that under induced conditions, i.e. the uninduced value is significantly greater in one of the strains, the induction ratio will appear very small. Where this is the case, it suggests that Rv2017 directly or indirectly regulates a repressor protein, which under uninduced conditions suppresses transcription. When the repressor is no longer present, the level of transcription is the same under both uninduced and induced conditions.

One would expect that when the individual components, i.e. the uninduced and induced conditions are not significantly different, the induction ratio would also not be significantly different. This was observed in the majority of cases with a few exceptions, that were in fact significantly different under induced conditions, when a less stringent p value was used ($p<0.05$).

Perhaps some of the most interesting observations were seen with genes that were significantly different under both uninduced and induced condition. The initial hypothesis was that these genes would all have had a significantly different induction ratio; however, this was not the case, just under half of the genes did not have a significantly different induction ratio. Of particular interest was *recA*, which fell into this category. The induction ratio appears to be

equal in ΔRv2017 strain compared to H37Rv; however it was clearly apparent from the uninduced and induced values that these were significantly lower in ΔRv2017 strain, by approximately 5-fold. This 5-fold decrease was consistent throughout the uninduced and induced values, thus resulting in an identical induction ratio. There are 9 genes (figure 8.11) that have similar induction ratios in ΔRv2017 strain compared to H37Rv, but show a significant decrease in expression under both uninduced and induced conditions. One possible explanation is that these genes are regulated by the same sigma factor, which recognises and controls transcription from their promoters. They are still induced, as the mechanism of induction has not been interrupted, yet the overall level of transcription is much less; this could be explained if the expression or activity of the responsible sigma factor is reduced or if another sigma factor were compensating for the reduction in the normal sigma factor. Interestingly, the expression of two sigma factors is significantly decreased under both uninduced and induced conditions in ΔRv2017 compared to H37Rv: *sigB* and *sigE* (see table 8.3). The decrease in expression of these sigma factors may have a role in the differential expression observed in others of the 118 genes involved in DNA-damage repair.

	H37Rv Uninduced		H37Rv Induced		ΔRv2017 Uninduced		ΔRv2017 Induced	
	Mean	S error	Mean	S error	Mean	S error	Mean	S error
sigB	4.670	0.482	4.865	0.604	0.843	0.073	1.259	0.138
sigE	2.723	0.438	3.138	0.412	1.082	0.075	1.086	0.131

Table 8.3: Expression level of two sigma factors with decreased expression in ΔRv2017 strain compared to H37Rv

The genes were identified in the 595 genes that were significantly different under both uninduced and induced conditions in the ΔRv2017 strain compared to H37Rv, using a Welsh's approximation to a T-test $p<0.01$ with the Benjamini and Hochberg FDR correction.

The other important question to address is: how does this data relate to the data obtained from the Δ*recA* strain of *M. tuberculosis*. Does Rv2017 regulate expression of genes in the DNA-damage regulon that are not regulated by the classical RecA/LexA system? In order to determine whether this is the case, the 59 genes with significantly different induction ratios were compared to data from the Δ*recA* strain (Rand *et al.*, 2003), classified in accordance with the expression patterns seen in the Δ*recA* strain (see table 8.4): group 1 genes were not expressed in Δ*recA* strain (21 genes, most with an SOS box) and therefore thought to be solely regulated by the RecA/LexA system; group 2 genes were partially expressed in Δ*recA* strain (28 genes, including *recA*), suggesting these gene were subject to dual regulation; group 3 genes were expressed to the same extent in the Δ*recA* strain (50 genes), suggesting they were not regulated by the classical RecA/LexA system and group 4 genes were expressed to a greater extent in Δ*recA* strain (13 genes), suggesting their expression may be negatively regulated indirectly by RecA/LexA. In this analysis, an additional group was identified; group 5 containing genes that were not identified as upregulated in Rand *et al.*, (2003) in response to DNA-damage, however, the conditions differed between this study and this Rand *et al.*, (2003).

Perhaps surprisingly, a large proportion of the genes (approximately 22%) fall into group 1, which are genes predicted to be regulated solely by the RecA/LexA system, interestingly 13 out of the 21 genes in this group showed reduced induction in the ΔRv2017 strain. This might be accounted for by the decreased overall expression of *recA*. Even though the induction ratio is the same in the ΔRv2017 strain compared to H37Rv, the actual expression level under both induced and uninduced conditions is approximately 5-fold lower in Rv2017 compared to H37Rv. This decrease in the level of expression of *recA*, may have a direct effect on the amount of RecA produced, which in turn would results in less RecA filament present in the cell,

Table 8.4

			H37Rv induction ratio		Rv2017 induction ratio		
	Systematic	Common	Mean	S error	Mean	S error	T-test
Group 1	Rv0336	Rv0336	12.07	2.81	1.73	0.18	5E-05
	Rv0515	Rv0515	12.89	2.83	1.52	0.23	4E-05
	Rv0516c	Rv0516c	4.76	0.76	1.62	0.10	0.0012
	Rv1000	Rv1000	6.95	1.11	1.32	0.14	0.0003
	Rv1378c	Rv1378c	12.47	4.30	2.28	0.39	0.0088
	Rv1702c	Rv1702c	3.37	1.01	1.09	0.06	0.0061
	Rv2578c	Rv2578c	5.80	1.18	1.10	0.08	0.0002
	linB	Rv2579	4.17	0.51	1.35	0.20	0.0003
	lexA	Rv2720	6.48	0.61	2.07	0.13	6E-06
	Rv3074	Rv3074	15.63	2.88	2.87	0.58	0.0038
	dnaE2	Rv3370c	14.16	3.55	1.59	0.25	0.0003
	Rv3395c	Rv3395c	12.80	4.42	1.10	0.05	0.006
	Rv3777	Rv3777	5.35	0.57	1.86	0.35	0.01
Group 2	Rv0094c	Rv0094c	6.80	1.38	1.29	0.17	0.0005
	Rv1148c	Rv1148c	8.39	1.07	1.45	0.22	1E-05
	Rv1588c	Rv1588c	10.06	2.99	1.38	0.10	0.0006
	Rv1945	Rv1945	8.34	2.03	1.56	0.17	0.0004
	Rv2717c	Rv2717c	3.98	0.65	1.48	0.19	0.0043
	Rv2718c	Rv2718c	6.16	0.76	1.68	0.37	0.0017
	Rv2719c	Rv2719c	6.66	0.70	1.45	0.25	0.0003
	Rv2979c	Rv2979c	4.75	1.31	1.46	0.17	0.0099
	Rv3466	Rv3466	7.85	2.55	1.27	0.07	0.0036
	Rv3467	Rv3467	5.56	1.40	1.28	0.18	0.0026
	Rv3828c	Rv3828c	5.07	1.16	1.69	0.18	0.0059
Group 3	Rv0922	Rv0922	4.18	0.89	1.33	0.17	0.0028
	Rv1277	Rv1277	5.48	0.82	1.42	0.21	0.0001
	fmt	Rv1406	3.93	0.48	1.01	0.08	3E-05
	uvrB	Rv1633	3.20	0.52	1.20	0.12	0.003
	Rv1765c	Rv1765c	6.47	0.48	2.01	0.23	2E-05
	Rv1833c	Rv1833c	4.56	1.17	1.36	0.17	0.0096
	Rv2014	Rv2014	6.18	1.41	1.18	0.14	0.0011
	Rv2015c	Rv2015c	9.39	1.74	2.04	0.28	7E-05
	Rv2191	Rv2191	8.90	1.56	1.25	0.11	5E-06
	Rv2791c	Rv2791c	7.01	1.68	1.70	0.13	0.0008
	Rv2792c	Rv2792c	6.13	1.83	1.29	0.15	0.0042
	Rv2884	Rv2884	3.10	0.53	1.46	0.16	0.0064
	Rv2885c	Rv2885c	8.16	1.47	1.52	0.13	0.0001
	thiL	Rv2977c	5.64	1.34	1.02	0.14	0.0002
	Rv2978c	Rv2978c	8.48	1.30	1.59	0.13	0.0001
	Rv3201c	Rv3201c	20.05	5.26	2.13	0.74	0.0003
	Rv3202c	Rv3202c	16.74	4.43	1.69	0.20	0.0001
	lhr	Rv3296	5.98	0.91	1.10	0.19	6E-05
	nei	Rv3297	4.10	0.65	1.39	0.19	0.0021
	Rv3517	Rv3517	4.92	1.24	1.15	0.08	0.0062
	fdxB	Rv3554	3.52	0.71	1.24	0.11	0.0054
Group 4	Rv1956	Rv1956	3.09	0.37	1.58	0.21	0.0095
	Rv2119	Rv2119	3.19	0.38	1.39	0.14	0.0015
	Rv2734	Rv2734	5.18	1.16	1.59	0.17	0.0093
Group 5	Rv0765c	Rv0765c	1.93	0.23	1.10	0.09	0.0056
	Rv0861c	Rv0861c	2.37	0.48	1.00	0.09	0.0062
	Rv0997	Rv0997	2.02	0.30	0.97	0.11	0.0073
	Rv1147	Rv1147	3.64	0.90	1.15	0.09	0.0091
	Rv2362c	Rv2362c	2.85	0.35	1.03	0.15	0.0008
	Rv2413c	Rv2413c	2.31	0.40	0.92	0.13	0.0066
	Rv2559c	Rv2559c	2.92	0.43	1.30	0.15	0.0026
	recX	Rv2736c	9.12	1.82	2.78	0.22	0.001
	ligB	Rv3062	2.55	0.43	0.99	0.09	0.0019
	Rv3075c	Rv3075c	2.75	0.22	1.17	0.14	0.0003
	Rv3645	Rv3645	2.32	0.25	1.23	0.04	0.0022

Table 8.4: Classification of 59 genes with significantly different induction ratios according to expression patterns seen in the Δ*recA* strain. The genes were grouped into 5 categories; group 1 genes were not expressed in Δ*recA* strain, group 2 were partially expressed in Δ*recA* strain, group 3 were expressed to the same extent in Δ*recA* strain, group 4 were expressed to a greater extent in Δ*recA* strain, and group 5 were not listed in the comparison between the Δ*recA* strain and H37Rv wild-type in Rand *et al.*, 2003.

thus resulting in reduced autocatalytic cleavage of LexA. This may result in a decrease in the levels of de-repression of the RecA/LexA operon, reflected a decreased level of induction of genes regulated solely by the RecA/LexA system. This could therefore account for the decrease in induction ratio of this sub-set of DNA-damage repair genes. However, this phenomenon could cause problems when addressing the possibility of whether the dual regulated genes (i.e. those partially induced in Δ*recA* strain) are partially regulated by Rv2017. The decrease in induction ratio observed in ΔRv2017 strain for 11 of the 28 genes in group 2 may also be due to the decreased level of transcription of RecA, and therefore decreased de-repression via LexA. A large proportion of genes also fell into category 3, a total of 21 out of 50 genes showed a decreased induction ratio compared in the ΔRv2017 strain compared to H37Rv: these genes were classified as those expressed to the same extent in H37Rv wild-type and the Δ*recA* strain. These genes are therefore thought to be regulated independently of the RecA/LexA system, however, Rv2017 does not appear to directly or indirectly regulate expression of all the genes in this category, therefore, although it appears that Rv2017 plays a role in regulation of genes in the DNA-damage response, it does not solely regulate expression of genes in a RecA dependent or RecA independent manner, but appears to regulate a subset of both categories. The genes in group 4 were expressed to a greater extent in Δ*recA* strain, however, none of these were expressed to a higher level in ΔRv2017 strain than H37Rv, and in fact, the induction ratio of 3 genes were decreased in the ΔRv2017 strain. The group 5 genes were not present in the microarray data from (Rand *et al.*, 2003), this is most likely due to the different induction conditions (optical density of induction and concentration of mitomycin C).

A total of 595 genes appear to be regulated by Rv2017 directly or indirectly, as they are significantly different under both uninduced and induced conditions. Consequently, it appears that determination of the Rv2017 regulon is more complicated that initially predicted. To

complicate matters further, Rv2017 appears to positively or negatively regulate the expression of 31 genes involved in transcriptional regulation via direct or indirect means. Consequently, it is impossible to determine with the data collated, whether the effects on transcription are as a direct result of the Rv2017 deletion, or as an indirect result, due to the sheer number of transcriptional regulators that appear to have their expression levels modified in ΔRv2017 strain.

The analysis of fold change of the genes significantly different under uninduced conditions $p<0.01$ with the Benjamini and Hochberg false discovery rate correction, has revealed that 100 genes are downregulated 5-fold or more in ΔRv2017 strain compared to H37Rv, and 90 genes are upregulated 5-fold or more in ΔRv2017 strain compared to H37Rv. The list of genes upregulated 5-fold or more in ΔRv2017 strain includes transcriptional regulators, and two component systems, along with PE and PPE genes. Interestingly two genes involved in homologous recombination were also upregulated in the ΔRv2017 strain; *recC*, upregulated by 6.58±1.27 fold and *recD*, upregulated by 2.18±0.22 fold. These genes are co-transcribed and form a complex with *recB*, but on checking the arrays it was found that *recB* was a bad spot, consistently throughout all the samples, so its expression could not be determined.

Genes that were 5-fold or more down regulated in ΔRv2017 strain include genes involved in rRNA synthesis, which may indicate that Rv2017 is a master regulator, as the conditions of treatment were the same for the H37Rv wild-type and ΔRv2017 strain. The decrease in expression of these genes, including other house keeping genes could be a direct result of the decrease in expression of the sigma factor *sigB*. Due to the nature of the data, it is impossible to determine which genes are directly regulated by Rv2017, and which are indirectly regulated, potentially through a transcriptional regulatory protein whose expression is controlled by

Rv2017; for example, WhiB1 is a transcriptional regulatory protein down-regulated in ΔRv2017 strain, which is thought to bind with *M. tuberculosis* CRP (Roger Buxton - personal communication). The repression of such a protein would therefore potentially affect all the genes regulated by CRP, thus indicating the difficulty of dissecting the Rv2017 regulon, from the regulons of other transcriptional regulators whose expression is altered in the ΔRv2017 strain. Nevertheless, this does raise the possibility that Rv2017 may in fact be a master regulatory protein, which may function as both an activator or repressor protein to positively and negatively regulate transcription at different genes.

9 Discussion

M. tuberculosis is an intracellular pathogen, which resides and replicates within macrophages (Graham and Clark-Curtiss, 1999; Mariani *et al.*, 2000). After receptor-mediated phagocytosis, *M. tuberculosis* prevents phago-lysosome fusion. However, this arrest of maturation of the phagosome is not universal, and in some cases phagosome maturation is enhanced by activation with IFN-γ (Kaufmann, 2001). Activated macrophage produces an array of DNA damaging agents, in the form of reactive oxygen (ROI) and nitrogen intermediates (RNI), which are known to damage DNA (Kaufmann, 2001). Therefore the repair of DNA-damage is thought to be of utmost importance in survival of *M. tuberculosis.* In a number of bacteria the expression of genes in the DNA-damage regulon is controlled by RecA/LexA; termed the SOS response, this system has been extensively studied in both *E. coli* and *B. subtilis.* It was recently discovered that the majority of genes in the DNA-damage regulon of *M. tuberculosis* were in fact regulated in a RecA independent fashion (Rand *et al.*, 2003), which lead to the question of what mode of regulation governed these DNA-damage repair genes. This project was designed to probe the alternative mechanism that was responsible for regulation of genes in the DNA-damage regulon that were regulated independently of the RecA/LexA system. A number of different possibilities were addressed regarding the mode of regulation of this subset of DNA-damage repair genes, and two different avenues were pursued to unravel the mode of regulation.

It has been suggested that the majority of regulation in bacteria takes place at the transcriptional level (Raman *et al.*, 2001). There are many different types of transcriptional regulation, that are controlled both temporally and spatially and culminate in a multi-factorial process of regulation. The gene expression of the sub-set of DNA-damage repair genes, defined by Rand *et al.*, (2003) as RecA independent, may be regulated by a sigma factor, which, by its specificity regulates

transcription from a certain regulon; the other alternative considered was that a regulatory protein, analogous to LexA, was responsible for the activation or suppression of genes in the RecA independent DNA-damage regulon. However, the microarray data published by Rand *et al.*, (2003) indicated that the RecA dependent and the RecA independent DNA-damage regulons are not mutually exclusive. Certain key genes, including *recA* itself, were partially induced in response to DNA-damage in the Δ*recA* strain of *M. tuberculosis*, suggesting that LexA was only partially responsible for regulation of these genes. The possibilities that a sigma factor or a predicted regulatory protein were responsible for regulation of transcription of a subset of the genes in the DNA-damage regulon were assessed.

9.1 The role of SigG

SigG was the most highly upregulated sigma factor in response to DNA-damage (Rand *et al.*, 2003). SigG was also upregulated in the Δ*recA* strain of *M. tuberculosis* suggesting that the expression and regulation of SigG were RecA independent.

A gene inactivation knockout of *sigG* was constructed in a laboratory strain of *M. tuberculosis*, H37Rv, using a deletion and insertion method, in which, a functional SigG was no longer produced. Complementation constructs were also produced for the Δ*sigG* strain to ascertain whether the phenotype observed was a direct result of the gene inactivation, or due to the indirect effects of the deletion on the two downstream co-transcribed genes Rv0181c and Rv0180c, or due to a secondary mutation elsewhere in the genome.

No differences were observed in the *in-vitro* growth rate for the Δ*sigG* strain and the full operon complement, compared to H37Rv. The Δ*sigG* strain was significantly more susceptible to

mitomycin C stress than the wild-type at a range of 0.02 to 0.2μg/ml. The full operon complement did not restore the viability back to wild-type, but was significantly less susceptible to mitomycin C stress in 4 out of the 5 tested concentrations than the Δ*sigG* strain. Mitomycin C causes interstrand cross links in the DNA (Paz *et al.*, 2004), which are generally repaired by homologous recombination; therefore one would expect upregulation of the *recA* and other genes involved in homologous recombination, and genes in the RecA/LexA regulon. Interestingly, these genes do not appear to be differentially expressed in the Δ*sigG* strain, despite the increased susceptibility to mitomycin C of the Δ*sigG* strain. It is possible that the increased susceptibility of Δ*sigG* strain to mitomycin C could be as a result of the significantly decreased expression of some of the cell wall/cell process genes and lipid metabolism genes. These decreases in expression may result in problems with cell wall formation in Δ*sigG* strain, which in turn, could make the mutant more susceptible to mitomycin C, as a higher proportion may be entering the cell.

Interestingly, preliminary mouse *in-vivo* data revealed that the Δ*sigG* strain was attenuated in comparison to H37Rv, which suggests that SigG or the SigG regulon is involved in virulence of *M. tuberculosis* in the mouse model of infection. Other ECF family sigma factor mutants have only shown attenuation in the mouse model of infection when time to death studies were performed: SigF (Chen *at el.*, 2000), SigE (Ando *et al.*, 2003), SigC (Sun *et al.*, 2004), and SigH (Kaushal *et al.*, 2002). No differences were observed in the CFU counts for the lung and spleen over a 20 day period for SigE (Ando *et al.*, 2003), whereas a SigF mutant showed decreased CFU compared to wild-type (Geiman *et al.*, 2004). The role of other sigma factors in *M. tuberculosis* had been identified using gene inactivation mutants. Analysis of these mutants revealed that SigH was responsible for regulation of other sigma factors, regulating inducible

gene expression of *sigE*, along with basal and inducible gene expression of *sigB*, which is subject to dual regulation by SigH and SigE (Raman *et al.*, 2001).

Analysis of the SigG locus revealed that the two downstream genes, Rv0181c and Rv0180c, are co-transcribed with SigG and may possibly function in the role of regulation of the sigma factors activity, as the majority of sigma factors are co-transcribed with their cognate anti-sigma factors (Raivio and Silhavy, 2001; Yoshimura *et al.*, 2004). Analysis of genes downstream of sigma factors, revealed that they are usually comprised of a transmembrane protein (Hughes and Mathee, 1998), with an extracytoplasmic sensory domain and an intracellular cytoplasmic domain that binds to its cognate sigma factor to prevent transcription of the sigma factors regulon (Yoshimura *et al.*, 2004) and a periplasmic domain which may act to detect environmental signals (Helmann, 1999). There are a wide variety of regulatory mechanisms governing sigma factor activity: regulation can take place at transcriptional, translational and post-translational levels (Helmann, 1999). Anti-sigma factors also operate in various ways to inhibit sigma factor-RNAP binding, which can be broadly grouped into three categories: export from the cell, as seen with the flagella biosynthesis anti-sigma factor FlgM of *Salmonella typhimurium*, partner switching modules as outlined with SigF of *B. subtilis* (i.e. regulation by an anti-anti sigma factor) and interactions with small molecules or protein ligands (Helmann, 1999). Sigma factors can also be synthesised as inactive pro-proteins, which undergo cleavage to form an active sigma factor (Haldenwang, 1995). Homology searches revealed the *sigG* locus is also present in *M. bovis* and shares a high degree of homology. The domain predictions and homology searches suggest that Rv0181c is a cytoplasmic protein, whereas Rv0180c appears to be a transmembrane protein with multiple transmembrane domains. Based on homology and domain predictions along with evidence from the regulation of other sigma

factors, it is possible that Rv0181c is an anti-sigma factor, and Rv0180c is an anti-anti sigma factor, which detect and respond to environmental signals to regulate the function of SigG.

The microarray data from the Δ*sigG* strain showed that the two downstream genes appear to have slightly reduced transcriptional in the Δ*sigG* strain compared to H37Rv. However, the limited decrease, particularly in translation, potentially observed in the Western blot suggests that the polar effects of the Δ*sigG* strain are minimal, and indicates that the phenotype of the Δ*sigG* strain is most likely a direct result of the gene inactivation of SigG. Although the deletion and insertion were not in-frame, this inclusion of the 3′ region of *sigG* in the knockout construct resulted in the proper formation of the stop codon at the end of *sigG*, so as not to interfere with any post-translational modification/processing.

Microarray data and potential Western data, indicated that the vast majority of expression of the *sigG* operon was independent of SigG, suggesting that SigG does not autoregulate, as is the case for a proportion of sigma factors (Raman *et al.*, 2004). However, primer extension and RNase protection assays of *sigG* revealed three separate transcriptional start sites, two of which are DNA-damage inducible, while the third promoter (P3) is not upregulated in response to DNA-damage, but appears to be autoregulated. The P1 and P2 promoters are regulated independently of SigG. Analysis of the promoter –10 and –35 regions supports the hypothesis that the P3 promoter is regulated by SigG, as they bore no similarity to the promoter motifs described for the ECF sigma factors or the primary sigma factor. Further analysis of the upstream regions of 5 genes upregulated in the Δ*sigG* strain, revealed that a potential SigG consensus of CGACC(R)(t/c)C-$N_{13\text{-}22}$-TGTCCG (where R is a/g/t) was present within 100bp upstream and downstream of the predicted translational start sites. There appears to be a greater degree of homology at the –35 site than at the –10 site, which has been observed before with other ECF

family sigma factors (Raman *et al.*, 2004). Interestingly, *nuoB*, Rv0655 and Rv0312 show a high degree of homology at both the –10 and –35 sites. Confirmation of these observations by either RNase protection or primer extension would enable clarification and further refinement a consensus motif, which could then be used in conjunction with the microarray findings to search for other genes regulated by SigG.

9.1.1 Identification of the SigG regulon.

The preliminary microarray analysis of the Δ*sigG* strain revealed that *ruvC* was partially induced in the Δ*sigG* strain, suggesting that *ruvC* may be partially regulated by SigG. This possibility was further analysed using primer extension and RNase protection assays to determine the transcriptional start sites of *ruvC*. As previously mentioned, *ruvC*, like *recA* was partially upregulated in response to DNA-damage in the Δ*recA* strain, and it has been shown that *recA* processes two transcriptional start sites, both of which are DNA-damage inducible, but only one of which is regulated by the repressor LexA (Davis *et al.*, 2002b; Movahedzadeh *et al.*, 1997). RNase protection assay confirmed that the P2 promoter of *recA* (containing the SOS box) showed complete abolition of expression in the Δ*recA* strain, suggesting that expression from the P2 promoter was completely dependent on RecA for derepression. In accordance with the findings (Movahedzadeh *et al.*, 1997), the P1 promoter was DNA-damage inducible even in the Δ*recA* strain, thus suggesting that induction of expression from this promoter is independent of RecA. There appeared to be a decrease by approximately 2-fold, in the level of expression in the Δ*sigG* strain from both the P1 and P2 promoters of *recA*, however, theses findings were not validated with the microarray data, which revealed there was no significant difference in the expression level of *recA* in the Δ*sigG* strain compared to H37Rv at the 1% level. The drawback

to this method is that one is not able to distinguish between the expression levels from individual promoters.

The primer extension assays revealed that *ruvC* possesses two transcriptional start sites, only one of which appeared to be DNA-damage inducible (P1). The P1 promoter, possesses a LexA binding site, and was only partially decreased in the Δ*recA* strain, whereas the P2 promoter appeared to be transcribed to a lesser extent in the Δ*sigG* strain. The RNase protection confirmed the observation that the P2 promoter does not appear to be DNA-damage inducible, however, neither the P1 nor the P2 promoter show differential expression by RNase protection in the Δ*sigG* strain. The RNase protection clearly shows that expression from the P1 promoter is not completely abolished in the Δ*recA* strain, thus suggesting there is another mechanism present, which is partially able to overcome the derepression of the P1 promoter of *ruvC* by LexA. This is particularly interesting when one looks at the potential promoter motifs identified upstream of the transcriptional start sites of the P1 promoters of both *recA* and *ruvC*. These promoters are both DNA-damage inducible and appear to be regulated at least partially by an alternative mechanism to the RecA/LexA system. Gamulin *et al.*, (2004) revealed the presence of a potential promoter motif, which they defined as the RecA-NP for *recA* non-dependent promoter. Analysis of the transcriptional start sites for *ruvC* reveal this motif is actually positioned in close proximity to the P1 promoter, in the potential –10 location. The –35 region is located more proximally in *recA*, and there is an alternative –35 sites for the P1 promoter of *ruvC* other than the RecA-ND, defined by Gamulin *et al.*, (2004). Nevertheless, it suggests that the P1 promoters of both *recA* and *ruvC* may be recognised by the same sigma factor. Interestingly, the region 2 of SigG shows the greatest degree of homology to the σ^{70}, and the –10 sites of *ruvC* show homology to both the σ^{70} and σ^{38} of *E. coli.* However the regulation of which sigma factor transcribes from a dual regulated promoter is more complicated than pure

competition, as in the case with σ^S and σ^{70}, architectural proteins such as Lrp, CRP, IHF and Fis have been implicated in determining which sigma factor initiates transcription (Hengge-Aronis, 1999), and the choice of sigma factor can also be modified by the pleiotropic regulator ppGpp, which has been shown to favour interactions of RNAP with alternative sigma factors at the expense of σ^{70} (Gralla, 2005). This is of particular interest, as it has also been alluded to that genes under the negative regulation of the LexA repressor have been de-repressed by ppGpp in the absence of RecA (Kvint *et al.*, 2000).

The differences observed in repression of the P2 promoter of *recA* and the P1 promoter of *ruvC* by LexA could be explained by the relative location of the LexA binding site. The sequences of the binding sites are identical for both *recA* and *ruvC* and vary from the consensus by 1bp. They also have a different spacer region, between the palindromic sites. The LexA binding site for the P2 promoter of *recA* is located over the RNAP binding site, and therefore most likely prevents binding of the RNAp-σ complex by obscuring the –10 and the –35 sites. However, the location of the LexA binding site for the P1 promoter of *ruvC* is downstream of the –10 promoter site, overlapping the transcriptional start site. This is interesting as the TrpR operon has both strong and weak TrpR boxes, depending on the location of the promoter –10 and –35 sites relative to the position of the TrpR box (Pittard *et al.*, 2005). It is possible that the location of the LexA repressor binding site enables transcriptional read through. In *ruvC*, the position of the LexA binding site would allow binding of the RNAP-σ complex, but the LexA repressor may possibly act as a road-block, preventing transcriptional elongation, rather than transcriptional initiation as is potentially the case for *recA*. It has been demonstrated that oscillation of the RNAP-σ complex at the site of a road-block can lead to transcriptional read through. Analysis of the location of the operator of the *lac* operon revealed that the Lac repressor was able to bind to the operator and did not prevent binding of the RNAP to the

promoter, yet the repressor blocked the clearance of the RNAP-σ complex from the promoter, and hence prevented transcription (Gralla, 1996). This repression was overcome *in-vitro* through oscillation of the RNAP-σ complex. Therefore it is possible that the LexA repressor only partially inhibits transcription via the position of the binding site rather than the affinity of the repressor for the SOS box.

Microarray data indicated that SigG was not involved in the regulation of genes involved in DNA-damage repair, but does regulate expression of a number of genes. Transcriptional analysis in the Δ*sigG* strain of *recA* and *ruvC*, genes which are partially regulated in a RecA independent manner, revealed that although preliminary microarray data and primer extension assays eluded to the possibility that *ruvC* was regulated by SigG, RNase protection assays revealed that SigG was not involved in regulation of expression of *ruvC* from either of the two promoters. The RNase protection result was confirmed by subsequent microarray analysis, which showed that the overall expression levels of *ruvC* were unaffected by the absence of SigG. It is noteworthy, that the expression level of *ruvC* from the P2 promoter was increased in the Δ*sigG* strain, which may have resulted from increased availability of RNAP in the absence of SigG. Sigma factor competition for the RNAP in the absence of SigG may have resulted in an increase in basal level of transcription.

RNase protection assay for *recA*, also partially regulated by RecA, lead to the tantalising possibility that *recA* P1 and P2 promoters were regulated partially by SigG. Two predicted regulatory proteins, Rv0232 and Rv3050c of the TetR/AcrR and AsnR family of transcriptional regulators respectively were downregulated in the Δ*sigG* strain, suggesting this decrease in expression of *recA* could be attributed directly to SigG, or indirectly via one of the two predicted regulatory proteins. Alternatively, SigE was upregulated under uninduced conditions

in the Δ*sigG* strain, although the level of SigH remained constant; however, SigE is only regulated by SigH under induced conditions (Raman *et al.*, 2001). SigE may regulate transcription of a repressor protein, therefore if this were the case, then the repressor would be upregulated in the Δ*sigG* strain, and could therefore result in decreased transcription of *recA* from both promoters. A common motif was identified upstream of the translational start sites of both *sigG* and *recA*, although the importance of this motif is unclear, as it is present with 1bp mismatch in close proximity to the predicted translational start sites (-150bp to +100bp) in 24 other mycobacterial genes.

The promoter similarity suggests the possibility that a sigma factor is responsible for regulation of expression of the RecA independently regulated genes. Analysis of the published sigma factor consensus sequences revealed that these do not appear to have homology to the P1 promoters of *recA* and *ruvC*. It is possible that *ruvC* could be transcribed from the same promoter by different sigma factors, which are able to elicit transcription from the same promoter. This type of compensation has been observed with over-expression of SigA which resulted in a decrease in expression of genes regulated by alternative sigma factors (Nystrom, 2004a). It has been observed with *E. coli*, that there is an overlap between the recognition of some promoter elements, there are cases where a single promoter can be regulated by more than one sigma factor, which is the case with σ^S and σ^{70} in *E. coli* (Tanaka *et al.*, 1993). Dual regulated promoters have similar –10 regions, which form the specific interactions with region 2 of the sigma factor.

Interestingly some genes repressed by LexA in *M. tuberculosis* have multiple LexA binding sites, as is the case for Rv2719c, which is divergently transcribed with LexA. Rv2719c possesses three LexA binding sites, which overlap the promoter recognition –10 and –35 sites,

or overlap with the predicted transcriptional start site. These sites however contain mismatches to the LexA consensus, therefore it was suggested that multiple LexA binding sites were present when there were two or more mismatches in the SOS box, this may allow regulation in the overall level of transcription depending on the degree of DNA-damage (Dullaghan *et al.*, 2002).

Regulation of transcription can be controlled by a dual mechanism, as observed with the *uspA* gene in *E. coli*, whereby the gene is subject to both positive and negative regulation. The repression by the FadR repressor can be overcome by the activator alarmone guanosine 3', 5'-bisphosphate (ppGpp), for certain genes in the operon, whereas *fad* itself is regulated by two activator molecules, ppGpp and the cAMP-CAP protein complex (Kvint *et al.*, 2000).

9.2 The role of an activator or repressor in DNA-damage

The second possibility was addressed, that a regulatory protein was potentially responsible for regulation of transcription of those DNA-damage inducible genes regulated independently of RecA. *In-vitro* binding assays, in the form of bandshift assays were unable to detect binding of a specific protein to the P1 region of *recA*, although binding of the LexA repressor to the P2 promoter was readily detectable. These regulatory proteins chosen for the *in-vitro* transcription covered a wide range of the transcriptional regulatory families, however, Rv2017 proved potentially the most interesting, due to homology with IrrR of *D. radiodurans*, which positively regulates *recA*, despite the presence of the LexA repressor (Narumi *et al.*, 2001).

The bandshift may not have been able to detect binding of an activator, as this process can be complicated as transcriptional regulation can take place at either proximal or distal sites. Distal activation occurs at enhancer sites located upstream of transcriptional start sites. Sig54 (σ^{54}) in

E. coli is part of the distal regulation, whereby, unlike the proximal enhancers, which enhance binding of the RNAP to the promoter recognition site by specific interactions with the alpha subunit of RNAP, the distal enhancers require the presence of an activator, and σ^{54}, which enables the RNAP-σ^{54} complex to bind to the promoter and remain inactive until the enhancer, causes the assembly of a large complex with ATPase activity via a signal transduction cascade (Merrick, 1993). The enhancer bound ATPase then makes contact with the RNAP most likely with the sigma subunit, and loops out the DNA region (Gralla, 1996), enabling initiation of transcription.

Analysis of the ΔRv2017 strain produced by deletion and insertion proved more fruitful. *In-vitro* growth curves revealed there was no difference between the growth of the ΔRv2017 strain and H37Rv under the conditions utilised. Interestingly the ΔRv2017 strain was hyposensitive to mitomycin C stress compared to H37Rv, in concentrations of mitomycin C greater than 0.02μg/ml, and preliminary time points for a mouse model of infection suggested that the ΔRv2017 strain was hypervirulent in comparison to H37Rv.

Time constraints did not allow the construction of a complement of ΔRv2017 strain. However, the RT-PCR performed to determine whether Rv2017 was mono or polycistronic revealed that Rv2017 was the second gene in an operon with Rv2016 located 5′ of Rv2017. RT-PCR also suggested that Rv2018 was also co-transcribed with Rv2017; Rv2018 is annotated in TubercuList to overlap with Rv2019, suggesting they also form a polycistron. The microarray data produced for the ΔRv2017 strain compared to H37Rv contradicts the RT-PCR data, as the expression levels of Rv2018 and Rv2019 are not significantly different under either uninduced or induced (mitomycin C 0.02 μg/ml) conditions. The microarray data for Δ*sigG* strain revealed

a significant decrease in expression of the two downstream co-transcribed genes, which suggests a potential problem with the RT-PCR. One could speculate that the promoter for Rv2018 overlaps with the 3′ region of Rv2017, which would make it appear as though the genes were co-transcribed, where in actual fact this was probably not the case.

Microarray analysis of the ΔRv2017 strain in comparison to H37Rv suggested that Rv2017 was partially involved in regulation of the DNA-damage repair regulon. Problems were encountered as with the Δ*sigG* strain microarray, when attempting to compare the data to that of Δ*recA* strain, as there was a 10-fold difference in the concentration of mitomycin C used for induction, but more importantly, only the induction ratio was available for the previous microarray data for the Δ*recA* strain (Rand *et al.*, 2003), limiting the information that could be obtained as compared to the availability of individual uninduced and induced results in this study. It did appear however, that Rv2017 was directly or indirectly responsible for regulation approximately half of the genes in the DNA-damage regulon. These genes were not limited to those regulated partially by RecA and independently of RecA, overlapping with the genes whose expression was dependent on RecA for derepression. Interestingly, part of the explanation may lie in the expression level of *recA* itself. At first glance using the induction ratio data, it appears that the level of induction of *recA* in the ΔRv2017 strain is the same as in the wild-type; however when the uninduced and induced values are assessed individually, there is a significant decrease in the expression level of *recA* under uninduced (t-test $p<0.01$) and induced (t-test $p<0.01$ + FDR) conditions, which, equates to an approximate 3.5-fold decrease in the expression level under induced conditions of *recA* in the ΔRv2017 strain. This decreased level of *recA* expression could result in a decreased quantity of RecA, which in turn would affect those genes partially and completely dependent on RecA for derepression.

With regard to the role of Rv2017 in regulation of the DNA-damage regulon, Rv2017 does not regulate all of the genes identified by Gamulin et al., (2004) as possessing a RecA-ND promoter motif, nor is the role of Rv2017 limited to RecA independent gene expression. Out of the 21 genes classified as DNA repair genes possessing the RecA-ND promoter motif, only *recA*, *ruvC*, *lhr*, *ssb*, *dnaB* and Rv0184 were significantly decreased in the ΔRv2017 strain in comparison to H37Rv. This indicates that Rv2017 and its regulon alone, are not fully responsible for regulation of genes induced in a RecA independent fashion.

M. tuberculosis has 196 predicted broad spectrum regulatory proteins (Cole *et al.*, 1998), of which 152 are predicted activator/repressor proteins, 30 are 2 component regulators, and 14 are serine-threonine kinases. In the ΔRv2017 strain, 7 of these broad-spectrum regulatory proteins were expressed to a lesser degree in ΔRv2017 strain than H37Rv, while 24 were upregulated in the ΔRv2017 strain. A comparison between the uninduced and induced expression levels revealed that these transcriptional regulators do not appear to be induced in response to mitomycin C stress. This suggests that the Rv2017 deletion has resulted in the differential expression of all of the broad spectrum transcriptional regulators, which may help explain why the expression of a huge proportion of genes was altered in the ΔRv2017 strain compared to H37Rv. This suggests that Rv2017 may act as a master regulator, affecting expression of a large proportion of genes in a possible cascade.

If Rv2017 acts as an activator, then potentially the most interesting genes are those that are downregulated in ΔRv2107 strain, as these may be regulated directly by Rv2017. Rv3477 is one of the genes most highly downregulated in the ΔRv2017 strain, and encodes a PE protein. This is of particular interest as the PE/PPE family are extracellular surface proteins, which act as potential antigens for the host immune response (Plotkin *et al.*, 2004), and form about 10% of

the mycobacterial genome (Chaitra *et al.*, 2005). Other genes downregulated include *ctaB* a cytochrome oxidase and *groEL2*, which is involved in heat shock response. Interestingly, both SigF of *M. tuberculosis* and SigB of *Streptomyces coelicolor* appear to have large regulons, including other transcriptional regulators, suggesting that although their specific regulons are small, they regulate a large number of other genes indirectly (Geiman *et al.*, 2004; Lee *et al.*, 2005). Both *sigB* and *sigE* are significantly decreased in the ΔRv2017 strain, as are certain operons involved in homologous recombination; *recC*, *D* and *G*, with no data available for *recB*. The general stress response chaperones DnaJ and DnaK are also downregulated in the ΔRv2017 strain, which suggests Rv2017 may play a direct or indirect role in stress response. However, it is noteworthy that the genes up/down regulated in the ΔRv2017 strain, appear to cover a wide range of functional groups, which further suggests that Rv2017 may be a master regulator.

In conclusion, it appears that the control of DNA-damage repair is complex, particularly as control of transcription appears to be a multifactorial process, which differs depending on the regulon, and often requires a combination of complex transcriptional regulation. A prime example of the complexity of transcriptional regulation is observed in the heat shock response in *B. subtilis*, which is regulated by at least 4 different mechanisms controlling different genes in the heat shock response. Class I genes, such as those that encode the molecular chaperones *gorESL* and *dnaK*, are regulated by the HecA repressor, which binds to a palindromic site in the operator, termed the CIRCE site (controlling inverted repeat of chaperone expression). The class II heat shock genes are regulated by the alternative sigma factor SigB (Grandvalet *et al.*, 2005), which account for a small proportion of the 709 genes with 4-fold differential expression in the Δ*sigB* strain (Price *et al.*, 2001). The class III genes are regulated by the CtsR repressor, which recognises and binds as a dimer to a heptanucleotide tandem repeat in the operator (Derre

et al., 2000). The class IV heat shock genes are regulated by an unknown mechanism (Grandvalet *et al.*, 2005). This is particularly relevant, as the control of the transcriptional repressors differs. HrcA is synthesised as an inactive protein, which is activated upon binding to GroEL; the active HrcA is then able to repress transcription by binding to the palindromic site of the operator. The repression is transiently lost under heat shock, modulated by GroE. Regulation of the CtsR repressor is somewhat different and involves degradation via proteases (ClpX and ClpP), while, ClpC is thought to protect CtsR from degradation under normal conditions (Derre *et al.*, 2000).

Further research is therefore required to dissect the complex network of regulation of the DNA-damage regulon, of which, I suspect only the tip of the iceberg has been discovered.

9.3 Where to begin

The research thus far has identified a number of tantalising possibilities for the alternative mechanism of regulation of the DNA-damage regulon. In order to further elucidate the possible mode of regulation, there are a number of avenues that it would be beneficial to pursue:

To determine a consensus promoter recognition site for SigG, primer extension/RNase protection assays could be performed using the 5 genes potentially directly regulated by SigG, to detect their transcriptional start site(s). This data could then these be used to design site directed mutagenesis and reporter fusion assays to define the SigG recognition consensus. Taqman quantitative RT-PCR would be used to confirm this SigG dependent expression, by looking for decreased levels of expression in the Δ*sigG* strain. This could also be used to

determine whether *recA* is partially regulated by SigG, as suggested by the primer extension and RNase protection assays.

The role of SigG in infection could be assessed by repeating the mouse *in-vivo* infections; alongside *in-vitro* infections of steady state and IFN-γ activated bone marrow derived macrophages. However, prior to this, both the full and partial operon complement should be re-tested for *in-vitro* viability.

The role of the two downstream co-transcribed genes in the regulation of SigG could be further addressed by re-synthesis of the SigG antibody, with a view to using the SigG, Rv0181c and Rv0180c antibodies in co-immunoprecipitations to determine if the two downstream genes are involved in regulation of SigG. Alongside this approach yeast-2-hybrid assays could be used to detect any interactions between SigG, Rv0181c and Rv0180c.

Determination of the Rv2017 regulon could be addressed using primer extension/RNase protection assays of the genes most highly downregulated in the ΔRv2017 strain, to identify a potential Rv2017 binding site and expression/purification of Rv2017 using a pET expression system could be performed; with a view to using purified Rv2017 in bandshift experiments with the P1 promoters of both *recA* and *ruvC* to determine if the decrease in expression of these genes was directly dependent on Rv2017.

The potential hypervirulence of the ΔRv2017 strain during infection could be assessed by using established *in-vivo* and *in-vitro* models (as outlined for Δ*sigG* strain).

10 References

Agger, E.M., and Andersen, P. (2002) A novel TB vaccine; towards a strategy based on our understanding of BCG failure. *Vaccine* **21**: 7-14.

Ando, M., Yoshimatsu, T., Ko, C., Converse, P.J., and Bishai, W.R. (2003) Deletion of *Mycobacterium tuberculosis* Sigma Factor E Results in Delayed Time to Death with Bacterial Persistence in the Lungs of Aerosol-Infected Mice. *Infect. Immun.* **71**: 7170-7172.

Bae, J.-B., Park, J.-H., Hahn, M.-Y., Kim, M.-S., and Roe, J.-H. (2004) Redox-dependent Changes in RsrA, an Anti-sigma Factor in *Streptomyces coelicolor*: Zinc Release and Disulfide Bond Formation. *Journal of Molecular Biology* **335**: 425-435.

Bailey, T.L., and Gribskov, M. (1998) Combining evidence using p-values: application to sequence homology searches. *Bioinformatics* **14**: 48-54.

Baldwin, N.E., and Dombroski, A.J. (2001) Isolation and characterization of mutations in region 1.2 of *Escherichia coli* sigma70. *Molecular Microbiology* **42**: 427-437.

Barton, G.M., and Medzhitov, R. (2002) Control of adaptive immune responses by Toll-like receptors. *Curr Opin Immunol* **14**: 380-383.

Bashyam, M., Kaushal, D., Dasgupta, S., and Tyagi, A. (1996) A study of mycobacterial transcriptional apparatus: identification of novel features in promoter elements. *J. Bacteriol.* **178**: 4847-4853.

Beaucher, J., Rodrigue, S., Jacques, P.E., Smith, I., Brzezinski, R., and Gaudreau, L. (2002) Novel *Mycobacterium tuberculosis* anti-sigma factor antagonists control sigmaF activity by distinct mechanisms. *Mol Microbiol* **45**: 1527-1540.

Bertrand-Burggraf, E., Hurstel, S., Daune, M., and Schnarr, M. (1987) Promoter properties and negative regulation of the *uvrA* gene by the LexA repressor and its amino-terminal DNA binding domain. *J Mol Biol* **193**: 293-302.

Bibb, M.J., and Buttner, M.J. (2003) The *Streptomyces coelicolor* Developmental Transcription Factor {sigma}BldN Is Synthesized as a Proprotein. *J. Bacteriol.* **185**: 2338-2345.

Black, C.G., Fyfe, J.A.M., and Davies, J.K. (1998) Absence of an SOS-like system in *Neisseria gonorrhoeae*. *Gene* **208**: 61-66.

Bone, A., Aertle A, Grzemska M (2001) Tuberculosis control in prisons, A manual for programme managers. WHO.

Borukhov, S., and Severinov, K. (2002) Role of the RNA polymerase sigma subunit in transcription initiation. *Res Microbiol* **153**: 557-562.

Borukhov, S., and Nudler, E. (2003) RNA polymerase holoenzyme: structure, function and biological implications. *Current Opinion in Microbiology* **6**: 93-100.

Brooks, P.C., Movahedzadeh, F., and Davis, E.O. (2001) Identification of Some DNA Damage-Inducible Genes of *Mycobacterium tuberculosis*: Apparent Lack of Correlation with LexA Binding. *J. Bacteriol.* **183**: 4459-4467.

Bucca, G., Brassington, A.M.E., Hotchkiss, G., Mersinias, V., and Smith, C.P. (2003) Negative feedback regulation of *dnaK, clpB* and *lon* expression by the DnaK chaperone machine in *Streptomyces coelicolor*, identified by transcriptome and *in vivo* DnaK-depletion analysis. *Molecular Microbiology* **50**: 153-166.

Busby, S., and Ebright, R.H. (1994) Promoter structure, promoter recognition, and transcription activation in prokaryotes. *Cell* **79**: 743-746.

Cabiscol, E., Tamarit, J., and Ros, J. (2000) Oxidative stress in bacteria and protein damage by reactive oxygen species. *Int Microbiol* **3**: 3-8.

Calamita, H., Ko, C., Tyagi, S., Yoshimatsu, T., Morrison, N.E., and Bishai, W.R. (2005) The *Mycobacterium tuberculosis* SigD sigma factor controls the expression of ribosome-associated gene products in stationary phase and is required for full virulence. *Cellular Microbiology* **7**: 233-244.

Camacho, L.R., Constant, P., Raynaud, C., Laneelle, M.-A., Triccas, J.A., Gicquel, B., Daffe, M., and Guilhot, C. (2001) Analysis of the Phthiocerol Dimycocerosate Locus of *Mycobacterium tuberculosis*. Evidence that this lipid is involved in the cell wall permeability barrier. *J. Biol. Chem.* **276**: 19845-19854.

Chaitra, M.G., Hariharaputran, S., Chandra, N.R., Shaila, M.S., and Nayak, R. (2005) Defining putative T cell epitopes from PE and PPE families of proteins of *Mycobacterium tuberculosis* with vaccine potential. *Vaccine* **23**: 1265-1272.

Chatterjee, D., Hunter, S.W., McNeil, M., and Brennan, P.J. (1992) Lipoarabinomannan. Multiglycosylated form of the mycobacterial mannosylphosphatidylinositols. *J Biol Chem* **267**: 6228-6233.

Chatterjee, D. (1997) The mycobacterial cell wall: structure, biosynthesis and sites of drug action. *Current Opinion in Chemical Biology* **1**: 579-588.

Chattopadhyaya, R., and Pal, A. (2004) Improved Model of a LexA Repressor Dimer Bound to *recA* Operator. *Journal of Biomolecular Structure and Dynamics* **21**: 681-689.

Checroun, C., Bordes, P., Leroy, O., Kolb, A., and Gutierrez, C. (2004) Interactions between the 2.4 and 4.2 regions of {sigma}S, the stress-specific {sigma} factor of *Escherichia coli*, and the -10 and -35 promoter elements. *Nucl. Acids Res.* **32**: 45-53.

Chedin, F., and Kowalczykowski, S.C. (2002) A novel family of regulated helicases/nucleases from Gram-positive bacteria: insights into the initiation of DNA recombination. *Mol Microbiol* **43**: 823-834.

Cheo, D.L., Bayles, K.W., and Yasbin, R.E. (1993) Elucidation of regulatory elements that control damage induction and competence induction of the *Bacillus subtilis* SOS system. *Journal of Bacteriology* **175**: 5907-5915.

Cole, S.T., Brosch, R., Parkhill, J., Garnier, T., Churcher, C., Harris, D., Gordon, S.V., Eiglmeier, K., Gas, S., Barry, C.E., III, Tekaia, F., Badcock, K., Basham, D., Brown, D., Chillingworth, T., Connor, R., Davies, R., Devlin, K., Feltwell, T., Gentles, S., Hamlin, N., Holroyd, S., Hornsby, T., Jagels, K., Krogh, A., McLean, J., Moule, S., Murphy, L., Oliver, K., Osborne, J., Quail, M.A., Rajandream, M.-A., Rogers, J., Rutter, S., Seeger, K., Skelton, J., Squares, R., Squares, S., Sulston, J.E., Taylor, K., Whitehead, S., and Barrell, B.G. (1998) Deciphering the biology of *Mycobacterium tuberculosis* from the complete genome sequence. *Nature* **393**: 537-544.

Colston M. J., D.E.O., Papvinasasundaram K.G. (2000) General recombination. In *Molecular Genetics of Mycobacteria.* W.R.jr, H.G.F.a.J. (ed): ASM press, pp. 85-91.

Courcelle, J., Khodursky, A., Peter, B., Brown, P.O., and Hanawalt, P.C. (2001) Comparative gene expression profiles following UV exposure in wild-type and SOS-deficient *Escherichia coli*. *Genetics* **158**: 41-64.

Daniels, D., Zuber, P., and Losick, R. (1990) Two amino acids in an RNA polymerase sigma factor involved in the recognition of adjacent base pairs in the -10 region of a cognate promoter. *Proc Natl Acad Sci U S A* **87**: 8075-8079.

Darst, S.A. (2001) Bacterial RNA polymerase. *Current Opinion in Structural Biology* **11**: 155-162.

Davis, E.O., Sedgwick, S.G., and Colston, M.J. (1991) Novel structure of the *recA* locus of *Mycobacterium tuberculosis* implies processing of the gene product. *Journal of Bacteriology* **173**: 5653-5662.

Davis, E.O., Dullaghan, E.M., and Rand, L. (2002a) Definition of the Mycobacterial SOS Box and Use To Identify LexA-Regulated Genes in *Mycobacterium tuberculosis*. *J. Bacteriol.* **184**: 3287-3295.

Davis, E.O., Springer, B., Gopaul, K.K., Papavinasasundaram, K.G., Sander, P., and Bottger, E.C. (2002b) DNA damage induction of *recA* in *Mycobacterium tuberculosis* independently of RecA and LexA. *Mol Microbiol* **46**: 791-800.

Demple, B., and Harrison, L. (1994) Repair of Oxidative Damage to DNA: Enzymology and Biology. *Annual Review of Biochemistry* **63**: 915-948.

Deretic, V., Philipp, W., Dhandayuthapani, S., Mudd, M.H., Curcic, R., Garbe, T., Heym, B., Via, L.E., and Cole, S.T. (1995) *Mycobacterium tuberculosis* is a natural mutant with an inactivated oxidative-stress regulatory gene: implications for sensitivity to isoniazid. *Mol Microbiol* **17**: 889-900.

Deretic, V., Song, J., and Pagan-Ramos, E. (1997) Loss of *oxyR* in *Mycobacterium tuberculosis*. *Trends Microbiol* **5**: 367-372.

Derre, I., Rapoport, G., and Msadek, T. (2000) The CtsR regulator of stress response is active as a dimer and specifically degraded in vivo at 37 degrees centigrade. *Molecular Microbiology* **38**: 335-347.

Dole, S., Nagarajavel, V., and Schnetz, K. (2004) The histone-like nucleoid structuring protein H-NS represses the *Escherichia coli* bgl operon downstream of the promoter. *Mol Microbiol* **52**: 589-600.

Dullaghan, E.M., Brooks, P.C., and Davis, E.O. (2002) The role of multiple SOS boxes upstream of the *Mycobacterium tuberculosis lexA* gene--identification of a novel DNA-damage-inducible gene. *Microbiology* **148**: 3609-3615.

Duncan, L., and Losick, R. (1993) SpoIIAB is an Anti-{sigma} Factor that Binds to and Inhibits Transcription by Regulatory Protein {sigma}F from *Bacillus subtilis*. *PNAS* **90**: 2325-2329.

Dye, C., Espinal, M.A., Watt, C.J., Mbiaga, C., and Williams, B.G. (2002a) Worldwide incidence of multidrug-resistant tuberculosis. *J Infect Dis* **185**: 1197-1202.

Dye, C., Williams, B.G., Espinal, M.A., and Raviglione, M.C. (2002b) Erasing the world's slow stain: strategies to beat multidrug-resistant tuberculosis. *Science* **295**: 2042-2046.

Earl, A.M., Mohundro, M.M., Mian, I.S., and Battista, J.R. (2002) The IrrE protein of *Deinococcus radiodurans* R1 is a novel regulator of *recA* expression. *J Bacteriol* **184**: 6216-6224.

Eiglmeier, K., Fsihi, H., Heym, B., and Cole, S.T. (1997) On the catalase-peroxidase gene, *katG*, of *Mycobacterium leprae* and the implications for treatment of leprosy with isoniazid. *FEMS Microbiol Lett* **149**: 273-278.

Eisen, J.A., and Hanawalt, P.C. (1999) A phylogenomic study of DNA repair genes, proteins, and processes. *Mutation Research/DNA Repair* **435**: 171-213.

Farr, S.B., and Kogoma, T. (1991) Oxidative stress responses in *Escherichia coli* and *Salmonella typhimurium. Microbiol Rev* **55**: 561-585.

Fenton, M., and Vermeulen, M. (1996) Immunopathology of tuberculosis: roles of macrophages and monocytes. *Infect. Immun.* **64**: 683-690.

Fernandes, N.D., Wu, Q.-l., Kong, D., Puyang, X., Garg, S., and Husson, R.N. (1999) A Mycobacterial Extracytoplasmic Sigma Factor Involved in Survival following Heat Shock and Oxidative Stress. *J. Bacteriol.* **181**: 4266-4274.

Fernandez de Henestrosa, A.R., Cune, J., Erill, I., Magnuson, J.K., and Barbe, J. (2002) A Green Nonsulfur Bacterium, *Dehalococcoides ethenogenes*, with the LexA Binding Sequence Found in Gram-Positive Organisms. *J. Bacteriol.* **184**: 6073-6080.

Fernandez De Henestrosa, A.R., Woodgate, R., Ogi, T., Ohmori, H., Aoyagi, S., Chafin, D., and Hayes, J.J. (2000) Identification of additional genes belonging to the LexA regulon in *Escherichia coli. Molecular Microbiology* **35**: 1560-1572.

Festenstein, R., Tolaini, M., Corbella, P., Mamalaki, C., Parrington, J., Fox, M., Miliou, A., Jones, M., and Kioussis, D. (1996) Locus Control Region Function and Heterochromatin-Induced Position Effect Variegation. *Science* **271**: 1123-1125.

Finn, R.D., Orlova, E.V., Gowen, B., Buck, M., and van Heel, M. (2000) *Escherichia coli* RNA polymerase core and holoenzyme structures. *EMBO J.* **19**: 6833-6844.

Flynn, J.L., and Chan, J. (2001) Immunology of tuberculosis. *Annu Rev Immunol* **19**: 93-129.

Friedberg, E.C. (2003) DNA damage and repair. *Nature* **421**: 436-440.

Friedberg, G. (1995) *DNA Repair and Mutagenesis*: ASM press.

Frischkorn, K., Sander, P., Scholz, M., Teschner, K., Prammananan, T., and Bottger, E.C. (1998) Investigation of mycobacterial *recA* function: protein introns in the RecA of pathogenic mycobacteria do not affect competency for homologous recombination. *Mol Microbiol* **29**: 1203-1214.

Gamulin, V., Cetkovic, H., and Ahel, I. (2004) Identification of a promoter motif regulating the major DNA damage response mechanism of *Mycobacterium tuberculosis*. *FEMS Microbiology Letters* **238**: 57-63.

Geiman, D.E., Kaushal, D., Ko, C., Tyagi, S., Manabe, Y.C., Schroeder, B.G., Fleischmann, R.D., Morrison, N.E., Converse, P.J., Chen, P., and Bishai, W.R. (2004) Attenuation of Late-Stage Disease in Mice Infected by the *Mycobacterium tuberculosis* Mutant Lacking the SigF Alternate Sigma Factor and Identification of SigF-Dependent Genes by Microarray Analysis. *Infect. Immun.* **72**: 1733-1745.

Georgiou, G. (2002) How to flip the (redox) switch. *Cell* **111**: 607-610.

Gomez M, S.I. (2000) Determinants of Mycobacterial Gene Expression. In *Molecular Genetics of Mycobacteria*. GF, H. (ed): ASM press, pp. 111 - 127.

Goodfellows (1986) *Bergey's Manual of Systematic Bacteriology*: Springer, biomedical sciences.

Gopaul, K.K. (2002) Transcription of the *Mycobacterium tuberculosis recA* gene. University College London.

Gopaul, K.K. (2003): University College London.

Goren, M.B., Hart, P.D.A., Young, M.R., and Armstrong, J.A. (1976) Prevention of Phagosome-Lysosome Fusion in Cultured Macrophages by Sulfatides of *Mycobacterium tuberculosis*. *PNAS* **73**: 2510-2514.

Graham, J.E., and Clark-Curtiss, J.E. (1999) Identification of *Mycobacterium tuberculosis* RNAs synthesized in response to phagocytosis by human macrophages by selective capture of transcribed sequences (SCOTS). *PNAS* **96**: 11554-11559.

Gralla, J.D. (1996) Activation and repression of *E. coli* promoters. *Curr Opin Genet Dev* **6**: 526-530.

Gralla, J.D. (2005) *Escherichia coli* ribosomal RNA transcription: regulatory roles for ppGpp, NTPs, architectural proteins and a polymerase-binding protein. *Molecular Microbiology* **55**: 973-977.

Grandvalet, C., Coucheney, F., Beltramo, C., and Guzzo, J. (2005) CtsR Is the Master Regulator of Stress Response Gene Expression in *Oenococcus oeni*. *J. Bacteriol.* **187**: 5614-5623.

Haldenwang, W.G. (1995) The Sigma-Factors of *Bacillus-Subtilis*. *Microbiological Reviews* **59**: 1-30.

Hansen, A.-M., Qiu, Y., Yeh, N., Blattner, F.R., Durfee, T., and Jin, D.J. (2005) SspA is required for acid resistance in stationary phase by downregulation of H-NS in *Escherichia coli*. *Molecular Microbiology* **56**: 719-734.

Helmann, J.D. (1999) Anti-sigma factors. *Curr Opin Microbiol* **2**: 135-141.

Helmann, J.D. (2002) The extracytoplasmic function (ECF) sigma factors. *Adv Microb Physiol* **46**: 47-110.

Hendrixson, D.R., and DiRita, V.J. (2003) Transcription of 54-dependent but not 28-dependent flagellar genes in *Campylobacter jejuni* is associated with formation of the flagellar secretory apparatus. *Molecular Microbiology* **50**: 687-702.

Hengge-Aronis, R. (1999) Interplay of global regulators and cell physiology in the general stress response of *Escherichia coli*. *Current Opinion in Microbiology* **2**: 148-152.

Henkin, T.M. (1996) Control of transcriptional termination in prokaryotes. *Annual Review of Genetics* **30**: 35-57.

Hong, H.-J., Paget, M.S.B., and Buttner, M.J. (2002) A signal transduction system in Streptomyces coelicolor that activates the expression of a putative cell wall glycan operon in response to vancomycin and other cell wall-specific antibiotics. *Molecular Microbiology* **44**: 1199-1211.

Hu, Y., and Coates, A.R.M. (1999) Transcription of Two Sigma 70 Homologue Genes, sigA and sigB, in Stationary-Phase *Mycobacterium tuberculosis*. *J. Bacteriol.* **181**: 469-476.

Hughes, K.T., and Mathee, K. (1998) The anti-sigma factors. *Annu Rev Microbiol* **52**: 231-286.

Humphreys, S., Stevenson, A., Bacon, A., Weinhardt, A.B., and Roberts, M. (1999) The alternative sigma factor, sigmaE, is critically important for the virulence of *Salmonella typhimurium*. *Infect Immun* **67**: 1560-1568.

Hutchings, M.I., Hoskisson, P.A., Chandra, G., and Buttner, M.J. (2004) Sensing and responding to diverse extracellular signals? Analysis of the sensor kinases and response regulators of *Streptomyces coelicolor* A3(2). *Microbiology* **150**: 2795-2806.

Iyer, V.N., and Szybalski, W. (1964) Mitomycins and Porfiromycin: Chemical Mechanism of Activation and Cross-Linking of DNA. *Science* **145**: 55-58.

Jager, W., Schafer, A., Puhler, A., Labes, G., and Wohlleben, W. (1992) Expression of the *Bacillus subtilis sacB* gene leads to sucrose sensitivity in the gram-positive

bacterium Corynebacterium glutamicum but not in Streptomyces lividans. *J. Bacteriol.* **174**: 5462-5465.

Jarlier, V., and Nikaido, H. (1994) Mycobacterial cell wall: structure and role in natural resistance to antibiotics. *FEMS Microbiol Lett* **123**: 11-18.

Jishage, M., Kvint, K., Shingler, V., and Nystrom, T. (2002) Regulation of sigma factor competition by the alarmone ppGpp. *Genes Dev.* **16**: 1260-1270.

Ju, J., and Haldenwang, W.G. (2003) Tethering of the *Bacillus subtilis* {sigma}E Proprotein to the Cell Membrane Is Necessary for Its Processing but Insufficient for Its Stabilization. *J. Bacteriol.* **185**: 5897-5900.

Kang, B.K., and Schlesinger, L.S. (1998) Characterization of mannose receptor-dependent phagocytosis mediated by *Mycobacterium tuberculosis* lipoarabinomannan. *Infect Immun* **66**: 2769-2777.

Kang, J.G., Paget, M.S., Seok, Y.J., Hahn, M.Y., Bae, J.B., Hahn, J.S., Kleanthous, C., Buttner, M.J., and Roe, J.H. (1999) RsrA, an anti-sigma factor regulated by redox change. *Embo J* **18**: 4292-4298.

Karakousis, P.C., Bishai, W.R., and Dorman, S.E. (2004) *Mycobacterium tuberculosis* cell envelope lipids and the host immune response. *Cellular Microbiology* **6**: 105-116.

Kaufmann, S.H. (2001) How can immunology contribute to the control of tuberculosis? *Nature reviews. Immunology* **1**: 20-30.

Kawakami, K., Kinjo, Y., Uezu, K., Miyagi, K., Kinjo, T., Yara, S., Koguchi, Y., Miyazato, A., Shibuya, K., and Iwakura, Y. (2004) Interferon-[gamma] production and host protective response against *Mycobacterium tuberculosis* in mice lacking both IL-12p40 and IL-18. *Microbes and Infection* **6**: 339-349.

Kleinsteuber, S., and Quinones, A. (1995) Expression of the *dnaB* gene of *Escherichia coli* is inducible by replication-blocking DNA damage in a *recA*-independent manner. *Mol Gen Genet* **248**: 695-702.

Kline, K.A., Sechman, E.V., Skaar, E.P., and Seifert, H.S. (2003) Recombination, repair and replication in the pathogenic *Neisseriae*: the 3 R's of molecular genetics of two human-specific bacterial pathogens. *Molecular Microbiology* **50**: 3-13.

Koomey, J.M., and Falkow, S. (1987) Cloning of the recA gene of *Neisseria gonorrhoeae* and construction of gonococcal recA mutants. *J Bacteriol* **169**: 790-795.

Kvint, K., Hosbond, C., Farewell, A., Nybroe, O., and Nystrom, T. (2000) Emergency derepression: stringency allows RNA polymerase to override negative control by an active repressor. *Mol Microbiol* **35**: 435-443.

Lane, D., Prentki, P., and Chandler, M. (1992) Use of gel retardation to analyze protein-nucleic acid interactions. *Microbiol Rev* **56**: 509-528.

Lee, E.-J., Karoonuthaisiri, N., Kim, H.-S., Park, J.-H., Cha, C.-J., Kao, C.M., and Roe, J.-H. (2005) A master regulator B governs osmotic and oxidative response as well as differentiation via a network of sigma factors in *Streptomyces coelicolor*. *Molecular Microbiology* **57**: 1252-1264.

Lee, S.J., and Gralla, J.D. (2001) Sigma38 (rpoS) RNA Polymerase Promoter Engagement via -10 Region Nucleotides. *J. Biol. Chem.* **276**: 30064-30071.

Lew, C.M., and Gralla, J.D. (2004) Mechanism of Stimulation of Ribosomal Promoters by Binding of the +1 and +2 Nucleotides. *J. Biol. Chem.* **279**: 19481-19485.

Li, W., Stevenson, C.E.M., Burton, N., Jakimowicz, P., Paget, M.S.B., Buttner, M.J., Lawson, D.M., and Kleanthous, C. (2002) Identification and Structure of the Anti-sigma Factor-binding Domain of the Disulphide-stress Regulated Sigma Factor [sigma]R from *Streptomyces coelicolor*. *Journal of Molecular Biology* **323**: 225-236.

Li, W., Bottrill, A.R., Bibb, M.J., Buttner, M.J., Paget, M.S.B., and Kleanthous, C. (2003) The Role of Zinc in the Disulphide Stress-regulated Anti-sigma Factor RsrA from *Streptomyces coelicolor*. *Journal of Molecular Biology* **333**: 461-472.

Lindgren, H., Stenman, L., Tarnvik, A., and Sjostedt, A. (2005) The contribution of reactive nitrogen and oxygen species to the killing of *Francisella tularensis* LVS by murine macrophages. *Microbes and Infection* **7**: 467-475.

Lisser, S., and Margalit, H. (1993) Compilation of E. coli mRNA promoter sequences. *Nucl. Acids Res.* **21**: 1507-1516.

Little, J.W. (1982) Control of the SOS regulatory system by the level of RecA protease. *Biochimie* **64**: 585-589.

Lodish H, B.D., Berk A, Lawrence Zipursky S, Matsudaira P, Darnell J (1995) *Molecular Cell Biology*. New York: Scientific American books.

Lonetto, M., Brown, K., Rudd, K., and Buttner, M. (1994) Analysis of the Streptomyces coelicolor sigE Gene Reveals the Existence of a Subfamily of Eubacterial RNA Polymerase {sigma} Factors Involved in the Regulation of Extracytoplasmic Functions. *PNAS* **91**: 7573-7577.

Lordi, G.M. (2000) Tuberculosis. In *Best Practice of medicine*: Merck Medicus.

Lorenz, M.G., and Wackernagel, W. (1994) Bacterial gene transfer by natural genetic transformation in the environment. *Microbiological Reviews* **58**: 563-602.

Mahenthiralingam, E., Marklund, B.I., Brooks, L.A., Smith, D.A., Bancroft, G.J., and Stokes, R.W. (1998) Site-directed mutagenesis of the 19-kilodalton lipoprotein antigen reveals No essential role for the protein in the growth and virulence of *Mycobacterium intracellulare*. *Infect Immun* **66**: 3626-3634.

Manganelli, R., Voskuil, M.I., Schoolnik, G.K., and Smith, I. (2001) The *Mycobacterium tuberculosis* ECF sigma factor E: role in global gene expression and survival in macrophages. *Molecular Microbiology* **41**: 423-437.

Manganelli, R., Voskuil, M.I., Schoolnik, G.K., Dubnau, E., Gomez, M., and Smith, I. (2002) Role of the extracytoplasmic-function sigma factor sigma(H) in *Mycobacterium tuberculosis* global gene expression. *Mol Microbiol* **45**: 365-374.

Manganelli, R., Provvedi, R., Rodrigue, S., Beaucher, J., Gaudreau, L., and Smith, I. (2004) Sigma factors and global gene regulation in *Mycobacterium tuberculosis*. *J Bacteriol* **186**: 895-902.

Mariani, F., Cappelli, G., Riccardi, G., and Colizzi, V. (2000) *Mycobacterium tuberculosis* H37Rv comparative gene-expression analysis in synthetic medium and human macrophage. *Gene* **253**: 281-291.

McAdams, H.H., and Shapiro, L. (2003) A bacterial cell-cycle regulatory network operating in time and space. *Science* **301**: 1874-1877.

Means, T.K., Lien, E., Yoshimura, A., Wang, S., Golenbock, D.T., and Fenton, M.J. (1999) The CD14 Ligands Lipoarabinomannan and Lipopolysaccharide Differ in Their Requirement for Toll-Like Receptors. *J Immunol* **163**: 6748-6755.

Medzhitov, R. (2001) Toll-like receptors and innate immunity. *Nat Rev Immunol* **1**: 135-145.

Merrick, M.J. (1993) In a class of its own the RNA polymerase sigma factor sigma 54 (sigma N). *Mol Microbiol* **10**: 903-909.

Miller, R.A., and Britigan, B.E. (1997) Role of oxidants in microbial pathophysiology. *Clin Microbiol Rev* **10**: 1-18.

Missiakas, D., and Raina, S. (1998) The extracytoplasmic function sigma factors: role and regulation. *Mol Microbiol* **28**: 1059-1066.

Mizrahi, V., and Andersen, S.J. (1998) DNA repair in *Mycobacterium tuberculosis*. What have we learnt from the genome sequence? *Molecular Microbiology* **29**: 1331-1339.

Mosrin-Huaman, C., Turnbough, C.L., and Rahmouni, A.R. (2004) Translocation of *Escherichia coli* RNA polymerase against a protein roadblock in vivo highlights a passive sliding mechanism for transcript elongation. *Molecular Microbiology* **51**: 1471-1481.

Movahedzadeh, F., Colston, M.J., and Davis, E.O. (1997) Determination of DNA sequences required for regulated *Mycobacterium tuberculosis* RecA expression in response to DNA-damaging agents suggests that two modes of regulation exist. *J Bacteriol* **179**: 3509-3518.

Narberhaus, F., Giebeler, K., and Bahl, H. (1992) Molecular Characterization of the Dnak Gene Region of *Clostridium-Acetobutylicum,* Including *grpE, dnaJ*, and a New Heat-Shock Gene. *Journal of Bacteriology* **174**: 3290-3299.

Narumi, I., Satoh, K., Kikuchi, M., Funayama, T., Yanagisawa, T., Kobayashi, Y., Watanabe, H., and Yamamoto, K. (2001) The LexA Protein from *Deinococcus radiodurans* Is Not Involved in RecA Induction following gamma Irradiation. *J. Bacteriol.* **183**: 6951-6956.

Naryshkin, N., Revyakin, A., Kim, Y., Mekler, V., and Ebright, R.H. (2000) Structural organization of the RNA polymerase-promoter open complex. *Cell* **101**: 601-611.

Nathan, C., and Shiloh, M.U. (2000) Reactive oxygen and nitrogen intermediates in the relationship between mammalian hosts and microbial pathogens. *PNAS* **97**: 8841-8848.

Neidhardt, F. (1996) Escherishia coli and Salmonella. Cellular and molecular biology. Washington DC: ASM press.

Niederhoffer, E.C., Naranjo, C.M., Bradley, K.L., and Fee, J.A. (1990) Control of *Escherichia coli* superoxide dismutase (*sodA* and *sodB*) genes by the ferric uptake regulation (*fur*) locus. *J Bacteriol* **172**: 1930-1938.

Nystrom, T. (2004) Growth versus maintenance: a trade-off dictated by RNA polymerase availability and sigma factor competition? *Mol Microbiol* **54**: 855-862.

O'Brien, R.J., and Nunn, P.P. (2001) The Need for New Drugs against Tuberculosis . Obstacles, Opportunities, and Next Steps. *Am. J. Respir. Crit. Care Med.* **163**: 1055-1058.

Paget, M.S., Kang, J.G., Roe, J.H., and Buttner, M.J. (1998) sigmaR, an RNA polymerase sigma factor that modulates expression of the thioredoxin system in response to oxidative stress in *Streptomyces coelicolor A3*(2). *Embo J* **17**: 5776-5782.

Paget, M.S., Leibovitz, E., and Buttner, M.J. (1999) A putative two-component signal transduction system regulates sigmaE, a sigma factor required for normal cell wall integrity in *Streptomyces coelicolor A3*(2). *Mol Microbiol* **33**: 97-107.

Paget, M.S.B., Molle, V., Cohen, G., Aharonowitz, Y., and Buttner, M.J. (2001) Defining the disulphide stress response in *Streptomyces coelicolor A3*(2): identification of the R regulon. *Molecular Microbiology* **42**: 1007-1020.

Papavinasasundaram, K.G., Colston, M.J., and Davis, E.O. (1998) Construction and complementation of a *recA* deletion mutant of *Mycobacterium smegmatis* reveals that the intein in *Mycobacterium tuberculosis recA* does not affect RecA function. *Mol Microbiol* **30**: 525-534.

Parish, T., Gordhan, B.G., McAdam, R.A., Duncan, K., Mizrahi, V., and Stoker, N.G. (1999) Production of mutants in amino acid biosynthesis genes of *Mycobacterium tuberculosis* by homologous recombination. *Microbiology* **145**: 3497-3503.

Parish, T., and Stoker, N.G. (2000) Use of a flexible cassette method to generate a double unmarked *Mycobacterium tuberculosis* tlyA plcABC mutant by gene replacement. *Microbiology* **146 (Pt 8)**: 1969-1975.

Park, S., and Imlay, J.A. (2003) High levels of intracellular cysteine promote oxidative DNA damage by driving the fenton reaction. *J Bacteriol* **185**: 1942-1950.

Paz, M.M., Kumar, G.S., Tomasz, M., Glover, M., and Waring, M.J. (2004) Mitomycin dimers: Polyfunctional cross-linkers of DNA. *Journal of Medicinal Chemistry* **47**: 3308-3319.

Pittard, J., Camakaris, H., and Yang, J. (2005) The TyrR regulon. *Molecular Microbiology* **55**: 16-26.

Plotkin, J.B., Dushoff, J., and Fraser, H.B. (2004) Detecting selection using a single genome sequence of *M. tuberculosis* and P. falciparum *Nature* **428**: 942-945.

Pomposiello, P.J., and Demple, B. (2001) Redox-operated genetic switches: the SoxR and OxyR transcription factors. *Trends Biotechnol* **19**: 109-114.

Price, C.W., Fawcett, P., Ceremonie, H., Su, N., Murphy, C.K., and Youngman, P. (2001) Genome-wide analysis of the general stress response in *Bacillus subtilis*. *Molecular Microbiology* **41**: 757-774.

Price, M.N., Huang, K.H., Alm, E.J., and Arkin, A.P. (2005) A novel method for accurate operon predictions in all sequenced prokaryotes. *Nucl. Acids Res.* **33**: 880-892.

Radman, M. (1975) SOS repair hypothesis: phenomenology of an inducible DNA repair which is accompanied by mutagenesis. *Basic Life Sci* **5A**: 355-367.

Raivio, T.L., and Silhavy, T.J. (2001) Periplasmic stress and ECF sigma factors. *Annu Rev Microbiol* **55**: 591-624.

Ramakrishnan, L., Federspiel, N.A., and Falkow, S. (2000) Granuloma-specific expression of Mycobacterium virulence proteins from the glycine-rich PE-PGRS family. *Science* **288**: 1436-1439.

Raman, S., Song, T., Puyang, X., Bardarov, S., Jacobs, W.R., Jr., and Husson, R.N. (2001) The Alternative Sigma Factor SigH Regulates Major Components of Oxidative and Heat Stress Responses in *Mycobacterium tuberculosis*. *J. Bacteriol.* **183**: 6119-6125.

Raman, S., Hazra, R., Dascher, C.C., and Husson, R.N. (2004) Transcription Regulation by the *Mycobacterium tuberculosis* Alternative Sigma Factor SigD and Its Role in Virulence. *J. Bacteriol.* **186**: 6605-6616.

Rand, L. (2003) The role of DNA repair genes in *Mycobacterium tuberculosis* pathogenesis. University college London.

Rand, L., Hinds, J., Springer, B., Sander, P., Buxton, R.S., and Davis, E.O. (2003) The majority of inducible DNA repair genes in *Mycobacterium tuberculosis* are induced independently of RecA. *Mol Microbiol* **50**: 1031-1042.

Ravisse, P., Rastogi, N., David, H.L., and Guelpa-Lauras, C.C. (1984) Experimental leprosy in the armadillo and nude mice: comparative histobacteriology and ultrastructure. *Acta Leprol* **2**: 327-339.

Saeyers, W.a. (2002) Bacterial pathogenesis. Vol. 2nd edition: ASM press.

Sambrook, F., Fritsch, E., and Maniatis, T. (1989) *Molecular cloning. A laboratory manual*: Cold Spring Harbor.

Sancar, A. (1994) Mechanisms of DNA excision repair. *Science* **266**: 1954-1956.

Sander, P., Bottger, E.C., Springer, B., Steinmann, B., Rezwan, M., Stavropoulos, E., and Colston, M.J. (2003) A *recA* deletion mutant of *Mycobacterium bovis* BCG confers protection equivalent to that of wild-type BCG but shows increased genetic stability. *Vaccine* **21**: 4124-4127.

Sassanfar, M., and Roberts, J.W. (1990) Nature of the SOS-inducing signal in *Escherichia coli*. The involvement of DNA replication. *Journal of Molecular Biology* **212**: 79-96.

Sassetti, C.M., Boyd, D.H., and Rubin, E.J. (2001) Comprehensive identification of conditionally essential genes in mycobacteria. *PNAS* **98**: 12712-12717.

Sassetti, C.M., Boyd, D.H., and Rubin, E.J. (2003) Genes required for mycobacterial growth defined by high density mutagenesis. *Molecular Microbiology* **48**: 77-84.

Schlesinger, L.S., Hull, S.R., and Kaufman, T.M. (1994) Binding of the terminal mannosyl units of lipoarabinomannan from a virulent strain of *Mycobacterium tuberculosis* to human macrophages. *J Immunol* **152**: 4070-4079.

Schnetz, K., and Wang, J. (1996) Silencing of the *Escherichia coli bgl* promoter: effects of template supercoiling and cell extracts on promoter activity in vitro. *Nucl. Acids Res.* **24**: 2422-2428.

Severinov, K. (2000) RNA polymerase structure-function: insights into points of transcriptional regulation. *Curr Opin Microbiol* **3**: 118-125.

Sharp, M.M., Chan, C.L., Lu, C.Z., Marr, M.T., Nechaev, S., Merritt, E.W., Severinov, K., Roberts, J.W., and Gross, C.A. (1999) The interface of sigma with core RNA polymerase is extensive, conserved, and functionally specialized. *Genes Dev.* **13**: 3015-3026.

Shi, L., Jung, Y.-J., Tyagi, S., Gennaro, M.L., and North, R.J. (2003) Expression of Th1-mediated immunity in mouse lungs induces a *Mycobacterium tuberculosis* transcription pattern characteristic of nonreplicating persistence. *PNAS* **100**: 241-246.

Shrivastava, T., Kumar, S., and Ramachandran, R. (2004) Cloning, expression, purification and crystallization of a transcriptional regulatory protein (Rv3291c) from *Mycobacterium tuberculosis* H37Rv. *Acta Crystallographica Section D: Biological Crystallography* **60**: 1874-1876.

Siegele, D.A., Hu, J.C., Walter, W.A., and Gross, C.A. (1989) Altered promoter recognition by mutant forms of the [sigma]70 subunit of *Escherichia coli* RNA polymerase. *Journal of Molecular Biology* **206**: 591-603.

Smith, B.T., Grossman, A.D., and Walker, G.C. (2002) Localization of UvrA and Effect of DNA Damage on the Chromosome of *Bacillus subtilis*. *J. Bacteriol.* **184**: 488-493.

Sohaskey, C.D., and Wayne, L.G. (2003) Role of narK2X and narGHJI in Hypoxic Upregulation of Nitrate Reduction by *Mycobacterium tuberculosis*. *J. Bacteriol.* **185**: 7247-7256.

Song, T., Dove, S.L., Lee, K.H., and Husson, R.N. (2003) RshA, an anti-sigma factor that regulates the activity of the mycobacterial stress response sigma factor SigH. *Mol Microbiol* **50**: 949-959.

Southern, E.M. (1975) Detection of specific sequences among DNA fragments separated by gel electrophoresis. *Journal Molecular Biology* **98**: 503-517.

Springer, B., Sander, P., Sedlacek, L., Ellrott, K., and Bottger, E.C. (2001) Instability and site-specific excision of integration-proficient mycobacteriophage L5 plasmids: development of stably maintained integrative vectors. *Int J Med Microbiol* **290**: 669-675.

Stewart, G.R., Snewin, V.A., Walzl, G., Hussell, T., Tormay, P., O'Gaora, P., Goyal, M., Betts, J., Brown, I.N., and Young, D.B. (2001) Overexpression of heat-shock proteins reduces survival of *Mycobacterium tuberculosis* in the chronic phase of infection. *Nat Med* **7**: 732-737.

Stewart, G.R., Wernisch, L., Stabler, R., Mangan, J.A., Hinds, J., Laing, K.G., Young, D.B., and Butcher, P.D. (2002) Dissection of the heat-shock response in *Mycobacterium tuberculosis* using mutants and microarrays. *Microbiology* **148**: 3129-3138.

Stohl, E.A., and Seifert, H.S. (2001) The *recX* gene potentiates homologous recombination in *Neisseria gonorrhoeae*. *Mol Microbiol* **40**: 1301-1310.

Storz, G., and Imlay, J.A. (1999) Oxidative stress. *Curr Opin Microbiol* **2**: 188-194.

Stover, C.K., de la Cruz, V.F., Fuerst, T.R., Burlein, J.E., Benson, L.A., Bennett, L.T., Bansal, G.P., Young, J.F., Lee, M.H., Hatfull, G.F., and et al. (1991) New use of BCG for recombinant vaccines. *Nature* **351**: 456-460.

Strong, M., Mallick, P., Pellegrini, M., Thompson, M., and Eisenberg, D. (2003) Inference of protein function and protein linkages in *Mycobacterium tuberculosis* based on prokaryotic genome organization: a combined computational approach. *Genome Biology* **4**: R59.

Sun, R., Converse, P.J., Ko, C., Tyagi, S., Morrison, N.E., and Bishai, W.R. (2004) *Mycobacterium tuberculosis* ECF sigma factor *sigC* is required for lethality in mice and for the conditional expression of a defined gene set. *Mol Microbiol* **52**: 25-38.

Tanaka, K., Takayanagi, Y., Fujita, N., Ishihama, A., and Takahashi, H. (1993) Heterogeneity of the Principal {sigma} Factor in *Escherichia coli*: The *rpoS* Gene Product, {sigma}38, is a Second Principal {sigma} Factor of RNA Polymerase in Stationary-Phase *Escherichia coli*. *PNAS* **90**: 3511-3515.

Tanaka, K., Kusano, S., Fujita, N., Ishihama, A., and Takahashi, H. (1995) Promoter determinants for *Escherichia coli* RNA polymerase holoenzyme containing sigma 38 (the rpoS gene product). *Nucl. Acids Res.* **23**: 827-834.

Toulme, F., Guerin, M., Robichon, N., Leng, M., and Rahmouni, A.R. (1999) In vivo evidence for back and forth oscillations of the transcription elongation complex. *Embo Journal* **18**: 5052-5060.

Travers, A.A., and Burgess R.R (1969) Cyclic re-use of the RNA polymerase sigma factor. *Nature* **222**: 537-540.

Volkert, M.R., and Landini, P. (2001) Transcriptional responses to DNA damage. *Current Opinion in Microbiology* **4**: 178-185.

Wayne, L.G. (1982) Microbiology of tubercle bacilli. *Am Rev Respir Dis* **125**: 31-41.

Walker, G.C. (1984) Mutagenesis and inducible responses to deoxyribonucleic acid damage in Escherichia coli. *Microbiol Rev* **48**: 60-93.

WHO (1993) World Health Forum 14.

WHO (2002) Tuberculosis - Fact sheet.

WHO (2003) HIV/AIDs and tuberculosis.

Withey, J.H., and DiRita, V.J. (2005) Activation of both *acfA* and *acfD* transcription by *Vibrio cholerae* ToxT requires binding to two centrally located DNA sites in an inverted repeat conformation. *Mol Microbiol* **56**: 1062-1077.

Wu, S., Howard, S.T., Lakey, D.L., Kipnis, A., Samten, B., Safi, H., Gruppo, V., Wizel, B., Shams, H., Basaraba, R.J., Orme, I.M., and Barnes, P.F. (2004) The principal sigma factor *sigA* mediates enhanced growth of *Mycobacterium tuberculosis* in vivo. *Mol Microbiol* **51**: 1551-1562.

Yan, S., Myler, P.J., and Stuart, K. (2001) Tetracycline regulated gene expression in *Leishmania donovani. Molecular and Biochemical Parasitology* **112**: 61-69.

Yoshimura, M., Asai, K., Sadaie, Y., and Yoshikawa, H. (2004) Interaction of *Bacillus subtilis* extracytoplasmic function (ECF) sigma factors with the N-terminal regions of their potential anti-sigma factors. *Microbiology* **150**: 591-599.

Zahrt, T.C., Song, J., Siple, J., and Deretic, V. (2001) Mycobacterial FurA is a negative regulator of catalase-peroxidase gene *katG. Mol Microbiol* **39**: 1174-1185.

Zahrt, T.C., and Deretic, V. (2002) Reactive nitrogen and oxygen intermediates and bacterial defenses: unusual adaptations in *Mycobacterium tuberculosis. Antioxid Redox Signal* **4**: 141-159.

Zhang, G., and Darst, S.A. (1998) Structure of the *Escherichia coli* RNA polymerase alpha subunit amino-terminal domain. *Science* **281**: 262-266.

Zheng, M., and Storz, G. (2000) Redox sensing by prokaryotic transcription factors. *Biochem Pharmacol* **59**: 1-6.

Appendix I: Media and solutions

Modified Dubos broth

K_2HPO_4	1g
$Na_2HPO_4.12H_2O$	6.25g
Na_3 citrate	1.25g
$MgSO_4.7H_2O$	0.6g
Asparagine	2g
10% Tween 80	5mls
Casamino acids (Difco)	2g
pH7.2 (2M NaOH)	
dH_2O upto 960mls	
Autoclave 121°C for 15 mins	

Freezing medium

K_2HPO_4	12.6g
Na_3 citrate	0.9g
$MgSO_4.7H2O$	0.18g
$(NH_4)_2SO_4$	1.8g
KH_2PO_4	3.6
Glycerol	96g
dH_2O to 1 litre	
Autoclave 121°C for 15 mins	

Lauria-Bertani agar (L-agar)

Tryptone (Difco)	10g
Yeast extract (Difco)	5g
NaCl	10g
Agar (Difco)	15g
dH_20 to 1 litre	

Lauria-Bertani broth (L-broth)

Tryptone (Difco)	10g
Yeast extract (Difco)	5g
NaCl	10g
pH7.5 (1M NaOH)	
dH_20 to 1 litre	
Autoclave 121°C for 15 mins	

Middlebrook 7H9 broth

Glycerol	2mls
7H9 medium powder (Difco)	4.7g
dH_2O to 900mls	
Autoclave 121°C for 10 mins	

Middlebrook 7H11 agar

Glycerol	5mls
7H11 medium powder (Difco)	21g
dH_2O to 900mls	
Autoclave 121°C for 10 mins	

Denhardt's reagent (50X)

Ficoll	5g
Polyvinylpyrrolidone	5g
BSA (Fraction V, Sigma)	5g
dH_2O to 500mls	
Filter sterilise and store at -20°C	

Z-buffer

$Na_2HPO_4.7H_2O$	0.06M
$NaH_2PO_4.H_2O$	0.04M
KCl	0.01M
$MgSO_4.7H_2O$	0.001M
β-merceptoethanol	0.05M
pH7.0	

Appendix II: Primers and probes

Primers and probes

	Forward	Reverse
co-transcription primers		
LD sigG Af/r	accaacagtgccccgcctatt	gccgcacgccttatctcg
LD sigG Bf/r	cctacggccgcctcactctgga	gcgtctggccggcgatgcta
LD sigG Cf/r	agccgtaccagcgttcttcc	tggccgccgttgttcatctc
LD sigG Df/r	ccctaccggcgtgaactgctc	ggtcttgcgcctcgggtgaatc
LD2016f/r	cctgcggccggcgtgaagat	cgtcctcggcggcggtgaact
LD2017f/r	ccaccaaccccacggagaacat	actgccggtcgggtggggaagag
LD2018f/r	gcgcttgcgtcccaggatttgtgc	ataccgtgccgcgacttgctctgc

Knockout construction and detection		
LD sigG up/low	gctctagagagtgggtcggtgttgtaagcctggac	cccaagcttataggatgaccgccgccgaagttgta
LDsigG 5' DC	gtggcggtggcacctggcacaa	gcgacctgcacgggaccaacatct
pLR11c 5'R	LDsigG low	gcaggctcgcgtaggaatcatc
sigG D f/r	ttcgcgggcaagtcctc	gcagcacgtcgcgcagcagcagta
sigG probe f/r	ggaattacatatgcatgcccgcggtggtcaag	atggatcccgcgcaacagttcgtcgtctatct
Rv2017 3'F/R	ccactagtccaccaaccccacggaggaca	gggcagccaagaccgaccact
Rv2017 5'F/R	tgtactagtccactgggcacggactaacc	cgctgccgggcctagttgcttatc
sigG compd1f/r	cgaacgtgacgtcatcgcggccgaaccgtc	gacggttcggccgcgatgacgtcacgttcg
Rv2017 probe f/r	ccatgcatagccggtgtctgtcca	cgtcctcggcggcggtgaactcc
Rv2017 D f/r	cgtgggcaagggtcaagcgttttc	cgatgggcccggtcgtcaacct
Hyg f/r	gacctgcacgggaccaacatcttc	cgcggccaggtccacgaagatgtt

RNase protection/primer extension primers		
LD sigG mid H	cccaagctttcacgtcaatgagcctacgcagagtctcc	
LD sigG mid2	cgctcccggtaatgact	
ruvC small f/r	aatctagaggtcggggccggctcaatctc	cgaagcttagctgccgaccacgcccactct
recA RNase F/R1	gatccggccaggctagcggtgttgagca	gaggcgcatcaccgaacctttgccgtaac
sigG RNase F/R1	atgcccgcggtggtcaag	tcggtgtgggcggagaagtc

sequencing primers		
pKP186 seq f/r	ccgtattaccgcctttgagtgagc	ggcataaaacgaaaggcccagtct
comp 186 seq f/r	tagcggcgggcatgctcg	ctatcgcttgggcgagca
M13 f/r	commercial (invitrogen)	commercial (invitrogen)

Bandshift probes	
RecA P1 forward	ctagatcattcggagcagccgacttgtcagtggctgtctctagtgtcacggccaaccga
RecA P1 reverse	ctagtcggttggccgtgacactagagacagccactgacaagtcggctgctccgaatgat
RecA P2 forward	ctagacgcggcgtgtcacacttgaatcgaacaggtgttcggctactgtggtgatcattcgga
RecA P2 reverse	ctagtccgaatgatcaccacagtagccgaacacctgttcgattcaagtgtgacacgccgcgt
Oligo P1 A Forward	ctagatcattcggagcagccgacttgtcagtga
Oligo P1 A reverse	ctagacactgacaagtcggctgctccgaatgat
Oligo P1 B Forward	cctagagccgacttgtcagtggctgtctctagtga
Oligo P1 B reverse	ctagtcactagagacagccactgacaagtcggct
Oligo P1 C Forward	ctagaggctgtctctagtgtcacggccaaccga
Oligo P1 C reverse	ctagtcggttggccgtgacactagagacagcct
Oligo P1 D Forward	ctagaatcgtggtgatcgactcggtggcggcgctga
Oligo P1 D reverse	ctagtcagcgccgccaccgagtcgatcaccacgat
Oligo P1 E Forward	tgaatcgaacaggtgttcggctac
Oligo P1 E reverse	gtagccgaacacctgttcgattca

Taqman primers and probes			
Gene	**probe**	**forward primer**	**reverse primer**
sigA	ttgagcagcgctaccttgccg	tcggttcgcgcctacct	tggctagctcgacctcctcct
sigG	cgcctggcgatatgcgcctg	caacagtgccccgcctat	ccgttggcgatcaacga
ruvC	caccaaaatccttgcgctgcaagct	gctcaggtcaccgcgatg	cggccggtgtcggtt
recA	ttcggggcaccacggcgat	accggcgcgctgaata	cgcggagctggttgatg

Appendix III: Microarray fold change Rv2017

Higher in H37Rv			
Gene name	Mean Fold change	SEM	Gene ID
Rv3489	-16.38	1.84E-02	Rv3489
PE	-15.70	1.25E-02	Rv3477
ctaB	-15.01	6.24E-03	Rv1451
groEL2	-13.31	1.14E-02	Rv0440
Rv1516c	-13.02	2.73E-02	Rv1516c
Rv0893c	-12.18	2.64E-02	Rv0893c
Rv0289	-11.70	1.14E-02	Rv0289
Rv3384c	-11.54	2.10E-02	Rv3384c
Rv3827c	-10.45	1.99E-02	Rv3827c
Rv3745c	-10.43	3.12E-02	Rv3745c
Rv3583c	-10.32	2.55E-02	Rv3583c
kasA	-9.99	5.43E-03	Rv2245
Rv1892	-9.40	2.95E-02	Rv1892
Rv1519	-9.37	4.70E-02	Rv1519
Rv1245c	-9.33	3.84E-02	Rv0287
Rv0287	-9.31	3.19E-02	Rv3418c
groES	-9.28	1.83E-02	Rv1133c
rplO	-9.10	2.77E-02	Rv0722
metE	-9.09	2.02E-02	Rv0280
rpmH	-8.51	3.63E-02	Rv0167
rpmD	-8.24	4.58E-02	Rv0291
PPE	-8.12	2.50E-02	Rv2840c
Rv0167	-8.09	2.24E-02	Rv3872
Rv0291	-7.84	1.97E-02	Rv1245c
Rv2840c	-7.81	1.87E-02	Rv0682
PE	-7.78	3.73E-02	Rv0850
rpsL	-7.77	2.47E-02	Rv2412
Rv0850	-7.70	3.29E-02	Rv2778c
rpsT	-7.70	2.99E-02	Rv1307
Rv2778c	-7.61	2.58E-02	Rv0723
atpH	-7.60	2.21E-02	Rv3136
PPE	-7.54	3.92E-02	Rv1872c
lldD2	-7.54	2.44E-02	Rv3443c
rplM	-7.53	1.95E-02	Rv3615c
Rv3615c	-7.51	2.83E-02	Rv0636

Higher in Rv2017			
Gene name	Mean Fold change	SEM	Gene ID
Rv0648	15.04	5.86E+00	Rv0648
Rv0600c	12.01	1.71E+00	Rv0600c
tcrA	11.45	3.00E+00	Rv0602c
Rv0842	10.79	2.31E+00	Rv0842
Rv2624c	10.53	2.13E+00	Rv2624c
Rv2407	10.42	4.68E+00	Rv2407
Rv2897c	10.38	3.48E+00	Rv2897c
Rv2648	9.99	3.21E+00	Rv2648
Rv3467	9.25	1.45E+00	Rv3467
Rv2205c	9.14	2.86E+00	Rv2205c
Rv2415c	9.08	2.65E+00	Rv2415c
adhE	9.03	5.02E+00	Rv0162c
Rv1259	8.86	1.72E+00	Rv1259
Rv0584	8.77	1.72E+00	Rv0584
Rv0094c	8.65	7.49E-01	Rv0094c
Rv0943c	8.58	1.89E+00	Rv0943c
Rv1965	8.48	2.70E+00	Rv1965
Rv1726	8.47	1.19E+00	Rv1726
Rv3446c	8.33	2.74E+00	Rv3446c
Rv0541c	8.32	1.36E+00	Rv0541c
Rv3529c	8.19	2.54E+00	Rv3529c
Rv0621	7.92	7.84E-01	Rv0621
Rv0614	7.70	1.40E+00	Rv0614
Rv0368c	7.63	1.16E+00	Rv0368c
Rv2278	7.60	3.10E+00	Rv2278
uspA	7.56	2.07E+00	Rv2316
Rv0622	7.33	9.86E-01	Rv0622
Rv1188	7.26	1.50E+00	Rv1188
Rv0953c	7.09	1.52E+00	Rv0953c
Rv3448	6.88	1.70E+00	Rv3448
Rv0077c	6.79	1.66E+00	Rv0077c
Rv2813	6.78	2.05E+00	Rv2813
PE	6.66	7.50E-01	Rv2340c
recC	6.58	1.27E+00	Rv0631c
Rv1999c	6.52	1.79E+00	Rv1999c

Rv0636	-7.47	2.32E-02	Rv3633
Rv3633	-7.44	1.13E-02	Rv1981c
nrdF	-7.34	4.11E-02	Rv0702
rplD	-7.32	3.17E-02	Rv0282
Rv0282	-7.28	1.96E-02	Rv0719
rplF	-7.15	2.02E-02	Rv0637
Rv0637	-7.13	2.77E-02	Rv1013
Rv1055	-7.11	5.46E-02	Rv0667
pks16	-6.89	1.85E-02	Rv2160c
rpoB	-6.89	2.26E-02	Rv3924c
Rv2160c	-6.88	4.43E-02	Rv3219
whiB1	-6.74	1.25E-02	Rv0701
rplC	-6.69	1.60E-02	Rv1066
Rv1066	-6.68	6.30E-02	Rv1993c
Rv1993c	-6.46	1.59E-02	Rv2816c
Rv2816c	-6.39	3.27E-02	Rv1196
PPE	-6.38	1.70E-02	Rv1518
Rv1518	-6.34	4.18E-02	Rv1195
PE	-6.31	1.81E-02	Rv3048c
nrdG	-6.25	5.07E-02	Rv1641
infC	-6.25	2.69E-02	Rv1322
Rv1322	-6.20	8.28E-02	Rv0665
Rv0665	-6.20	4.00E-02	Rv3019c
Rv3019c	-6.19	2.66E-02	Rv3135
sigB	-6.15	3.45E-02	Rv1388
PPE	-6.13	4.92E-02	Rv0309
mIHF	-6.12	2.43E-02	Rv1630
Rv0309	-6.12	3.18E-02	Rv0653c
rpsA	-6.10	1.92E-02	Rv0608
Rv0653c	-6.04	1.91E-02	Rv1308
Rv0608	-6.02	4.33E-02	Rv1831
atpA	-6.02	2.50E-02	Rv2186c
Rv1831	-5.96	3.16E-02	Rv1054
Rv2186c	-5.95	4.06E-02	Rv2909c
Rv1054	-5.94	4.73E-02	Rv1247c
rpsP	-5.94	6.10E-02	Rv3047c
Rv1247c	-5.92	4.63E-02	Rv3183
Rv3047c	-5.86	7.11E-02	Rv3456c
Rv3183	-5.83	6.30E-02	Rv3277
rplQ	-5.78	2.54E-02	Rv0350
Rv3277	-5.75	5.11E-02	Rv1055
dnaK	-5.69	3.90E-02	Rv0700

Rv0574c	6.49	1.02E+00	Rv0574c
Rv2627c	6.49	2.25E+00	Rv2627c
Rv0259c	6.44	1.35E+00	Rv0259c
idsA	6.32	1.21E+00	Rv3398c
Rv0021c	6.23	1.72E+00	Rv0021c
PPE	6.22	1.10E+00	Rv0096
Rv2655c	6.17	1.60E+00	Rv2655c
narK2	6.00	1.18E+00	Rv1737c
Rv3184	5.99	1.57E+00	Rv3184
Rv3333c	5.92	9.56E-01	Rv3333c
ufaA1	5.90	1.04E+00	Rv0447c
Rv0836c	5.88	1.24E+00	Rv0836c
Rv0572c	5.81	8.60E-01	Rv0572c
Rv0592	5.80	1.32E+00	Rv0592
rocA	5.80	1.37E+00	Rv1187
Rv2305	5.77	5.90E-01	Rv2305
Rv0090	5.77	8.76E-01	Rv0090
Rv0163	5.77	2.39E+00	Rv0163
echA2	5.74	1.08E+00	Rv0456c
Rv3326	5.71	1.44E+00	Rv3326
Rv1722	5.67	1.05E+00	Rv1722
pknK	5.67	9.68E-01	Rv3080c
fdhD	5.66	1.20E+00	Rv2899c
Rv0843	5.66	1.08E+00	Rv0843
Rv1190	5.61	9.09E-01	Rv1190
purT	5.60	3.90E-01	Rv0389
amt	5.48	1.20E+00	Rv2920c
Rv1763	5.46	1.56E+00	Rv1763
Rv0687	5.45	6.59E-01	Rv0687
Rv0697	5.44	7.56E-01	Rv0697
Rv1757c	5.42	1.67E+00	Rv1757c
Rv0161	5.41	1.68E+00	Rv0161
Rv0492c	5.37	7.69E-01	Rv0492c
Rv3201c	5.36	8.51E-01	Rv3201c
Rv3660c	5.32	6.26E-01	Rv3660c
Rv1112	5.32	9.14E-01	Rv1112
Rv2167c	5.32	1.24E+00	Rv2167c
Rv3185	5.30	1.57E+00	Rv3185
galT	5.30	1.50E+00	Rv0619
Rv2049c	5.30	2.74E+00	Rv2049c
hycD	5.28	5.31E-01	Rv0084
Rv1575	5.22	1.14E+00	Rv1575

rpsJ	-5.58	2.90E-02	Rv1344
Rv1344	-5.58	5.46E-02	Rv1464
Rv1464	-5.53	1.29E-02	Rv3856c
Rv3856c	-5.52	2.91E-02	Rv1361c
PPE	-5.50	2.45E-02	Rv2927c
Rv2927c	-5.49	4.01E-02	Rv1072
Rv1072	-5.44	2.50E-02	Rv0639
nusG	-5.43	6.46E-02	Rv3866
Rv3866	-5.43	1.91E-02	Rv3487c
lipF	-5.41	4.02E-02	Rv2247
accD6	-5.36	1.81E-02	Rv0685
tuf	-5.34	2.89E-02	Rv1080c
greA	-5.31	2.19E-02	Rv0283
Rv0283	-5.25	2.04E-02	Rv2381c
mbtD	-5.22	2.45E-02	Rv3407
Rv3407	-5.18	6.49E-02	Rv3316
sdhC	-5.16	4.59E-02	Rv2710
Rv0292	-5.12	2.84E-02	Rv0292
groEL1	-5.11	2.94E-02	Rv3417c
Rv3300c	-5.10	8.23E-02	Rv3300c
rpsG	-5.10	4.26E-02	Rv0683
atpD	-5.07	4.03E-02	Rv1310
Rv2376c	-5.06	2.60E-02	Rv2376c

cysM3	5.22	8.93E-01	Rv0848
Rv0846c	5.22	1.23E+00	Rv0846c
Rv3380c	5.21	1.57E+00	Rv3380c
Rv0796	5.20	1.49E+00	Rv0796
Rv0311	5.19	1.56E+00	Rv0311
Rv0494	5.19	1.60E-01	Rv0494
Rv1588c	5.15	5.29E-01	Rv1588c
Rv2621c	5.12	5.03E-01	Rv2621c
Rv1936	5.09	9.47E-01	Rv1936
Rv3537	5.08	1.68E+00	Rv3537
lppB	5.07	6.46E-01	Rv2544
PPE	5.06	1.15E+00	Rv3621c
Rv3186	5.05	1.55E+00	Rv3186
xylB	5.02	6.48E-01	Rv0729
Rv2488c	5.01	1.19E+00	Rv2488c

Appendix III: Gene with a 5-fold of more differential gene expression in ΔRv2017 strain compared to H37Rv. Fold change was calculated as ΔRv2017 strain expressed as a proportion of H37Rv, genes were identified that were 5-fold different in expression level between ΔRv2017 strain compared to H37Rv. The left column reprewsents the reciprocal fold change (inducted with -) therefore genes are expressed to a lower level in ΔRv2017 strain compared to H37Rv. Whereas the right hand column represents genes which are upregulated in ΔRv2017 strain by more than 5-fold compared to H37Rv.

Appendix IV - Keystone abstract

A Novel Mechanism Regulating DNA-Damage Inducible Gene Expression in *Mycobacterium tuberculosis*

Lisa Dawson and Elaine Davis, Division of Mycobacterial Research, National Institute for Medical Research, Mill Hill, London,UK.

Mycobacterium tuberculosis (*Mtb*) is an intracellular pathogen, which causes human tuberculosis. Infected macrophage produce reactive oxygen and nitrogen intermediates, known to damage DNA; therefore DNA damage repair is thought to be important in survival of *Mtb* in the host. RecA is an integral part of the DNA damage repair system, being highly conserved and ubiquitous. In *Mtb* the *recA* gene is expressed from two promoters. One promoter (P2) is regulated by LexA, while the other promoter (P1) remains DNA damage inducible independently of the classical LexA/RecA system. Studies using gel shift assays have failed to detect a repressor or activator protein which binds the P1 promoter from total cell free extracts of *Mtb*, unlike the P2 promoter, which clearly binds LexA. This may be due to low levels of expression. Therefore, five proteins with predicted regulatory functions, which are induced following DNA damage in both wild type and Δ*recA* strains of *Mtb*, are being expressed to examine binding individually.

Alternatively, regulation of gene expression from the P1 promoter could be controlled by a sigma factor. Sigma factors are protein subunits of RNA polymerase, which confer specificity of binding to the promoter of a specific gene. The function and/or expression of sigma factors can be regulated, resulting in regulation of expression of the genes they transcribe. The sigma factors SigG, SigE and SigH are induced following DNA damage in both wild type and Δ*recA* strains of *Mtb*. A *sigG* knockout is being constructed and will be used alongside *sigE* and *sigH* knockouts (kindly provided by R.N.Husson) to determine if any of these sigma factors regulate gene expression of the P1 promoter of *recA*.

Lisa Dawson

Poster session 2